

2013-09-13

Myxoma Virus Therapy of Malignant Gliomas in Murine Syngeneic Models: Translating Barriers to Therapy

Zemp, Franz Joseph

Zemp, F. J. (2013). Myxoma Virus Therapy of Malignant Gliomas in Murine Syngeneic Models: Translating Barriers to Therapy (Doctoral thesis, University of Calgary, Calgary, Canada).

Retrieved from <https://prism.ucalgary.ca>. doi:10.11575/PRISM/27049

<http://hdl.handle.net/11023/967>

Downloaded from PRISM Repository, University of Calgary

UNIVERSITY OF CALGARY

Myxoma Virus Therapy of Malignant Gliomas in Murine Syngeneic Models:

Translating Barriers to Therapy

by

Franz J. Zemp

A THESIS

SUBMITTED TO THE FACULTY OF GRADUATE STUDIES
IN PARTIAL FULFILMENT OF THE REQUIREMENTS FOR THE
DEGREE DOCTOR OF PHILOSOPHY

DEPARTMENT OF MEDICAL SCIENCE

CALGARY, ALBERTA

SEPTEMBER, 2013

© Franz J. Zemp 2013

Abstract

High grade glioma has an almost universally fatal outcome. Failure of current treatment modalities has prompted the investigation into non-traditional therapies. Oncolytic virus therapy entails the use of replication competent viruses that selectively infect, replicate and kill cancer cells. This multi-modal therapy can function to directly kill cancer cells, stimulate anti-tumour immune responses, and be engineered to express additional anti-tumour activities. Despite promising preclinical studies in xenograft models, clinical trials have demonstrated no overwhelming treatment responses. Interestingly, syngeneic glioma models have shown results more typical of what was seen in the clinic.

This study was undertaken to identify the potential immune-effectors mediating Myxoma virus (MYXV) clearance in immunocompetent mouse models. MYXV is a rabbit-specific poxvirus that has oncolytic properties in cancer cell lines, having previously been shown to ‘cure’ human xenograft models. We found that syngeneic murine glioma lines derived from *Nf1^{+/-}Trp53^{+/-}* mice formed aggressive, gliosarcoma-like tumours in the brains of C57Bl/6 mice, but MYXV administration resulted in a very transient infection and no treatment efficacy. Further, a new syngeneic glioma model was created through culturing spontaneous gliomas from these mice as neurospheres. These lines displayed stem cell markers and produce highly invasive gliomas when grafted into the brains of immunocompetent C57Bl/6 mice.

We hypothesized that Type-I interferon (IFN α/β), could be playing a role in this resistance. However, it was found that MYXV treatment did not elicit an IFN α/β response in these glioma lines *in vitro* or *in vivo*. Further, engineered ablation of IFN α/β signalling in the glioma *in vivo* had no change in treatment outcome.

Immunophenotyping the glioma microenvironment found these gliomas were heavily infiltrated with microglia and macrophages, just as has been shown in human patients. Ablation of tumour-resident macrophages, not treatment-recruited macrophages, resulted in a significant increase in viral infection in the tumours that resulted in a mild survival advantage; however, the virus was still rapidly cleared in these animals. NK and T cell populations were also recruited to the tumour. Interestingly, ablation of both these populations, but not either one alone, resulted in a robust, durable infection in the tumour that resulted in survival benefit.

Preface

Portions of the work presented within this thesis have previously been published in academic, peer-reviewed journals. As required by the University of Calgary thesis guidelines, full citations for these articles and an account of the division of labor are described below. All work has been published in journals that do not require written copyright permissions to reproduce in a thesis dissertation. Unless otherwise stated here, all work presented within this thesis was performed by Franz J. Zemp.

A portion of the text in the **Chapter 1** has been revised from a review article listed below. **Figure 1.2** was also adapted from this publication. All portions of text and figures used were written or prepared by FJZ.

Zemp FJ, Corredor JC, Lun X, Muruve DA, Forsyth PA. 2010. Oncolytic viruses as experimental treatments for malignant gliomas: using a scourge to treat a devil. *Cytokine Growth Factor Rev.* 21(2-3): 103-17.

Portions of the text and figures in **Chapter 3 and 4** have been used from two recently published articles. **Figures 3.3, 3.4, 4.2, 4.3, 4.4, 4.5, 4.6, 4.7, 4.8, 4.9, 4.10** and **Table 3.1 and 3.2** were fully or partially published in the journals listed below. All experiments and portions of text and figures used were written or prepared by FJZ, except for Figure 4.7 A, where the immunohistochemistry was performed by Lori Maxwell.

Zemp FJ, Lun X, McKenzie BA, Zhou H, Maxwell L, Sun B, Kelly JJ, Stechishin O, Luchman A, Weiss S, Cairncross JG, Hamilton MG, Rabinovich BA, Rahman MM, Mohamed MR, Smallwood S, Senger DL, Bell J, McFadden G, Forsyth PA. 2013. Treating brain tumor-initiating cells using a combination of myxoma virus and rapamycin. *Neuro Oncol.* 15(7): 904-20.

Zemp FJ, McKenzieBA, Lun XQ, Reilly K, McFadden G, Yong VW, Forsyth PA. 2013. Resistance to oncolytic Myxoma Virus therapy in NF1^{+/-}/p53^{+/-} syngeneic mouse glioma models is independent of IRF-9 dependent tumour signalling. *PLoS One.* 8(6): e65801.

Acknowledgements

First and foremost, I would like to thank my loving, beautiful, and most importantly, understanding wife, **Krista**. Thank you for all the love and support, especially over the past year. And to my son **Oliver**, you are still new to the world, but your smiles and laughs helped me through to the end. I am so excited to share the things I have learned with you.

Thank you to my **Mother** and **Father**, for all the love and support over the years on my incredibly long journey through academia.

To **Dr. Peter Forsyth**, thank you for welcoming me into your lab, and providing the support and mentorship which allowed me to “follow my nose” throughout my studies. The lessons I have learned from you go far beyond the laboratory.

To **Dr. Wee Yong**, I cannot thank you enough for taking me into your foster care and helping through when times got tough. CCR2-deficient mice, brilliant!

To **Dr. Frank Jirik** and **Dr. Dan Muruve**, thank you for your guidance and encouragement while sitting on my committee. To **Dr. May Ho** for taking the time to be my internal external examiner for both my candidacy exam and thesis defence. And to **Dr. Samuel Rabkin** for coming to Calgary as my external examiner.

Thank you to **Dr. Jennifer Chan** for all the times you ‘had a minute’ to chat about my work or look at a slide.

A very special thank you to **Dr. Xueqing Lun**, who taught me many of the *in vivo* procedures I performed in this thesis. But most importantly, taught me how to hold a pair of scissors.

Thank you to all the members of the **Forsyth and Yong laboratories** for their help and support along the way. Special thank you to **Dr. Sam Lawn** for the introspective chats and laughs, and **Brienne McKenzie** for your eagerness to help, learn and endure. And especially to **Lori Maxwell**, who was often the only one able to save me from myself.

Thank you to my collaborators, **Dr. Grant McFadden** and **Dr. Karlyne Reilly**, as without Myxoma virus and syngeneic cell lines, this project could never have happened.

Thank you to **Evelyn Boland** who always made sure the behind the scenes workings were in order, even when it wasn’t her job anymore. And to **Molly Chisholm** who helped me take good care of my mice.

Finally, a huge thank you to the **University of Calgary**, **Alberta Innovates – Health Solutions**, the **Izaak Walton Killam Foundation**, and the **Canadian Institute of Health Research Vanier Scholarships**. You provide more than salary, but instill confidence and a sense of purpose that drives research.

Table of Contents

1. LITERATURE REVIEW	1
1.1. Malignant gliomas: Characteristics from the clinic	1
1.1.1. Incidence and prognosis.....	1
1.1.2. The molecular characteristics of high grade gliomas	2
1.2. The glioma microenvironment.....	5
1.2.1. Glioma immunosuppression	6
1.2.2. Microglia and peripheral monocyte/macrophages in the glioma microenvironment.....	9
1.2.2.1. Microglia ontogeny and normal function	9
1.2.2.2. Glioma-associated microglia and macrophages: Clinical analysis.....	13
1.2.2.3. Glioma-associated microglia and macrophages: Functions	15
1.3. Animal models of gliomas for the preclinical evaluation of therapeutics.....	19
1.3.1. Types of preclinical glioma models: Grafts.....	20
1.3.2. Types of preclinical glioma models: Spontaneous glioma models.....	23
1.3.3. Types of preclinical glioma models: Brain tumour-initiating cells	28
1.4. Oncolytic viruses.....	31
1.4.1. The role of monocytes/macrophages in oncolytic therapy for the CNS	37
1.4.2. The role of natural killer cells in oncolytic therapy for the CNS.....	39
1.4.3. Oncolytic viruses for the treatment of glioma	44
1.4.3.1. Oncolytic viruses for the treatment of glioma: Clinical trial summary	47
1.4.3.2. Oncolytic viruses for the treatment of glioma: Preclinical Trials	50

1.4.4.	Myxoma virus as a candidate oncolytic virus for gliomas	54
1.4.4.1.	Myxoma virus biological characteristics.....	56
1.4.4.2.	Myxoma virus as an anti-glioma agent.....	65
1.5.	Literature review summary, overall hypothesis and specific aims	68
2.	MATERIALS AND METHODS.....	72
2.1.	Cell Culture	72
2.1.1.	Mouse adherent cell lines: Origins and culture techniques	72
2.1.2.	Human adherent cell lines: Origins and culture techniques.....	72
2.1.3.	Mouse brain tumour-initiating cell lines: Origins and culture techniques..	73
2.1.4.	Human brain tumour-initiating cell lines: Origins and culture techniques.	75
2.2.	Myxoma virus: Strains and <i>in vitro</i> infection and replication assays	76
2.2.1.	Myxoma virus strains and propagation.....	76
2.2.2.	Myxoma virus infection and replication <i>in vitro</i>	77
2.3.	Viability assays and drug treatments.....	77
2.3.1.	AlamarBlue®	77
2.3.2.	Thiazolyl blue tetrazolium bromide (MTT) assay	78
2.4.	Cytokine measurements <i>in vitro</i>	78
2.4.1.	HEK-Blue and B16-Blue assays for IFN α/β	78
2.4.2.	Reverse transcriptase (RT)-PCR.....	79
2.4.3.	IFN α/β reporter plasmid.....	79
2.4.4.	ELISA: Single and multi-cytokine ELISA luminex – <i>in vitro</i>	80

2.5.	Creation of modified NPcis cell lines	80
2.5.1.	Lentiviral packaging and transfection.....	80
2.5.2.	Interferon responsive firefly luciferase construct for the stable transfection of cell lines.....	81
2.5.3.	IRF9 knockdown in NPcis cell lines.....	82
2.6.	Stem cell marker expression in mBTIC lines.....	84
2.6.1.	Western blotting.....	84
2.6.2.	Immunocytochemistry/Immunofluorescence	84
2.7.	H&E and immunohistochemistry.....	85
2.7.1.	Mounting frozen sections.....	85
2.7.2.	H&E staining frozen sections	85
2.7.3.	Immunohistochemistry for Myxoma virus, glioma markers, and confirmation of knockdown.....	86
2.8.	Mouse strains and genotyping.....	87
2.8.1.	Mice strains.....	87
2.8.2.	Genotyping mice.....	87
2.9.	Intracranial surgeries	88
2.9.1.	Orthotopic tumour implantation	88
2.9.2.	Intracranial treatments	88
2.10.	<i>In vivo</i> monitoring of viral infection and replication.....	89

2.10.1.	In vivo viral replication	89
2.10.2.	Monitoring viral infection with bioluminescence imaging.....	89
2.11.	Immunophenotyping the glioma microenvironment before and after intracranial MYXV treatment	90
2.11.1.	Multi-cytokine ELISA in vivo	90
2.11.2.	IFN α/β ELISA in vivo.....	90
2.11.3.	Flow cytometry for immunocytes in the glioma microenvironment.....	90
2.12.	Other mouse treatments.....	92
2.12.1.	Clodronate liposome administration	92
2.12.2.	Minocycline administration.....	93
2.12.3.	Diphtheria toxin administration	93
2.12.4.	CD161(NK1.1) administration.....	93
2.13.	Statistical analysis	94
3.	CHARACTERIZING SYNGENEIC C57BL/6 MURINE GLIOMA MODEL FOR PRECLINICAL STUDIES OF MYXOMA VIRUS THERAPY	95
3.1.	Introduction	95
3.2.	Results	99
3.2.1.	MYXV treatment of GL261 and B8 in vitro	99
3.2.2.	In vitro response of NPcis lines to Myxoma virus infection	101
3.2.3.	Characterization of NPcis tumours in vivo	104

3.2.4.	In vivo response of NPcis lines to Myxoma virus infection.....	106
3.2.5.	Creation and characterization of murine brain-tumour initiating cell lines	111
3.2.6.	Response of mBTIC lines to Myxoma virus oncolytic therapy in vitro ...	123
3.3.	Discussion	126
4.	THE ROLE OF TYPE-I INTERFERON IN MEDIATING TREATMENT FAILURE IN NPcis PRECLINICAL GLIOMA MODELS	135
4.1.	Introduction	135
4.2.	Results	140
4.2.1.	Species-specificity of type-I interferon and protection of NPcis cell lines by exogenous type-I interferon	140
4.2.2.	NPcis cell line type-I interferon production in response to MYXV in vitro or in vivo	142
4.2.3.	Creation of interferon insensitive NPcis cell lines through IRF9 knockdown	147
4.2.4.	Testing human cell lines for type-I interferon production following Myxoma virus infection.....	151
4.3.	Discussion	157
5.	IMMUNOCYTE-MEDIATED MECHANISMS OF MYXOMA VIRUS TREATMENT RESISTANCE IN NPcis ORTHOTOPIC MODELS.....	163
5.1.	Introduction	163

5.2.	Results	167
5.2.1.	The K1492 tumour microenvironment after Myxoma virus treatment	167
5.2.2.	The role of resident and recruited monocytoïd cells in mediating Myxoma virus treatment failure in the K1492 model	184
5.2.3.	The role of NK, NKT and T cells in mediating Myxoma virus treatment failure in the K1492 model	208
5.3.	Discussion	225
6.	OVERALL IMPACT AND FUTURE DIRECTIONS	236
6.1.	AIM I: Characterizing relevant syngeneic glioma models	236
6.2.	AIM II: Interrogating the role of type-I interferon in Myxoma virus treatment failure in syngeneic glioma models	239
6.3.	AIM III: Immunophenotyping the syngeneic glioma microenvironment before and after Myxoma therapy and identifying potential cellular mediators of treatment resistance.....	241
6.4.	Overall thoughts and conclusions	246

List of Tables

Table 1.1: Oncolytic viruses for gliomas in completed clinical trials - Overview	48
Table 1.2: Oncolytic viruses for gliomas in clinical trials – In progress or planned	49
Table 1.3: Oncolytic viruses in preclinical models of syngeneic gliomas – Overview ...	52
Table 2.1: Origins and strains of mice used.....	87
Table 2.2: Antibodies used immunophenotyping the K1492 microenvironment before and after Myxoma treatment.....	92
Table 3.1: <i>In vivo</i> growth characteristics of NPcis glioma lines implanted in C57Bl/6 mice.....	105
Supplementary Table 1: NPcis Litter #1. DOB: 2011.08.11	279
Supplementary Table 2: NPcis Litter #2. DOB: 2011.11.17	280
Supplementary Table 3: NPcis Litter #3. DOB: 2011.12.21	281

List of Figures and Illustrations

Figure 1.1: Overall characteristics of malignant gliomas.....	4
Figure 1.2: Immunosuppression in the glioma microenvironment.....	7
Figure 1.3: How microglia and glioma infiltrating monocytes/macrophages can enhance glioma tumourogenesis.....	18
Figure 1.4: Oncolytic viruses have the potential to elicit an anti-tumour response through a number of mechanisms.	45
Figure 1.5: The clinical conundrum.....	54
Figure 1.6: Myxoma virus infection and replication.	63
Figure 2.1: Dissection of NPCis mouse brain at autopsy.	75
Figure 2.2: Creation of a type-I interferon responsive luciferase reporter construct in a lentiviral reporter plasmid.....	83
Figure 3.1: B8 and GL261 cell lines have differing susceptibility to MYXV infection and MYXV-mediated cell death in vitro.	101
Figure 3.2: Preliminary tests of NPCis cell lines show the lines have variable susceptibility to MYXV infection and MYXV-mediated cell death in vitro.....	102
Figure 3.3: NPCis cell lines have variable susceptibility to MYXV infection and MYXV-mediated cell death in vitro.....	104
Figure 3.4: K1492 and K1861 form aggressive intracranial tumours in C57Bl/6 mice.	106
Figure 3.5: MYXV treatment in vivo results in only transient infection of the tumour and results in no therapeutic efficacy.	111
Figure 3.6: Three of seventeen NPCis animals followed found putative astrocytoma-like lesions..	114
Figure 3.7: Formalin-fixed paraffin embedded sections of lesions demonstrate that both FJZ0309 and FJZ0528 are high-grade gliomas..	115

Figure 3.8: Lesions cultured from NPcis mouse brains readily formed neurospheres in mouse neural stem cell media and displayed multi-lineage differentiation in response to fetal bovine serum.....	117
Figure 3.9: Mouse glioma neurosphere cultures expresses neural stem cell markers and markers of differentiation doing different CNS lineages.....	121
Figure 3.10: mBTIC lines FJZ0309, FJZ0528 and FJZ1116 all form infiltrative tumours when implanted into C57Bl/6 mice.	122
Figure 3.11: Murine BTIC lines FJZ0309, FJZ0528, and FJZ1116 and human BTIC lines BT025 and BT048 in response to Myxoma virus treatment in vitro.	126
Figure 4.1: Differences between xenograft and syngeneic glioma models that could explain the resistance to Myxoma therapy in vivo.	139
Figure 4.2: Type-I Interferon is not cross-reactive between human and murine glioma lines.	141
Figure 4.3: NPcis cell lines are protected by exogenous murine IFN β	143
Figure 4.4: NPcis cell lines do not produce any functional type-I interferon to Myxoma virus in vitro yet retain the ability to produce type-I interferon to other stimuli.	145
Figure 4.5: Type-I Interferon is not produced in the K1492 glioma microenvironment in vivo.	146
Figure 4.6: IRF9 knockdown results in loss of protection of type-I interferon in K1492 in vitro.	148
Figure 4.7: K1492 IRF9 knockdown persists in vivo, but makes no difference in viral replication or treatment efficacy.	150
Figure 4.8: Conventional glioma cell lines do not produce type-I interferon in response to Myxoma virus.	152
Figure 4.9: Human brain tumour-initiating cell lines do not produce type-I interferon in response to Myxoma virus.	154
Figure 4.10: Non-transformed human cell types do not produce type-I interferon in response to Myxoma virus.	156

Figure 5.1: Hypothesized mechanism for Myxoma virus treatment resistance.....	168
Figure 5.2: Immunophenotyping of the K1492 glioma microenvironment by flow cytometry with or without Myxoma virus treatment.....	172
Figure 5.3: K1492 orthografts in C57Bl/6 mice are highly infiltrated by microglia and macrophages.	174
Figure 5.4: Immunophenotyping of the K1492 glioma microenvironment in response to sterile injury.	175
Figure 5.5: Tumour-resident and recruited NK cells in K1492 treated with Myxoma virus.....	178
Figure 5.6: The recruited population of CD45 ^{high} CD11b ⁺ in Myxoma treated K1492 tumours consists of monocytes, granulocytes NK cells and T cells.	181
Figure 5.7: Cytokine and Chemokines significantly regulated in the K1492-glioma microenvironment.	183
Figure 5.8: K1492 orthografts in CB17-SCID mice have similar microglial and monocyte infiltration to C57Bl/6, but U87 lacks extensive infiltration.....	186
Figure 5.9: CCL2 in the glioma microenvironment may in part be tumourally-derived and regulated by growth factor signalling.	186
Figure 5.10: CCR2-deficient mice fail to recruit any peripheral monocytes/macrophages to the K1492 tumour before or after Myxoma treatment.....	189
Figure 5.11: CCR2-deficient mice have unaffected microglial activation and tumour-recruitment but are largely devoid of monocyte/microglia within the K1492 glioma. ..	191
Figure 5.12: CCR2-deficient have an exaggerated recruitment of NK, NKT and T cells to the K1492 glioma in response to Myxoma treatment.....	193
Figure 5.13: CCR2-deficient mice have a significant increase in the amount of infection, but not replication occurring after Myxoma virus administration which translates into a mild increase in survival of treated animals.	196
Figure 5.14: Clodronate liposome administration results in depletion of peripheral monocyte infiltration at three days post Myxoma virus administration.	198

Figure 5.15: Ablation of peripheral monocytes results in no significant change in viral luciferase or survival in K1492 glioma-bearing mice.....	200
Figure 5.16: CD11b::DTR mice display toxicity to diphtheria toxin administration. ...	202
Figure 5.17: CD11b::DTR mice bearing K1492 gliomas have resident glioma-infiltrating microglia and recruited CD45 ^{high} CD11b ⁺ ablated after diphtheria toxin administration. Loss of these cell types results in significant increase in Myxoma luciferase expression.	204
Figure 5.18: Spontaneous NPcis gliomas in C57Bl/6 mice have microglia and/or monocyte activation and recruitment that may correlate with grade of the tumour.	206
Figure 5.19: Minocycline administration in the K1492 model enhances early Myxoma virus infection but does not result in survival benefit.....	207
Figure 5.20: K1492 gliomas implanted in immunodeficient IL2R γ -deficient mice have a persistent tumour infection that results in an increase in survival benefit.	211
Figure 5.21: Immunophenotyping the K1492 glioma microenvironment in IL2R γ -deficient mice shows no recruitment of peripheral immunocytes in response to Myxoma treatment.	213
Figure 5.22: RAG1-deficient animals are devoid of all CD3 populations in the K1492 microenvironment before or after Myxoma treatment, but the NK cell population remains the same.	216
Figure 5.23: RAG1-deficient mice have a subtle impediment to viral clearance from the K1492 glioma but this does not translate to a change in treatment efficacy.	218
Figure 5.24: IL2R γ -deficient and IL2R γ -Rag-deficient mice have identical viral clearance kinetics and similar survival benefit in response to Myxoma virus treatment.	220
Figure 5.25: Ablation of peripheral NK cells does not change viral luciferase clearance from K1492-bearing CD57Bl/6 mice, nor change treatment efficacy.....	222
Figure 5.26: U87 orthoxenografts in Rag1 ^{-/-} or Rag1/IL2R γ ^{-/-} mice show similar trends of viral clearance kinetics and treatment efficacy in the K1492 model.	224

Supplementary Figure 1: Example of flow cytometry scatter plot with large and small gate..... 278

Supplementary Figure 2: Percent CD45 of clodronate liposome experiment.. 278

List of Symbols, Abbreviations, Nomenclatures

Abbreviation	Definition
AA	anaplastic astrocytoma
AdV	adenovirus
BTIC	brain tumour-initiating cells
CED	convection enhanced delivery
CPA	cyclophosphamide
CNS	central nervous system
CSCH	cancer stem cell hypothesis
DMEM	Dulbecco's modified Eagle medium
dpi	days post implantation (referring to tumour)
dpTx	days post treatment (mostly intracranial MYXV)
DT	diphtheria toxin
DTR	diphtheria toxin receptor
DV	dead virus
ECM	extracellular matrix
EMV	extracellular mature virion
FBS	fetal bovine serum
FFU	fluorescent focus forming units
GBM	glioblastoma multiforme
GFP	green fluorescent protein
GIM	glioma infiltrating monocytes/macrophages
HDi	histone-deacetylase inhibitors
hpi	hours post-infection
HSV	Herpes simplex virus
IFN α/β	type-I interferon
IMV	intracellular mature virion

IRF	interferon regulatory factor
ISG	interferon-stimulated gene
ISRE	interferon stimulated response element
LB	Luria broth
mBTIC	mouse brain tumour-initiating cell
MCMV	mouse cytomegalovirus
MEF	mouse embryonic fibroblast
MHC	major histocompatibility complex
MMP	matrix metalloproteases
MOI	multiplicity of infection
MTD	maximum tolerated dose
MTT	thiazolyl blue tetrazolium bromide
MV	Measles virus
MYXV	Myxoma virus
NCR	natural cytotoxicity receptors
NK	natural killer cell
NKR	natural killer cell receptor
NKT	natural killer T cell
NDV	Newcastle disease virus
NPcis	<i>C57Bl/6 Trp53^{+/-}/Nf1^{+/-}</i> mice
NoTx	no treatment
NSC	neural stem cells
PAMP	pathogen-associated molecular pattern
PBS	phosphate buffered saline
PFU	plaque-forming unit
PGE2	prostaglandin E2
PRR	pattern-recognition receptor

ORF	open reading frame
OV	oncolytic virus
RFP	red fluorescent protein
RV	Reovirus
SCID	severe combined immunodeficient
TCGA	The Cancer Genome Atlas
TLR	Toll-like receptor
T _{reg}	regulatory T cells
VEGF	vascular endothelial growth factor
VSV	Vesicular stomatis virus
VV	Vaccinia virus
WHO	World Health Organization

1. LITERATURE REVIEW

1.1. Malignant gliomas: Characteristics from the clinic

1.1.1. Incidence and prognosis

Malignant brain and nervous system cancers in adults are relatively rare, with ~25,000 new cases predicted to be diagnosed in North America in 2013.^{1,2} Gliomas, cancers of glial cell origin, are expected to make up 15,000-20,000 of these cases, with 60-70% being accounted for by glioblastoma multiforme (**GBMs**, grade IV) and 10-15% by anaplastic astrocytomas (**AAs**, grade III).²⁻⁴ However, despite the low incidence rate of these cancers, intensive research into novel glioma therapies is fuelled by their dismal survival rates. This is punctuated by the 12-15 month median survival rate of GBMs,^{3,5} which has remained nearly unchanged for 25 years despite modern surgical and chemotherapeutic advances.⁶ Further, although the median age of diagnosis is ~55 years of age for high-grade gliomas,^{3,5} this median is widely distributed with disease commonly found in younger patients less than 40 years of age. Anaplastic astrocytomas have a less aggressive course, with a median survival of 2-3 years,⁷ but will progress to GBMs with all patients inevitably succumbing to disease.

Current therapies for malignant glioma include surgical resection followed by radiotherapy and concurrent or adjuvant chemotherapy, most often the DNA alkylation agent temozolomide (TEMODAR®).^{3,5} Additional treatments aimed at alleviating the physiological and neurological side-effects of the tumours, seizures and intracranial edema for example, are also common. However, the failure of these therapies to significantly improve the survival highlights the need for more effective treatments.

1.1.2. *The molecular characteristics of high grade gliomas*

The World Health Organization (**WHO**) classification of gliomas is based upon the morphological representation of the neoplasm through histology.⁸ Simply put, astocytomas look like astrocytes and oligodendrogliomas look like oligodendrocytes. Grading these tumours is assigned through several other histological characteristics. For example, while both WHO grade III AAs and WHO grade IV GBMs both have astrocytic characteristics with nuclear atypia and high mitotic activity, GBMs are further classified by areas of necrosis and microvascular proliferation.^{8,9} Both of these grades are highly infiltrative, with single cells invading the brain parenchyma. This makes complete surgical resection largely impossible. This, coupled with their a glioma's radio- and chemo-resistance render them essentially incurable.^{4,8-10}

GBMs, the most common and aggressive of the MGs, have been extensively characterized, are divided into 'primary' and 'secondary' GBMs. Primary GBMs (>90% of these tumours) arise *de novo* appearance with no evidence of a prior, less malignant lesion. In contrast, secondary GBMs progress from lower grade lesions (usually WHO Grade II diffuse astocytomas or WHO Grade III AAs).^{8,9} Despite the differences in their origin, the resulting WHO Grade IV lesions are morphologically indistinguishable. However, primary and secondary GBMs do differ genetically. Secondary gliomas are associated with the mutations that are characteristic of WHO Grade II and Grade III astrocytic gliomas, mainly *TP53* (>65%) and *IDH1/2* mutations (50-80%). Primary gliomas have far less frequent *TP53* mutations (25-33%) and *IDH1/2* mutations are rare (3-7%).^{4,8,9} The differences between these glioma types are summarized in **Figure 1.1**.

The Cancer Genome Atlas (**TCGA**) is a multi-center collaboration organized to characterize the diversity of genetic alterations in GBMs. Through gene sequencing, expression analysis and copy number analysis, it has confirmed previous observations and identified new mutations and signalling pathways that are critical in GBMs. The TCGA study was integral in moving this field forward, as it identified multiple genetic players that commonly result in dysfunction in three core pathways; the p53 pathway (87%), Retinoblastoma pathway (78%), and Receptor-tyrosine kinase signalling (88%).¹¹

The data generated by the TCGA, in addition to an extensive amount of expression and sequencing sets published in the literature, has allowed the classification of GBMs into several subgroups based on gene-expression profile and mutational status. The most notable of these studies used the TCGA expression data, subsequently confirmed in independent data sets, to show that GBMs cluster into 4 subgroups, Classical, Mesenchymal, Neural and Proneural.¹² Although these subgroups were derived from an expression signature that includes over 200 genes, these subtypes cluster with known genetic alterations in GBMs. For example, the Classical subtype is associated with chromosomal *EGFR* amplifications and *CDKN2A/B* homozygous deletions with activated Sonic-Hedgehog and Notch signalling. Mesenchymal subtypes with chromosomal or expression loss of *NF1* and *PTEN*, and activated NFκB signalling. The Proneural subtype is characterized by *PDGFRA* chromosomal amplification, oligodendrocyte gene expression patterns, as well as *IDH1* and *TP53* mutation. The Neural subtype is characterized through the expression of neuronal genes. Similar groupings have been made in other studies,¹³ and highlight the heterogeneity of these lesions despite the

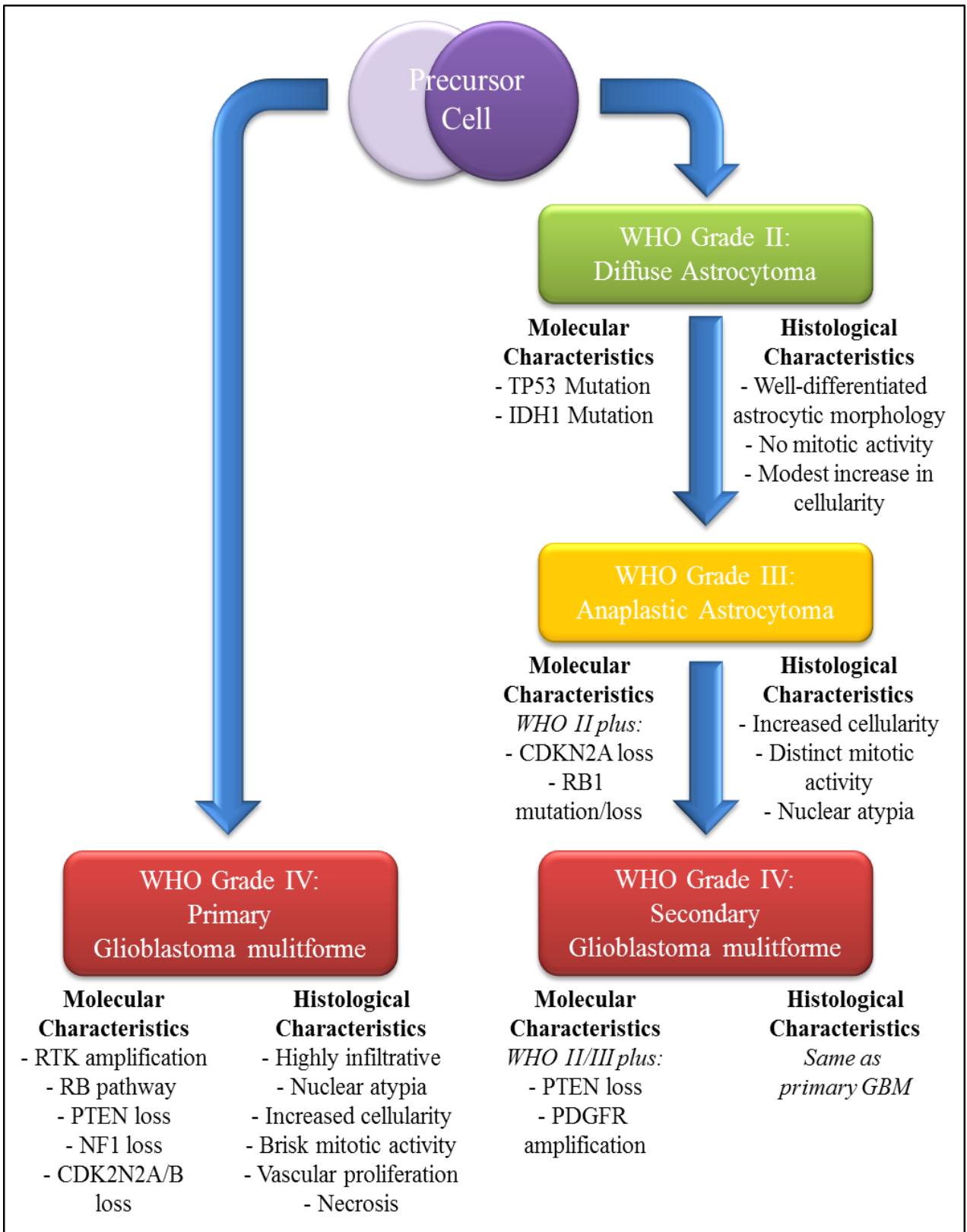


Figure 1.1: *Overall characteristics of malignant gliomas.* Primary and secondary glioblastoma multiforme (**GBM**) arise from precursor cells of unknown origin that may or may not be common to each arm of the disease. Secondary GBMs arise from lower grade gliomas while primary GBMs arise *de novo*. The most dramatic difference between primary and secondary gliomas is the mutation of IDH1 and mutation/loss of TP53 in secondary gliomas. This figure has been modified from ref. 8 and 9.

characterized through the expression of neuronal genes. Similar groupings have been made in other studies,¹³ and highlight the heterogeneity of these lesions despite the uniform, morphological-based diagnosis of GBM. Current work aims at associating these subtypes with treatment regimens targeting the genetic defects and pathway dysfunction displayed by these subtypes; however, this will inevitably be complicated by the heterogeneity of these tumours *in situ*, which have been shown to display several subtypes within a single patient.^{14,15}

The fundamental understanding of the key pathways driving gliomagenesis, and how these GBMs can differ between patients (and even differ within themselves), will allow future studies/trials to devise therapeutic strategies to target key compartments and exploit potential weaknesses. However, as with many cancers, the complexity of the tumour itself goes beyond just the genetics and includes interactions with other cell types in the tumour microenvironment.

1.2. The glioma microenvironment

The malignant glioma *in situ* has numerous interactions with its environment, many of which are involved in manipulating its ‘host’ to sustain its growth and evade its detection. For example, high-grade gliomas are highly vascular,^{16,17} and use various

methods to divert and create a blood-supply, a process termed neovascularization. The mechanisms of neovascularization are complex and poorly understood, but what is pertinent here is the appreciation of the complexity by which the GBM can sustain its growth. From simply migrating to pre-existing vasculature (co-option), to inducing the formation of new vessels (angiogenesis and vascularization), to becoming its own vasculature (vascular-mimicry and glioblastoma-endothelial transdifferentiation), the GBM microenvironment coordinates signals and manipulates the stroma to fit its needs.¹⁶

1.2.1. Glioma immunosuppression

Another key component in the glioma microenvironment is the recruitment of significant numbers and types of immunocytes. The glioma inflammatory environment is an interesting predicament; it has been shown that human gliomas have a number of different immunocytes that infiltrate the tumour,¹⁸⁻²² suggesting that an anti-glioma immune response may be occurring. Indeed, it has been suggested that gliomas are potentially immunogenic tumours with a number of identified glioma antigens.^{23,24} However, despite the presence of these immunocytes an effective anti-tumour immune response seems to be largely impaired on account of a number of glioma-derived immunosuppressing factors. (**Figure 1.2**).

The glioma is a highly immunosuppressed environment, with numerous pathways in which it can suppress anti-tumour immune responses. This is a process known as immune escape, and has recently been added as one of the 'Hallmarks of Cancer' in the revised edition published by Hanahan and Weinberg.²⁵ At its most basic level, gliomas can facilitate immune escape through the modulation of immunostimulatory receptors. Gliomas modulate their Major-Histocompatibility Complex (**MHC**) receptors, down-

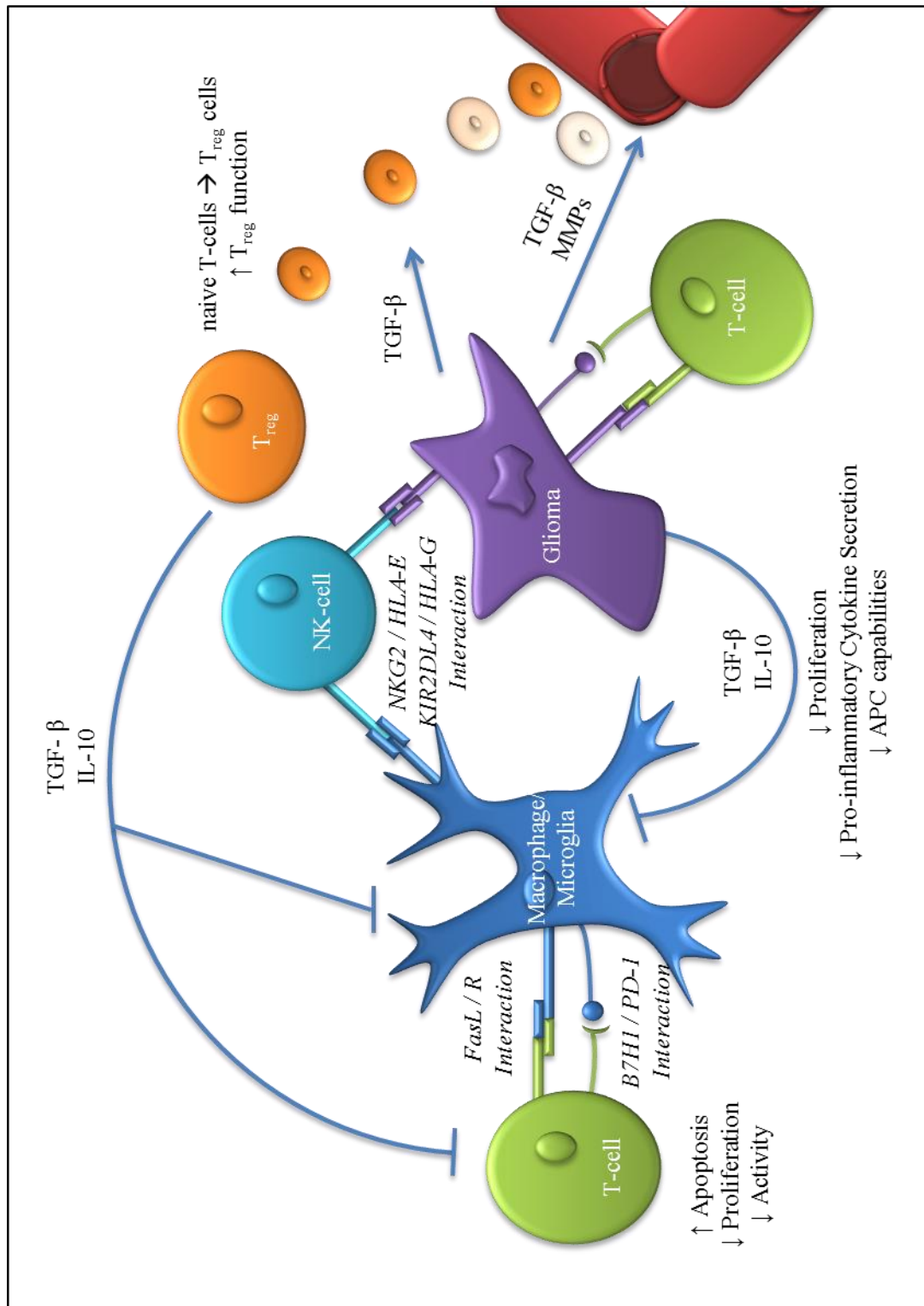


Figure 1.2: *Immunosuppression in the glioma microenvironment.* TGFβ and IL10 have numerous effects on several immunocytes in the microenvironment and can be derived from the glioma or T_{reg} cells. Cell-cell immunosuppressive interactions by the tumour or infiltrating microglia/monocytes/macrophages can suppress killer cell responses. Adapted from Zemp et al., 2010.

regulating immunostimulatory classical MHC-I receptors (HLA-A, -B, -C)²⁶ and up-regulating immunosuppressive non-classical MHC-I receptors HLA-G^{27,28} and HLA-E.²⁹⁻
³¹ This regulation functions to inhibit antigen-specific T cell responses to the tumour (loss of classical MHC-I) while off-setting potential cytotoxic killer cell responses to the loss of classical MHC-I expression (up-regulation of HLA-G and HLA-E). Further, gliomas can express the Fas Ligand (**FasL**) which can induce apoptosis in anti-tumour cytotoxic T-cells and NK cells that express the Fas receptor.^{32,33} Similarly, gliomas express the T-cell co-stimulatory molecule B7-H1, which interacts with the receptor PD-1 on activated lymphocytes to inhibit their function.^{34,35}

Gliomas also secrete potent immunosuppressive molecules such as TGF- β , IL-10, and prostaglandin E2.³⁶⁻³⁸ The most prominent of these molecules is TGF- β , which plays multiple major roles in glioma biology in addition to immunosuppression such as sustaining proliferation, migration, angiogenesis, treatment resistance, and maintaining glioma tumor initiating cell tumorigenicity.³⁸⁻⁴¹ Collectively, these immunosuppressive molecules function to decrease the activity, proliferation, and pro-inflammatory cytokine secretion of anti-tumour immunocytes.³⁶⁻³⁸ TGF- β also attracts and induces the differentiation of regulatory T-cells (CD4⁺CD25⁺FOXP3⁺, **T_{reg}**), which have numerous immunosuppressive effects (**Figure 1.2**).⁴²⁻⁴⁴

Infiltrating microglia and glioma-infiltrating monocytes/macrophages also function in mediating immunosuppression. This will be discussed in a subsequent section as these immunocytes heavily infiltrate the glioma microenvironment and play multiple roles in gliomagenesis.

1.2.2. Microglia and peripheral monocyte/macrophages in the glioma microenvironment

Brain-resident microglia and infiltrating peripheral monocytes/macrophages (glioma-infiltrating monocytes/macrophages; **GIMs**) are widely described in glioma patients,¹⁸⁻²² and may make up one-third of the tumour mass.⁴⁵ Since microglia are a specialized brain-resident immunocyte, a discussion about ‘normal’ microglia follows.

1.2.2.1. Microglia ontogeny and normal function

Microglia are colloquially referred to as ‘macrophages’ of the central nervous system (CNS). Indeed, many major organs in the body are populated by their own resident macrophages; Kupffer cells of the liver, osteoclasts of the bone, alveolar macrophages of the lung, and so on, each specialized to function in those tissues. However, whether or not microglia are in fact macrophages is still a matter of contention, one that is partially rooted in a debate over their ontogeny.

The origin of microglia in the CNS has been hotly contested for decades; however, recent studies have solidified the evidence to suggest that microglia are of mesodermal lineage, specifically of myeloid origin.⁴⁶⁻⁴⁸ The current paradigm holds that myeloid-derived microglia progenitors migrate to the CNS early in foetal development and divide to populate the CNS in the second trimester of humans and E10-19 in rodents.⁴⁶⁻⁴⁸ It is these cells that constitute the original long-lived microglial population seen in the developing animal and into adulthood. These developmental-derived microglia uniformly populate the entire CNS, making up ~10% of the total adult brain cell population.^{47,48} The turnover of these cells in steady-state conditions is thought to mainly involve microglia self-renewal, as well as a small percentage that are recruited and differentiated from

blood-derived progenitors.^{48,49} Given the ontogeny of microglia, the fact that they express some traditional markers of members of the mononuclear phagocyte system (F4/80, CR3(CD11b) and FcγRII/III^{46,48,50}), and some of their immune effector functions (to be discussed below), strongly suggest that microglia are a CNS-resident macrophage.

Microglia have been described as the brain's 'sensor of pathology',⁵¹ and are known to be involved in all known CNS disease states. This is not to say that steady-state microglia are dormant, although these type of microglia are referred to as 'resting'. Resting microglia are highly ramified, extending multiple processes into their microenvironment. These processes actively probe their surroundings,⁵² sampling interstitial fluid, resident cell populations such as astrocytes and neurons, and possibly even detecting the functional state of neuronal synapses.⁵³ Remarkably, it has been calculated that microglia survey the entire CNS for damage or infection in this manner every several hours,⁵² proving to be true, highly active, sentinels of the CNS.

In contrast to other tissue-specific macrophages, resting microglia are kept in a 'immunoquiescent' state, with down-regulated MHC, cytokine-secretory, and reactive oxygen/nitrogen species production. This is thought to occur through the ambient levels of immunosuppressive cytokines in the CNS, such as TGF-β and prostaglandin-E2 (PGE2), and cell-cell interactions within the CNS, such as neural CD200 and microglial CD200R.^{50,54} Indeed, the very nature of the CNS and the functions it performs demands that these cells keep their potential cytotoxicity in check.

Microglia have evolved to mediate pathological states to which the CNS is most commonly exposed, namely removing dead/dying/infected cells. The CNS is a highly

pro-apoptotic environment, where steady-state neurons and glial cells exist in a fine balance between life and death. Damaged or infected neurons and glia up-regulate pro-apoptotic factors, including TNFR and FASR,⁵⁵ in response to damage or infection, triggering extrinsic apoptotic pathways mediated by ligands expressed on or secreted by microglia.⁵⁰ The onset of apoptosis results in the recognition of cell surface apoptotic cell-associated molecular patterns such as lipid phosphatidylserine, that are recognized by microglial cells triggering their phagocytic engulfment. It is critical that apoptotic cells are removed quickly from the CNS, as late stage apoptotic cells can spill their neurotoxic contents.^{50,55}

The ability of microglia to phagocytose apoptotic cells is a consequence of their activation. Microglia are activated by a number of different stimuli, such as ‘danger’ or ‘stranger’ signals that are specific to the type of pathological state in the brain. ‘Danger’ signals can include extracellular purines, most notably ATP, that are released by damaged neurons and recognised by metabotropic receptors (P2X and P2Y family members) on microglia.⁵⁶ Serum proteins, which are normally excluded from the brain by the blood-brain barrier, also function as danger signals, and are a sign of blood-brain-barrier-breach.⁵⁰ ‘Stranger’ signals are often associated with pathogen-associated molecular patterns (**PAMPs**) which are recognized by pathogen-recognition receptors (**PRRs**) on microglia. As the name implies, PAMPs are pathogen-derived molecules recognized as foreign by the innate immune system. PRRs expressed by microglia include Toll-like receptors (**TLRs**; TLR1 through 9 are expressed in mouse and human systems^{46,57}) retinoic acid-inducible gene I (RIG-I)-like helicases (RIG-I and MDA5),⁵⁸ nucleotide-binding domain, leucine-rich repeat containing (NOD-like) receptors,⁵⁹ and scavenger

receptors.⁶⁰ Many of these receptors are further up-regulated upon activation. In addition to the microbial PAMPs that these receptors recognise, many of them, especially TLRs and scavenger receptors, are capable of recognizing endogenous ligands as ‘danger’ or altered-self ‘stranger’ signals. This is especially important in the case of neuronal injury, as apoptotic cells display ligands that can both activate microglia and then signal their phagocytosis. Resting microglia can also be activated by proinflammatory cytokines secreted by other glia or neurons, including GM-CSF, TNF α , IFN β and IFN γ .^{46,50,54}

Activation of these cells through pathogen or damage-associated molecules results in an activated phenotype with increased proliferation, motility, phagocytic activity, and cytokine/growth factor secretion. Activation of microglia is a continuum, with ‘resting/ramified’ microglia possessing small bodies and long, thin tendril-like processes, intermediate states that include the shortening and bulking of the processes and cell body, and full activation results in an amoeboid phenotype that is morphologically and immunohistochemically indistinguishable from recruited peripheral monocytes.^{46,50} These fully activated microglia are licensed to phagocytise, proliferate and migrate. This activation can lead to a positive-feedback such that activated microglia will release an array of cytokines and chemokines, activating and recruiting additional microglia, a process defined as microgliosis. Additionally, chemokines, cytokines and other enzymes released upon activation can potentially function to weaken the blood-brain barrier and attract additional innate and adaptive immunocytes from the periphery. Concordantly, microglia activation results in a dramatic increase in MHC I and II expression and co-stimulatory molecules CD80, CD86 and CD40; however, the ability of microglia to act as efficient antigen-presenting cells is grossly contested in the literature.^{46,50,54,61}

Investigation into the function of microglia often looks at the proinflammatory aspects of these cells, but microglia can also promote tissue repair. In models of neuronal injury, there are two phases to microglial activation, acute and chronic.⁶² Acute activation is highly proinflammatory with secretion of TNF α , IL-1 β , IL-6 and reactive oxygen/nitrogen species. It is this immediate acute activation state that is thought to exacerbate the injury response. However, microglia at injured sites may undergo what is known as a chronic activation state, with down-regulated proinflammatory secretions, an increase in secretion of immunosuppressive IL-10 and PGE2, and the secretion of growth factors. This activation state is associated with neuroregeneration and healing. These chronically activated microglial state will be discussed more in the subsequent section, as these are the same phenotype as those which infiltrate gliomas. However, looking at how the brain keeps these cells in check, and how chronically activated microglia act, it must already be apparent how a glioma can manipulate and hijack these systems.

1.2.2.2. Glioma-associated microglia and macrophages: Clinical analysis

As mentioned, it is not possible to distinguish by microscopic appearance or histology activated amoeboid microglia from recruited peripheral monocytes that differentiate into macrophage-like cells in the CNS. Some of the earliest studies to look at infiltration of these cells in glioma used a combination of histological and morphological techniques to identify these cells collectively. One of the earliest study to quantify microglial/GIM infiltration in human gliomas was by Morantz et al (1979), where they found >40% of cells within GBMs were of a macrophage phenotype.⁶³ They quantified this through a primitive tumour cell suspension that included an antibody labelling to Fc and C3 receptors. One of the earliest studies to use macrophage specific antibodies

[CD68(EBM/11)] in human gliomas found that “EBM/11 reactive cells were ubiquitous and quite numerous in gliomas.”⁶⁴ And finally, investigation into this macrophage infiltrate in low- and high-grade gliomas using FMC33(unknown antigen; reported to be macrophage specific) and CD11b(OKM1) antibodies found that high-grade gliomas were significantly more infiltrated than low-grade-gliomas (25.87 vs 36.46% of tumor cells).¹⁹ Further studies have shown that the highly activated, amoeboid phenotype increases with glioma grade.^{50,65,66}

It is possible to distinguish microglia from GIMs through flow cytometric analysis using a combination of the common leukocyte antigen (CD45) and other macrophage markers (ie, MAC1 (CD11b), F4/80). Microglia have low-intermediate CD45 expression and a macrophage marker (ie, CD45^{low-intermediate}CD11b⁺), whilst peripherally recruited GIMs have high levels of CD45 and a macrophage marker (ie, CD45^{high}CD11b⁺).^{46,67} Parney et al., 2009, used these markers assessing microglia and macrophages from 9 patient tumours, finding that microglia and macrophages could infiltrate the tumour, contributing up to 4 and 15% of the total cells isolated from surgical resection, respectively.²² Another study looking at 6 patients with high-grade glioma found that 1% of the total cells were CD45⁺CD11b⁺;²¹ however, personally judging by the scatter plots presented in the paper these results are questionable.

Finally, changes in infiltrates in the glioma microenvironment can be assayed utilizing gene expression arrays. For example, the TCGA data was utilized to associate levels of necrosis in GBMs, finding that a necrotic signature was strongly associated with the mesenchymal GBM subtype.^{12,68} Interestingly, GIM accumulation is often found in areas associated with the high levels of necrosis and hypoxia, which was already noted in

the earliest of studies.⁶⁴ Indeed, another recent study has demonstrated that inflammatory infiltrate, including microglial and macrophage expression signatures, cluster into the mesenchymal GBM subtype.⁶⁹ The question then arises, are tumour associated microglia and GIMs merely a consequence of scavenging necrotic tissue or do they have larger pro- or anti-glioma functions?

1.2.2.3. Glioma-associated microglia and macrophages: Functions

Given the morphological and histological indistinguishability between activated amoeboid microglial and GIMs, it could be postulated that their functions within the glioma may be overlapping. However, it would not be surprising to find discrete functions for these similar yet inherently different cell types. This next section discusses some of the interactions between gliomas, microglia and GIMs, and an attempt will be made to try and distinguish which cell type was examined.

Given the proapoptotic and phagocytotic abilities of microglia and macrophages, it could be hypothesized that they function in anti-tumour immunity. However, microglia and GIMs isolated from glioma patients are shown to be ‘immunoinert’, not expressing proinflammatory cytokines, and with suppressed MHC and co-stimulatory molecules.^{21,22} However, these cells may be playing an alternative role in the microenvironment, acting as tumour-associated macrophages (**TAMs**) described in other cancers⁷⁰ or chronically activated microglia. These TAMs are thought to be very similar to M2, ‘alternatively’ activated macrophages. Peripheral macrophages can be divided into, at the simplest level, M1 and M2 macrophages. M1 macrophages are associated with pro-inflammatory responses and M2 macrophages with inflammation resolution and wound healing.^{70,71} Microglia as well have been proposed to have these characterizations,^{72,73} albeit are not

synonymous with M2 macrophages.⁷⁴ Both M2 macrophages and/or M2 microglia can be induced by IL-4, IL-10 and IL-13, TGF- β , and PGE-2, and are characterized by increased expression of IL-10, IL-1 α , Arginase-1 and scavenger receptors.^{70,75-77} Normal M2 macrophages are involved in tissue-remodelling, immunosuppression and pro-angiogenic processes, correlating to the ‘healing’ after inflammatory insult.^{70,75} It is easy to see how the M2 phenotype of macrophage or microglia can be co-opted as a tumour-promoting agent. Below are some examples from the literature of specific glioma-associated microglial and GIM functions.

M2 phenotypes function in immunosuppression and down-regulating inflammatory responses to promote tissue remodelling and healing. Indeed, the main immunosuppressive molecules secreted by gliomas, TGF- β , IL-10 and PGE-2 (**Chapter 1.2.1; Figure 1.2**), are known M2 inducing factors. Microglia are also known to be a prominent source of IL-10,⁷⁸ and PGE-2.⁷⁹ Interestingly, IL-10 is an activator of STAT3 signalling, a known ‘oncopathway’ in glioma, mediating cellular survival, proliferation, self-renewal, and invasion.⁸⁰ STAT3-signalling is also a signature of the mesenchymal GBM subtype.⁹ Interestingly, STAT3 inhibitors have shown to reverse the immunosuppression of microglial and GIMs in murine models, reactivating the antitumour potential of these cells.^{81,82} Further immunosuppressive actions of microglia/GIMs include the expression of receptors HLA-E, HLA-G,⁸³ and B7-H1,^{84,85} as well as the FasL.⁸⁶ (**Figure 1.2**) Indeed, the immunosuppressive nature of these infiltrating immunocytes mirrors what is already reported to be done by the glioma itself.

Microglia and GIMs are also known to perpetuate glioma progression through increasing glioma invasiveness and driving proliferation. Secretion of metalloproteases

(MMPs) by these cells function to degrade the extra-cellular matrix (ECM), allowing for glioma invasion and release of ECM-bound growth factors. MMP levels in glioma, especially MMP2 and MMP9, are correlated with the level of glioma invasiveness in patients.⁸⁷ An innovative experiment using *ex vivo* cultured brain slices demonstrated that glioma invasion was mediated by glioma-secreted MMP2 that was somehow activated by microglia.⁸⁸ Depletion of microglia using clodronate liposomes resulted in limited glioma invasion and restoration of microglia re-promoted invasion.⁸⁸ A follow-up study demonstrated that gliomas secrete MMP2 as a pro-enzyme, which is cleaved and made functional by microglial expressed MT1-MMP.⁸⁹ Induced MMP-9 expression from gliomas has recently been shown to be through microglial/GIM secretion of TGF- β .⁹⁰ In addition to MMP secretion and activation, microglia can also drive cellular proliferation, survival and angiogenesis of gliomas through the secretion of growth factors such as EGF, VEGF, BDNF and SCF.^{91,92} A summary of these processes can be seen in **Figure 1.3**.

Given the cancer stem cell hypothesis may apply to gliomas (see section 1.3.3), we can speculate on the roles microglia may play mediating the differentiation and/or pluripotency of these populations, as they have with normal neural stem cells.^{62,93,94} And finally, M2 microglia and macrophages are also known to help induce angiogenesis.⁹⁵ Collectively, these glioma associated microglia and GIMs seem to play diverse roles in stimulating many aspects of gliomagenesis.

However, given the plasticity of both microglia and monocytes/macrophages, perhaps these infiltrating cells can be used to suppress gliomas? Indeed, several studies have shown that microglia and macrophages kill glioma cells *ex vivo* through either induction

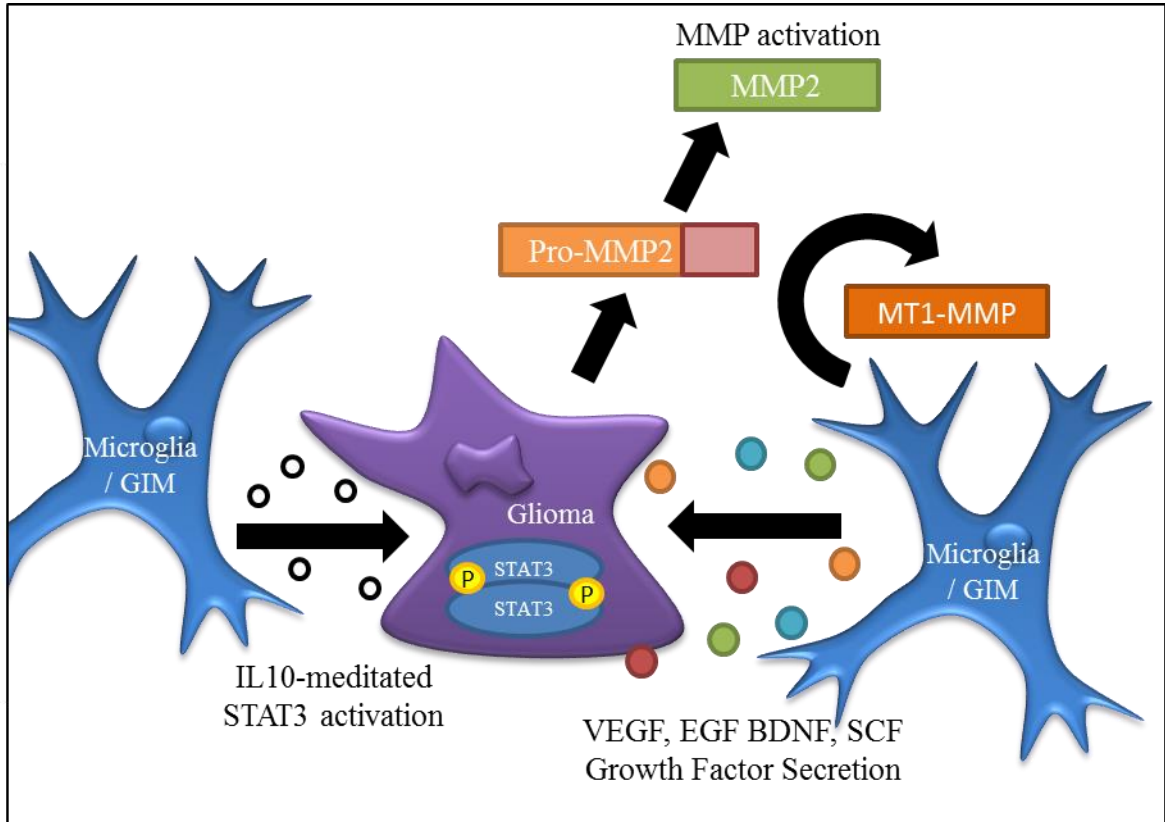


Figure 1.3: How microglia and glioma infiltrating monocytes/macrophages can enhance glioma tumourogenesis. Description in text.

of apoptosis^{96,97} or autophagy.⁹⁸ Unfortunately, both these studies used primary ‘normal’ microglia cultures activated by either LPS or IFN γ . These naïve microglia have not been effected by the glioma microenvironment so perhaps these results are misleading. Interestingly, a very recent study has shown that brain-tumour derived microglia display an M2 phenotype, and can induce the proliferation and migration of glioma stem cells; however, these microglia could be switched to an M1 microglial phenotype through application of the RIG-I/TLR3 agonist polyI:C.⁹⁹ These microglia no longer simulated invasion and migration, but instead induced the death and phagocytosis of the glioma cells. This is very similar to a project in Dr. Yong’s laboratory that showed the immunosuppressed nature of tumour-derived microglia compared to non-pathogenic

microglia. Here normal microglia were able to induce the differentiation of human glioblastoma brain-tumour initiating cells, yet tumour-derived microglia could not. However, upon stimulation with a putative TLR agonist, this phenotype was reversed (unpublished data). Collectively, these experiments suggest that the glioma-associated microglia and GIMs can be switched from pro- to anti-tumour functions.

The above only covers some of the topics in the glioma microenvironment that are pertinent to the experiments done in this thesis, with additional interactions between gliomas and astrocytes,^{91,100} and normal neural stem cells,^{101,102} among others cell types¹⁰³ having been described. Additionally, as with many cancers, the glioma microenvironment can be very necrotic and hypoxic. Unfortunately, space limitations do not permit the discussion of all these cell types; however, suffice to state that the glioma microenvironment is complex and multi-faceted.

1.3. Animal models of gliomas for the preclinical evaluation of therapeutics

Although the genetic and molecular interactions within glioma cells can be modelled in a culture dish, the glioma microenvironment is complex with many extra-glioma interactions playing important roles in the etiology and treatment of the disease. The presence of growth factors, chemokines, cytokines, and extracellular matrix proteins that are not glioma-derived are excluded in *in vitro* culture studies. These interactions could potentially have profound effects on treatment outcome through activating redundant pathways, activating treatment resistance pathways and/or mediating treatment delivery to the tumour. We believe that modelling these interactions in animal models is most appropriate for the interrogation of gliomagenesis and evaluating therapeutic interventions.

Establishing models of cancer in animals is a contested subject, as there are a number of important considerations: What is the correct animal species? Which type of graft to use? Where should the graft be grown? Should we even use a graft at all? Indeed, the use of inappropriate preclinical models for testing cancer therapeutics is thought to be one of the main reasons for the repeated failure of Phase II and III cancer clinical trials.¹⁰⁴

1.3.1. *Types of preclinical glioma models: Grafts*

Grafting tumours into animal models has been the mainstay of glioma preclinical testing. This involves the surgical transplantation of cell lines grown in culture into animals. The species of cell line used and the placement of the graft within the animal dictate what types of microenvironmental interactions will occur.

A xenograft uses human glioma cell lines in animal models. This requires immunodeficient animals as human grafts in immunocompetent mice could provoke anti-graft immune responses which could cause the rejection of the graft or confound experimental results. It is important to determine which type of immunocompromised animal to use, as the commonly used mouse strains for xenografts all display specific immunodeficiencies. For example, Nude mice have a mutation in *Foxn1*, leading to the absence of thymic epithelial cells and thus no T cell development.¹⁰⁵ Severe combined immunodeficient (SCID) mice have a mutation in *protein kinase, DNA activated, catalytic polypeptide* (SCID^{Prkdc}) which results in defects in non-homologous end joining of DNA double strand breaks as well V(D)J recombination,¹⁰⁶ leaving these mice devoid of B and T cell populations. Crossing SCID^{Prkdc} mice onto a strain of mice called non-obese diabetic (NOD), produces the NOD-SCID mouse which has no B or T cell populations, very limited numbers of NK cells, no serum complement, and limitations in

macrophage maturation.¹⁰⁷ These are the three most commonly used immunodeficient mice in cancer research, yet their potential cellular interactions with the tumour microenvironment are dramatically different. It is easy to envision similar experiments utilizing different immunocompromised mouse models giving dissimilar results.

Xenografts can be heterotopic or orthotopic. Heterotopic xenografts are mainly subcutaneous grafts established in the flank of an immunocompromised mouse. The relevance of such grafts in glioma models is questionable, as the CNS is such a specialized environment. In contrast, orthotopic grafts are placed in the same environment from which the tumour was derived; i.e., glioma orthoxenografts are grown in the brain, breast cancer orthoxenografts are grown in the mammary fat pad. This is especially important when studying diseases such as gliomas, as the CNS microenvironment is very different from the rest of the mouse, having specialized cell types (astrocytes, microglia) and ECM components.¹⁰⁸ Preserving potential interactions between the tumour and these CNS specific components is important to the accuracy of modelling gliomas.

Orthoxenografts, however, do have inherent problems. The necessity of an immunocompromised mouse removes, at the least, interactions with T cell populations. T_{regs} were briefly discussed earlier in this chapter as an important part of glioma immunosuppression, while other T cell populations are critical to many glioma immunotherapies making xenografts inappropriate for these types of studies.¹⁰⁹ In addition to missing cell interactions, many chemokines and cytokines have species-specific interactions, such as Type-I¹¹⁰⁻¹¹² and Type-II¹¹³ interferons, GM-CSF,¹¹⁴ and members of the TNF α family.¹¹⁵ As such, these factors produced in the murine glioma

microenvironment may have no effect on the human tumour. Finally, orthoxenografts derived from conventional glioma cell lines that have been passaged for many generations in serum no longer display some of the defining characteristics of GBMs in patients, lacking single cell infiltration, tumour heterogeneity, necrosis, and robust angiogenesis (this is described in detail in Chapter 1.3.3).

An alternative to the orthoxenograft is a syngeneic orthograft, essentially implanting a mouse glioma in the brain of a mouse or a rat glioma in the brain of a rat. These syngeneic murine or racine glioma cell lines are harvested from animals bearing spontaneous gliomas. The two most common lines are the GL261 and CT2A models, which were chemically induced gliomas in C57Bl/6 mice that have been retained through tissue culture. A lesser known syngeneic glioma model in B6D2F₁ mice is the 4C8 line, which was originally derived from transgenic mice expressing the *c-neu* oncogene driven by the myelin-basic protein promoter.¹¹⁶ Syngeneic orthografts obviously retain any species-specific interactions, but also are capable of being implanted into fully-immunocompetent animals. These syngeneic glioma models are essential to any preclinical studies where an intact immune system is needed, such as active immunotherapies.¹⁰⁹ However, I would argue that the complex, multi-faceted, and immune-infiltrated nature of the glioma microenvironment, which can only be fully represented in syngeneic orthotopic models, should be part of the standard for preclinical modelling in treatment-related studies.

The major limitation to these models is that they are NOT human tumours, meaning they may not retain signalling cascades and specific-drug interactions that would be found in the clinic. Further, these syngeneic glioma lines suffer from the same

consequences as passaging human cell lines in serum cultures, mainly the selection of homogenous cell populations that no longer represent the original tumours from which they were derived.

1.3.2. Types of preclinical glioma models: Spontaneous glioma models

Spontaneously arising gliomas in animal models are the *de novo* creation of a tumour in the CNS which starts with the mutations in a single or small number of cells that subsequently transform into a growing glioma. Presumably these models undergo all the necessary aspects of gliomagenesis, from immune escape to neovascularization, making these models very relevant in the study of human gliomas. These models have become very important to the study of glioma biology and therapeutic testing, as these models often best recapitulate the histopathology and etiology of the disease.¹⁰⁴

There are a number of ways to induce gliomas in the brain of an animal; chemical induction, viral administration, the genetic overexpression of oncogenes, or the knockout of tumour-suppressors. Thanks to broad scale, concerted genomics efforts, we have a deeper understanding for the core pathways and key genes that are altered in gliomas, and the development of animal models for these diseases is greatly increasing in number whilst also increasing in relevancy. Targeted genetic approaches have largely made the chemical induction of spontaneous brain tumours an obsolete technique, as the random mutations driving these gliomas are often not as relevant to the human disease. For example, GL261, the most commonly used syngeneic cell line in the C57Bl/6 mouse (178 pubmed hits vs. 19 for the CT2A line), is driven off a point-mutation in K-RAS.¹¹⁷ Although the RAS pathway is aberrantly regulated in the majority of human GBMs, only 2% of patients have a mutated RAS.¹¹ Interestingly, many of the commonly used

syngeneic glioma lines in rats (C6, 9L, T9, RG2, F98¹¹⁸) and mice (GL261¹¹⁹, CT2A¹²⁰) are derived from chemically induced gliomas. Further, they were all derived between 25-40 years ago, indicating their extensive passage in culture.

Viral-induced gliomagenesis is an interesting and efficient way of inducing gliomagenesis in animal models. The best known is the RCAS-Tva system, which uses a strain of avian retrovirus, Rous sarcoma virus (RSV), to transduce genes of interest into mouse cells bearing the viral receptor Tva.¹²¹ Genetically engineered mice that express the Tva gene under the control of tissue specific promoters direct viral infection and stable transgene expression to these tissues. In glioma studies, Tva has been expressed under the *GFAP* promoter (astrocytes and astrocytic precursors)^{122,123}, *NESTIN* promoter (neural stem cells)^{122,124}, and the *CNP* promoter (oligodendrocyte precursor promoter)¹²⁵ to induce the expression of various transgenes including PDGF- β ,^{122,125} EGFRvIII,¹²³ K-RAS,¹²⁶ and activated AKT,¹²⁶ among others. The insertion of these genes, and/or combination of genes, resulted in the formation of gliomas in mice of varying grades and histological features. Further, crossing the Tva mice to different null or heterozygous backgrounds can add to the genetic alterations possible through this system. This is an excellent system to introduce specific oncogenes and markers in a predictable and cell-type-specific manner.

Genetically engineered models using tissue specific or whole-organism knockouts have also been used to develop spontaneous gliomas in mice. The first genetic model to target glioma tumour-suppressors in using knockout mice was the *Nf1*^{+/-}/*Trp53*^{+/-} heterozygous mice.¹²⁷ *Nf1* and *Trp53* genes are located within 7 cM, and the mutant mice generated were selected to have the mutations on the same chromosome such that these

mutations were linked. These mice are termed NPcis mice (a major reagent utilized in this thesis), and developed varying grades of glioma with high penetrance that depended on mouse strain, gender, and gender of the parent carrying NPcis locus.¹²⁷⁻¹³¹ Throughout this thesis, I refer to this model as NPcis mice that are on the C57Bl/6 background.

NPcis mice have an average lifespan of 7-8 months, with astrocytoma's developing with ~40-70% penetrance (depending if the male or female parent was carrying the NPcis locus).^{127,128} However, mice that lived longer than 6 months (ie, did not succumb to shorter latency tumours), had a 92% penetrance of brain lesion.¹²⁷ Given the promiscuousness of P53 deregulation in cancer (lost or mutated in nearly 50% all human cancers¹³²), it is not surprising that NPcis mice develop other tumour types, most notably soft-tissue sarcomas, histiocytic sarcomas, pheochromocytomas, and lymphomas.¹²⁸ It has been speculated that if mice did not succumb to these shorter-latency tumours, that 100% of these mice would develop high-grade astrocytomas.¹²⁷

The grade of these tumours also is related to the gender of the NPcis offspring, with female mice developing astrocytomas less frequently but of an overall higher grade.^{130,131} This is interesting, as males are more prone to developing gliomas in the human population (WHO Gr. III, 1.31:1 male:female, WHO Gr. IV, 1.26:1 male:female).⁸ The greater chance of progression to grade IV GBMs in the NPcis female mice is thought to be a consequence of these mice living longer on average than males, with an increased time for the tumour to progress.^{130,131} Averaged between the sexes, these tumours appeared as 40% low-grade (WHO Grade II), with high-grade gliomas occurring at 50% WHO Grade III and 10% WHO Grade IV.

In the NPcis model, tumorigenesis occurs as the mice age and lose the wildtype copy of *Trp53* and *Nf1*, two of the most commonly lost or mutated genes in human glioma.¹¹ Given the observation that both low grade and high grade tumours can arise in this model and that one of the initial hits to tumorigenesis is loss of *Trp53*, it is suggested that these represent secondary GBM models.^{127,133}

Unfortunately, this model does have a low penetrance of grade IV GBMs. Another limitation of these mice, since it is a global *Nf1*^{+/-}/*Trp53*^{+/-}, loss of a single copy of one of these genes can result in effects on other cells in the mouse. For example, it has been shown that global *Nf1*^{+/-} mice will develop optical gliomas by ~3 months of age, but a targeted astrocyte *Nf1* deletion will not result in any gliomagenesis.^{134,135} Interestingly, it was found that activated *Nf1*^{+/-} microglia in the tumour microenvironment specifically enhances the growth of *Nf1*^{-/-} astrocytes, demonstrating the importance of the microenvironment¹³⁶ and raising some interesting questions about these models and the role of NF1 loss in gliomas.

In order to more specifically ablate these highly relevant glioma tumour-suppressors, different combinations of floxed *Nf1* and germ-line *Trp53* mutations have been used with a GFAP-Cre mouse to target *Nf1* loss to astrocytes.¹³⁷ This study demonstrated that when *Nf1* loss preceded *Trp53* loss (*Nf1*^{fl/fl}/*Trp53*^{+/-} mice), only 1/18 mice developed astrocytoma's. Conversely, *Nf1*^{+fl}/*Trp53*^{-/-} mice or *Nf1*^{+fl}/*Trp53*^{+/-} developed astrocytoma with 100% penetrance, strongly suggesting that *Trp53* loss must precede *Nf1* loss in this model of astrocytoma. Further, in the *Nf1*^{+fl}/*Trp53*^{+/-} model, 70% of the astrocytomas were deemed WHO Grade IV GBMs at time of death (~27.5 weeks, 6.4 months). The discrepancy in tumour progression between this model *Nf1*^{+fl}/*Trp53*^{+/-} and

Nf1^{+/-}/*Trp53*^{+/-} is an interesting phenomena which does not seem to be addressed in the literature. It could be attributed to strain effects or pathologist biases, but it also could suggest that in high-grade astrocytoma models, global *Nf1* heterozygosity is preventing the progression of these tumours. Although this model does increase the penetrance to Grade IV GBMs, given the array of grades found, this model is also a representative of secondary gliomas.

The above study also found that mice harbouring GBMs had activated AKT signalling, which is associated with PTEN loss in human GBMs. Further work has investigated the addition of *Pten*^{+/fl} on the *Nf1*^{+/fl}/*Trp53*^{+/fl} mice. This addition drastically reduced survival, with all mice dying of astrocytomas, of which ~90% were WHO Grade IV-equivalent GBMs.¹³⁸ The rate at which these gliomas occurred suggest that PTEN loss in human patients is a contributing factor to the progression of secondary GBMs or perhaps an initiating event in primary GBMs.

Many other transgenic mouse models have been described, including astrocytic overexpression of activated RAS,¹³⁹ astrocytic overexpression of *PDGFA* in a *Trp53*^{-/-} background,¹⁴⁰ and mature astrocytic loss of *Trp53*, *Pten* and *Rb1*,¹⁴¹ among others. The discussed models cover some of the aspects that are looked at when building genetically induced mouse models, and lays out an interesting progression of ideas stemming for the original observation of *Nf1* and *Trp53* loss-of-heterozygosity induced astrocytomas in mice. The recent advances in our understanding of glioma genetics coupled with the progressing simplicity of mouse transgenics, will undoubtedly bring numerous more models into the literature.

1.3.3. *Types of preclinical glioma models: Brain tumour-initiating cells*

The glioma-cell of origin has been a hotly contested, the major candidates are the multipotent adult neural stem cells (**NSCs**) or from committed or partially committed cells from the astrocytic or oligodendrocytic lineage.¹⁴² Studies using spontaneous gliomas in mice have provided mixed results. For example, studies using the *Trp53/Nf1* model have suggested that NSC are the glioma cell of origin,^{137,138,143} while others suggest that in a similar model driven by the same tumour suppressors has an oligodendrocyte precursor cell of origin.¹⁴⁴ The details of these studies, and many others, will not be discussed here, and clearly more work must be done to answer these questions and translate them back into the clinic. It will suffice to say the ‘cancer-stem cell hypothesis’ has found its way into the glioma world.

The cancer stem cell hypothesis suggests that tumorigenesis is driven by a set of rare, slowly cycling cells with the capacity for indefinite self-renewal and multipotency.¹⁴⁵ Tissue-specific stem cells could be prime targets of transformation as their potential for self-renewal coupled with their longevity could act as an indefinite reservoir for tumour-cell synthesis. Progress has been made towards validating this model, first in hematopoietic cancers where putative ‘cancer stem cells’ were first discovered.^{146,147} More recently, and more conservatively named, tumour initiating cells have been discovered in several solid tumours such as breast,¹⁴⁸ melanoma,¹⁴⁹ prostate,¹⁵⁰ colorectal,¹⁵¹ lung,¹⁵² as well as many others cancers. Brain tumour-initiating cells (**BTICs**) have also been described.^{153,154}

BTICs functionally defined and are primary glioma specimens cultured under neurospheres-promoting conditions, which use neurobasal media supplemented with EGF

and FGF. In contrast, traditional cell cultures use of Dulbecco's modified Eagle medium (DMEM) formulations supplemented with fetal bovine serum. These conditions have been shown to allow for the proliferation and maintenance of adult murine and human neural stem cells *in vitro*.^{155,156} Gliomas often appear as primitive, undifferentiated cells that express neural stem cell markers such as NESTIN,¹⁵⁷ SOX2,¹⁵⁸ OCT4,¹⁵⁹ BMI1.¹⁶⁰ Patient samples cultured as neurosphere retain these markers, as well as a capacity to self-renew (asymmetric cell division), and differentiate into other CNS lineages (multi-lineage differentiation).^{4,145,154,161-163}

So how does the 'Cancer Stem Cell' hypothesis (CSCH) change the way we look at gliomas? The CSCH suggests a hierarchical system, whereby there is only a (relatively) small number of tumour-initiating cells, with the bulk of the tumour being aberrantly differentiated 'tumour transit amplifying cells' with limited potential for replication, and on their own cannot form neurospheres in culture or form tumours when transplanted in mice.^{4,145} One of the first descriptions of BTICs found this, with 100 putative BTICs able to form tumours in orthotopic xenografts in mice, while 1×10^5 non-BTIC like tumour cells isolated from the same specimen could not form tumours when injected in mice.¹⁵⁴

Further, the CSCH would predict that gliomas would be heterogeneous in nature due to the aberrant differentiation of transformed transient amplifying cells in the tumour microenvironment. It would also predict that therapies that are unable to kill these BTICs *in situ* would not result in any durable responses as these BTICs could then repopulate the tumour. Both of these characteristics do fit what is seen in human gliomas. Tumour heterogeneity is a hallmark of GBMs, as suggested by its very name, (Glioblastoma

multiforme). Secondly, BTICs have been found to be chemo- and radio-resistant,¹⁶⁴⁻¹⁶⁶ suggesting they indeed may act as treatment-resistant ‘disease reservoirs.’¹⁶¹⁻¹⁶³

Unfortunately, the CSCH hypothesis BTICs is fraught with controversy, mostly revolving around semantics and cellular markers, of which I will not discuss further. What cannot be lost in this controversy is the fact that glioma specimens cultured as neurospheres better retain the characteristics of the original tumours from which they were derived. A pivotal study took freshly dissociated glioma specimens and cultured them either in the conventional manner with serum or under neurospheres conditions with EGF and FGF.¹⁶² It was found that glioma samples cultured in serum lost all the stem-like markers (NESTIN, SOX2, BMI, MSI1) and after several passages lost their heterogeneity and became a monoculture of aberrantly differentiated cells. After only 3 passages in serum, their transcriptional profile began drifting from that of the original tumour, and by 7-13 passages had similar transcriptional profiles more similar to the conventional glioma cell lines used for decades (ie, U87, U251). These lines grown in serum also had to ‘learn’ to grow, reaching a plateau of growth followed by an unlimited and exponential growth. These late passage serum cultures regained their ability to form tumours in mice, but these tumours did not phenocopy the characteristics of the patient tumour, many growing as a well demarcated ‘golf-ball’ tumours as seen with the conventional cell lines. On the contrary, these same tumours cultured under neurospheres conditions retained their stem cell markers, capacity for self-renewal and multi-lineage differentiation, and maintained a steady growth rate continuously in culture. Most importantly, the transcriptional profile of these cells grown in under stem cell culture conditions closely maintained the signature that was seen in the original patient tumour

for over 30 passages. Further, these BTICs orthotopically grafted into immunodeficient mice produced infiltrative tumours as was seen in the patient from which they were derived. This maintenance of gene expression in GBM neurospheres and a detailed histological examination of their orthoxenograft phenotype were also performed in a study of 15 GBM patients. Here it was shown that discrete characteristics of particular patients GBMs, such as a PNET or oligodendglioma components or Giant Cell GBM subtypes, were recapitulated in neurosphere orthoxenografts. Very interestingly, this study showed that copy-number alterations that appeared in the neurospheres occurred in only a subset of patient tumour cells, perhaps suggesting that neurosphere cultures enriched for the stem-cell like component of human tumours.¹⁶³

These studies, as well as the original studies that demonstrated that these BTICs can form a ‘better xenograft,’^{145,154} strongly suggests that the neurosphere culture system is superior to glioma lines grown in serum. It is not to say here whether the existence of these cells confirms the cancer-stem cell hypothesis for GBMs, as this is likely a very complicated question. What is important is that it appears that maintaining the dedifferentiated nature of glioma specimens in culture is critical for retaining their relevant tumorigenic properties and genetic signatures.

1.4. Oncolytic viruses

Oncolytic virus (**OV**) therapy uses replication competent viruses that selectively infect and kill cancer cells. Viruses are highly specific infectious particles, often with very limited species and tissue tropisms. Their life cycle is dependent on the virus being able to enter, replicate and disperse from a target cell. This is combated by a host that has evolved a number of strategies to limit viral replication. As such, viral tropism is often

limited to the cells of a host where the virus has evolved to bypass these anti-viral responses.

The idea of using viruses as cancer therapy arose from observations of cancer remission in patients coinciding with natural viral infections. Documented observations of infection-induced remissions began over a century ago, and have intensified as modern medicine matured. 'Formal' clinical evaluation of viruses as cancer therapeutics in the mid-20th century utilized viral-infected human tissues, saliva and sera injected into cancer patients, in some cases achieving durable responses.¹⁶⁷ However, since these trials used naturally occurring, non-attenuated viruses (hepatitis-inducing viruses,¹⁶⁸ West Nile virus¹⁶⁹ and Mumps virus¹⁷⁰) treatment resulted in patient infection and associated sequelae such as hepatitis and/or encephalitis. Following these 'ethically-questionable' initial studies, the field lay dormant for several decades until it was revitalized through advances in molecular biology and virology.

Modern 'Oncolytic viruses' exploit natural viral trophic restrictions to limit viral infection to tumour cells. For example, adenoviruses (**AdV**) and Measles viruses (**MV**) have defined receptor requirements for entering a target cell;¹⁷¹ thus genetically altering these receptor requirements to cancer-specific receptors 're-targets' these viruses to cancer cells. In the context of gliomas, a prime example is MV re-targeted to EGFRvIII, a mutant EGFR receptor found only in a subset of human gliomas.¹⁷²

Other OV, such as oncolytic Vaccinia virus (**VV**), Herpes Simplex Virus (**HSV**) and Vesicular stomatis virus (**VSV**), utilize ubiquitously expressed cell surface proteins^{171,173,174} making infection of a wide variety of cell types possible. In this case,

tumour-specific tropism is achieved by exploiting cancer-specific cellular phenotypes. The inherent nature of cancer cells as highly proliferative, anti-apoptotic, and/or immunodeficient/immunosuppressed provides optimal replication environments for many viruses. Indeed, most viruses contain gene products that function to elicit such states in the normal host cells and are necessary for viral tropism. As such, viral genes aimed at promoting these characteristics are dispensable for infection and replication in cancer cells, but not 'normal' cells. Deletion of these tropism genes in oncolytic viruses allows for tumour-specific replication.¹⁷⁵ Having been able to more selectively target cancer cells, modern OV's have been intensely studied in the preclinical and clinical settings for a variety of neoplasms.

In its infancy, modern OV's were perhaps viewed as a 'fringe' therapy for several decades. However, the legitimization of this therapy can be seen through the sheer number of recent clinical trials, with no less than 75 trials currently completed, on-going or recruiting.¹⁷⁵ In addition, the purchase of BioVex, Inc, which held the rights to the oncolytic virus OncoVex^{GM-CSF}, was recently purchased by Amgen for 1 billion dollars.¹⁷⁶ OncoVex^{GM-CSF}, now referred to as Talimogene laherparepvec, is a HSV-based OV that expresses GM-CSF, and has just completed Phase III clinical trials in late stage melanoma. Remarkably, this OV was shown to increase response rates from 6% to 26% over GM-CSF treatment according to interim analysis (www.amgen.com). The only other Phase III clinical trial in OV's used an oncolytic adenovirus, now termed Oncorine. This study incorporated intratumoral injections of Oncorine with conventional chemotherapy (cisplatin plus 5-fluorouracil), and found the addition of OV to this regimen doubled the response rates from ~40% to ~80%.¹⁷⁷

So why are OV_s garnering much clinical interest? And why do they seem to be enhancing our current therapeutic regimes? One of the most appealing tenants of OV therapy is the treatment's conceivable self-potential, which hinges on the infection, replication, and spread of the virus throughout the tumor and possibly even to metastatic sites on intratumoural and systemic delivery of OV_s. Further, and most importantly, is the multifaceted anti-tumour activity of OV_s. Multipronged therapeutics such as these may overcome problems such as tumour heterogeneity that limits the effectiveness of monotherapies.

The multifaceted nature of OV antitumor activity begins with infection-based tumour cell death. Cell death following viral infection can occur as a natural part of the viral lifecycle or a consequence of cellular response to viral infection. Investigation into OV infection-based tumour cell death has revealed that a multitude of cell death mechanisms may occur. For example, oncolytic VSV-induced cell death has been intricately dissected to demonstrate a PKR and FAS dependent induction of apoptosis,¹⁷⁸ a mechanism which has been shown to be retained in glioma cell lines.¹⁷⁹ More genetically complex viruses, however, are thought to down-regulate apoptotic machinery. In such instances, it has been demonstrated that these oncolytic viruses kill host cells through the autophagy pathway, as has been demonstrated for HSV¹⁸⁰ and AdV.¹⁸¹ Interestingly, this ability to induce tumour-killing cell death programmes has been exploited to try and enhance oncolytic activity. Expression of apoptosis-inducing transgenes, such as TRAIL,¹⁸² or autophagy-inducing transgenes, such as Beclin1,¹⁸³ in oncolytic AdV has increased viral killing of tumour cells. However, it is important to consider that the early induction of cell-death mechanisms in tumour cells could result in the premature abortion of viral

replication. Thus, the effect of these transgenes should be carefully weighed against advantages of using replication competent viruses.

It has recently been shown that some oncolytic viruses are capable of targeting tumour vasculature, resulting in the inhibition of tumour-blood supply. There are several methods in which OV's are thought to be capable of targeting tumour vasculature. The first is through the direct infection and killing of tumour-associated vasculature, as has been shown for VSV,¹⁸⁴ VV¹⁸⁵ and HSV¹⁸⁶ oncolytic viruses. Alternatively, some viruses such as oncolytic AdVs contain viral proteins that limit angiogenesis. The viral E1A protein has been shown to directly downregulate pro-angiogenic vascular endothelial growth factor (**VEGF**) receptor in tumour cells, resulting in the inhibition of tumour-induced angiogenesis.¹⁸⁷ Further, OV's have been genetically engineered to express anti-angiogenic factors such as soluble VEGF receptors, endostatin, angiostatin, plasminogen, thrombospondin, amongst others.¹⁸⁸

Viruses are potent elicitors of host immune responses. Robust anti-viral cytokine and cellular responses can occur in response to oncolytic viral infection, resulting in enhanced anti-tumour activity. Viral infection with oncolytic viruses can lead to the tumoural or stromal secretion of proinflammatory molecules such as Type-I and -II interferons and TNF α , among others. Interestingly, these cytokines themselves have been employed as anti-cancer therapeutics as single agents. Type-I interferons are the quintessential anti-viral cytokine, capable of being produced by many cell types in the body and inducing an 'anti-viral state' upon ligand recognition. Prior to the introduction of specific small-molecule inhibitors, Type-I interferon, specifically IFN α 2, had been a front-line therapeutic for a variety of blood cancers, with additional efficacy found in melanoma,

bladder and renal cancer.¹⁸⁹ The function of systemically delivered IFN α 2 has been controversial, but is largely thought to occur through the induction of pro-apoptotic interferon stimulated genes^{189,190} and the stimulation of anti-tumour immunocytes.¹⁹¹⁻¹⁹⁵ TNF α has a similar mode of action, and is still locally administered in non-resectable soft-tissue sarcomas and melanoma metastases.^{196,197} Thus, production of anti-viral cytokines in response to OV treatment adds an additional layer of anti-tumour action, acting on both infected and non-infected tumour cells.

The production of anti-viral/pro-inflammatory agents through OV infection inevitably results in the recruitment of peripheral immunocytes. As discussed in the following sections on preclinical and clinical trials of OVs in syngeneic glioma models, the recruitment of these immunocytes has been seen as both a boon and a bane. On one hand, the activation and recruitment of anti-viral immunocytes to the infected tumour has been touted as a method to overcome tumour immunosuppression and activate anti-tumour immunity. In this instance, the oncolysis of cells has been seen to release tumour-associated antigens to act in anti-tumoural responses.¹⁷⁵ Further, the swift recruitment of innate immunocytes can clear infected-tumour cells, enhancing therapeutic benefit whilst concomitantly inhibiting effect viral spread. It is likely that in most instances the innate immune processes that are limiting viral infection are in fact the same processes that will be governing OV effectiveness in the clinic. As such, a discussion regarding the major immune-infiltrating immunocytes following OV therapy for gliomas and their potential roles in therapy will be discussed. In terms of experimental glioma experiments, the cell types that have been investigated in the literature are monocytes/macrophages and NK cells

1.4.1. The role of monocytes/macrophages in oncolytic therapy for the CNS

Monocytes are the hematopoietic stem cell-derived precursors of macrophages and dendritic cells. These cells are produced in the bone marrow and egress to the peripheral blood, circulating for 2-3 days before infiltrating a target tissue and differentiating into tissue-specific macrophages and dendritic cells.¹⁹⁸ Circulating monocytes can also be directly recruited to sites of inflammation, dividing and differentiating on site as directed by inflammatory cues.

In the case of CNS inflammation, monocytes have been shown to be recruited to inflammatory sites through the chemokine receptor CCR2 in models of experimental autoimmune encephalitis,¹⁹⁹ ischemic injury,²⁰⁰ Alzheimer's disease²⁰¹ and West Nile²⁰² and HSV encephalitis²⁰³; however, other chemokine receptors can play axillary roles. For example, the CXCL12/CXCR4 signalling axis has been shown to control perivascular cuff formation, limiting parenchymal infiltration of CXCR4⁺ immunocytes, including monocytes.^{204,205} Further, both Very late antigen-4 (VLA-4) and leukocyte function antigen-1 (LFA-1) have been shown to be important integrins in the recruitment of monocytes to the CNS.^{206,207} Once recruited to the inflamed brain, monocytes differentiate into macrophages that are immunohistochemically identical to activated microglia cells and are thought to assume similar functions (see Chapter 1.2.2.1).^{46,50}

The recruitment of monocytes from the periphery in response to CNS infections seems to have disease-specific functions, and can function to provide both neuroprotective and neurodestructive roles. For one, infiltrating monocytes have been shown to act as 'carriers' of disease, providing entry to the CNS for viruses such as HIV.²⁰⁸ However, more often is the case that these cells play active roles in anti-viral

immunity. The loss of circulating monocytes has been shown to increase viral loads and mortality in encephalitic models of HSV,²⁰⁹ Sindbis virus²¹⁰ and Mouse hepatitis virus,²¹¹ suggesting they play important roles in managing CNS infection. In these incidences, these cells were shown to be responsible for recruiting and activating T cell responses through Il-12 and CCL5 secretion, as well as the induction of IFN γ . Macrophages in viral infections in peripheral organs are also responsible for the production of Type-I IFN and TNF α ²¹² as well as the direct phagocytosis of both infected cells^{213,214} and viral particles themselves.^{215,216} All of these functions could prove important in mediating the premature clearance of OV_s from a tumour.

Several studies have demonstrated a robust recruitment of monocytes/macrophages/activated microglia upon treatment of intracranial gliomas with JX-594 (vvDD),²¹⁷ HSV,^{218,219} MV¹⁷² and MYXV²²⁰ through immunohistochemical staining for various monocytoid markers. This has also been observed in clinical GBM samples after HSV²²¹ and Adv²¹⁹ OV treatment. These cells have been indirectly implicated in mediating OV clearance from the tumour through the use of immunosuppressive compounds such as rapamycin and cyclophosphamide, which were shown to inhibit the recruitment of these cells after OV administration in preclinical models.^{217,218,220} Of note however, is the ubiquitous nature of these compounds which can inhibit/ablate multiple immunocytes, thus more precise ablation techniques should be used to interrogate the role of these cells.

Only a single study has examined direct monocyte/macrophage ablation on OV effectiveness in glioma models.²¹⁹ This study employed a syngeneic rat glioma model with intracranial HSV administration and peripheral monocyte/macrophage ablation

using intravenous clodronate liposomes. The peripheral depletion of these cells resulted in a 5-fold increase in OV titres recovered from the tumour, and an increase in area of infected tumour from 4% to 16%. Being as clodronate liposomes do not enter the brain when administrated systemically, so does not target microglia or tumour-resident macrophages, the authors then grew *ex vivo* in brain slices harbouring intracranial gliomas. These tumour-bearing slices treated with clodronate liposomes depleted the CD68⁺ cells in the slice, and resulted in a 10-fold increase in titres isolated from the brain. These data suggest that both infiltrating peripheral monocytes and resident microglial/macrophages play a role in the clearance of OV. The authors hypothesized that these cells were involved in the immediate phagocytosis of viral particles. Interestingly, however, cyclophosphamide resulted in an 80% tumour infection and 100-fold increase in titres, suggesting that other cells types were effecting OV temporal infection.

1.4.2. *The role of natural killer cells in oncolytic therapy for the CNS*

Natural killer (NK) cells are innate immunocytes derived from lymphoid progenitors in the bone marrow. Here, these cells mature to express specific chemotactic receptors, adhesion molecules and effector functions before entering into circulation where they transiently survey peripheral organs for inflammatory cues and then re-enter circulation.^{222,223} Upon encountering inflammatory signals these cells are programmed in a tissue-specific manner to excerpt tissue- and stimuli-specific functions.

NK cells main effector functions are involved in the clearance and control of tumours and pathogens, particularly, virally-infected cells. This is perhaps best emphasised by the multitude of NK evasion strategies employed by many different viruses.²²⁴ In response to infected and transformed cells, NK cells function in an antigen-independent fashion to

identify and destroy these targets. NK cells exert cytotoxic functions through a number of ways, all of which encompass the activation of apoptotic pathways in the target cell. Firstly, and most commonly associated with NK cell-mediated cytotoxicity, is NK cell degranulation.²²⁵ Perforin and granzymes are the key components of this pathway, and are expelled from the NK cells (degranulated) from specialized cellular organelles. Here, the target cell membrane is 'punctured' by secreted perforin molecules which allow the entry of a family of proteases termed granzymes to enter the target cell. These granzymes function to cleave numerous proteins within the cell, particularly initiator caspases, which result in the immediate induction of the apoptotic programme. Alternatively, NK cells can mediate target cell death through the secretion of TNF α , TRAIL, or FasL, inducing extrinsic apoptotic pathways in cells displaying the cognate receptors.²²⁵ In addition to these cytotoxic functions, NK cells are also involved in the production of IFN γ in the inflammatory environment, polarizing adaptive immune responses to favour anti-viral/tumour (T_H1) immunity. The cytotoxic effector functions are primed and enhanced in the inflammatory environment by cytokines such as IFN α/β , IL-12, IL-15, and IL-18.^{222,223}

As with all directed cytotoxic activities within an organism, NK cell targeting must be accurate in order to limit bystander tissue damage and autoimmunity. The current paradigm holds that NK effector function is regulated through an array of NK cell receptors (**NKRs**) that elicit ligand-based activation or inhibition signals.^{222,223} Under steady-state conditions inhibitory signalling dominates, resulting in the lack of an NK response. However, transformed or virally-infected cells can display activation receptors

and/or lose inhibitory receptors, signalling their ‘stressed’ state and inducing NK cell-mediated effector functions.

This balance was first identified through discovery of cells lacking MHC-I resulting in an activation of NK cell-mediated cytotoxicity.²²⁶ As discussed in Section 1.2.1, gliomas, as with many cancers, can lose expression of MHC-I presumably to counteract antigen-specific cytotoxic T cell responses against tumour-associated antigens.²⁶ This also occurs during many viral infections as a strategy to disguise viral antigens.²²⁷ As such, MHC-I acts as an inhibitory ligand on inhibitory NKRs, which signal through intracellular immunoreceptor tyrosine-based inhibitory motifs (ITIMs) to oppose activation.²²⁸ Thus, attempts of adaptive immunoevasion through inhibiting expression of MHC-I can lead to activation of a robust NK-mediated innate immune response.

Alternatively, transformed or virally infected cells can express activating ligands, many of which signal through immunoreceptor tyrosine-based activating motifs (ITAMs) or DNAX-activating protein (DAP) intermediates to induce NK effector programs.²²⁸ The ligands for these receptors can be quite diverse and include both host- and viral-encoded elicitor molecules. Stress-induced host ligands MIC-A, MIC-B and ULBP-1 – 4 in humans, and RAE-1, MULT-1, H60 in mice, are recognized by the conserved NKG2D receptor. These molecules have been shown to be expressed on transformed cells as a result of the activation of oncogenic stress such as DNA-damage, heat-shock protein and senescence-associated pathways.²²⁹ These stress-induced ligands can also be induced upon viral infection, with some viruses capable of limiting host expression.²³⁰

Another group of activating receptors known as natural cytotoxicity receptors (**NCR**) are potent inducers of NK cell effector function, and consist of NKp46, NKp80, NKp30

and NKp44 in humans, and NCR1 (an NKp46 orthologue) in mice. These receptors signal NK cell effector function through recognition of membrane bound viral hemagglutinins and some tumour-specific antigens.^{223,228} Other viral products that can directly activate NK cells include mouse cytomegalovirus (MCMV) m157 viral protein which is recognized by Ly49H on NK cells, and is a major determinate of susceptibility to MCMV infection in mice.²³¹ Other activating and inhibiting receptors exist on human and/or mouse NK cells, but further discussion is beyond the scope of this section. Of note, however, is the ability of NK cells to directly target antibody coated cells for destruction through a process called antibody-dependent direct cytotoxicity.²²³ Given the major roles NK cells can play in anti-tumour and anti-viral immunity, it seems prudent that they would play substantial roles in oncolytic viral therapy. In terms of gliomas, the role of NK cells has only just started to be elucidated.

The first study to document NK cell infiltration in glioma models utilized a syngeneic rat model with HSV.²¹⁸ It was found that an immediate (6 hours post-injection) up-regulation of NK cell markers (NKR-P1) occurred and diminished by 72 hours, as determined by immunohistochemistry. Cyclophosphamide was found to inhibit the infiltration of macrophages (CD68⁺) cells and microglial (CD163⁺) into these tumours, but did not affect the recruitment of the NKR-P1⁺ cells. However, it was shown that cyclophosphamide inhibited NK cell activation, as measured by a dramatic decrease in intratumoural IFN γ levels. This NK inactivation by cyclophosphamide was confirmed with *in vitro* studies. Interestingly, a follow-up study by the same authors demonstrated that in Nude mice bearing U87 orthoxenografts, cyclophosphamide did inhibit recruitment of NK cells to these gliomas to increase tumoural infection and viral titres.²³²

Taken with the previously described role of cyclophosphamide enhancing HSV infection and replication in gliomas by inhibiting the recruitment of microglia and macrophages, this demonstrates that cyclophosphamide can target numerous immunocytes infiltrating gliomas following OV treatment. However, given the ubiquitous nature of cyclophosphamide on immunocytes, these studies do not isolate the role that NK directly.

The first study to delineate the role of NK cells in the OV therapy was published at the end of last year.²³³ This substantial study demonstrated that HSV therapy is significantly attenuated by NK cell infiltration, with NK ablation studies increasing *in vivo* viral titres by ~3-fold in U87-bearing Nude mice. It was subsequently shown that infection of glioma cells with HSV resulted in the up-regulation NK activating ligands on U87 glioma cells that were recognized by NKp30 and NKp46 natural cytotoxicity receptors. This study suggested that viral distribution throughout the tumour was mediated through the swift targeting of infected tumour cells by NK cells, removing these ‘viral factories’ to halt viral replication and spread. This was the first study to directly implicate NK cells as major players in limiting OV therapy through the swift clearance of OV from the tumour.

Alternatively, we have shown that a natural oncolytic virus, Myxoma virus, can have its anti-tumoural properties enhanced when coupled with NK adoptive therapy in immunocompetent mouse models.²³⁴ Here we demonstrated that MYXV causes a down-regulation of MHC-I through the viral protein M153. This loss of inhibiting ligand resulted in activation of NK cell cytotoxic activity, enhancing anti-tumour therapy when administering MYXV and adoptive NK cells *in vitro* and *in vivo*.

Summarizing these sections, the literature suggests that immediate innate immune responses to the tumour through the phagocytosis of viral particles or viral infected cells by microglia and recruited monocytes/macrophages coupled to the swift clearance of infected tumour cells by NK cells explains why mouse glioma models (and possibly patients) that retain these interactions do not have robust OV infections nor extended viral replication, resulting in a lack of anti-tumour efficacy. It appears that these immune responses, especially in terms of the NK cell compartment, have the possibility to enhance OV therapy if it could be controlled such as to allow more tumoural infection.

Oncolytic viruses are truly multi-modal therapies, able to provoke anti-tumour responses through a variety of mechanisms, including direct tumour killing, activation of anti-tumour cytokines and cellular immune responses, and targeting tumour blood supply. The variety of ways that OVs can concomitantly target tumours allows a greater possibility of overcoming the heterogeneous nature of tumours.

1.4.3. Oncolytic viruses for the treatment of glioma

As mentioned, early OV clinical case reports in the mid-20th century were often marred by viral neurotropism that led to severe and often fatal neurotoxicity.^{167,169,235} These results imposed an obvious barrier to OV therapy for brain malignancies. However, as the molecular aspects of biology and virology were slowly unravelled, the use of selected or genetically engineered viruses attenuated for the absence of neurotropism began to emerge. What could be considered the first modern pre-clinical trial of an attenuated OV for the therapy of malignant gliomas was published by Martuza et al.,²³⁶ who showed that an engineered strain of HSV showed strong efficacy *in vitro*, as well as in mouse heterotopic and orthotopic mouse xenografts of human

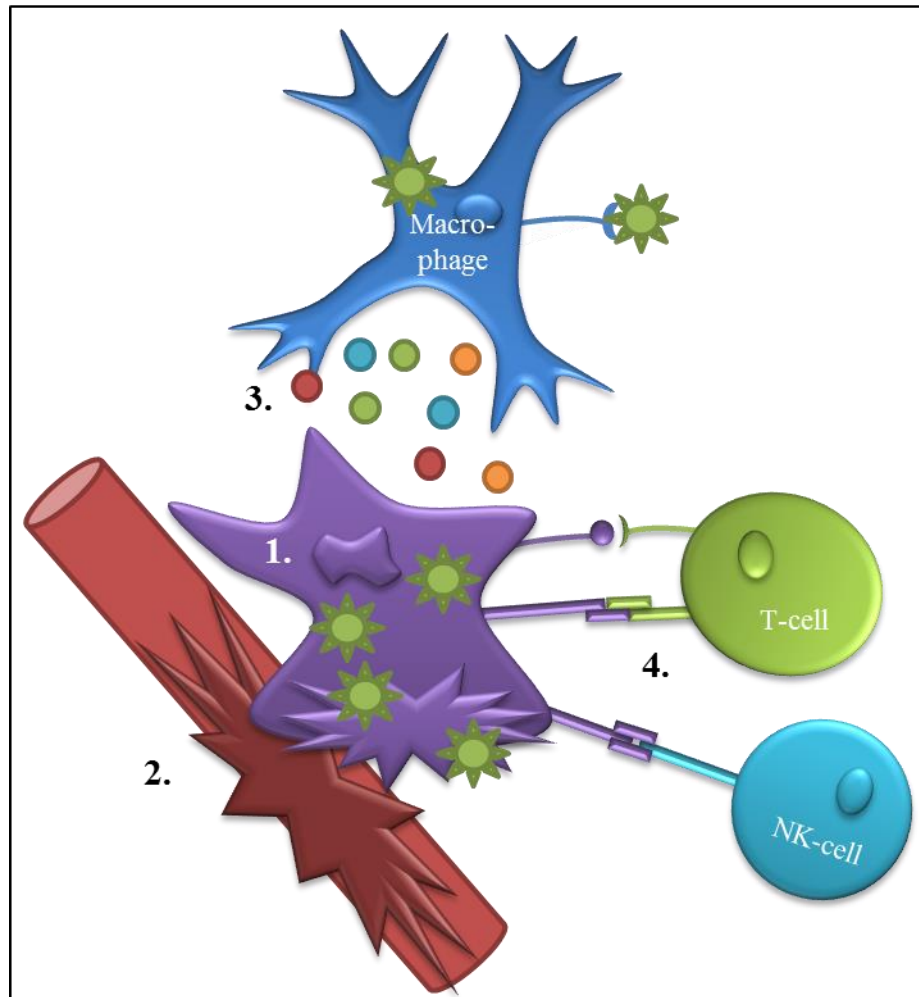


Figure 1.4: *Oncolytic viruses have the potential to elicit an anti-tumour response through a number of mechanisms. Oncolytic viruses induce cancer cells death through: 1) Direct infection of cells causing tumour cells to die through lysis, apoptosis or autophagy; 2.) Infection in the tumour microenvironment destroys blood vessels feeding the tumour; 3.) Detection of virus in the tumour microenvironment causes an anti-viral cytokine responses that have anti-tumour properties; 4.) Infection of the cell alters immunomodulatory receptors on the tumour cells allowing for targeting by cytotoxic killer cells.*

gliomas. In this instance, attenuation of HSV for decreased neuropathogenicity was achieved through a large deletion of the thymidine kinase gene, limiting viral replication to actively replicating cells only. Several other attenuated HSV viruses with engineered mutations targeting the HSV viral tropism gene $\gamma_1-34.5$, and other tropism genes, arose

shortly thereafter with equivalent preclinical efficacy with even further reduced neurotoxicity.²³⁷⁻²³⁹

The next attenuated virus studied for the treatment of gliomas was the attenuated AdV, dl1520, now termed ONYX-015.²⁴⁰ Initially it was believed to selectively target *TP53*-mutated or deleted cells, making gliomas an excellent target. The original publications found *in vitro* efficacy of a *TP53*-mutated glioma cell line, with little or no treatment benefit *in vitro* or *in vivo* in mouse xenografts with a wildtype *TP53* cell line.^{240,241} Subsequent studies with this virus in mouse heterotopic xenografts of primary patient gliomas found ONYX-015 had significant antitumour activity in human gliomas regardless of *TP53* activity.²⁴² The function of the E1B-55 kDa protein is now thought to be part of a viral induced ubiquitin E3 ligase complex, forcing the degradation of many proteins, including *TP53*, in addition to having important functions in blocking the induction of Type-I interferon stimulated genes.²⁴³

Preclinical studies of OV_s in gliomas in the 1990s were largely limited to attenuated HSV_s and AdV_s; indeed, these were the first viruses to enter human glioma clinical trials. However, the new millennium supplied an entire new arsenal of possible viruses for use in glioma therapy that have completed or entered into clinical trials. Further, we are now far past the initial days of discovery using OV_s for glioma treatment. Modern studies have moved on to start improving these OV_s through engineering transgenes, retargeting viruses, and finding optimal combination treatments with chemotherapeutics.

1.4.3.1. Oncolytic viruses for the treatment of glioma: Clinical trial summary

Eight formal clinical trials of OV therapy for MGs have been completed to date (summarized in **Table 1.1**). We have previously published an extensive review on the details of these trials.²⁴⁴ The four viral backbones that have been reported in clinical studies thus far are: 1) HSV; 2) Newcastle Disease Virus (**NDV**); 3) AdV; 4) Reovirus (**RV**). However, several more viruses on their way or in the clinic for glioma patients (**Table 1.2**)

To summarize these clinical trial overall, it was found that these viruses were safe, with no maximum tolerated dose (**MTD**) reached, and some anti-glioma activity found in a handful of patients. These are the same outcomes one would find with nearly all Phase I studies using novel agents with two exceptions; a **MTD** is virtually always found with cytotoxic agents, and

several extensive responses have been seen, including a tumor regression in one trial in which there was no evidence of tumor at autopsy.²⁴⁵ Given that the goal and design of these Phase I studies is to determine safety, and not efficacy, these trials can be considered an overwhelming success on one level; however, some readers still may find the small number of responders disconcerting.

Several other clinical trials for gliomas are underway or in development (**Table 1.2**). These trials focus on testing new viruses (retargeted Adenovirus, Measles virus, attenuated Polio virus, Parvovirus) and optimizing routes of delivery (mainly through convention enhanced delivery, **CED**). As can be seen by this flourish of clinical activity, OV therapy for MGs is expected to have promise.

Table 1.1: Oncolytic Viruses for Gliomas in Completed Clinical Trials - Overview

Virus (strain)	Genetics	Study Type	Patient Number	Dose/Schedule/ Route of Administration/MTD	Reported Toxicities	Efficacy	Ref.
HSV-1 (G207)	γ_1 -34.5 gene deletion lacZ insertion in U _L 39	phase I	21	1×10^6 to 3×10^9 pfu/single injection/ intratumoural to enhancing area/ No MTD	no toxicity/serious adverse could be ascribed to the treatment	6/21 neurological status improvement 8/21 tumor volume decrease (MRI)	246
HSV-1 (G207)	γ_1 -34.5 gene deletion lacZ insertion in U _L 39	phase I	9	1.5×10^8 to 1×10^9 pfu/ intratumoral injections pre- and post- resection/No MTD	AE possibly or probably related: Grade III Seizure (22%); Grade II/III Fever (22%); Grade II/III Hemiparesis/Hemiagnosia (44%)	None found (not designed to measure)	221
HSV-1 (HS-1716)	γ_1 -34.5 gene deletion	phase I	9	1×10^3 to 1×10^5 pfu/single injection/ intratumoural/No MTD	no toxicity/serious adverse could be ascribed to the treatment	3/9 responders, 5/9 stable (MRI) 1/9 smaller, 2/9 stable (SPECT)	247
HSV-1 (HS-1716)	γ_1 -34.5 gene deletion	phase I	12	1×10^5 pfu/single injection/ intratumoural/No MTD	no toxicity/serious adverse could be ascribed to the treatment	Not measured	248
HSV-1 (HS-1716)	γ_1 -34.5 gene deletion	phase I	12	1×10^5 pfu/single injection/ intratumoural/resection cavity/ No MTD	no toxicity/serious adverse could be ascribed to the treatment	3/12 disease-free for 15-22 months	249
AdV (ONYX-015)	E1B-55kD gene deletion	phase I	24	1×10^7 to 1×10^{10} pfu/single injection/tumour bed post- resection/No MTD	no toxicity/serious adverse could be ascribed to the treatment	None found	250
Reovirus	Wildtype virus	phase I	12	1×10^7 to 1×10^{10} pfu/single injection/intratumoural/No MTD	No grade III/IV adverse effects possibly or probably related	1/12 disease-free survival (>6 years)	245
NDV (NDV-HUJ)	selected NDV (lentogenic)	phase I/II	14	0.1×10^9 - 1.1×10^{10} IU dose escalation w/ 3 cycles of 5.5×10^{10} /No MTD	Grade I/II fever 5/14 (45%)	1/14 complete response 3/14 long-term survival	251

MTD - Maximum tolerated dose

Table 1.2: Oncolytic Viruses for Gliomas in Clinical Trials - In-progress or Planned

Virus (strain)	Administration Route	Genetics	Study Type / Status	ClinicalTrials.gov identifier	Principle Investigator
RV	Intratumoural with CED	Wildtype	Phase I/II Enrollment Complete	NCT00528684	James M Markert, MD University of Alabama
NDV (NDV-HUJ)	Intratumoural	selected NDV (lentogenic)	Phase I/II Planned	NCT01174537	Hadassah Medical Organization
AdV (Ad-Δ24-RGD)	Intratumoural	24bp deletion in E1A and RGD fiber	Phase I No longer recruiting	NCT00805376	Frederick F. Lang, MD MD Anderson, Texas
AdV (Ad-Δ24-RGD)	Intratumoural with CED	24bp deletion in E1A and RGD fiber	Phase I / II recruiting	NCT01582516	Clemens Dirven, MD PhD Erasmus Center
MV (MV-CEA)	Intratumoural	MV Edmonson strain that expresses human carcino-embryonic antigen	Phase I / recruiting	NCT00390299	Evanthia Galanis, MD Mayo Clinic, Minnesota
Poliovirus (PVSR1PO)	Intratumoural with CED	native IRES replaced with human rhinovirus type-2 IRES	Planned	NCT01491893	Matthias Gromeier, MD Duke University
Parovirus (ParvOryx01)	Intratumoural	Wildtype Rat Virus	Phase I/II Recruiting	NCT01301430	Anders Unterberg, MD PhD University of Heidelberg

1.4.3.2. Oncolytic viruses for the treatment of glioma: Preclinical Trials

The first and most important, albeit somewhat surprising, lesson learned from the OV clinical trials in gliomas is that OVs are safe when administered directly into the brain. However, the initial excitement in developing OV therapy was based on the simple concept that a small infection would be sufficient to begin a rapid, pan-tumoural infection producing a cure. This has proven not to be true. In fact, despite the reasonably high inoculums (1×10^5 – $>1 \times 10^9$ PFUs), the studies that investigated the extent of infected tumour and the duration of the infection demonstrated that this is a transient infection that is readily cleared. This most likely explains the somewhat disappointing response rates found thus far.

These clinical results are very different to what has repeatedly been shown in the literature for the efficacy of oncolytic viruses in preclinical models for gliomas. In fact, several OVs have shown a high percentage of ‘cured’ animals with a single intratumoral injection in mouse glioma orthoxenografts,²⁵²⁻²⁵⁴ while both HSV-207 and HSV-1716 produced robust viral infection or replication and measurable efficacy in mouse glioma subcutaneous or orthotopic xenografts.^{238,255} Although there are many reasons for this discrepancy, the model in which these viruses are tested is likely to blame for these untranslatable findings. As would be suggested by the several studies that looked at immune infiltrate in the clinical tumours post-inoculation, these therapies produce a robust immune response that could be clearing the viral infection before the virus can sufficiently replicate throughout the tumour. As such, it could be anticipated that OV preclinical trials in immunocompetent orthotopic models would more closely recapitulate

what we have seen in the clinic thus far. **Table 1.3** summarizes the preclinical studies using OV_s in orthotopic syngeneic glioma models.

When comparing the results of neuroattenuated HSV in syngeneic orthotopic models to what has been seen in the clinic, there seems to be a very reasonable correlation. HSV treatment alone has little effect in syngeneic orthotopic gliomas, with complete viral clearance occurring between 3 and 7 days after treatment. Interestingly, ‘armed’ oncolytic HSV with immunostimulatory elements seems to be able to recruit anti-tumour immunocytes to bolster HSV efficacy. ‘Armed’ OV_s contain transgenes under the control of viral or host promoters such that these genes are expressed in the targeted cancer cell. These have included pro-drugs, tumour-suppressors, ECM degrading components, and additional immunomodulatory genes.²⁴⁴

Other OV_s used in immunocompetent preclinical models resulted in similar results, with the vast majority of these studies demonstrating that oncolytic viruses alone have very little or no effect in syngeneic intracranial tumours. Again, viral infection seems to rarely last longer than 7 days post treatment, with little evidence of viral replication. When significant treatment benefit is found in these models with virus alone, it is only when very high inoculums are used in very small tumours. To put this in perspective, in the JX-594 experiments, 10,000 cells were implanted in the brains of mice, followed by 5×10^7 PFUs the next day to the same location in the brain. Even if these cells doubled in that time, that is a 2500:1 ratio of virus:tumour cells, or 2500 MOI. What is incredible is that this type of ratio still does not cure animals, suggesting the virus is unable to spread to all the cells even in these microscopic tumours. This literature suggests that unless all or many of the cells are infected at treatment, there is no benefit

Table 1.3: Oncolytic Viruses in Preclinical Models of Syngenic Gliomas - Overview

Virus	Genetics	Dose/ Admin route	Tumour Line / Time of Treatment	Survival	Replication / Clearance	Important Notes	Ref.
Herpes simplex	γ 1-34.5 gene deletion	1×10^6 PFU / Intratumoural	GL261-mouse / 5 dpi	19 dpi control vs. 26 dpi virus	N/A	Immunosuppressive IL-10 expressing virus abrogated survival advantage.	256
Herpes simplex	γ 1-34.5 gene deletion	1×10^7 PFU / Intratumoural	4C8-mouse / 7 dpi; 21 dpi	54 dpi control vs. 72 dpi virus, 7 dpi Tx; No change with 21 dpi Tx	Virus cleared by 6 dp Tx	Immunostimulating IL-12 expressing virus increased survival to 97 days.	257
Herpes simplex	γ 1-34.5, ICP6, and α 47 deletion	2×10^6 PFU / Intratumoural	CT2A-mouse / 6 dpi	No significant change (death ~20dpi)	N/A	Immunostimulating Flt-3 expressing virus resulted 40% of mice 'cured'	258
Herpes simplex	ICP6 deleted	2×10^7 PFU / Intratumoural	D74-rat / 7 dpi	12 dpi control vs. 15 dpi virus	Largely cleared by 3 dp Tx	Removal of PBMCs using cyclophosphamide decreased viral clearance and survival	259
Reovirus	Wildtype	1×10^9 PFU / Intratumoural	RG2-rat / 4 dpi; 9L-rat / 4 dpi	RG2 -19 dpi control vs. 24 dpi virus; 9L - 27 dpi control vs. 40 dpi virus;	Virus present at 5 dp Tx, 6000-fold less than injected	Cyclophosphamide administration did not alter survival or viral clearance kinetics	260
Vaccinia	Viral TK and VGF deleted	1×10^9 PFU / Intravenous	RG2-rat / 5 dpi; F98-rat / 7 dpi	RG2 -14 dpi control vs. 18 dpi virus; F98 - ~18 dpi control vs. ~24 dpi virus;	Virus persistence to 7 dp Tx	Immunosuppressive drugs cyclophosphamide and rapamycin increased infection and treatment efficacy	261
Vaccinia	Viral TK and VGF deleted, GM-CSF addition	5×10^7 PFU / Intracranial	RG2-rat / 1 & 4 dpi, 8, 13 & 18 dpi	Early Tx -19 dpi control vs. 26 dpi virus; Late Tx - 19 dpi control vs. 36 dpi virus	Viral transgene expression observed until 10 dp Tx	Immunosuppressive drug rapamycin increased infection and treatment efficacy	217
Vaccinia	Viral TK and VGF deleted, GM-CSF addition	1×10^7 PFU / Intracranial	GL261-mouse / 1, 4 & 10 dpi, 8, 13 & 18 dpi	Early Tx - ~23 dpi control vs. ~33 dpi virus; Late Tx - No significant change	Loss of viral transgene expression between 6-8 days	Immunosuppressive drug rapamycin increased infection and treatment efficacy only in early dose experiment	217
Vesicular stomatitis	delta51 mutation	5×10^8 PFU / Intravenous	RG2-rat / 2 & 5 dpi	No significant change (death ~17dpi)	N/A	Immunosuppressive drug rapamycin increased treatment efficacy	262
Myxoma	Wildtype	1×10^7 PFU / Intracranial	RG2-rat / 5 dpi	RG2 - no significant change (death ~19 days)	Cleared between 3 and 5 dp Tx	Immunosuppressive drug rapamycin increased infection and treatment efficacy	220

dpi - days post implantation
dp Tx - days post treatment

from viral therapy alone. One may argue that treating these small tumours so soon after implantation may in fact be mimicking OV therapy after surgical resection; however given the overall lack of single cell infiltration observed by these older syngeneic models, and such a small timeframe that they have to infiltrate, it is doubtful that this recapitulates that scenario.

Of note in many of these studies is that immunosuppressive compounds such as cyclophosphamide and rapamycin are able to either enhance the initial infection or delay viral clearance, allowing for a more robust tumour infection and more thorough tumour destruction. This strongly suggests that the immune system in these animals is indeed clearing the virus before significant tumour infection can occur.

It seems counterintuitive that in several instances adding immunostimulating molecules to the virus can enhance therapeutic efficacy, while in others the addition of immunosuppressive therapeutics to the treatment regimen can enhance infection and delay viral clearance. Indeed, there appears to be two views of this in the OV field, those who wish to recruit the immune system and those that wish to inhibit it (**Figure 1.5**). This ‘clinical conundrum’ will have to be resolved in order to maximize OV therapy in the clinic. However, it is likely that optimal OV therapy will need the combination of both these strategies. Or, as shown by my data in this thesis, the most effective strategy may be first to temporarily inhibit the innate immune response so that the OV can rapidly spread throughout the tumor and infect each tumor cell. This would be followed by an enhanced immune response that utilizes both anti-viral and anti-tumor responses to recruit immunocytes to clear infected tumor cells. One can envisage a treatment strategy that would utilize temporary immunosuppressive compounds to achieve this.

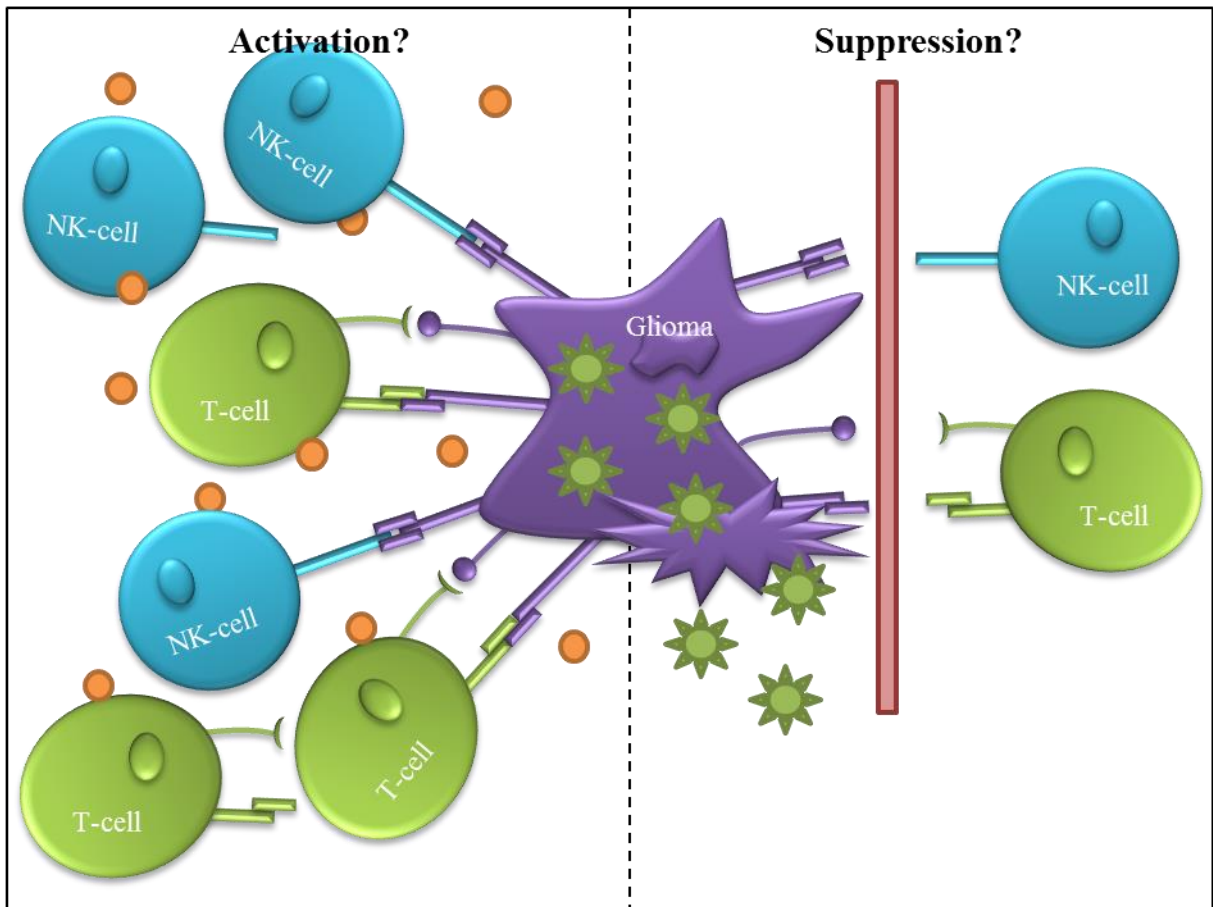


Figure 1.5: *The clinical conundrum.* Should we be trying to harness the potential therapeutic benefit of the anti-viral response or should we try and suppress it to achieve greater viral infection and replication rates?

1.4.4. *Myxoma virus as a candidate oncolytic virus for gliomas*

A newcomer into the OV world, and the recent OV of choice in the Forsyth laboratory, is Myxoma Virus (**MYXV**). MYXV is a member of the Pox virus family (*Poxviridae*), *Chordopoxvirinae* subfamily, and the *Leporipoxvirus* genus. The natural host of MYXV is believed to be the South American tapeti (*Sylvilagus brasiliensis*) and the North American brush rabbit (*Sylvilagus bruneii*), where MYXV causes a mild, benign fibrosis at the site of infection. The virus is passively transmitted by mosquito and other biting arthropod vectors, and infection in bitten animals are contained to the

epidermis at the site of inoculation.^{263,264} However, MYXV was first discovered through a lethal, systemic infection termed Myxomatosis, that occurs in the European rabbit (*Oryctolagus cuniculus*). In this instance, MYXV is capable of spreading from the epidermal fibromas to the deeper dermal layers, where MYXV can subsequently infect circulating leukocytes to systemically disperse the virus and set-up secondary sites of infection.²⁶³⁻²⁶⁵ European rabbits infected with MYXV develop numerous, systemic tumours accompanied by a complete immune collapse, with death occurring from overwhelming infections of normally benign microorganisms.²⁶⁵

This very narrow host range and lethal infection in European rabbits has been exploited as a 'biological weapon' against the introduced rabbit population in Australia in 1950. Rabbit populations were decimated, and in some areas within a year of release the Myxomatosis killed greater than 99% of the rabbit population.^{263,264} Since then, both MYXV and rabbit populations have evolved, slowly resulting in less lethal infections. This release of MYXV in Australia, and a similar release in Europe, has provided a unique opportunity for the study of viral-host co-evolution in nature.

As could be imagined, prior to the release of a non-native virus *en masse* could be performed, MYXV safety to humans and endemic animal populations was heavily scrutinized, and nearly 20 years of safety testing was performed before approval for its release was granted by the Australian parliament (www.csiro.au). Amazingly, MYXV tropism is so specific that a non-lagomorph vertebrate has never been shown to be infected, including humans, with no evidence of even sero-conversion in areas where the virus has been released.²⁶⁶

Several strains of MYXV have been isolated, but most of the work characterizing this virus and the strain used in oncolytic studies, is the Lausanne Strain, one of the oldest strains on biological record.²⁶⁴ As such, any MYXV referred to herein is referring to this strain. Further, most of the work characterizing MYXV has been in relation to its *Chordopoxvirinae* cousin, Vaccinia virus (VV), a member of the *Orthopox* genus. VV has been deemed the prototypical poxvirus due to its importance as a vaccine and its relation to the human pathogen Variola virus, the etiologic agent of Small Pox. This is complicated by the fact the *Leporipoxvirus* genus encode 15-20% less proteins than members of the *Orthopox* genera,²⁶⁷ and are amongst the few members of the *Poxviridae* family known to cause tumour-like cutaneous, fibrotic lesions,²⁶⁸ suggesting differing modes of infection, replication and/or pathogenesis; however, when areas of MYXV virus virology are not known, aspects of VV were implemented.

1.4.4.1. Myxoma virus biological characteristics

As with all poxviruses, MYXV consists of a nucleocapsid core surrounded by a single lipid bilayer. This collective structure is termed the intracellular mature virion (IMV), and is a large (300 x 250 x 200 nm), brick-shaped structure that is thought to be the main infectious particle produced, and is thought to be released through cellular lysis.²⁶⁹ However, as with other poxviruses, MYXV is capable of producing additional infectious forms, such as the extracellular mature virion (EMV). This form contains an additional host-derived membrane, which is thought to facilitate systemic infection in MYXVs natural host, lagamorphs. MYXV purification techniques destroy the extra-membrane during purification techniques,²⁷⁰ so most *in vitro* studies are conducted with the IMV. This is especially prudent in the case of the oncolytic viral studies discussed below.

Analysis of the IMV proteins in MYXV has recently been performed.²⁶⁷ The nucleocapsid was found to consist of 14 proteins, the most abundant of which were M099L, M092L, and M058R, homologues of VV major structural core proteins, providing scaffolding for the nucleocapsid. The remaining core proteins are enzymes involved in initiating replication in the host cells, such as viral RNA polymerase (M068R), transcription factors (M072L, M096L), DNA helicase (M086L), and a Holliday junction resolvase (M112L). All of the identified core proteins shared close homology to VV proteins, except for M151, a *Leporipoxvirus* virulence factor which is a serine proteinase inhibitor implicated in inhibiting cleavage of caspases initiating apoptosis and interleukin-1 β maturation.²⁷¹

The protein envelope surrounding the nucleocapsid core was found to contain 4 proteins, M060R, M071L, M115L, and M093L.²⁶⁷ Interesting, M071L and M115L are the VV homologues of A27L and H3L, 2 of the 4 VV membrane proteins known to be necessary for viral attachment to the host cellular membrane. Both A27L and H3L have been shown to bind cell surface heparin sulphate,²⁷² implicating cell surface glycosaminoglycans as important mediators of MYXV host cell attachment.

Important to note here is that VV has been shown to have greater than 80 proteins as part of the IMV, ~60 in the nucleocapsid and ~20 in the viral membrane.²⁷² This is in stark contrast to the 17 proteins identified in the MYXV IMV.²⁶⁷ Whether this is a consequence of the more intensive study of the prototypical poxvirus VV or if this is a consequence of a fundamentally different, and less complex, viral attachment and entry method utilized by MYXV has yet to be determined; however, given that other known

VV core proteins have known homologues in MYXV,²⁷³ it is likely that subsequent studies will uncover further viral proteins within the MYXV IMV.

Intensive studies looking at the host cellular mediators of MYXV adherence have not been conducted. VV has been more thoroughly studied, and has been shown that the virus binds cell surface glycosaminoglycans, specifically heparin sulphate with the A27L and H3L viral proteins, chondroitin sulphate with D8 and extracellular laminin with A26.^{272,274} As mentioned, MYXV contains A27L and H3L homologues, as well as a D8 homologue,²⁷⁵ but no A26L.²⁷⁶ This suggests that MYXV may also adhere to heparin sulphate and chondroitin sulphate but not laminin. This was recently demonstrated with exogenous heparin sulphate being shown to competitively inhibit cell binding of VV and MYXV, while laminin only inhibited binding of VV.²⁷⁷ It is currently unknown if chondroitin sulphate also inhibits MYXV binding, or what other factors mediate this initial step in MYXV infection.

Membrane fusion and virus entry into the host-cell are the next steps in viral infection, and a highly contentious issue within the *Poxviridae* family. The major entry mechanisms that have been proposed are outer membrane fusion and receptor-stimulated endocytosis. Membrane fusion simply suggests that the membrane surrounding the IMV fuses with the host plasma membrane and releases the nucleocapsid into the cytoplasm. The endocytic pathway involves the viral adhesion-mediated stimulation of host receptors that induce endocytosis of the virion, followed by membrane fusion with the endocytic vesicle membrane to release the capsid into the cytoplasm. In terms of the prototypical VV, experimental evidence for both pathways exists, and seems to be dependent on the cell type examined, strain of VV, and the experimental methods employed. However,

recent evidence strongly favours the endocytic pathway, macropinocytosis specifically, as the favoured route.^{272,274} A study examining morphological characteristics of infected rabbit kidney cells (RK13) in culture with electron microscopy found a number of MYXV virions within vesicles within the cytoplasm, suggesting that MYXV was entering these cells utilizing a similar endocytic pathway.²⁷⁸ Interestingly, a comparison of VV and MYXV cell entry was performed on a panel of human cancer cell lines,¹⁷³ an important study considering both these viruses are oncolytic candidates. Here it was found that MYXV and VV may actually employ different methods of host cell entry in human cancer cells, with data suggesting that MYXV could enter independently of endosomal acidification and tyrosine kinase-dependent endocytic pathways. It is likely that the entry methods of MYXV, as with VV, is host cell-type dependent and requires further study.

Regardless of the method of entry, MYXV must participate in membrane fusion, either at the plasma membrane or the vesicle membrane, for entry of the nucleocapsid into cytoplasm. This still remains as somewhat of a mystery for most members of the *Poxviridae* family, and has never been investigated for MYXV. In VV, however, recent studies demonstrate that a group of 12 proteins present in the IMV membrane form the fusion/entry complex and are required for entry.²⁷⁴ Interestingly, these proteins were not seen in the initial survey of MYXV membrane or core proteins,²⁶⁷ but the MYXV genome does contain conserved or semi-conserved homologues of these proteins.²⁷³ Again, this is an area of the literature that needs further experimentation; however, given the close homology of these proteins, it would appear these viruses use analogous fusion mechanisms.

The MYXV genome is 161.8 Kb of double-stranded DNA, and, as with all Poxviruses, is arranged as a single linear fragment with terminal inverted repeats and closed hairpin loops at each end.^{269,273} The genome contains 171 open-reading frames (**ORF**), almost 50% of which are proposed to be under control of early viral promoters.²⁷³ Upon entry into the cytoplasm, the nucleocapsid initiates transcription from ORFs containing early promoters. These early ORFs code proteins that are involved in viral genome replication, host modulatory proteins, and transcription factors that initiate the transcription of intermediate ORFs. All viral mRNAs are capped and polyadenylated using viral encoding enzymes, mimicking eukaryotic mRNAs such that host ribosomes will translate these messages. Cessation of early gene transcription in VV is thought to occur through the dissociation of the nucleocapsid, a process termed uncoating.²⁶⁹ Viral genome replication is thought to occur at this point, which, in the case of VV, occurs through the formation of viral genome concatamers which are resolved just prior to packaging.²⁶⁹

Intermediate gene transcription occurs following the completion of DNA replication, and mostly encodes enzymes and factors necessary for the on-set of late gene expression, as well as several early packaging components.^{273,279} The products of late ORFs are the components of the IMV (structural and enzymatic proteins needed for the infection of subsequent cells) as well as proteins that regulate the packaging of these elements with replicated dsDNA genome.

There has only been a single study examining the morphogenesis of MYXV. Here electron microscopy was utilized to observe viral infection and replication *in vitro* in rabbit kidney cell lines.²⁷⁸ This study found similar assembly dynamics to what had

previously been observed for VV.²⁶⁹ Assembly begins with the production of a crescent membrane structure that is presumably then packed with the genome and core proteins. This crescent structure is then closed to form the outer membrane of the IMV, followed by the condensation of the genome and core proteins to form the internal nucleocapsid structure.²⁷⁸ Subsequent enveloping strategies can also occur, whereby material from the golgi apparatus, endosomes and/or plasma membrane can be utilized to form two additional membrane structures; one which mediates fusion with the host outer plasma membrane to facilitate export, and the other two mask viral particles once released from the cell. As mentioned earlier, these infectious particles are not used in initial oncolytic studies as these membranes are lost in during the purification of the virus.²⁷⁰

Given the size of mature poxviruses, transport of the packaged virus to the plasma membrane for viral egress is an active process. In the case of VV, transportation of the mature, double enveloped viruses from viral assembly factories to the cell surface occurs along microtubules using both host kinesins and viral kinesin mimics (ie, F12L, A36).²⁸⁰ Upon contact with the exterior host plasma membrane, the outer viral envelope fuses, releasing the virion to the exterior. While some of these virions are immediately released following fusion, others remain bound to the outer plasma membrane. These viruses signal actin polymerization cascades within the host cell, resulting in the production of virus-tipped actin projectiles exuding from the host cell.^{269,276} These actin projectiles are important for the efficient dissemination of virus to neighboring cells. Again, limited studies have investigated the exact egress strategies of MYXV, but the several that have been conducted suggests that it is very similar to what has been described in VV.^{276,278,281} Interestingly, an additional strategy has been identified whereby it has been suggested

that MYXV can travel to neighboring cells through cytoplasmic corridors that attach neighboring cells, allowing the virus to infect neighboring cells without subjecting itself to the external immune responses.²⁷⁸

A summary of the above discussed putative infection and replication mechanisms can be seen in **Figure 1.6**.

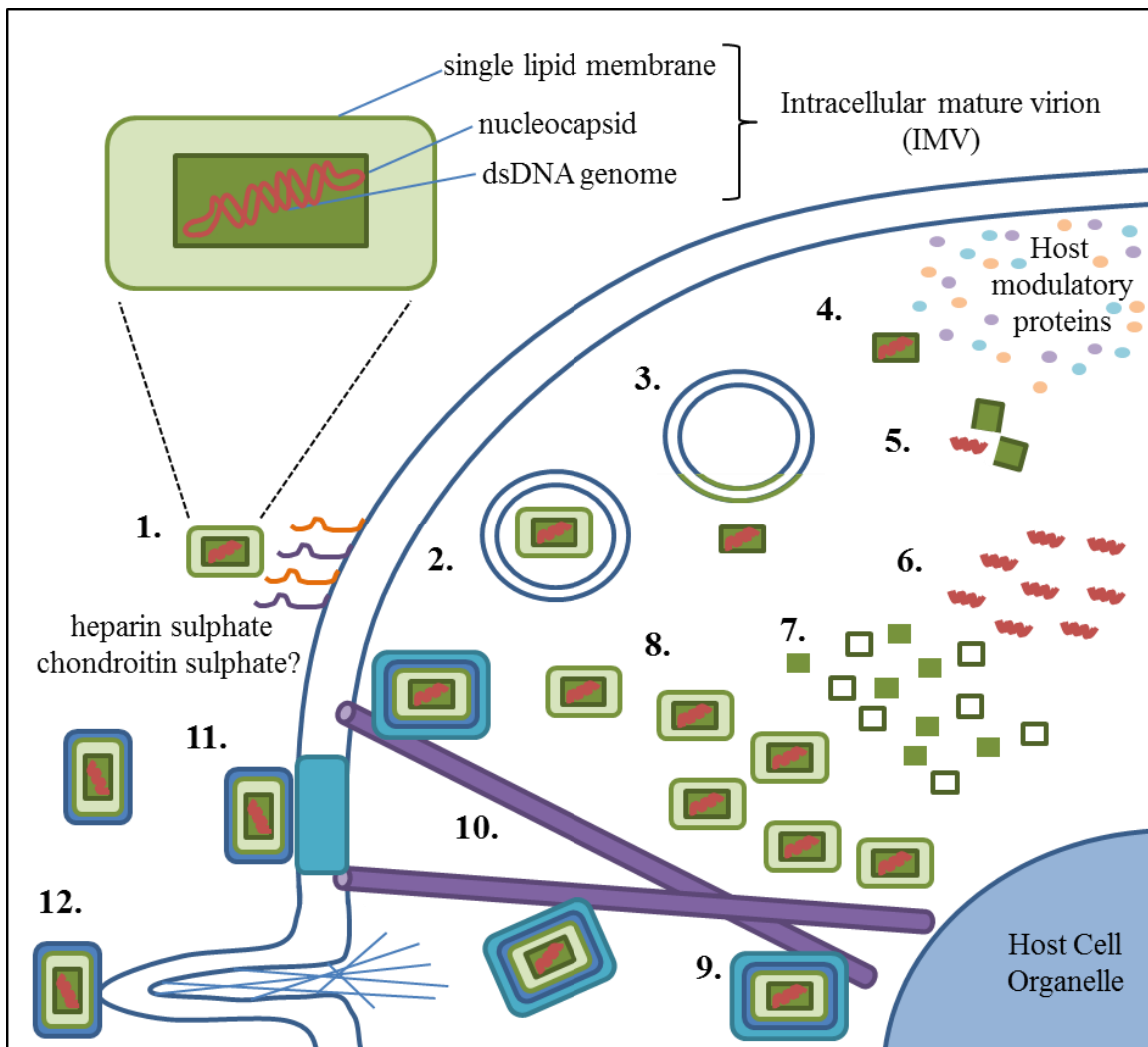


Figure 1.6: *Myxoma virus infection and replication.* In oncolytic virus studies, the purification techniques results in infection of cancer cells with the intracellular mature virus (IMV). 1 – The MYXV IMV binds the host cell possible adhering to membrane glycosaminoglycans such as heparin sulphate and chondroitin sulphate. 2 – Presumably, MYXV entry into the cytoplasm can occur through host cell-mediated endocytosis (shown) or fusion with the external plasma membrane. 3 – Membrane fusion with the endocytic vesicle releases the viral nucleocapsid. 4 – Early gene expression begins for genome replication and host modulatory proteins. 5 – Nucleocapsid uncoating stops early gene expression. 6 – Viral genome replication. 7 – Intermediate and late gene expression occurs after genome replication, coding for proteins involved in packaging the virus and the components of the IMV. 8 – Packaging of virus into the most abundant infections form, the IMV. 9 – Two subsequent membranes derived from the golgi, endocytic vessicle or endoplasmic reticulum can envelope the IMV. 10 – These enveloped viruses are transported to the host plasma membrane through active transport along microtubules. 11 – The outer membrane than fuses with the plasma membrane, which can release the single enveloped virus. 12 – some released virus remains attached to the external plasma membrane and signals the formation of actin-projections to ‘push’ envelopedvirions to neighboring cells. Finally, not shown, is a major dissemination pathway for MYXV that is thought to be through intracellular connections called ‘cytoplasmic corridors.’

Myxoma virus is perhaps best studied through the numerous host modulatory proteins they encode. These proteins combat the host response to viral infection, mainly by preventing apoptosis, evading immune responses, and with some poxviruses, inducing cell cycle progression. These proteins can approximately be categorized as viroceptors, virokines, and virotransducers/inhibitors.^{269,282} Most of these factors are expressed as part of the early transcriptome immediately after infection.²⁷³

Viroceptors are a group of viral proteins that have evolved to act as decoy receptors, binding host cytokines, chemokines and/or growth factors. Likely the best described for MYXV is the product of the M007L/R ORF, M-T7. M-T7 is a rabbit IFN- γ receptor homologue that has lost its intracellular and transmembrane domains. This secreted, cell-free receptor functions to bind and sequester IFN γ signalling in the infection microenvironment through competitive inhibition.²⁸³ Similarly, the M001R/L ORF codes a secreted receptor which binds and inhibits host chemokines (M-T1),²⁸⁴ while the

M002R/L ORF codes a secreted decoy TNF receptor (M-T2).²⁸⁵ Other, membrane bound viroceptors include the M141R and M128L, which are functional viral mimics of host immunosuppressive modules CD200²⁸⁶ and CD47,²⁸⁷ respectively.

Virokines are secreted viral proteins that mimic host cytokines and growth factors. For MYXV, the best described virokine is M010L, which is a functional homologue to rabbit epidermal growth factor (EGF),²⁸⁸ and along with M131R,²⁶⁸ provides mitogenic signalling responsible for the formation of tumour-like cutaneous lesions in host lagomorphs.

Finally, virotransducers/inhibitors are proteins that usually function intracellularly to inhibit anti-viral mechanisms of infected cells. MYXV in particular, is especially well known for the number of anti-apoptotic proteins it encodes. For example, M011L²⁸⁹ and, putatively, M146R²⁷³ binds and inhibits anti-apoptotic proteins of the BCL2 family, while M005R/L inhibits cyclin-dependent kinase induced apoptotic programs.²⁹⁰ The protein product of M151R, SERP2, is a proteinase-inhibitor shown to inhibit apoptosome and granzyme-directed cleavage of caspases, the final initiators of the apoptotic program.²⁷¹ Additional, non-apoptosis related virotransducers/inhibitors also exist, such as M013L and M150L (inhibits NFκB function),²⁹¹ M153L (inhibits MHC-I cell-surface expression),²⁹² and M029L and M156R (PKR inhibitors),²⁹³ amongst many others.
282,294,295

Many of these host modulatory proteins are vitally important for functional MYXV infection and replication in its lagomorph host, and it is easy to infer that some of these proteins could be of importance when considering MYXV as an oncolytic virus. However, this is incredibly complicated by the fact that many of these proteins are

species-specific. For example, the soluble receptors M-T2 and M-T7 have both been shown to specifically bind rabbit TNF α and IFN γ , respectively, with no binding affinity for any other species tested, including murine and human.^{285,296} It is not known what other proteins are species-specific or cross-specific, and this is an important aspect to keep in mind when using oncolytic viruses whose natural tropism is other than humans.

1.4.4.2. Myxoma virus as an anti-glioma agent

The above discussion highlights many of the reasons MYXV is appealing as an oncolytic virus: 1.) The dsDNA genome is large and capable of being engineered to introduce large transgenes of interest; 2.) Cytoplasmic replication prevents the exchange of genetic material between the cancer cell and the virus; 3.) A host range that is extremely narrow; 4.) Proven track record for safety in humans and other non-human species. Of course, it can also kill cancer cells.

The oncolytic activity of MYXV was first shown in screen on 21 NCI cancer lines, where 15 (>70%) were able to be productively infected with the virus.²⁹⁷ The oncolytic activity of MYXV was immediately tested in preclinical models of glioma, using a panel of established glioma cell lines and primary patient specimens, demonstrating that MYXV could infect, replicate and kill these lines at relatively low multiplicities of infection (0.1 – 10 **MOI**).²⁵³ Astoundingly, MYXV was shown to ‘cure’ nearly 100% of orthoxenografts in nude mice when treated with 5.0×10^6 PFU twelve days after tumour implantation. MYXV infection and replication extended past 42 days post treatment, and titres only dropped as a result of the tumour being destroyed. These results were very exciting, and were subsequently extended into medulloblastoma orthoxenografts (cure of 60% of mice)²⁹⁸ and rhabdoid orthoxenografts (cure of 67% of mice)²⁹⁹, with both

models producing durable intratumoural infections. Recently, MYXV was found to be able to infect, replicate and kill human brain-tumour initiating cell lines, albeit they were more refractory to the therapy than had been seen in conventional cell lines.³⁰⁰ This translated *in vivo*, with no durable ‘cures,’ but significant survival benefit (30-50% increase in survival). BTICs also displayed persistent infection up to at least 21 days post-infection, with concomitant rapamycin treatment able to increase viral replication rates in the tumour and further extended survival.

As mentioned, rapamycin was found to increase *in vivo* viral replication of MYXV, JX-594 and VSVΔ51 (**Table 1.3**); its mechanism of action has only briefly been mentioned. Rapamycin inhibits the mammalian-target of rapamycin complex’s (mTORC1 and, partially, mTORC2), which is a very complicated and important central signalling complex. Its role in cancer therapy is thought to occur through the inhibition of mTORC1 inhibiting phosphorylation of P706K1 and 4EBP1, which are both involved in regulation of translational processes, resulting in cell cycle arrest and autophagy.³⁰¹ In immunity, mTORC1 and mTORC2 play roles in T and B cell proliferation and activation, Type-I interferon responses, antigen presentation, and antibody production.³⁰² The diverse actions of this drug make the exact mechanism through which it functions *in vivo* to enhance OV therapy difficult to discern.

However, it has been shown that rapamycin will also increase MYXV replication *in vitro* in some of the human and rat cell lines we have tested *in vitro*.^{220,298,300} Part of the tropism of MYXV in cancer cells is thought to occur through the constitutional activation of AKT,^{303,304} which often occurs as a consequence of perpetual growth factor signalling or the absence of a negative regulator PTEN (both of these events are common in

GBMs¹¹). Rapamycin inhibition induces mTORC1 to up-regulate AKT activation, possibly by inhibiting IRS1 to activate IGF-1 signalling,³⁰⁵ thus in cells where AKT is only partially activated, rapamycin treatment may further up-regulate AKT activity to enhance tropism.³⁰⁴ The fact that rapamycin both enhances viral tropism to cancer cells while potentially inhibiting anti-viral immune responses, and has already been shown to have significant anti-glioma activity in the clinic,³⁰⁶ makes rapamycin a very viable candidate for combination therapy in the clinic with OV_s for gliomas.

Although touched on briefly already, the study we performed in the immunocompetent RG2 and F98 syngeneic rat models has showed quite different results than the orthoxenografts. Despite seeing such robust viral infection for extended periods of time in several different orthoxengraft models, MYXV virus was cleared from the tumour-bearing brain very swiftly, with little recoverable virus from the tumour at day 3 and none by day 7. Interestingly, rapamycin significantly enhanced this infection/replication *in vivo*. We also enhanced infection/replication using convection enhanced delivery (CED), which is a system to slowly infuse a large volume of therapeutic through a catheter to a localized position within or around the tumour. This system allows for larger volumes to be delivered while dramatically increasing the distribution of the therapeutic.³⁰⁷ This system in the RG2 model also increased viral infection and viral titres within the tumour, and when combined with rapamycin had a lengthy infection that remained stable in the tumour for greater than 12 days. Without rapamycin administration, CED delivered MYXV was cleared by this time, but increased initial infection. CED with MYXV alone only provided a very small survival benefit, but rapamycin included in this regimen increased survival by over 2.5-fold. Collectively

these data suggest that MYXV in syngeneic rat models is cleared very quickly and intracranial virus administration is not adequately infecting even these small tumours. Inhibition of immunity and/or increasing tumour susceptibility while maximizing viral delivery will be key to advancing this therapy. Future studies interrogating how this MYXV is cleared from the syngeneic glioma microenvironment are warranted.

1.5. Literature review summary, overall hypothesis and specific aims

The study of oncolytic virotherapy is complex, bridging the disciplines of cancer biology, virology and immunology. Further, when administering these viruses to a notoriously virus-sensitive organ such as the brain, the complexity of this therapy increases dramatically. What the above literature review was aimed to accomplish was to demonstrate the intricacies of human gliomas, especially their interactions with the ‘normal’ brain and immune system, and how many of these intricacies can only be modelled in orthotopic grafts or spontaneous models of glioma in immunocompetent animals. Also, it covers how oncolytic virotherapy lies in a delicate balance between being overwhelmed by innate immunity such that it is cleared before any treatment benefit can occur with being able to subvert tumour-induced immunosuppression to activate an anti-tumour immune responses. Given the divergent roles the immune system can play in mediating the efficacy of this therapy, I hope it is clear that appropriate immunocompetent mouse models should be used when analyzing the potential for this therapy in glioma patients.

This has been demonstrated when looking at the discrepancies between preclinical studies and clinical outcomes of oncolytic therapy for gliomas. Unlike the preclinical models that demonstrate durable and robust infection rates resulting in ‘cures,’ the two

clinical studies^{221,249} in human glioma patients demonstrated that: 1.) the virus is cleared very quickly, and 2.) that this clearance is accompanied by a robust immune infiltrate. Collectively with the other trials we can add a third point, that overall OV therapy is not effective in glioma patients. What is striking is the similarity of these results to what has been demonstrated in the few studies investigating how syngeneic orthotopic glioma models react to OV treatment.

Studies using oncolytic viruses in syngeneic glioma models more closely resemble the clinical results. In these studies, OV therapy alone is rarely sufficient to find therapeutic benefit. Further, lasting tumoural infection and viral replication is often limited to several days, not weeks. In the studies that did find therapeutic benefit with OV alone, microscopic orthografts are treated with virus soon after implantation. These tiny tumours are likely being ‘saturated’ with virus, biasing these results towards therapeutic efficacy. However, when suppressing putative virus clearing immune effectors with chemotherapeutics, we can see increased viral infection, replication, and/or efficacy in syngeneic models. This strongly suggests that immediate anti-viral immune responses are responsible for clearing OVs before anti-tumour activity can occur.

Despite the sporadic use of orthotopic syngeneic models in the literature, there has only been several studies that robustly characterized the immune response to intracranial oncolytic virus administration. Given the role the immune system may play, this is a largely under-investigated area. Further work is warranted to assess which immune effectors are limiting viral infection/replication and which may be able to enhance anti-glioma activity. These responses, which may be general in a larger

neuroinflammation sense, will likely have caveats applicable to each oncolytic virus used.

During the duration of my thesis I tried to model my experiments as closely as possible to relevant clinical obstacles. To achieve this, I used primary murine glioma cell lines orthografted into immunocompetent mice with macroscopic tumours in an attempt to delineate immune effectors dictating Myxoma virus therapeutic outcomes under the overall hypothesis that:

A fully immunocompetent glioma model will be refractory to oncolytic Myxoma virus therapy due to rapid anti-viral responses that will clear the infection before significant anti-tumour activity will occur. Inhibition of these factors to achieve viral replication and pan-tumoural infection will result in significant therapeutic benefit.

To test these hypotheses, I undertook the following specific aims, each demarcated into its own chapter.

AIM I (Chapter 3): To find or create murine syngeneic glioma lines derived from spontaneous tumours with relevant human glioma genetics. These lines must be susceptible to MYXV infection and replication *in vitro*. These lines must closely resemble the features associated with human gliomas when orthotopically implanted in syngeneic mice. Ideally, these mice would be on the C57Bl/6 background.

AIM II (Chapter 4): To interrogate type-I interferon responses in syngeneic models with Myxoma virus. Given the specific nature of type-I interferons, it was hypothesized that these cytokines would play a key role in dictating viral infection and replication in syngeneic models.

AIM III (Chapter 5): To immunophenotype the syngeneic glioma microenvironment to identify candidate immune cell populations that may be mediating premature Myxoma virus clearance from the tumour. We hypothesized that tumour-resident or recruited immunocytes may be involved and that ablating these cell populations transgenically or pharmacologically could enhance viral infection and replication in the glioma.

2. MATERIALS AND METHODS

2.1. Cell Culture

2.1.1. Mouse adherent cell lines: Origins and culture techniques

NPcis cell lines (K1492, K1861, K1491 and K5001) were derived from C57Bl/6 *Trp53^{+/-}/Nf1^{+/-}* mice,^{127,131,133} and were a kind gift from Dr. Karlyne Reilly (NCI Frederick). The RasB8 (**B8**) cell line was derived from astrocytoma-bearing transgenic GFAP-V¹²Ha-ras ICR mice¹³⁹ and was a kind gift from Dr. Abhijit Guha's laboratory (Sick Kids Center for Research and Learning, Toronto). GL261 cell lines were obtained from Dr. Luc Vallieres' laboratory (Laval University, Montreal). B16-Blue was purchased from InvivoGen (#bb-ifnab, InvivoGen). These mouse lines were grown in High Sucrose DMEM (#11965, Gibco) containing 10% fetal bovine serum (**FBS**; Invitrogen), and B16-Blue with ZeocinTM (100 mg/ml). Cells were grown at 37°C in a humidified 5% CO₂ incubator (ThermoScientific), and passaged at 80-90% confluence. Cells were harvested or passaged using a 0.05% Trypsin-EDTA (#25300, Gibco) following a brief wash with phosphate buffered saline (PBS). Cells were tested for mycoplasma at regular intervals.

2.1.2. Human adherent cell lines: Origins and culture techniques

U87 and U251 cell lines were obtained from the American Type Culture Collection (Manassas, VA, USA), and HS68 human foreskin fibroblasts cells were a kind gift from Dr. Karl Riabowol's laboratory (University of Calgary). These cells lines were cultured in Dulbecco's modified Eagle medium F12 (#11330, Gibco) with 10% FBS. HEK-Blue cells were purchased from InvivoGen (#hkb-ifnab, InvivoGen). These were cultured in High Sucrose Dulbecco's modified Eagle medium (#11965, Gibco) containing 10% FBS

and Zeocin™ (100 mg/ml) and Blastocidin (30 µg/ml). Human fetal astrocytes were a kind gift from Dr. Wee Yong's laboratory (University of Calgary) and derived as previously described.¹⁰⁰ These cells were maintained in GIBCO DMEM (#11700-077, Invitrogen), 0.1mM DMEM non-essential amino acids, 1mM sodium pyruvate, 1mM L-glutamine, 0.1% dextrose, 100ug/mL Pen/Strep (Invitrogen) and 10% FBS. All cell lines were grown at 37°C in a humidified 5% CO₂ incubator (ThermoScientific), and passaged at 80-90% confluence using 0.05% Trypsin-EDTA (#25300, Gibco). Cells were tested for mycoplasma at regular intervals.

2.1.3. Mouse brain tumour-initiating cell lines: Origins and culture techniques

Mouse brain-tumour initiating cell lines (**mBTICs**) FJZ0309, FJZ0305, and FJZ1116 were created from C57Bl/6 *Trp53*^{+/-}/*Nf1*^{+/-} mice^{127,131,133}. NPcis mice were a kind gift from Dr. Karlyne Reilly (NCI Frederick), and continued to be bred at the University of Calgary's Clara Christie Centre for Mouse Genomics facility. NPcis mice were bred to wildtype C57Bl/6 mice (#000664, Jackson Laboratories), and all litters genotyped by digesting tail snips with DirectPCR reagent (Cat # 101-T; Viagen Biotech, Inc.) and analyzed by PCR (Primers and reaction conditions in **Appendix 1**). Mice heterozygous for both transgenes were transferred into the Biohazard unit and monitored for symptoms of tumour burden, which most often included large necrotic sarcomas, abdominal masses, loss of weight, ataxia, and/or limb paralysis. All mice were sacrificed by ketamine/xylazine anesthetic followed by cervical dislocation when tumour burden or symptoms resulted in difficulty of the animals feeding, grooming or ambulating. All protocols were reviewed and approved by the Animal Care Committee of the University of Calgary (Protocol #AC12-0034).

Sacrificed animals had their whole brains immediately removed, and transferred to a culture dish containing cold 1 x PBS and 2 x Pen/Strep antibiotic solution (#15140, Invitrogen). Brains were then cut in approximately 1-2 mm coronal sections in the dish with a razor, with every other section removed and flash frozen for cryogenic sectioning (Thermo Shandon Cryotome E; **Figure 2.1 A**). Sections were H&E stained (see below protocol) and examined by microscopy for brain lesions. Any brain lesions were microdissected from the corresponding areas on the tissue remaining in the PBS solution. Removed lesions were then mechanically dissociated using sterile scissors in a new culture dish with 15 mL of 1 x PBS 2 X Pen/Strep, and then spun for 5 min at 2000 RPM. Pellets were then re-suspended and further mechanically dissociated in 100 μ L of mouse neural stem cell media [Mouse NeuroCult NSC Basal Media with Mouse NeuroCult NSC Proliferation Supplements (#05700 and #05701, Stem Cell Technologies) plus EGF (20ng/ml; Sigma), FGF2 (20ng/ml; Chemicon) and 2 μ g/mL of heparin sulfate (StemCell Technologies)]. The re-suspended cells were then placed in 12mL of mouse stem cell media with 1 x Pen/Strep and 5 μ g/ml plasmocin (InvivoGene) in low adherence culture flasks (Sarstedt, #83.1810.502), and fed every 3-4 days until spheres started to develop. Mouse neurospheres were dissociated using Accumax (SCR006, Millipore) and expanded until the second passage, when frozen stocks were created by freezing cells in mouse stem cell media plus 10% dimethyl sulfoxide (Sigma) and storing in liquid nitrogen storage units. Further culture of mBTICs was done in the absence of antibiotics and plasmocin. Carcasses of sacrificed animals also went through a gross autopsy for analysis of additional tumours.

Wildtype mouse neural stem cells were harvested from the subventricular zone of CD1 mice, and were a kind gift from Dr. Jennifer Chan. These cells were cultured in the same manner as the mBTICs.

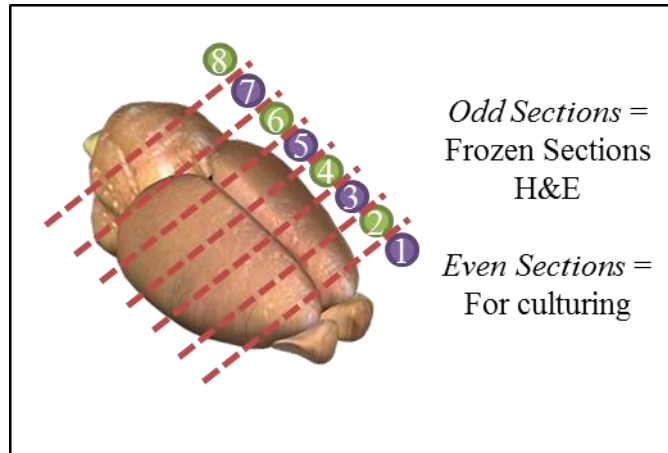


Figure 2.1: *Dissection of NPcis mouse brain at autopsy.* NPcis mice sacrificed as a result of complications arising from tumour burden had their brains removed and examined for astrocytoma formation. Brains were sliced coronally in 1-2 mm sections, and every other section flash frozen, sections cut, and stained with H&E. Sections were examined for visible lesions, and any present were dissected out of corresponding area of tissue and placed in culture.

2.1.4. Human brain tumour-initiating cell lines: Origins and culture techniques

Human brain-tumour initiating cells (**BTICs**) were obtained from the Clark H. Smith Neurologic and Pediatric Tumor and Related Tissue Bank, Calgary, Alberta, Canada, and created as described elsewhere.³⁰⁸⁻³¹¹ These lines were cultured under neurosphere conditions in human stem cell media [Human NeuroCult NS-A Basal Medium plus Human NeuroCult NS-A Proliferation Supplements (#05750 and #05753, Stem Cell Technologies) plus EGF (20ng/ml; Sigma) and FGF2 (20ng/ml; Chemicon)]. Brain tumour cell cultures were passaged as needed by dissociating spheres using Accumax (SCR006, Millipore) and seeding culture flasks (Falcon, #353109) with single cells.

2.2. Myxoma virus: Strains and *in vitro* infection and replication assays

2.2.1. Myxoma virus strains and propagation

Viruses (vMyx-GFP, vMyx-FLuc,³⁰⁰ and vMyx-RFP³¹²) were obtained from the McFadden laboratory or grown in our laboratory as described.²⁷⁰ Briefly, BGMK cells were plated in expanded surface roller bottles (Fisher #06-419-9) in 120mL of complete MEM (Invitrogen #26140-079) + 10% FBS in 37°C, 5% CO₂ incubators (Thermo) equipped with a bottle roller and grown until 80% confluent (2-3 days). All but 20mL of media was then removed, and MYXV added at an MOI of ~0.05. Rolling continued for 1 hour, and then 100 mL of fresh MEM added, and continued to roll. After 72 hours, media is removed, and cells washed and trypsinized and collected in 50 mL falcon tubes. Cells were pelleted by centrifugation of 1930 x g at 4°C for 5 minutes, pellets resuspended in 5 mL of 10 mM Tris-HCl (pH 8.0). Purification is conducted by sonicating the solution in a cup sonicator 2 x 1 minute, with a 1 minute rest interval on ice in-between, with the sonicator containing a 1:1 ratio of ice:water. The solution was then further homogenated in a sterile, pre-chilled 40 mL Dounce homogenizer, and the homogenate spun at 1040 x g at 4°C for 15 minutes. Supernatant was stored, and pellet resuspended in Tris-HCl and Dounce homogenization and spin repeated. Supernatants were combined and carefully layered on a sucrose cushion of 36% sucrose in 10 mM Tris-HCl (pH 8.0), and spun for 80 minutes at 58,267 x g at 4°C. Virus pellet was then re-suspended in 1.5 mL of 10 mM Tris-HCl (pH 8.0) and then further purified by careful layering over a 24 - 40% sucrose gradient (2 mL each of 40, 36, 32, 28 and 26% sucrose in 10 mM Tris-HCl) and spun for 40 minutes at 33,518 x g at 4°C. The viral band was carefully removed, and respun for 60

minutes at 43,780 x g at 4°C, and virus pellet finally resuspended in 10 mM Tris-HCl (pH 8.0), aliquoted, and stored at -80°C. Virus titre was determined as described below.

UV-inactivated MYXV (dead virus; **DV**) was prepared by irradiating virus with UV light for 4 hours, and tested for infection on permissive BGMK cells.

2.2.2. *Myxoma virus infection and replication in vitro*

Viral titres on adherent cell lines were performed as previously described.^{220,253,270,298} Briefly, cells were plated at 2.5×10^4 cells/well in a 24-well plate overnight, and then infected the following morning with indicated MOI of MYXV. Input virus was placed in a well with media but containing no cells and harvested as the experimental time points were harvested. Supernatants from infected cells were collected, subjected to three freeze thaw cycles at -80°C and then plated in serial dilution on 80-90% confluent BGMK cells plated in 6-well plates. GFP (vMyx-GFP) or mCherry (vMyx-FLuc) foci were then counted on the BGMK lawn and viral titres calculated as fluorescent focus forming units (**FFU**) per mL.

Viral infection and replication was qualitatively assessed via early viral gene expression of GFP under the synthetic early/late vaccinia virus promoter^{220,253,270,298} at indicated times post infection. Cells and GFP fluorescence were observed by microscopy (Zeiss inverted microscope with AxioVision v4.5 Software).

2.3. Viability assays and drug treatments

2.3.1. *AlamarBlue*®

To detect viability of adherent or neurosphere cultured cell lines *in vitro* by AlamarBlue® (Invitrogen), cells were plated in 100 µL of media in 96-well plates

overnight, and then given treatment the following day. Cell viability was measured at the indicated time point by addition of 10 μ L alamarBlue reagent as described by the manufacturer. Values were obtained by measuring fluorescence with a 544 nm excitation and 590 nm emission (Molecular Devices SpectraMax M2 spectrophotometer, using SoftMax Pro software) after ~2 hours of incubation at 37°C (dependent on cell type). Viability is often shown as percent control, whereby the treatment values are divided by the control values.

2.3.2. *Thiazolyl blue tetrazolium bromide (MTT) assay*

Initial experiments used thiazolyl blue tetrazolium bromide (MTT) viability assays. Here, cells were seeded in 24-well plates (2.5 $\times 10^4$ cells/well) the previous night, and then given treatment as per the experimental conditions. Media was removed at desired time point, and 300 μ L 5mg/mL thiazolyl blue tetrazolium bromide (Sigma) in 1 x PBS was added for 3 hours and incubated at 37°C. 300 μ L of stop solution (20% SDS in 50% dimethyl formamide) was then added and the plate was placed on a circular shaker for 1 hour at room temperature. Solution was then mixed and 200 μ L added to a clear bottom 96-well plate in duplicate, and absorbance measured at 560 nm (test) and 630 nm (reference). Final values used were the test minus the reference wavelengths.

2.4. Cytokine measurements *in vitro*

2.4.1. *HEK-Blue and B16-Blue assays for IFN α/β*

Quantitating functional Type-I IFN *in vitro* was performed using HEK-Blue and B16-Blue interferon reporter cell lines. Experimental supernatant was obtained by plating cell lines overnight in 96-well plates, and then treating with the listed stimulus. Extracellular

polyI:C (pI:C EC; Cal-tech) was 25 $\mu\text{g}/\text{mL}$ placed directly on cells, while intercellular polyI:C referred to 1 $\mu\text{g}/\text{mL}$ packaged in lipofectamine 2000 (Invitrogen) at a 3:1 lipofectamine:polyI:C ratio. 20 μL of the supernatant from the treated cells was added to 96-well plates containing 180 μL of media containing ~50,000 HEK-Blue or ~75,000 B16-Blue cells, grown previously for 24 hours in 37°C incubator. 20 μL of the media was then transferred to 180 μL of QUANTI-Blue (InvivoGen), incubated for 3 hours, and then SEAP levels determined using a spectrophotometer (Molecular Devices SpectraMax M2 spectrophotometer, using SoftMax Pro software) at 650 nm.

2.4.2. Reverse transcriptase (RT)-PCR

To confirm IFN α/β production or to measure the induction of the listed genes at the transcriptional level, RNA was collected (Qiagen RNeasy Plus) from cell lines plated at 2.5×10^5 cells/well in 6-well plates seeded overnight and treated with the listed stimulus. cDNA was created with SuperScript II Reverse Transcriptase (Invitrogen) and PCR performed using Taq Polymerase (Invitrogen). Primers sequences found in **Appendix 1**.

2.4.3. IFN α/β reporter plasmid

5.0×10^3 cells stably transfected with the ISRE::FLUC plasmid (**Chapter 2.5.2**) were plated in black-sided/clear-bottom 96-well plates (655986, Greiner bio-one). Cells were then treated with the listed stimulus. At the designated time post-treatment, D-luciferin (Caliper LifeSciences) solution was added to each well to a final concentration of 0.15 mg/mL. Plates were covered and transported to the Xenogen IVIS 200 system where

luciferase expression was measured and quantified through luminescence using the associated software Live Image v4.1 (Caliper, LifeScience).

2.4.4. *ELISA: Single and multi-cytokine ELISA luminex – in vitro*

NPcis cells lines K1492, K1861 and K1491, along with GL261 were plated at 5.0×10^4 cells/well in 24-well plates overnight. The following morning, the cells were treated with exogenous polyI:C, vMyx-GFP, or DV, and supernatants collected 24 hours after treatment. A 32-plex ELISA from Eve Technologies (Calgary, Alberta) was performed on these supernatants.

For measuring CCL2 in response to different growth factors, 2.5×10^4 K1492 cells were plated in 96-well plates overnight, serum-starved for 8 hours and then given 10 ng/mL of EGF, FGF2, or PDGF. Supernatants were harvested 24 hours later for analysis of CCL2 as measured by an ELISA kit following the instructions listed in the manufacturers protocol (Ebioscience, 88-7391-86).

2.5. **Creation of modified NPcis cell lines**

2.5.1. *Lentiviral packaging and transfection*

ISRE::FLUC and IRF9 shRNA plasmids were co-transfected into HEK-293 METR cells with pMD2.G (VSV.G env) and pCMV-deltaR8.91 envelope and packaging plasmids (kind gifts from Dr. Brain Rabinovich; MD Anderson). Supernatant was discarded 12 hours after infection, and then collected following 24 and 48 hours. Supernatants were then concentrated ~50X using Amicon Ultra 100K centrifugal filters (#UFC910008, Millipore) and added to K1492 or U87 cells with 1.6 µg/mL of polybrene (Sigma) overnight.

2.5.2. *Interferon responsive firefly luciferase construct for the stable transfection of cell lines*

To create an interferon-responsive firefly luciferase construct for the stable transfection of cell lines, we combined pieces of two plasmids. The main backbone for the construct was the lentiviral vector pLV430 oFL-T2A-mCherry, which we have previously used to label human BTIC lines.³¹¹ This plasmid contains a murine optimized firefly luciferase and mCherry reporter separated by a T2A cleavage sequence.³¹³ These reporter genes are driven off of a MSCV LTR promoter. This strong, constitutively active promoter was exchanged with five copies of the interferon stimulated response element (ISRE) containing a minimal TATA box promoter found in the PATHdetect ISRE *cis*-Reporting System (#219092, Stratagene; **Figure 2.2**). Briefly, the response element and minimal promoter area on the PATHdetect plasmid were amplified by PCR using forward and reverse primers that contained *Cl*I and *Pf*I restriction sites, respectively (see **Appendix 1** for primer sequences). This PCR fragment was then cloned with the Zero Blunt® TOPO® PCR Cloning Kit with One Shot® TOP10 Chemically Competent *E. coli* (#K2800, Invitrogen) and single colonies selected from Luria Broth plates (**LB**; #12795-084, Invitrogen) with Kanamycin (50 µg/mL). Plasmids were then purified from overnight cultures of these colonies in liquid LB with Kanamycin (50 µg/mL) using QIAprep Spin Miniprep Kit (#27104, Qiagen). Finally, both the Zero Blunt® TOPO® and pLV430 plasmids were cut with *Cl*I (R0197S, NEB) and *Pf*I (R0595S, NEB) restriction enzymes, gel purified (#28704, Qiagen), and ligated (T4 Ligase, # 46300, Invitrogen). Ligated constructs were checked by restriction digest, and vector/insert combos of the correct size transformed into DH5α *E. coli* selected on LB plates

containing 50 µg/mL ampicillin (Sigma). Single colonies were picked, expanded in liquid LB with 100 µg/mL ampicillin, and plasmids isolated (QIAprep Spin Miniprep Kit, # 27104, Qiagen) and sequenced (University of Calgary Sequencing Facility). The resulting plasmid is henceforth referred to as ISRE::FLUC, and packaged into a lentivirus and transfected into cell lines as described above (**Figure 2.2 B**).

2.5.3. *IRF9 knockdown in NPCis cell lines*

shRNA constructs in K1492 and K1861 were created using a set of Sigma Mission IRF9 shRNAs (Catalogue numbers and Sequences in **Appendix 1**) or Scrambled (#SHC002) in pLKO.1-puro vectors. The shRNA vectors was co-transfected into HEK-293 METR cells with pMD2.G (VSV.G env) and pCMV-deltaR8.91, and lentivirus particles isolated and concentrated as described in the previous section. One day after infection, media was removed and replaced with DMEM (#11965, Invitrogen) with 1.0 µg/mL of puromycin (#A11138-03, Invitrogen). shRNA pool of the knockdown were screened by pre-treating K1492 with 10 U/mL of mIFN β (PBL Interferon Source) and infecting with 2 MOI of vMyx-GFP. It was identified that shRNA ‘clone 5’ had the most infected cells as measured by GFP foci. Next, we derived single colony clones from ‘clone 5’ IRF9 knockdown and the Scrambled control. These single colonies were again screened, and it was found that clone 5.4 had the least protection with exogenous IFN β from vMyx-GFP infection, while scrambled controls remained protected. Clone 5.4 was chosen for all subsequent experiments.

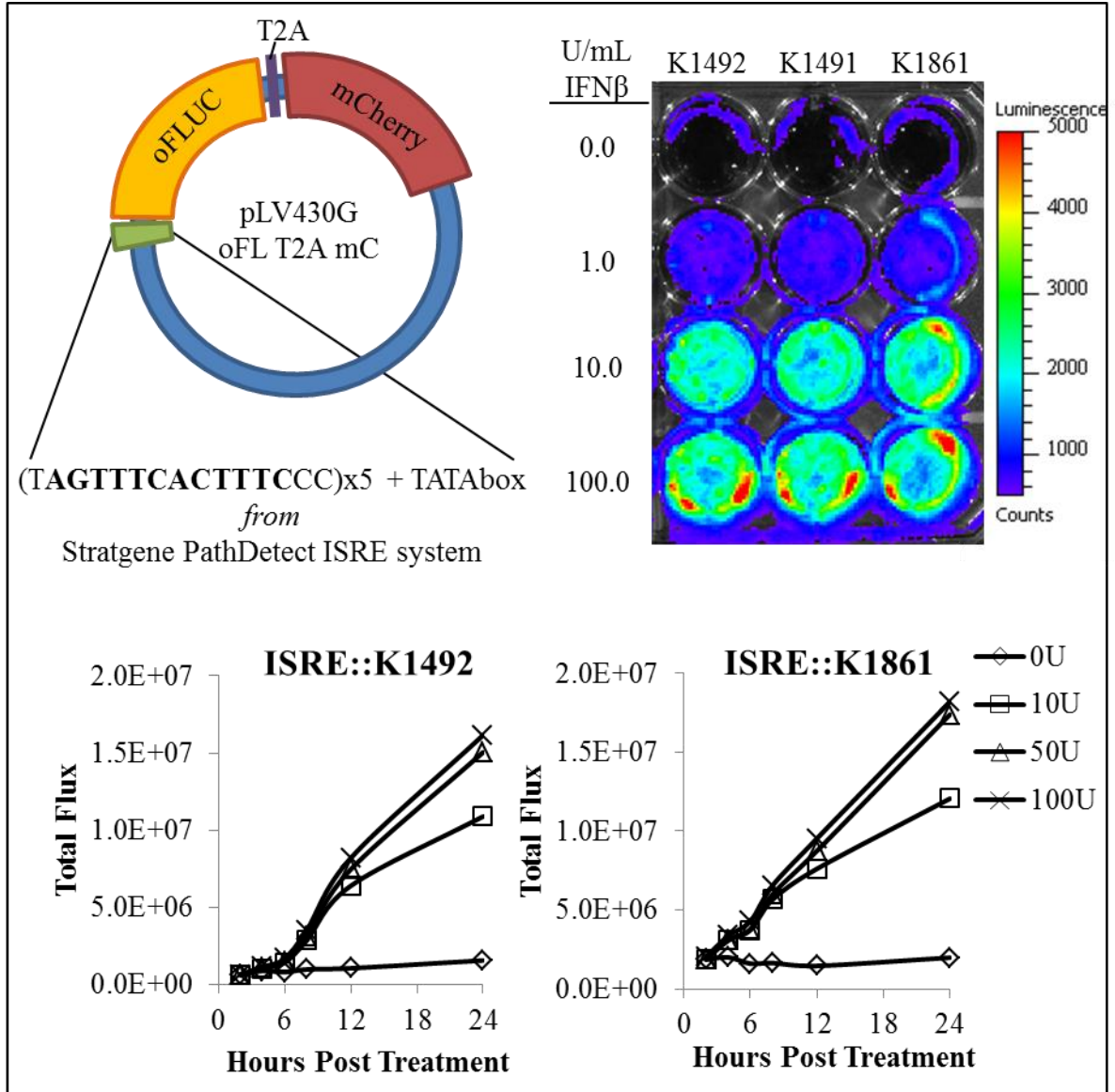


Figure 2.2: Creation of a type-I interferon responsive luciferase reporter construct in a lentiviral reporter plasmid. The interferon responsive elements and minimal TATA box promoter found in the Stratgene PathDetect ISRE system was cut out and spliced into the pLV430G oFL T2A mC plasmid, replacing the MSCV LTR promoter with this regulatory element. This plasmid packages in a lentiviral system, and easily transfects cell lines to make them responsive to IFN α/β in a dose and time-dependent manner.

2.6. Stem cell marker expression in mBTIC lines

2.6.1. Western blotting

For stem cell markers, 2.5×10^5 early passage mBTICs were dissociated into single cells and plated in 6-well plates in mouse stem cell media in the presence or absence of 1% FBS, and harvested 7 days later. Western blots were performed using 50 μ g of total protein run on in 12% polyacrylamide gels (37.5:1 acrylamide:bis-acrylamide; BioRad) and transferred onto nitrocellulose membranes (BioRad). Western blot antibodies were SOX2 (Millipore AB5603, 1:1000) and TUJ1 (Sigma T2200, 1:1000) and were detected using a goat anti-rabbit HRP (Pierce 31460, 1:10000). Nestin (Millipore MAB353, 1:1000), GFAP (Millipore MAB360, 1:1000), BMI-1 (Millipore 05-637, 1:1000) and OLIG2 (Millipore MabN50, 1:1000) were detected using goat anti-mouse HRP (Pierce 31430, 1:5000).

2.6.2. Immunocytochemistry/Immunofluorescence

Immunocytochemistry/immunofluorescence was performed by spinning spheres onto slides with Cytofunnels (Thermoscientific, A78710005) Cells were fixed with 4% paraformaldehyde for 20 mins, then rinsed twice with cold PBS. Cell membranes were permeabilized for 10 min with PBS containing 0.25% Triton X-100, and then blocked with 10% goat serum in PBS with 0.3 M glycine. Primary antibodies were diluted in PBS with 10% goat serum and placed on slides in a dark, humidified chamber at room temperature for 1 hour. Secondary antibodies were diluted in 10% goat serum in PBS and incubated in same chamber for 1 hour. Coverslip mounting and DAPI staining were done simultaneously using VECTASHIELD® Mounting Media with DAPI (H-1200, Vector). Antibodies used were SOX2 (Millipore AB5603, 1:200) and TUJ1 (Sigma T2200, 1:200)

and were detected with goat anti-rabbit RFP (Jackson 115.012.003, 1:200). NESTIN (Millipore MAB353, 1:100), GFAP (Millipore MAB360, 1:200), BMI1 (Millipore 05-637, 1:200) and OLIG2 (Millipore MABN50, 1:200) were detected with goat anti-mouse GFP (Invitrogen A11029, 1:200). Slides were then analyzed by microscopy (Zeiss inverted microscope with AxioVision v4.5 Software).

2.7. H&E and immunohistochemistry

2.7.1. Mounting frozen sections

Frozen sections were mounted using OCT (Tissue-Tek, 4583). Mouse brains were removed and then placed on dry ice until partially frozen. Brains were then cut coronally using a razor blade (0.5mm behind injection site if tumour and/or virus treated) and placed face down on clear plastic mounting tray with a small layer of mounting media on the bottom. Mounting bracket was then placed overtop and filled with mounting media. These blocks were then set in a metal dish containing ~5mm of 100% ethanol place in a Styrofoam container containing dry ice. Frozen blocks were then sectioned using a Thermo Shandon Cryotome E and/or stored at -80°C.

If frozen sections were being cut from brain slices from NPCis mice for examination of brain lesions, the slice of brain was mounting on Tissue Tec mounting media on a mounting bracket, covered with a thick layer of mounting media, and then flash frozen using the freezing press in the Thermo Shandon Cryotome E.

2.7.2. H&E staining frozen sections

Frozen sections were fixed in formyl alcohol (10% 37.5% Formaldehyde in 100% ethanol) for a minimum of 2 minutes, and rinsed briefly with water. Slides were place in

haematoxylin for 4 minutes, rinsed with water, placed in 1% glacial acetic acid in 100% EtOH for 10 seconds, rinsed with water, and then dipped in 0.5% ammonia in ddH₂O for 10 secs and then rinsed with water. Slides were then dehydrated in successive 70% and 100% EtOH for 10 seconds, placed in 0.1% Eosin in 100% EtOH for 10 seconds and two successive washes in 100% EtOH for 10 seconds each. Staining was then preserved with two successive 10 seconds dips in xylene. Coverslips were added to slides and fixed with toluene-based mounting reagent (TBS SHUR/mount)

2.7.3. Immunohistochemistry for Myxoma virus, glioma markers, and confirmation of knockdown

K1492 and K1861 glioma-bearing mice were sacrificed, and brains placed in 10% buffered formalin for a minimum of 48h. Brains were then cut coronally approximately 0.5 mm behind the injection site and mounted in paraffin blocks, and the first and last slides cut were stained using standard H&E by AIRG Histology Services or Foothills Hospital Histological services. Immunohistochemistry was performed using the MT-7e (McFadden Laboratory; 1:1000) and IRF9 (Proteintech, Cat #14167-1-AP; 1:500) was detected using a biotinylated goat anti-rabbit (Vector; 1:300) and vectastain elite ABC reagent (Vector, PK-6100). GFAP (Chemicon #MAB360; 1:500) and S100b (Abcam #ab14849; 1:100) were detected using the Vector MOM kit (BMK-2202). Slides were mounted, counterstained and viewed with a Zeiss inverted microscope (Axiovert 200M) and a Carl Zeiss camera (AxioCam MRc).

2.8. Mouse strains and genotyping

2.8.1. Mice strains

Table 2.1 shows the names and source of the mice purchased. Whenever possible, six to eight week-old female mice were used. The animals were housed in a vivarium maintained on a 12-hour light/dark schedule with a temperature of $22 \pm 1^\circ\text{C}$ and a relative humidity of $50 \pm 5\%$. Food and water were available *ad libitum*. RAG1/IL2R γ -null mice were created by crossing a female RAG1-null mouse with a male IL2R γ -null mouse, and selecting homozygotes to breed progenies for experiments. These homozygotes were then inbred to receive mice for experimentation. CD11b::DTR mice were backcrossed to C57Bl/6 mice for a further 4 generations, and homozygotes then selected and bred.

Table 2.1: *Origins and strains of mice used*

In-Text Name	Strain Name	Producer/Origin	Strain Number
C57 or WT	C57BL/6	Jackson Labs	000664
<i>Rag1</i> -null	B6.129S7- <i>Rag1</i> ^{tm1Mom} /J	Jackson Labs	002216
<i>Ccr2</i> -null	B6.129S4- <i>Ccr2</i> ^{tm1Ifc} /J	Jackson Labs	004999
<i>Il2rg</i> -null	B6.129S4- <i>Il2rg</i> ^{tm1Wjl} /J	Jackson Labs	003174
CD11b::DTR	B6.FVB-Tg(ITGAM-DTR/EGFP)34Lan/J	Jackson Labs	006000
SCID	<i>Icr-Prkdc</i> ^{scid}	Charles River	236

2.8.2. Genotyping mice

Mice were genotyped through tail snips performed by the CCCMB facility at the University of Calgary. Tails were placed in 300 μL of DirectTail Lysis Reagent (#102-T,

Viagen) with 0.4 mg/mL of Proteinase K (Sigma) and incubated at 55°C on a shaker platform overnight. Tails were then placed at 85°C for 45 mins, and then 2 µL used in 20 µL PCR reaction using recombinant DNA Taq polymerase (10342, Invitrogen). Primer sequences and specific reactions are listed in **Appendix 1**.

2.9. Intracranial surgeries

2.9.1. Orthotopic tumour implantation

For orthotopic injections of NPCis cell lines, the cells were prepared in a 2.5×10^4 cell/µL PBS solution and 2 µL (5×10^4) cells implanted into the right striatum of mice as described previously.^{220,253,262,308} Briefly, mice were anesthetized with ketamine/xylazine, a small incision made in the scalp, and a 0.5-mm burr hole made 1.5–2 mm right of the midline and 0.5–1 mm posterior to the coronal suture. Stereotactic injection used a 10-µL syringe (Hamilton Co., Reno, NV) with a 30-gauge needle, inserted through the burr hole to 3 mm, mounted on a Kopf stereotactic apparatus (Kopf Instruments, Tujanga, CA). The needle was left in place for 60 seconds, and then slowly withdrawn over a 60 second period. For survival studies, animals were followed until they lost $\geq 20\%$ of body weight or had trouble ambulating, feeding, or grooming.

2.9.2. Intracranial treatments

Intracranial injection of 5×10^6 FFU of vMyx-FLuc or vMyx-GFP, PBS, DV or polyI:C (Caltech) was performed on day 14 for all lines, unless otherwise stated. Treatments were intratumourally administered using the same stereotactic technique as described above, and through the same burr hole created for the tumour implantation. All

animal work procedures were in accordance with the Guide to the Care and Use of Experimental Animals published by the Canadian Council and all protocols were reviewed and approved by the Animal Care Committee of the University of Calgary (Protocol #AC12-0034).

2.10. *In vivo* monitoring of viral infection and replication

2.10.1. In vivo viral replication

Viral recovery from tumour-bearing mice was done at day 0 (~30 mins post-infection), 1, 3, 5, and 7 days post-infection. Animals were sacrificed and the tumour-bearing hemisphere crushed in the 500 μ L of cold PBS using a small pestle, and then sonicated (2 x 2sec, 10% Amplitude; Fisher Scientific Sonic Dismembrator Model 500), and spun at 3000 x G for 15 minutes and frozen. Supernatants were thawed and then titred on BGMK cells as described above.

2.10.2. Monitoring viral infection with bioluminescence imaging

Bioluminescence from the vMyx-FLuc-infected cells was imaged with the Xenogen IVIS 200 system by intraperitoneal injection of D-Luciferin, Firefly, potassium salt, (#119222, Caliper Life Sciences) made to 30 mg/mL in PBS and filter sterilized through a 0.2 μ M filter. Luciferin was given at a dose of 5 μ L/g. Data were analyzed by drawing a region of interest around the entire skull and measuring the total luminescent emission from that area in units of Total FLUX.

2.11. Immunophenotyping the glioma microenvironment before and after intracranial MYXV treatment

2.11.1. Multi-cytokine ELISA in vivo

Animals were sacrificed and the tumour-bearing hemisphere crushed in the 500 μ L of cold PBS using a small pestle, sonicated (2 x 2sec, 10% Amplitude; Fisher Scientific Sonic Dismembrator Model 500), spun at 3000 x G for 15 minutes, then filtered through a 0.22 μ M filter, and frozen. A 32-plex ELISA was performed by Eve Technologies (Calgary, Alberta) on these samples.

2.11.2. IFN α / β ELISA in vivo

To measure IFN α / β production *in vivo* following listed treatments, we used C57Bl/6 mice bearing 14 day K1492 tumours. Mice were sacrificed at designated time points post-treatment, and brains removed. The tumour-bearing hemisphere was dissected out, and placed in 500 μ L cold PBS in a 1.5 mL microfuge tube. Brains were crushed in the tube using a micropestle, sonicated (2 x 2sec, 10% Amplitude; Fisher Scientific Sonic Dismembrator Model 500), and spun at 3000 x G for 15 minutes. Supernatants were then diluted to normalize protein levels (Bradford Assay; BioRad) and applied to Mouse Verikine Interferon α (#42120), β (#42400) and γ (#42600) ELISA kit from PBL Interferon Source as per the manufacturer's protocol.

2.11.3. Flow cytometry for immunocytes in the glioma microenvironment

Flow cytometry of immunocytes in the glioma microenvironment required the isolation of these cells from the brain. Mice bearing 12 day K1492 glioma orthografts were treated with vMyx-GFP or PBS, or left untreated, and then sacrificed for flow

cytometry 3 days following treatment, 15 days post-K1492 implantation. To isolate immunocytes, animals were anesthetized with ketamine/xylazine, and then cardiac perfused with 6 mL of PBS. Brains were removed from the animals, and tumour-bearing hemisphere placed in 2.5 mL of RPMI 1640 (GIBCO) with 2% FBS. Tumor-bearing hemispheres were then homogenized through a 70 μ M strainer and rinsed with 10 mL RPMI 1640 2% FBS, and then brought to a final volume of 12.5 mL in a 50 mL Falcon tube. Each sample was then mixed with 5.4 mL of Isotonic Percoll [9 parts Percoll (GE) to 1 part 10 x PBS (d = 1.123 g/L)], and then underlaid with 5 mL of Percoll 1.08 (2.25 mL 1 x PBS, 4 mL Isotonic Percoll /per gradient). Samples were then spun for 1200 x G for 30 mins at 20°C. Myelin debris in top gradient was then removed by a pipette, and the 10 mL above the interface taken into a new 50 mL Falcon and 25 mL of RPMI 1640 2% FBS added. Samples were then spun for 300 x G for 15 minutes at 4°C, and then supernatant removed and pellet re-suspended in 1 mL of 1 x PBS with 0.5% FBS (FLOW-PBS).

Next, cells were aliquoted into staining groups in flow cytometry tubes, topped up to 2 mL of 1 x PBS with 0.5% FBS, and then spun at 300 X G for 6 minutes at 4°C. Pellets were then resuspended in 95 μ L of FLOW-PBS and 2 μ L of Mouse BD Fc Block (rat IgG_{2b} anti-mouse CD16/CD32 monoclonal antibody; Cat. No. 553141) for 5 minutes at 4°C. This was followed by the addition of 1 μ L of one or a combination of the antibodies found in **Table 2.2**. Isotype control cocktails were run using one or a combination of the isotype controls, as the experiment dictated. Cells were incubated for 4°C at room-temperature for 30 mins in the dark, and then 2 mL of FLOW-PBS was added and cells

spun at 300 X G for 6 minutes at 4°C. Supernatant was then carefully decanted, and the cells re-suspended in FLOW-PBS and spun again. Cells were then re-suspended in 250 µL of FLOW-PBS and then 250 µL of 8 % formaldehyde (Sigma) in FLOW-PBS. Cells were then either immediately analyzed, or stored at 4°C overnight, and then analyzed the next morning on an Attune™ Acoustic Focusing Cytometer with Blue/Red lasers using the corresponding software.

2.12. Other mouse treatments

2.12.1. Clodronate liposome administration

Clodronate liposomes were obtained from Dr. Nico van Rooijen (ClodronateLiposomes.org). K1492-bearing C57Bl/6 mice were administered 200 µL of Clodronate Liposomes or control Liposomes (Vehicle) via tail vein injection at -1, 0, 1 and 2 days post-MYXV treatment, which corresponded to 11, 12, 13 and 14 days-

Table 2.2: *Antibodies used immunophenotyping the K1492 microenvironment before and after Myxoma treatment*

Antibody	Isotype Control
PE rat IgG _{2b} ,κ anti-mouse CD45 (BD 553081)	PE rat IgGb κ anti-mouse (BD 556925)
PerCP-Cy5.5 rat IgG _{2b} ,κ anti-mouse CD11b (BD 561114)	PerCP-Cy5.5 rat IgGb κ (BD 552991)
APC Ar Ham IgG ₁ ,κ anti-mouse CD3ε (BD 533066)	APC Ar Ham IgG ₁ , κ anti-mouse (BD 553874)
PE-Cy7 rat IgG _{2a} ,κ anti-mouse Ly6G (BD 560601)	PE-Cy7 rat IgG _{2a} κ (BD 552784)
PE-Cy7 ms IgG _{2a} ,κ anti-mouse CD161 (NK1.1) (BD 561111)	PE-Cy7 mouse IgG _{2a} ,κ anti-mouse (BD 550927)

post K1492 implantation. Animals were sacrificed for flow cytometry analysis of glioma-infiltrating leukocytes or followed for viral infection and survival.

2.12.2. Minocycline administration

Minocycline hydrochloride was obtained from (Sigma) and diluted in DMSO and heated to 37°C immediately before every treatment. Although very well tolerated in humans, reaching therapeutic serum concentrations of minocycline in mice is difficult.³¹⁴ As such, an aggressive strategy to reach these concentrations before MYXV administration. K1492-bearing C57Bl/6 mice were started at 50 mg/Kg twice a day starting at 10 dpi for two days (10-11 dpi), then 50 mg/Kg once a day for 5 days (12-16 dpi), and then dropped on a maintenance dose of 25 mg/Kg for 3 days (16-19 dpi). Administration of vMyx-FLuc was given at 14 dpi.

2.12.3. Diphtheria toxin administration

Diphtheria toxin (unicked; **DT**) was obtained from List Biological Laboratories (#150) and reconstituted in sterile water and frozen in 500 µL aliquots. In preliminary experiments, C57Bl/6 mice were administered 10 ng/g or 25 ng/g via intraperitoneal injection every second day, doses shown previously to ablate cell types of interest.³¹⁵⁻³¹⁷ For studies with MYXV, 10 ng/g was administered to K1492-bearing C57Bl/6 animals at 11, 13 and 15 dpi, with viral administration at 14 dpi.

2.12.4. CD161(NK1.1) administration

Functional grade low-endotoxin CD161(NK1.1; PK130 antigen) or isotype control antibody was purchased from BioLegend (#108712 and #400224). For preliminary experiments looking at depletion of NK cells in the spleen, a single intraperitoneal

injection of 200 µg of antibody was given to C57Bl/6 mice. For measuring the effect of NK cells on Myxoma replication, CD161 or isotype control was given to K1492-bearing C57Bl/6 animals at 13 and 15 dpi, with vMyx-FLuc administered on 14 dpi.

2.13. Statistical analysis

All data were processed and graphed in either MS Excel 2010 or Prism GraphPad v5.0. Statistics were also performed in these programs. All data was assumed to be normally distributed, and F-tests were used determine if homoscedastic or heterodastic t-tests were used. All t-tests were two-sided and values were considered to be statistically significant at $p < 0.05$. *In vivo* luciferase monitoring produced highly variable data, thus distributions could not be considered normal, and non-parametric Mann-Whitney (Wilcoxon Rank Sum) tests were conducted. Survival curves were generated by the Kaplan-Meier method, and statistics were determined using the Log-rank Mantel-Cox test for all treatments together unless otherwise noted.

3. CHARACTERIZING SYNGENEIC C57BL/6 MURINE GLIOMA MODEL FOR PRECLINICAL STUDIES OF MYXOMA VIRUS THERAPY

3.1. Introduction

One of the most appealing tenants of oncolytic virus (OV) therapy is the treatment's self-potential, which hinges on the infection, replication, and spread of the virus throughout the tumor. Several OVs have been evaluated in glioma clinical trials and although safe, only a handful of clinical responses have been observed and evidence of tumour infection and viral replication was limited to very few patients.^{221,249} This is in stark contrast to what has been demonstrated in pre-clinical xenograft glioma models, where robust tumour infection and replication result in promising survival benefits, with even durable 'cures' being shown in intracranial mouse models with recombinant Poliovirus,²⁵² Reovirus,²⁵⁴ and Myxoma virus²⁵³.

So why are clinical results so disappointing (**Chapter 1.4.1.1**)? This discrepancy could be a function of the preclinical models utilized to study the efficacy of these viruses. Much of the preclinical work examining OV therapy in gliomas has been in hetero- or orthotopic xenografts of human tumor cells in immunocompromised mice. Xenografts possess two important, but potentially overlapping limitations that compromise their utility for the preclinical testing of OVs. Firstly, the immunocompromised nature of these models inevitably affects the profile of immune infiltrates within the tumour microenvironment. By changing the cellular components of the tumour stroma, the cytokine, chemokine, and growth factor networks are fundamentally changed, which may be vitally important in predicting factors that limit OV treatment efficacy. Secondly, the antiviral signaling networks that exist within the murine tumour microenvironment may not signal effectively to the human tumour due to

inter-species receptor-ligand incompatibility. Xenografts thus ignore many potential interactions between the glioma and its microenvironment prior to or during OV treatment. These interactions are potentially of great importance, especially when considering immune-glioma interactions that could result when infecting a glioma with a replication-competent virus. The retention of these factors in syngeneic models could explain the treatment failure we observe in these models and patients.

We have previously found differences between human xenograft and murine syngeneic glioma models using MYXV, whereby MYXV has robust viral replication and often cures immunocompromised mice bearing orthotopic human brain-tumor xenografts (orthoxenografts),^{234,253,298} but does not have significant replication or efficacy in syngeneic rodent orthografts.²²⁰ The lack of strong efficacy of OVs in immunocompetent glioma models is worrisome, as the rat syngeneic tumours used somewhat recapitulate human gliomas¹¹⁸ and retain immune cell populations/stromal interactions found in glioma patients. In order to interrogate the contributions that may affect efficacy of OVs in glioma patients, relevant murine models in the C57Bl/6 background would be ideal, as this background has numerous mutant and transgenic strains that could assist in delineating these mechanisms. As such, **the main objective of this introductory chapter was to identify and/or create syngeneic C57Bl/6 murine glioma cell lines for the preclinical testing of MYXV and other glioma therapeutics.**

The first experiments investigated the use of the RasB8 (**B8**) cell line, which was derived from astrocytoma-bearing transgenic GFAP-V¹²Ha-ras ICR mice,¹³⁹ and the GL261 cell line derived from C57Bl/6 mice receiving intracranial injections of 3-methylcholantrene.¹¹⁹ *In vitro* characterization of this line demonstrated that B8 was

highly susceptible to MYXV infection, replication and viral-mediated cell death, but GL261 was resistant to the virus, with little infection noted through fluorescent early gene expression even at high viral titers *in vitro*. These lines were deemed inappropriate for further preclinical testing in C57Bl/6 mice as the B8 model was produced in ICR mice, thus not syngeneic, and GL261 was inherently resistant to MYXV infection.

Next, primary mouse glioma cell lines derived from C57Bl/6 NPcis mice (*Trp53*^{+/-}/*Nf1*^{+/-}) were investigated. These mice spontaneously develop high-grade gliomas that recapitulate many clinical phenotypes of the human disease.^{127,128,131} The resulting cell lines show loss-of-heterozygosity of *Nf1* (encoding neurofibromin) and *Trp53* (encoding p53) in addition to PDGFR α expression,¹³³ clinically relevant molecular features seen in many GBM patients.^{11,12} These lines displayed a range of susceptibility to MYXV infection and replication *in vitro*, but all succumb to viral mediated cell death at high MOIs. Two of these lines, K1492 and K1861, were orthotopically grafted into C57Bl/6 mice and produced aggressive gliomas bearing astrocytic tumour markers. However, intracranial injection of MYXV failed to result in sustained viral replication or treatment efficacy. In fact, only very minimal tumour infection that was completely resolved by 5 to 7 days post-infection was found. These NPcis lines were found to be relevant preclinical models to move forward and interrogate the mechanisms of treatment failure in syngeneic models in the C57Bl/6 background.

Despite K1492 and K1861 proving to be acceptable models, their *in vivo* appearance did not represent a classical glioma, having a spindle-like appearance and lacking distinct single-cell infiltration. As such, an investigation to further improve our model system was performed using an alternative culture method that has been shown to better retain *in vivo*

glioma characteristics. Primary glioma specimens cultured under neurosphere promoting conditions¹⁵⁵ (as opposed to adherent, serum-containing cultures as above) has been shown to have a number of advantages. Most importantly, they more robustly retain the original tumor expression patterns whilst being able to better recapitulate the original tumour growth characteristics *in vivo* in orthotopic grafts.^{308,318,319} These cultures retain neural-stem cell markers and the stem-like abilities of self-renewal and multi-lineage differentiation,^{4,161,308,319-321} preserving the undifferentiated state observed in gliomas *in situ*. Importantly, these stem-like cells within gliomas have been identified to be both chemo- and radio-resistant¹⁶⁴⁻¹⁶⁶ and may act as treatment-resistant ‘disease reservoirs’^{4,161,319,320} responsible for the inevitable recurrence seen in nearly all glioma patients. Herein, primary gliomas isolated and cultured in this manner and displaying these properties are referred to as brain-tumour initiating cells (**BTICs**).

To generate a syngeneic mouse BTIC model, NPcis mice (*Trp53^{+/-}/Nf1^{+/-}*) in the C57Bl/6 background were used. NPcis mice were bred and followed until they were sacrificed due to a collection of symptoms often deriving from peripheral tumour formation. Upon death, brains were examined for lesions through histology, and confirmed neoplastic lesions were microdissected and grown as neurospheres in mouse neural stem cell media supplemented with EGF and FGF. These lines grew readily as spheres, stained for stem cell markers, differentiated in serum into several CNS-related lineages, and stained for several types of differentiation markers. Further, when grafted into the brains of immunocompetent C57B/6 mice, they retained characteristics of the original tumours from which they were derived. Although still in early days of characterization, we are confident that these lines represent murine brain tumour-

initiating cells. Interestingly, they are all highly resistant to MYXV infection, replication and cell death.

These lines potentially represent a large step forward for the preclinical study of gliomas in the immunocompetent microenvironment. Further studies characterizing their exact nature are warranted, and investigations into their glioma sub-type and treatment sensitivities could be of great interest to the glioma research field.

3.2. Results

3.2.1. MYXV treatment of GL261 and B8 *in vitro*

GL261 and RasB8 (**B8**) cell lines were the first lines obtained in the laboratory for the intent of testing intracranial MYXV treatment in orthotopic grafts in C57Bl/6 mice. Interestingly, these two lines had completely opposite responses to MYXV infection *in vitro*. B8 was highly susceptible to infection (**Figure 3.1 A**), with 50% and 15% viability following 0.1 and 1.0 MOI MYXV treatment at 48 hours post-infection (**hpi; Figure 3.1 B**). Conversely, GL261 had very little infection with MYXV as measured by GFP fluorescence under the control of the early viral promoter (**Figure 3.1 A**), and infection resulted in 98% and 74% viability at 48 hpi at 0.1 and 1.0 MOI (**Figure 3.1 B**). These cell lines were significantly more susceptible (B8) and resistant (GL261) to our bench mark cell line U87 at both MOIs. As suggested by the early gene expression, B8 resulted in a productive infection with cell-free virus recovered at 48, 72 and 96 hpi (**Figure 3.1 C**). GL261 resulted in no recovery of functional cell-free virus. Of note here, is the relatively low titres, despite such abundant infection noted in **Figure 3.1 A**. This was due to

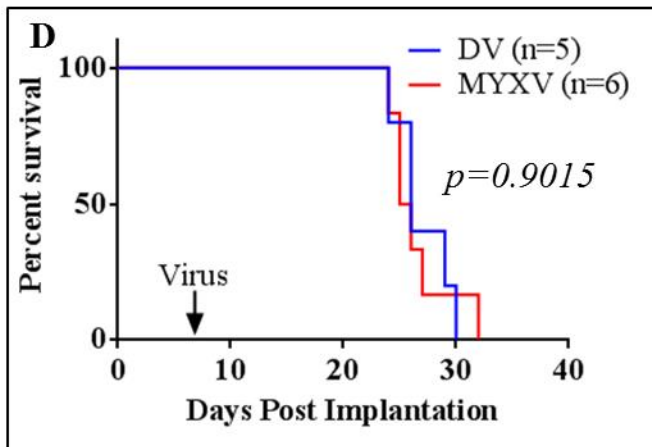
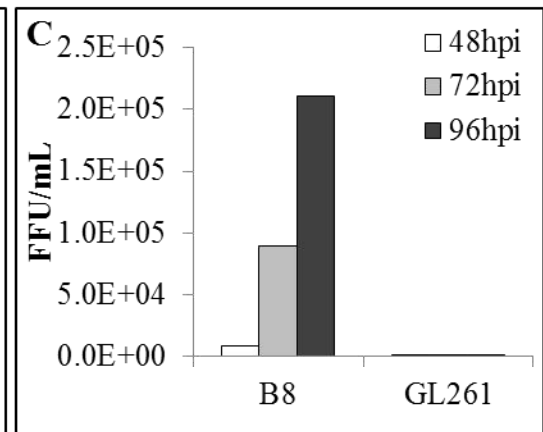
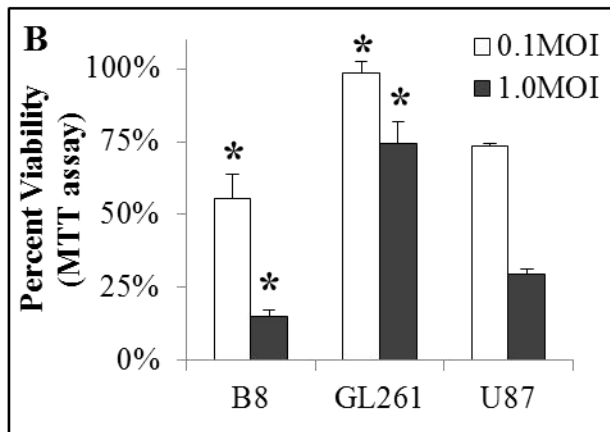
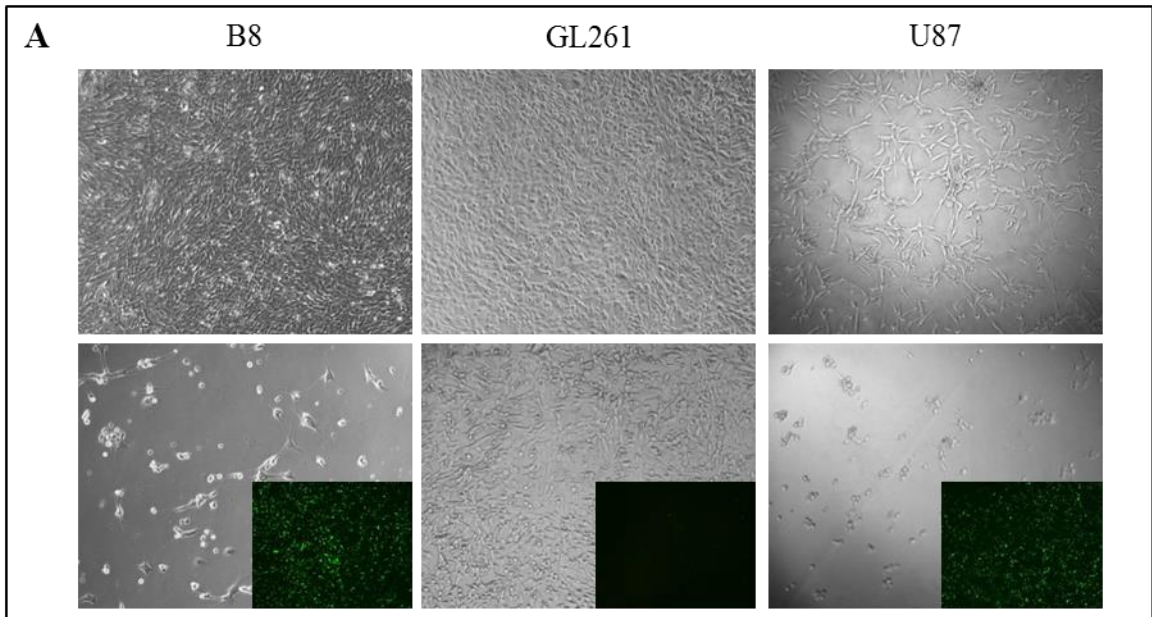


Figure 3.1: B8 and GL261 cell lines have differing susceptibility to MYXV infection and MYXV-mediated cell death *in vitro*. **A** – Mouse B8 and GL261, and human U87 cell lines infected with 1.0 MOI vMyx-GFP (bottom row; 100X phase/contrast, 25X GFP inlay) or control (top row; 100X phase/contrast) at 72 hpi. **B** – Percent viability B8 (n=3), GL261 (n=5) and U87 (n=4) as treated with given MOI of vMyx-GFP at 48 hpi. DV equivalent of 1.0 MOI. Asterisks represent significant difference from U87 (t-test, p<0.05). **C** – Viral titres (focus-forming units (FFU/mL) from infected B8 and GL261 lines at 48, 72, and 96 hpi titred on BGMK cells. Only supernatant titred in this experiment (n=2). **D** – Intracranial implantation of 1×10^4 GL261 in C57Bl/6 mice treated with a single intracranial injection of 5×10^6 PFUs of vMyx-GFP at 7 days-post implantation. All error bars in this figure represent standard error.

the experimental design of the experiments, such that only the supernatant was harvested, leaving infected cells behind. However, as the majority of MYXV replication is the production of intracellular mature virions, this was deemed an inaccurate method for determining replication, and all future experiments harvested both cells and supernatant. However, given the lack of any recoverable virus and no early gene expression, it is clear that GL261 cannot replicate the virus.

Despite being inherently resistant to the virus *in vitro*, there remained the possibility that the inflammatory response of injecting live MYXV intracranially in GL261-bearing C57 animals would result in an anti-tumour response, especially as GL261 has been shown to be quite susceptible to immunotherapies.³²² However, there was no change in efficacy seen between dead virus treatment (DV) and vMyx-GFP treatment (**Figure 3.1 D**) *in vivo*.

3.2.2. *In vitro response of NPcis lines to Myxoma virus infection*

The NPcis cell lines, K1492, KR158D, and K5001 (classified as derived from Grade III gliomas) and K1861, K1491 and K4622 (classified as derived from Grade II gliomas),¹³³ were kind gifts from Dr. Karlyene Reilly (NCI Fredrick). Four of these lines

were chosen for further *in vitro* studies based on the original assessment of their susceptibility to MYXV infection (not shown), MYXV-induced cell death (**Figure 3.2 A**), and viral replication. (**Figure 3.2 B**) These lines, K1492, K1861, K1491, and K5001 represented two lines from each of the Grade III and Grade II groups, and within each group could either support robust viral infection/replication or not (**Figure 3.2B**).

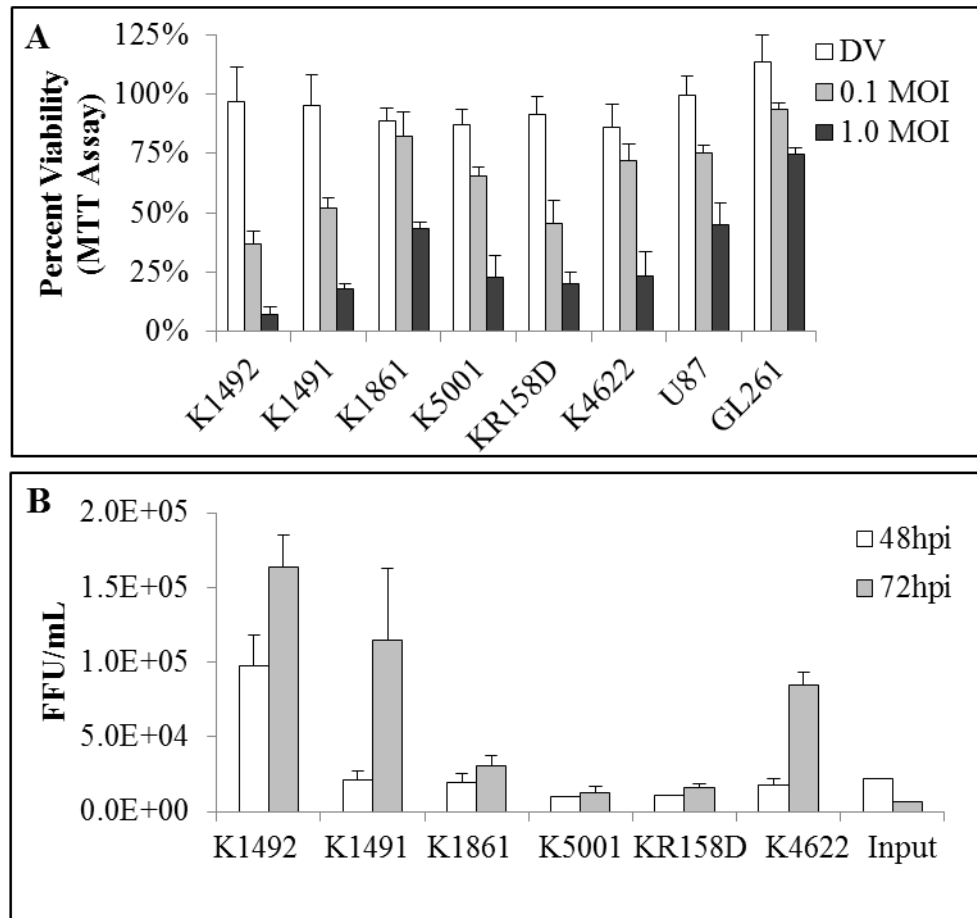
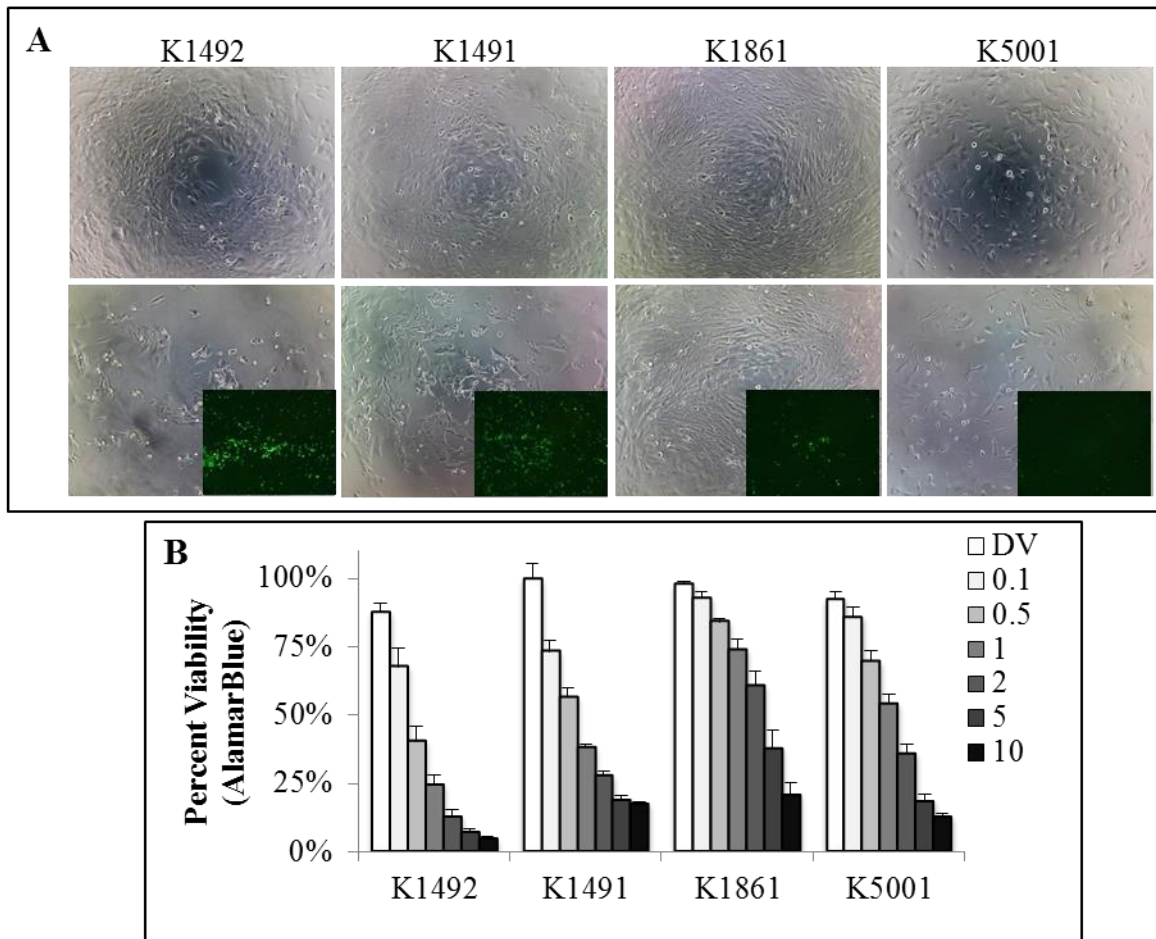


Figure 3.2: Preliminary tests of NPcis cell lines show the lines have variable susceptibility to MYXV infection and MYXV-mediated cell death *in vitro*. **A** – Percent viability of NPcis cell lines versus U87 and GL261 cell lines infected with 0.1 or 1.0 MOI vMyx-GFP measured 48 hpi via MTT assay (n=4). DV equivalent to 1 MOI. **B** – Viral recovery was titred on BGMK cells from infected NPcis cells lines at 48 and 72 hpi. Only supernatant titred in this experiment. All error bars represent standard error.

Examining these four cell lines in response to MYXV treatment *in vitro* using the AlamarBlue assay for viability (replaced the MTT assay in our laboratory) found very similar results to the preliminary study. Despite these lines being derived from the same genetic background and having the same *Trp53* and *Nf1* null driving mutations,^{127,131,133} we found a large variability in MYXV infection and replication rates (**Figure 3.3 A, B, C**). K1491 and K1492 provided the most robust viral replication, producing high titres of 6.1×10^7 and 1.8×10^8 at 72 hpi. These lines were also the most sensitive to viral treatment, with 1 MOI resulting in ~25% and ~38% viability at 48 hpi, respectively.



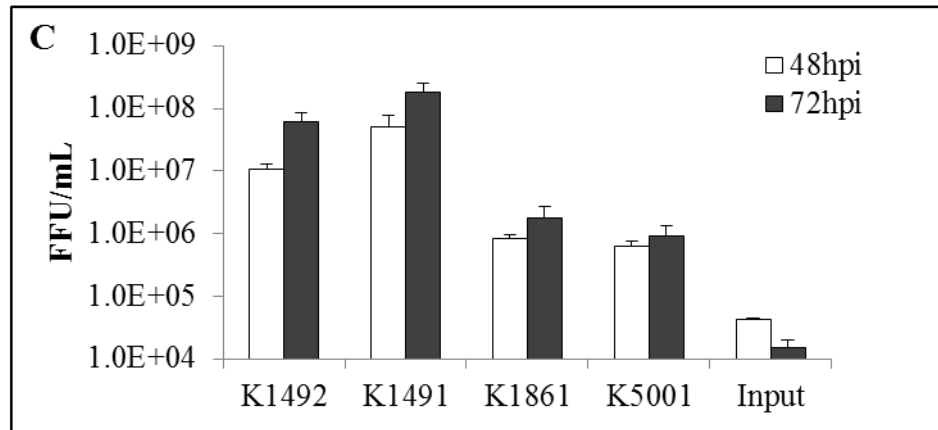


Figure 3.3: *NPcis* cell lines have variable susceptibility to *MYXV* infection and *MYXV*-mediated cell death in vitro. **A** – *NPcis* cell lines infected with 1.0 MOI vMyx-GFP (bottom row; 100X phase/contrast, 25X GFP inlay) or control (top row; 100X phase/contrast) at 48hpi. **B** – Percent viability of *NPcis* cell lines at 48 hpi with vMyx-GFP as measured by Alamar blue (n=4). Error bars represent standard error. **C** – Viral recovery of supernatant and infected cells titred on BGMK cells from infected *NPcis* cell lines at 48 and 72 hpi (n=4). Input virus is vMyx-GFP seeded in wells with no cells. Error bars represent standard error and all cell lines are significantly elevated over the input at for that time-point.

Conversely, K1861 was the most resistant to cell death with ~74% viability at 1 MOI at 48 hpi, but was killed by the virus at higher MOIs (21% viability with 10 MOI, 48 hpi). K5001 had intermediate sensitivity to viral mediated cell death. These more resistant cell lines markedly differed in their ability to replicate the virus, with K1861 and K5001 unable to reach the high titres seen in the other lines, but still able to produce functional virions following infection.

3.2.3. Characterization of *NPcis* tumours in vivo

To establish which lines we would utilize for *in vivo* studies, we implanted 5.0×10^4 cells in the right striatum of C57Bl/6 mice. All mice succumbed to the tumours, but survival varied (**Figure 3.4 A**). Only K1492 and K1861 reproducibly produced intracranial tumours, whilst K1491 and K5001 both tended to produce large extracranial tumour masses with or without a corresponding intracranial tumour (**Table 3.1**). K1492

and K1861 orthotopically implanted in C57Bl/6 mice produced aggressive tumours (**Figure 3.4 B**). Despite having protruding tendrils into the adjacent brain parenchyma, these tumours appear to have a defined tumour border and overall lacked the single cell infiltrate pattern that can appear in astrocytic tumours. Microscopically, these tumours were composed of spindle cells arranged in bundles with a focal storiform pattern. Immunohistochemistry shows patchy expression of GFAP and S100b protein in tumour cells (**Figure 3.4 B**), a feature seen in some GBM patients.⁸ The histologic features and immunohistochemical profile are consistent with a gliosarcoma, a glioblastoma variant that has a similar evolution and prognosis. It is easy to speculate that this morphological change to a more mesenchymal phenotype was acquired through culture of the primary cells in serum,^{162,323,324} since it has been shown that the sarcomatous component in glioblastoma represents an aberrant differentiation of the glioblastoma cells.⁸ As the main purpose of this study was to identify intracranial glioma models in immunocompetent C57Bl/6 mice for the pre-clinical modelling of OV, we deemed K1492 and K1861 relevant for use in our subsequent experiments.

Table 3.1: *In vivo* growth characteristics of NPCis glioma lines implanted in C57Bl/6 mice.

Line	Median Survival	Tumour at Day 25	Extra-Cranial Tumour Outgrowth
K1492	36 days	100% (4/4)	0% (6/6)
K1861	44 days	100% (6/6)	17% (1/6)
K1491	58 days	25% (1/4)	100% (8/8)
K5001	74.5 days	75% (3/4)	100% (6/6)

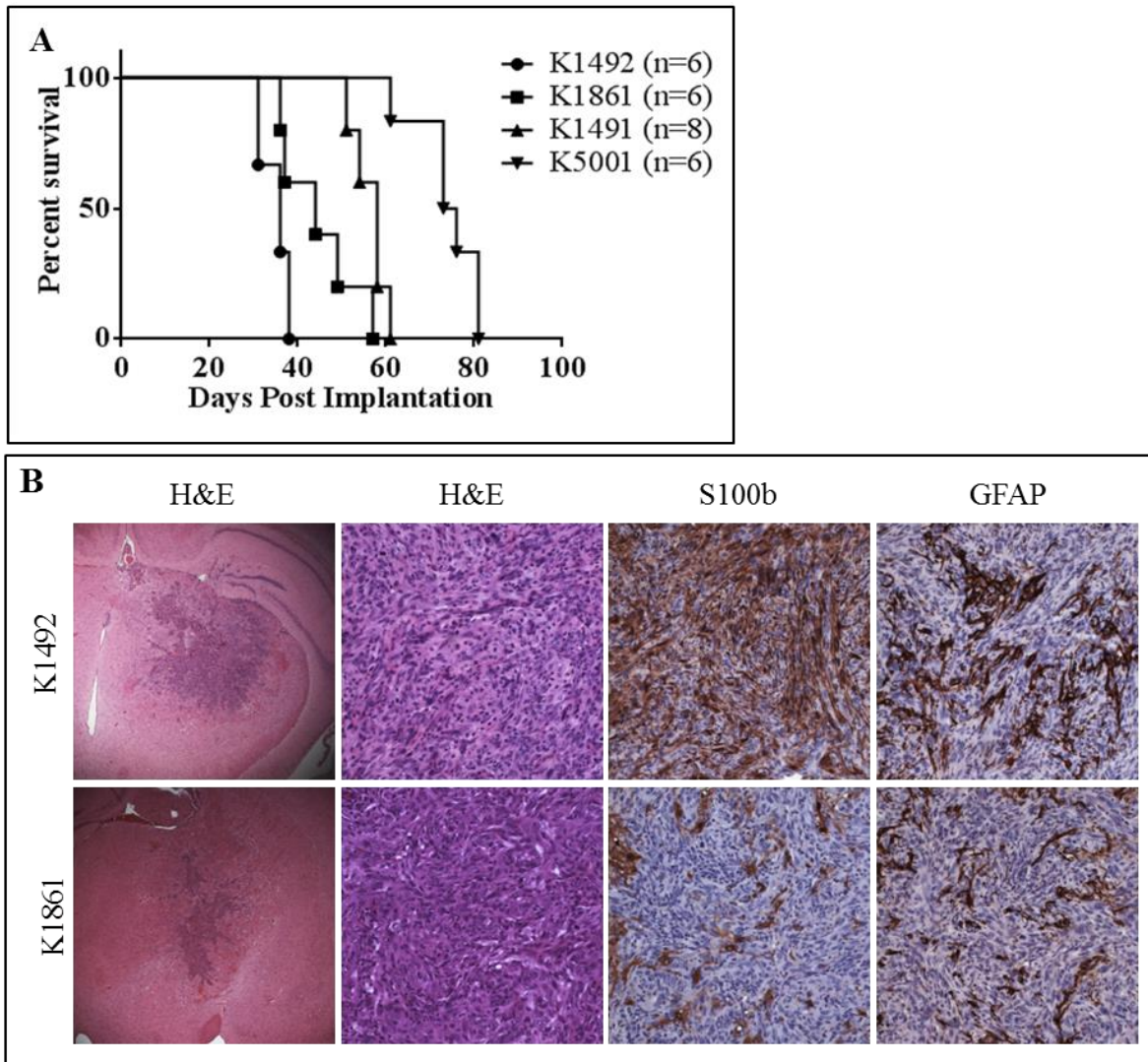
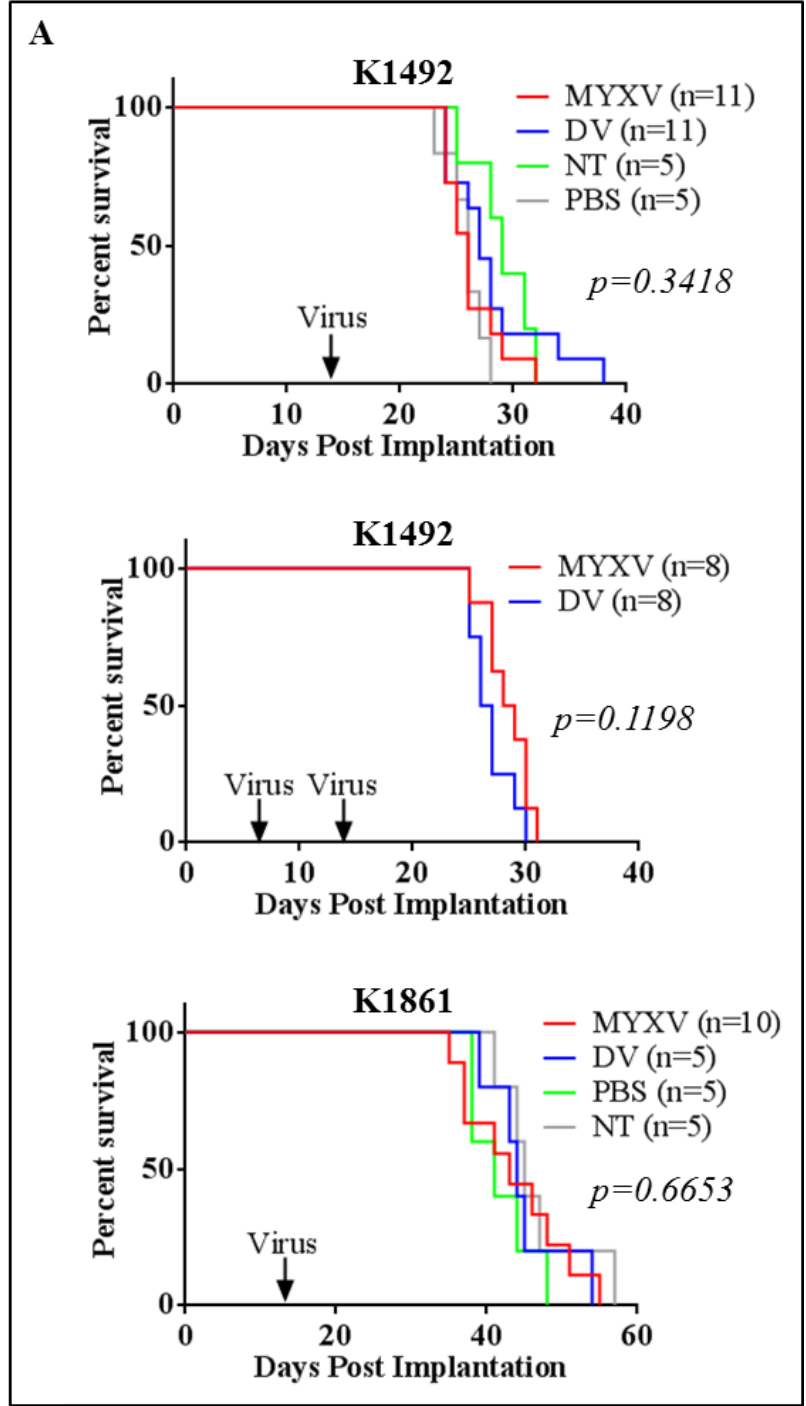


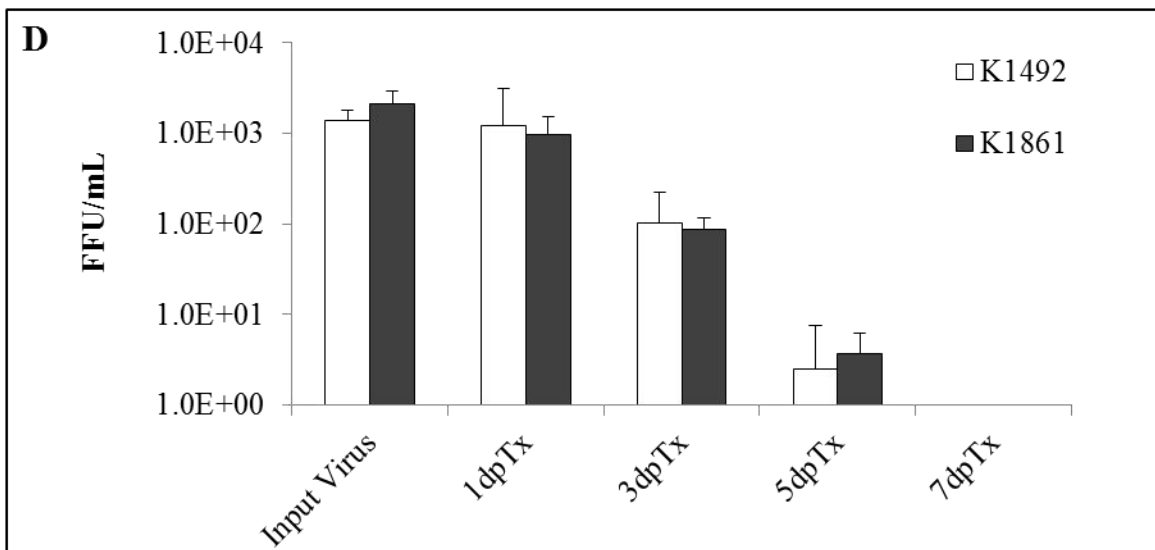
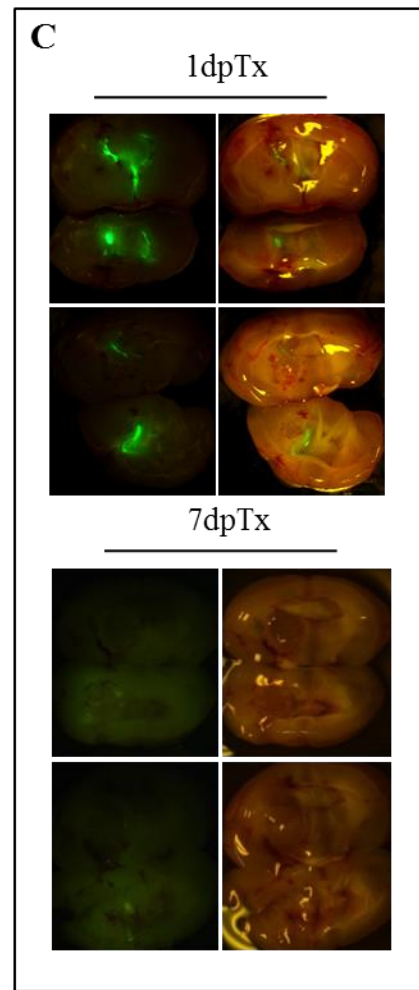
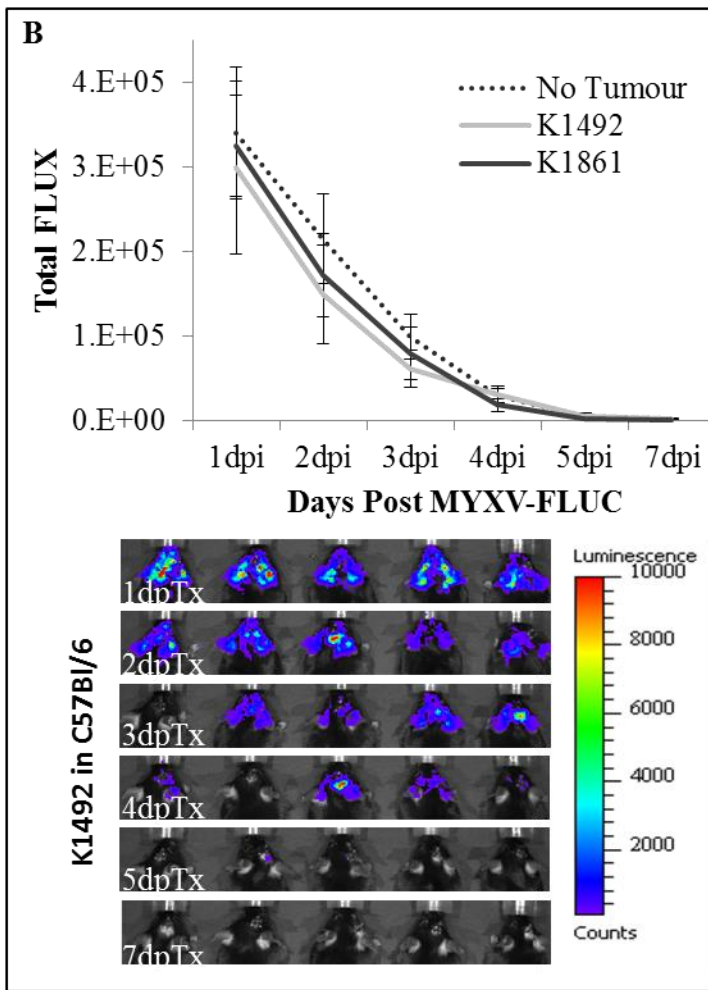
Figure 3.4: *K1492 and K1861 form aggressive intracranial tumours in C57Bl/6 mice.* **A** – Survival study of NPcis mice with 5×10^4 cells of K1492, K1861, K1491 and K5001 implanted into the right straitum of C57Bl/6 mice. **B** - Histopathology of 14 day K1492 and K1861 by H&E (first column 25X, second column 200X) and astrocytic markers S100b (200X) and GFAP (200X).

3.2.4. In vivo response of NPcis lines to Myxoma virus infection

K1492 and K1861 were treated with an intratumoral inoculation of 5×10^6 PFU of an MYXV construct that expresses Firefly luciferase, vMyx-FLuc, at 14 days post-implantation (**Figure 3.5 A**), a dose previously found to be efficacious in other intracranial models.^{253,298,325} All mice succumbed to tumour burden with no therapeutic

benefit [26, 27, 26, and 29 days median survival for MYXV, dead virus (**DV**), PBS or No treatment (**NoTx**), respectively] for K1492 (Log-rank Mantel-Cox test; $p=0.3418$ comparing all treatments), and 43, 44, 41, and 45 days median survival in K1861 (Log-rank Mantel-Cox test; $p=0.6653$, comparing all treatments). Further, two treatments of 1×10^7 PFU of vMyx-FLuc at 7 and 14 days in K1492, the most susceptible line *in vitro*, showed no therapeutic benefit (26.5 and 28.5 median survival for DV and MYXV, respectively, $p=0.1198$; **Figure 3.5 A**). There was no viral replication as measured by viral luciferase activity (**Figure 3.5 B**), with complete clearance of bioluminescent activity by 5 days post-treatment (**dpTx**). These viral clearance kinetics were closely mimicked with viral recovery assays from the tumour (**Figure 3.5 D**). Interestingly, the viral luciferase activity measured in these models did not differ from non-tumour-bearing animals, and seemed to be a consequence of minor off-target infection of cells in the ventricles (**Figure 3.5 C**) as previously described with intraventricular MYXV administration.³²⁶ However, IHC staining for the early MYXV viral protein, M-T7, found that there was indeed a small proportion of the tumour infected at 1 dpi, with very little evidence of tumour infection at 3 dpi and none at 7 dpi (**Figure 3.5 E**). These results demonstrate that the input virus underwent only very transient infection of these tumours, without any sustained viral replication in the tumour beds, and no measurable therapeutic benefit.





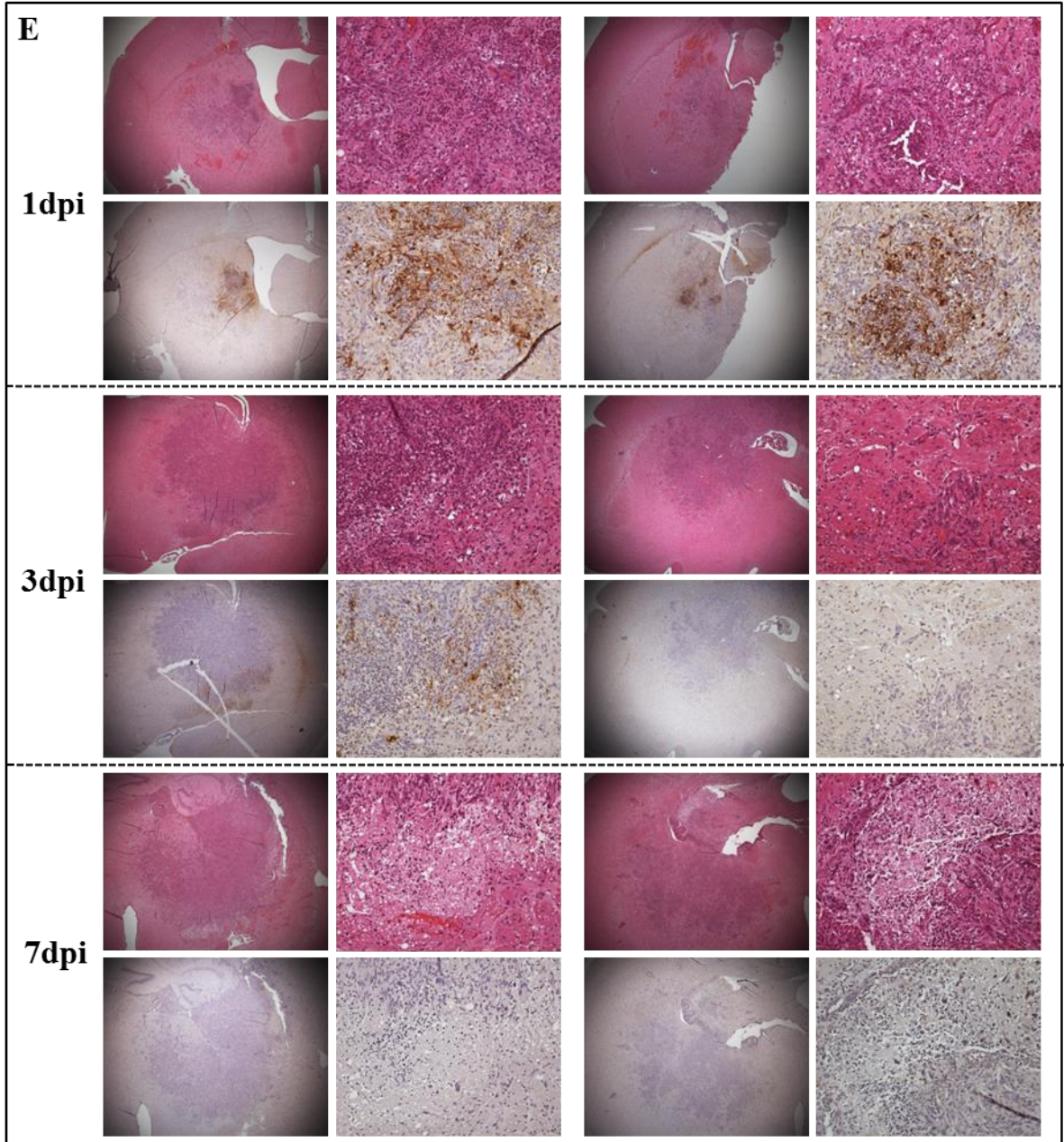


Figure 3.5: *MYXV treatment in vivo results in only transient infection of the tumour and results in no therapeutic efficacy.* **A** - 5×10^4 cells of K1492 and K1861 were intracranially implanted in C57Bl/6 mice and received 5×10^6 PFUs (single injection at day 14) or 1×10^7 PFUs (double injection at day 7 and 14) of vMyx-FLuc (MYXV), UV-inactivated virus (DV), PBS, or no treatment (NoTx). **B** – Luciferase measured (Total FLUX) from region-of-interest around the entire mouse skull following 5×10^6 PFUs vMyx-FLuc in K1492 (n=8), K1861 (n=10) at 14 days post-tumour implantation or no tumour (n=5). **C** – K1492-bearing C57Bl/6 mice with a single injection of vMyx-GFP at 14 days post-tumour implantation, and brains removed, sliced and viewed on a fluorescent dissecting microscope at 1 and 7 days post-virus administration. **D** – Viral recovery from K1492 (n=4) and K1861 (n=4) tumours following intracranial treatment with vMyx-FLuc. Input virus represents mice where virus was recovered <1 hour post-injection. **E** – Immunohistochemical staining on formalin-fixed paraffin-embedded sections for early MYXV protein MT-7 in 14 day K1492 at 1, 3 and 7 days post-treatment (Left 25X; Right 100X). All error bars represent standard error.

3.2.5. Creation and characterization of murine brain-tumour initiating cell lines

Although relevant for our purposes of interrogating oncolytic viral resistance in immunocompetent models (**Chapters 4 and 5**), the K1492 and K1861 lines did not completely phenocopy glioma characteristics when grown *in vivo*; mainly, these lines lacked single-cell infiltration away from the tumour mass as I universally found in patients. Since it has been described in the literature that primary human glioma specimens cultured as neurospheres were better able to retain *in vivo* growth characteristics, we grew primary mouse gliomas as neurospheres and preliminarily assessed their usefulness as a preclinical glioma model.

A detailed protocol on the creation of these lines can be found in **Chapter 2.1.3**. Briefly, mouse brain-tumour initiating cell lines (**mBTICs**) FJZ0309, FJZ0305, and FJZ1116 were created from C57Bl/6 *Trp53^{+/-}/Nf1^{+/-}* (**NPcis**) mice,^{127,128,131,133} a kind gift from Dr. Karlyne Reilly (NCI Frederick), and bred at the University of Calgary breeding facilities. Heterozygote mice for these litters were then monitored for tumour burden,

most often presenting as large necrotic sarcomas, abdominal masses, loss of weight, ataxia, and/or limb paralysis. These mice were then sacrificed, had their whole brains aseptically removed, and then cut coronally into 1-2 mm sections. Alternating sections were flash frozen or retained in sterile saline (**Figure 2.1**). Flash frozen portions were mounted and sectioned, H&E stained, and examined by microscopy for brain lesions. Any discovered brain lesions would then have this tissue micro-dissected from the corresponding areas on the tissue remaining in the sterile saline solution.

Three litters, for a total of 17 NPcis heterozygous mice, were obtained from breeding NPcis female mice to male C57Bl/6 (wildtype), a combination shown to give a larger percentage of astrocytoma-bearing animals than breeding male NPcis mice to female wildtype.¹²⁸ All mice perished within one year of birth, with a median survival of 218 days (~7.2 months; **Figure 3.6 A**), comparable to what has been previously shown for NPcis mice in this background.¹²⁷ The short lifespan of the NPcis loci in the C57Bl/6 background was due to the preponderance of short latency tumours, and 12 of the 17 mice died from obvious tumour burden visible before or after autopsy. These tumours appeared as soft-tissue sarcomas and/or lymphomas, with two possible pheochromocytomas, tumour types previously shown to occur in these animals.^{127,128} Three animals were sacrificed due to neurological deficits, such as limb paralysis and/or ataxia, with no obvious lesions in the brain or rest of the body. Finally, one animal was found dead with no autopsy, and one was sacrificed due to an unnoticed dental malocclusion. This is summarized in **Supplementary Tables 1, 2 and 3**.

Three of the 17 animals were found to have obvious brain lesions and the tumours and resulting cell lines were named according to the days they were sacrificed, FJZ0309,

FJZ0528 and FJZ1116 (**Figure 3.6 B**). Of these, FJZ0309 was found in a mouse sacrificed at 219 days old due to a large, putative soft-tissue sarcoma on a hind limb. Analysis of the brain sections found a large tumour mass that seemed to be growing up and out of the lateral ventricle. No other tumours were found in this mouse. FJZ0528 was

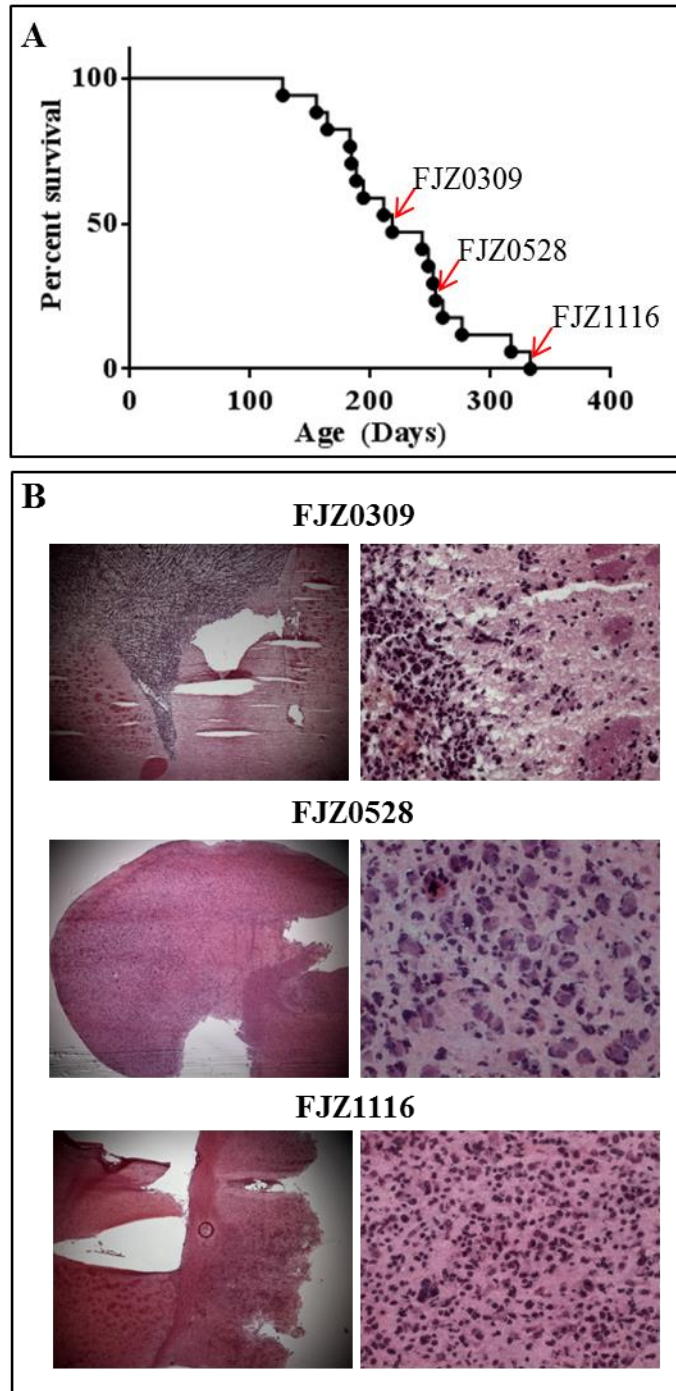


Figure 3.6: *Three of seventeen NPcis animals followed found putative astrocytoma-like lesions. A – Survival of seventeen animals from three C57Bl/6 NPcis litters, with red arrows denoting the animals that had confirmed brain lesions that resulted in cultured neurosphere lines. B – Original frozen sections stained with Haematoxylin and Eosin from sacrificed NPcis animals showing neoplastic lesions (left 25x magnification; right 400x magnification).*

derived from a mouse sacrificed at 254 days for extensive hyperactivity and tachypnea. Examining the brain, even before cryogenic sectioning, showed a large mass in the lateral ventricle that was unfortunately lost during cryogenic sectioning. However, H&E of these frozen sections showed a highly infiltrative and diffuse tumour throughout the cerebral cortex. Other possible lesions in this animal included enlarged adrenals and bloody, spotted lungs. Finally, FJZ1116 was found in a mouse sacrificed at 333 days, and had an incredibly large body, but a small emaciated face. Upon autopsy, this mouse was found to have major metastatic disease that was very prominent in the liver, lungs and spleen. Cryosectioning the brain discovered a smaller hyperplastic lesion in the upper frontal cortex. A fourth animal was found to have a very small lesion, but this could not be conclusively differentiated from a freezing artifact, and cells cultured from this area did not result in growth in culture (*data not shown*).

Sections that were used for microdissection of tumours for cell culture were formalin fixed and paraffin embedded for future immunohistochemical analysis. Unfortunately, the originally observed lesion in these sections was only retained in the FJZ0309 and FJZ0528 tumours (**Figure 3.7**). Initial pathology of the FJZ0309 tumour found that it was a hypercellular tumour composed of atypical elongated to oval nuclei with coarse chromatin and high, consistent GFAP staining. There were frequent mitoses indicative of a high mitotic index, and was highly vascular with, signs of neo-vascularization. There

were only limited signs of necrosis and the tumour was infiltrative into adjacent tissue. Taken collectively, this tumour was seen as the murine version of a human WHO grade IV tumour. FJZ0528 was a mid-high grade glioma, the mitoses were less frequent than FJZ0309 and there were no signs of any abnormal vasculature or necrosis. This tumour was highly infiltrative, positive for GFAP staining, and formed secondary structures such as perineuronal satellitoses. This tumour was deemed similar to a WHO grade III tumour.

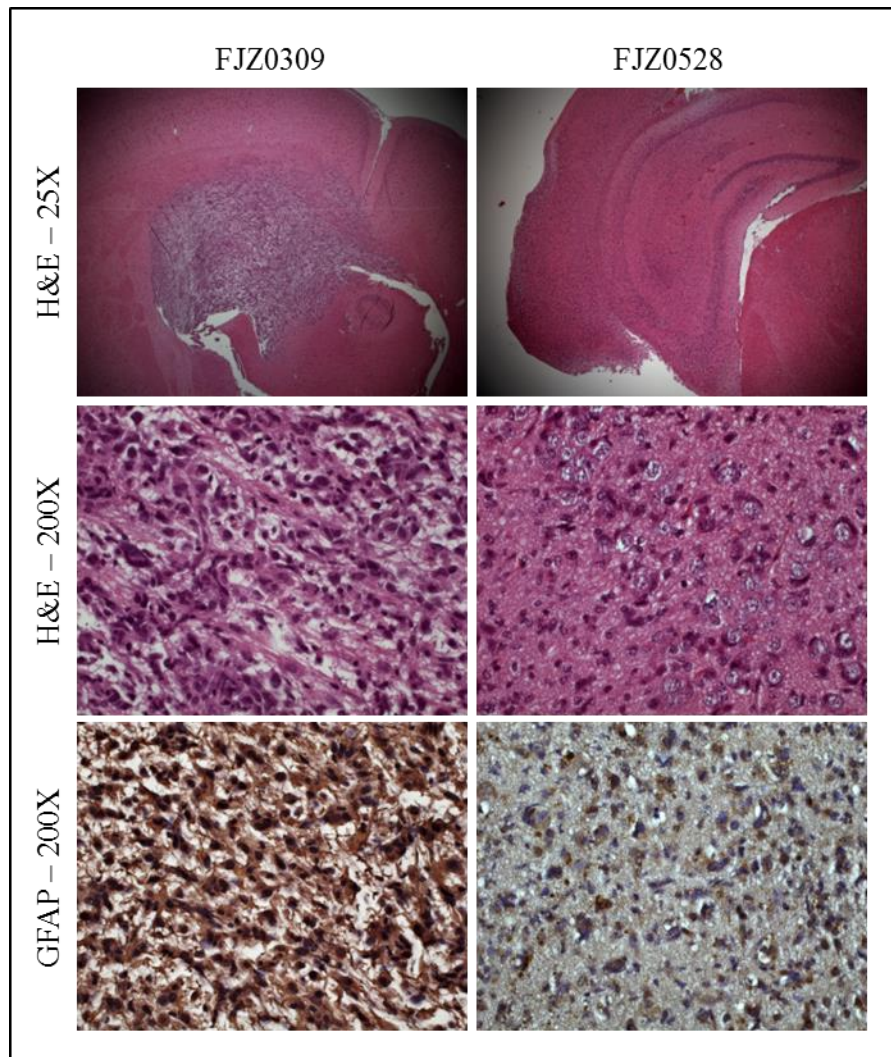


Figure 3.7: Formalin-fixed paraffin embedded sections of lesions demonstrate that both FJZ0309 and FJZ0528 are high-grade gliomas. FJZ0309 and FJZ0528 sections stained with Haematoxylin and Eosin or a murine glial-fibrillary protein. Magnification as labelled.

Finally, FJZ1116 was analyzed from the initial frozen sections. It was found to have a bizarre appearance with clustering of cells with a reasonable amount of neuropil, frequent mitoses, small necrotic foci, and normal vasculature. The initial pathology suggested that this was a glioneuronal tumor, an astrocytoma with primitive neuroectodermal tumour characteristics, or even a primitive neuroectodermal tumour itself. Further staining of all these sections will allow for more complete pathology and diagnosis in the future.

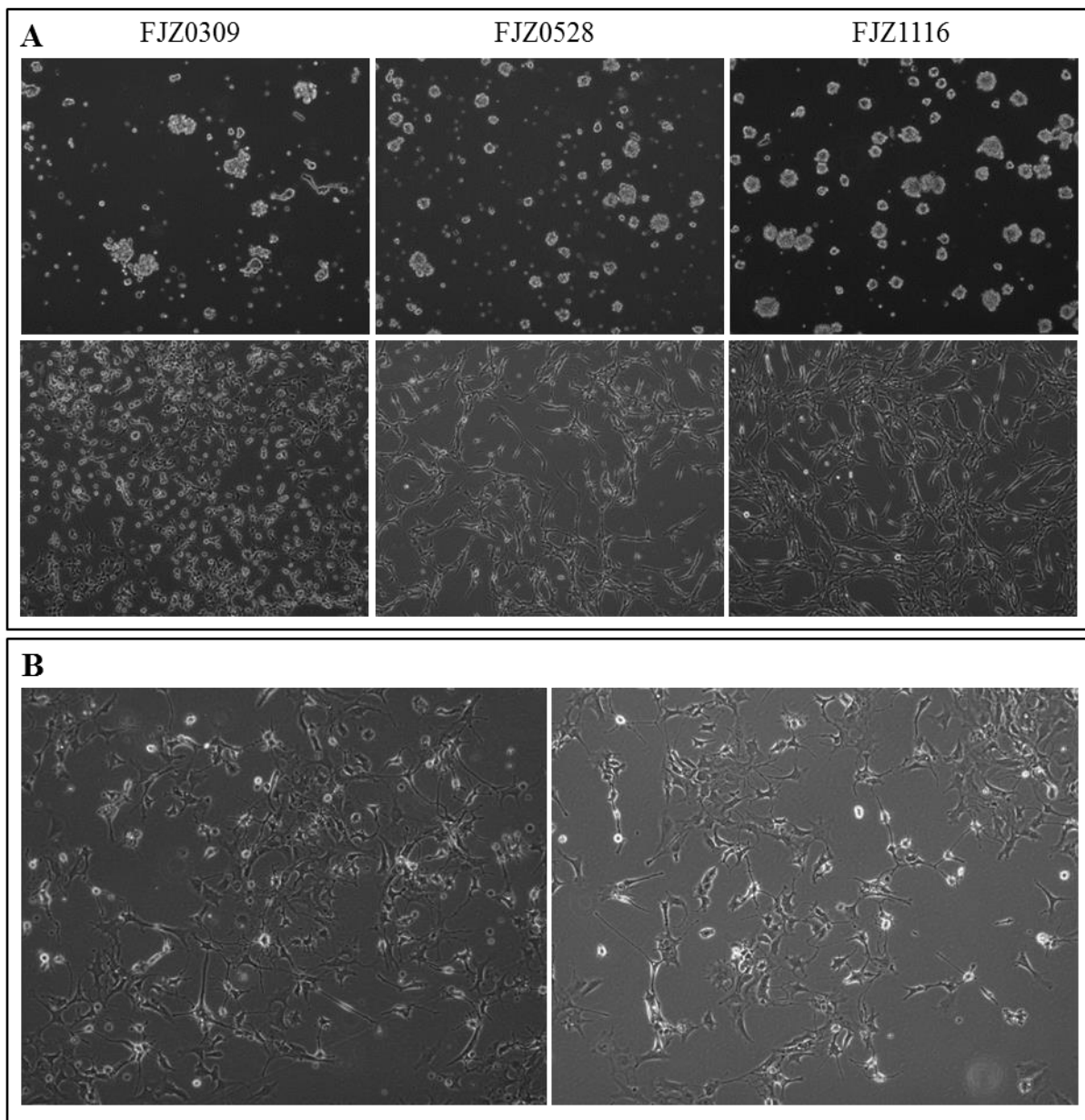


Figure 3.8: Lesions cultured from NPcis mouse brains readily formed neurospheres in mouse neural stem cell media and displayed multi-lineage differentiation in response to fetal bovine serum. **A** – Three putative mBTIC lines were placed in mouse neural stem cell media supplemented with EGF, FGF, and heparin sulphate with (*below*) or without (*above*) 1 % fetal bovine serum. Pictures were taken 7 days following plating of 2.5×10^5 cells in 6 well plates (100X magnification). **B** – Single cell FJZ0309 placed in high-sucrose DMEM with 10% fetal-bovine serum for 5 days show multilineage differentiation as defined by cellular morphology. (200X magnification).

Next, we analyzed the spheres themselves. In all these studies, spheres were passaged to a maximum of 4 to 5 passages. All lines were frozen down from primary samples at passage 2. FJZ0309 formed neurospheres in mouse neural stem cell media supplemented with EGF, FGF2 and heparin sulphate within the first 72 hours, while FJZ0528 and FJZ1116 formed neurospheres in culture within 10 days of being harvested. When placed in 1% fetal bovine serum, these neurospheres appeared to differentiate and lay down on the culture plate (**Figure 3.8 A**), capable of taking on the morphology of several different neural cells, including neurons, astrocytes and even-microglia like cells (**Figure 3.8 A/B**). Although not well depicted in this figure, the spheres formed by the FJZ0309 cells were loosely coherent, consisting of heterogeneous cell sizes, but overall having larger cells than the other lines. FJZ0528 or FJZ1116 formed compact neurospheres more representative of what we have seen in the human BTIC cultures (**Figure 3.11 A**). Further, FJZ0309 appeared to have larger nuclei than the other mBTICs, perhaps suggesting that these cells have some complex genome amplifications.

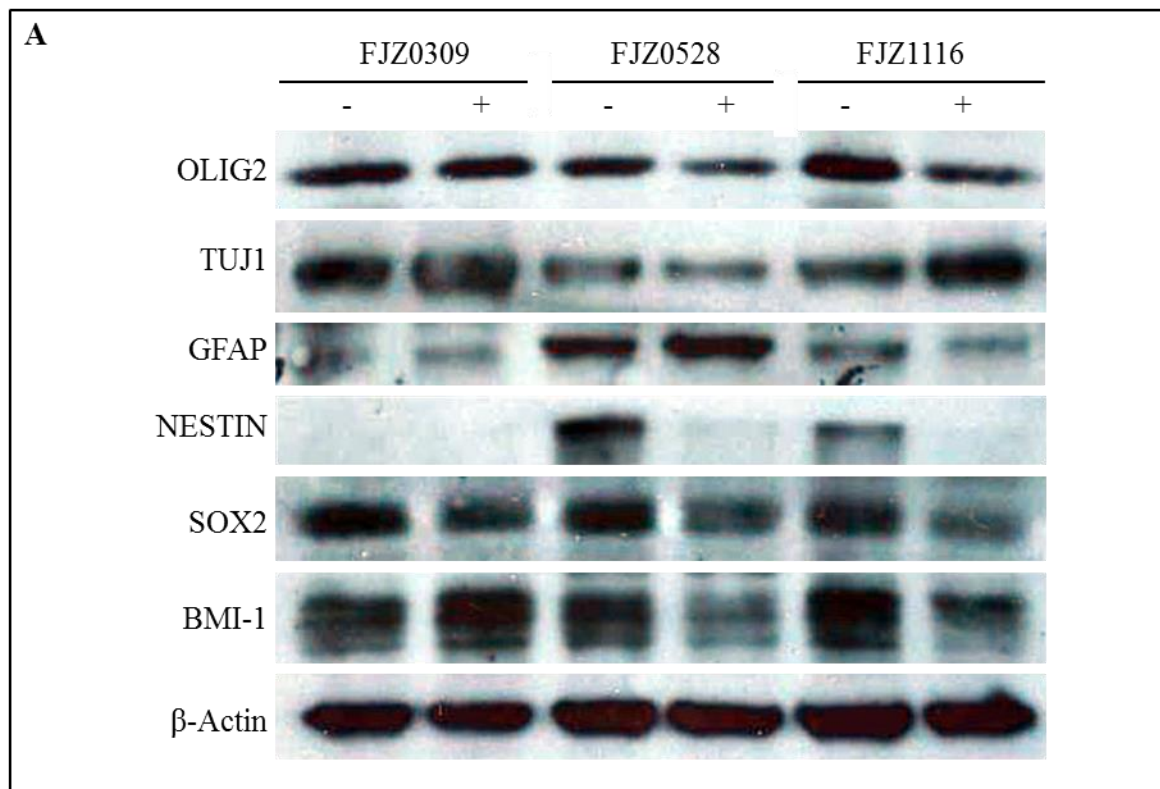
The multilineage potential of these cells strongly suggested these were glioma stem-like cells. As such, neural stem cell markers NESTIN¹⁵⁷, SOX2¹⁵⁸ and BMI1¹⁶⁰ were assayed in these lines, along with differentiation markers for oligodendrocytes (OLIG2),

astrocytes (GFAP) and neurons (TUJ1), as often used in BTIC studies.^{162,300,308,321} First, Western blots for these markers were performed on these lines grown as spheres in mNSC media or differentiated in mNSC media plus 1% fetal bovine serum for 7 days (**Figure 3.9 A**). All the spheres expressed the neural stem cell markers SOX2 and BMI1, while only FJZ0528 and FJZ1116 expressed NESTIN, which was completely lost after differentiation in serum. SOX2 decreased in all lines in response to differentiation, while BMI1 decreased in lines FJZ0528 and FJZ1116 and appeared to be up-regulated in FJZ0309. All the lines expressed high levels of the oligodendrocyte marker OLIG2 which remained unchanged in FJZ0309 in response to serum, but decreased in FJZ0528 and FJZ1116. TUJ1, a neuronal marker, and GFAP, an astrocyte marker, seemed conversely correlated in the lines, where TUJ1 was highly expressed and induced upon differentiation in FJZ0309 and FJZ1116, while higher levels of GFAP that further increased in response to serum was seen in FJZ0528.

Next, mBTIC neurospheres were spun onto glass slides and the presence of these markers was confirmed using immunocytochemistry (**Figure 3.9 B**). These markers very closely mimicked what was seen in the Western blots, with high expression in all the lines of BMI1 and OLIG2, and lower but present expression of SOX2. These markers stained most cells that remained of the sphere, but OLIG2 and BMI1 did tend to have higher expression in the cells towards the middle of the sphere. NESTIN had the most intense expression in FJZ1116, but there were nearly no spheres remaining on the FJZ0528 slide, and the small spheres that remained had NESTIN positive cells. FJZ0309 had no conclusive NESTIN positive cells. The differentiation markers TUJ1 and GFAP

followed very similar expression patterns as the Western blots, with TUJ1 highest in the FJZ0309 and FJZ1116 lines, and GFAP positive cells only found in the FJZ0528.

Of note, the putative glioma stem cell surface markers CD133¹⁵⁴ and CD15³²⁷ were analyzed. The first experiment examined was performed only on FJZ0309, and found 17.5% PROMININ1 (CD133) positive cells and 1.5% SSEA1 (CD15) positive cells, compared to 2.5% and 0.4%, respectively, in cells differentiated in 10% fetal bovine serum for 5 days (*data not shown*). However, these experiments were repeated in all the lines, and no significant CD133 and CD15 staining was found in any line. However, the subsequent use of these antibodies has failed to produce any positive results in our or other labs for any cell lines with these antibodies. Future experiments need to be performed with Western blot and/or immunocytochemistry to assay these markers.



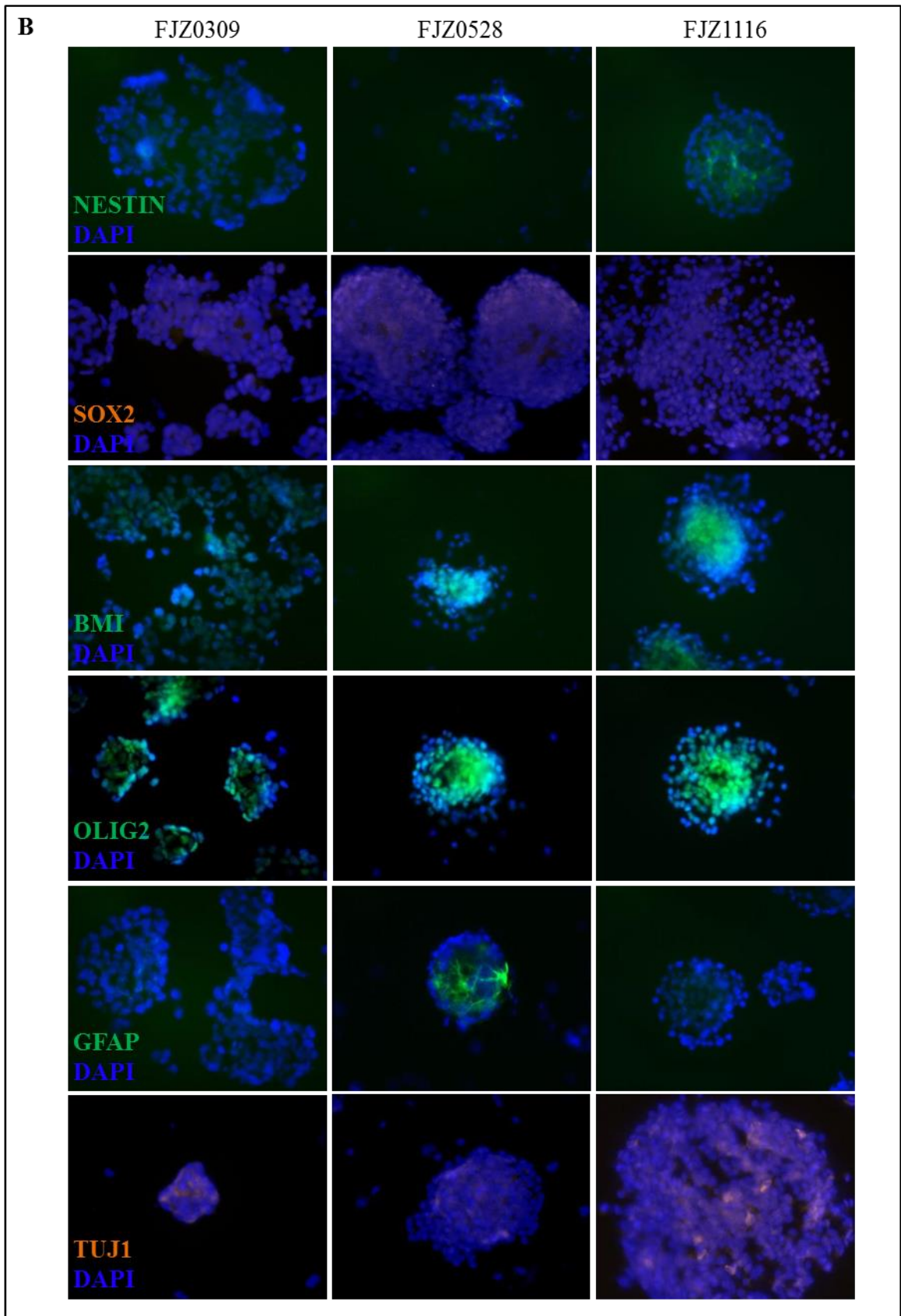


Figure 3.9: *Mouse glioma neurosphere cultures expresses neural stem cell markers and markers of differentiation doing different CNS lineages.* **A** – Western blot analysis of lines FJZ0309, FJZ0528, and FJZ1116 dissociated as single cells and placed in mouse neural stem cell media supplemented with EGF, FGF, and heparin sulphate with (+) or without (-) 1% fetal bovine serum and harvested 7 days later for protein. **B** - FJZ0309, FJZ0528, and FJZ1116 grown in flasks until neurospheres reached a manageable size, and were spun onto slides using cytospin funnels. Immunocytochemistry was performed using the listed antibodies (green names – anti-mouse FITC labelled secondary; red names – anti-rabbit RFP labelled secondary) and counterstained with DAPI (400X magnification).

To consider these cells Brain-Tumour Initiating Cells, it was important to determine if they formed brain tumours in mice. Further, it was important that these cells be able to graft into fully immunocompetent C57Bl/6 animals. In preliminary experiments 5.0×10^4 cells were implanted into the right striatum just as previously described, and a cohort was sacrificed at 25 days-post implantation (**dpi**) for analysis and the remainder of the animals left for survival studies. At 25 dpi, of the two mice analyzed, both FJZ0309 implanted mice had sizable tumours that seemed to migrate in the vicinity of the lateral ventricle (**Figure 3.10 A**). These tumours had single cell infiltrate throughout the brain parenchyma. Mice died shortly thereafter with an average survival of 34 dpi. Of the animals implanted with FJZ1116, only 1 of 3 (33%) was found to have a tumour. Although small, this tumour was highly infiltrative. Mice were still alive 100 days post implantation. FJZ0528 intracranial implants results in 2 of 3 mice developing tumours at 25 dpi. These were small, yet highly invasive tumours that invaded beyond the initial tumour injection site and well into the brain parenchyma without forming an obvious tumour mass. Several instances of perinuclear satellitosis were also observed, as seen in the original tumour. Survival studies were not performed in this line. The pathology observed here must be confirmed through a formal pathology report.

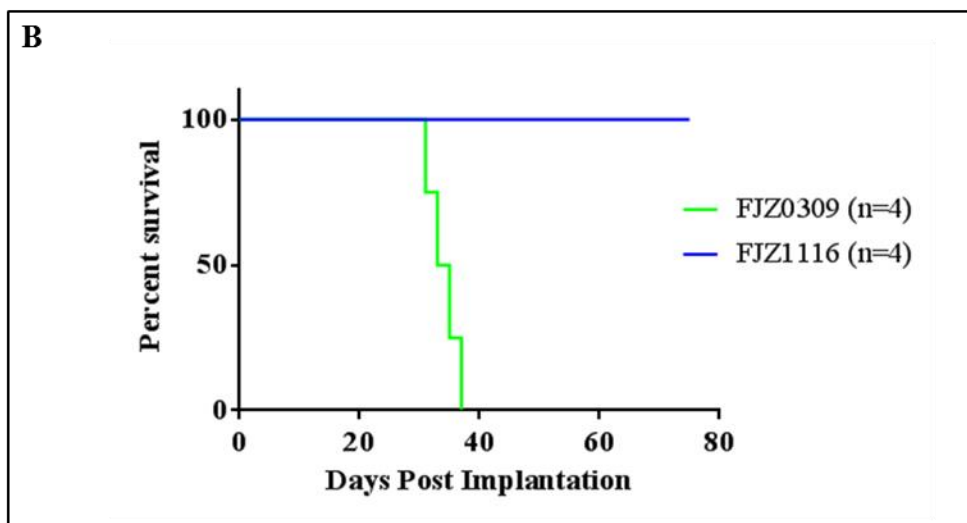
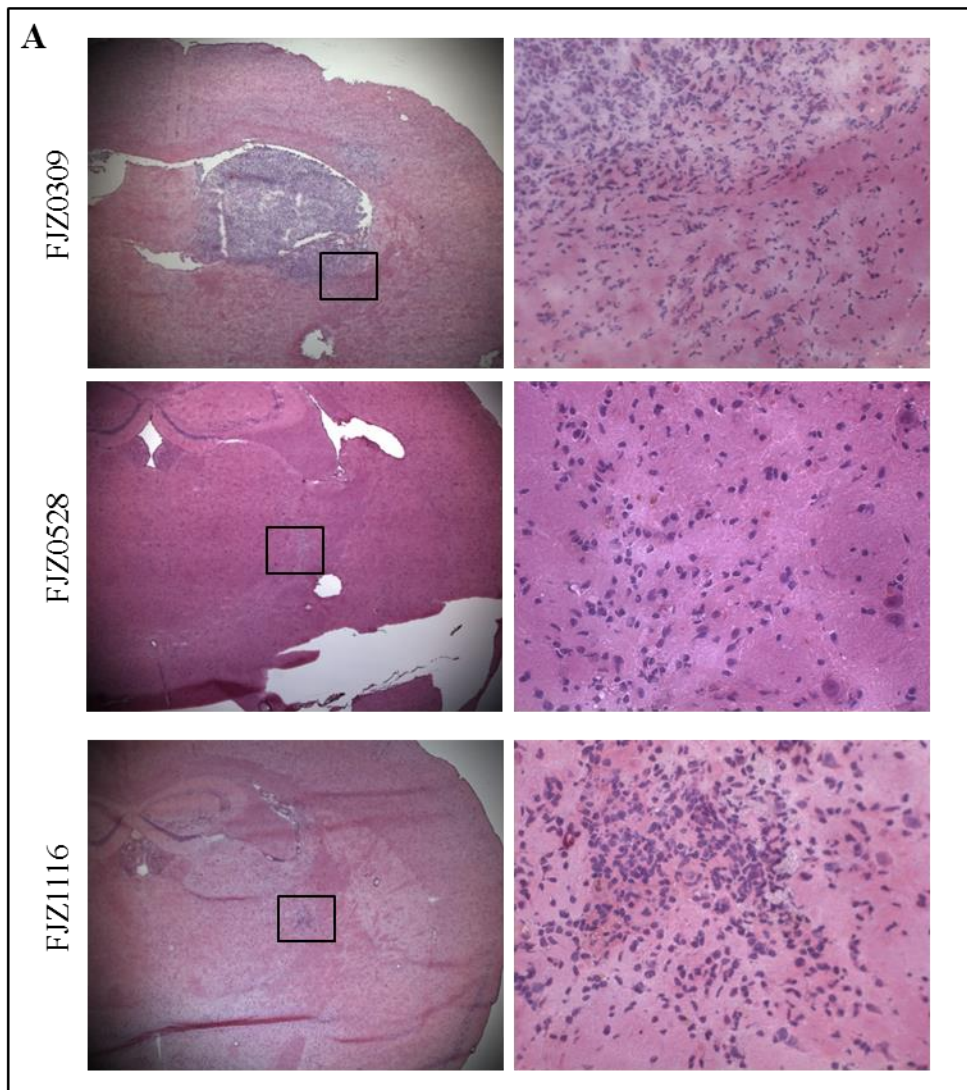


Figure 3.10: *mBTIC lines FJZ0309, FJZ0528 and FJZ1116 all form infiltrative tumours when implanted into C57Bl/6 mice. 5.0x10⁴ mBTICs were implanted into the right striatum of C57Bl/6 mice and mice were then sacrificed for histology or studied for survival. A - Frozen sections from brains of implanted mBTICs at 25 days post-implantation. (Left, 25 X magnification; Right, 400X magnification). B – Survival of animals implanted with mBTICs.*

These results demonstrate that glioma cells isolated directly from spontaneous astrocytomas in mice and grown under neural stem cell conditions contain markers that have been shown to be expressed in previously published ‘glioma stem cells.’ All the lines tested can at least initiate a tumour in C57BL/6 mice, these lines were designated ‘Murine Brain Tumour-Initiating Cells’ (**mBTICs**). Although only preliminary work, these have the potential to become an important part of future preclinical glioma studies.

3.2.6. Response of *mBTIC* lines to *Myxoma virus oncolytic therapy* in vitro

Next determined was the susceptibility of these mBTICs to MYXV therapy. We recently found that human BTICs were more refractory to MYXV treatment than conventional glioma cell lines, but are still able to be infected and support robust viral replication, eventually killing these cells.³⁰⁰ Surprisingly, all of our mBTICs were very resistant to MYXV infection (**Figure 3.11 A**), with almost no GFP expression in FJZ0309 and only sparse amounts seen in FJZ0528 and FJZ1116 infected with 5 MOI of vMyx-GFP and viewed at 120 hours post-infection. This is in stark contrast to what is seen in the human lines BT025 and BT048, two of the more resistant human BTIC lines,³⁰⁰ which have intense GFP staining throughout the spheres that are infected with virus. Next, these lines were infected with vMyx-RFP (**Figure 3.11 A**), which has the red fluorescent protein (RFP) under the control of the control of the poxvirus P11 late promoter.³¹² There seemed to be comparable amounts of GFP and RFP expression in these lines, suggesting that mBTICs infected with the virus are able to progress until Late

stage viral gene expression. Complementing these infection studies was a preliminary examination of actual viral replication within these lines, harvesting cells and supernatant for analysis of the production of functional MYXV virions (**Figure 3.11 B**). These results closely mimicked the fluorescent microscopy studies, where very little viral replication was seen in FJZ0309, replicating to 2.5×10^3 FFU/mL, while FJZ0528 and FJZ1116 replicated to 9.3×10^4 and 3.6×10^4 FFU/mL, respectively. The human BTICs reached titres of 2.8×10^5 and 1.6×10^6 FFU/mL for BT048 and BT025 and the NPCis serum-cultured cell line K1492 reached very high titres of 4.6×10^7 FFU/mL, very similar to what was seen in Chapter 3. Of note, statistics could not be performed in this experiment as this experiment was only repeated twice.

Finally, cell viability was measured in these lines in response to MYXV treatment (**Figure 3.11 C**). As could be predicted by the infection and replication experiments, FJZ0309 was completely resistant to viral infection, even at 25 MOI. mBTICs FJZ0528 and FJZ1116 succumbed to some form of viral-mediated cell death at higher MOIs, but remained quite resistant compared to other cells lines we have tested. For example, 10 MOI resulted in ~20% viability in the human BTICs, while mBTICs FJZ0528 and FJZ1116 had ~50% viability and FJZ0309 ~90%. To keep this in perspective, 10 MOI on K1492 at 48 hpi resulted in almost complete cell death (**Figure 3.2**). Collectively, these experiments demonstrate that these mBTIC lines are resistant to MYXV infection and MYXV-mediated cell death, even more so than human BTIC lines. It will be interesting in the future to look at mechanisms behind MYXV resistance and to their susceptibility to other clinically relevant treatments.

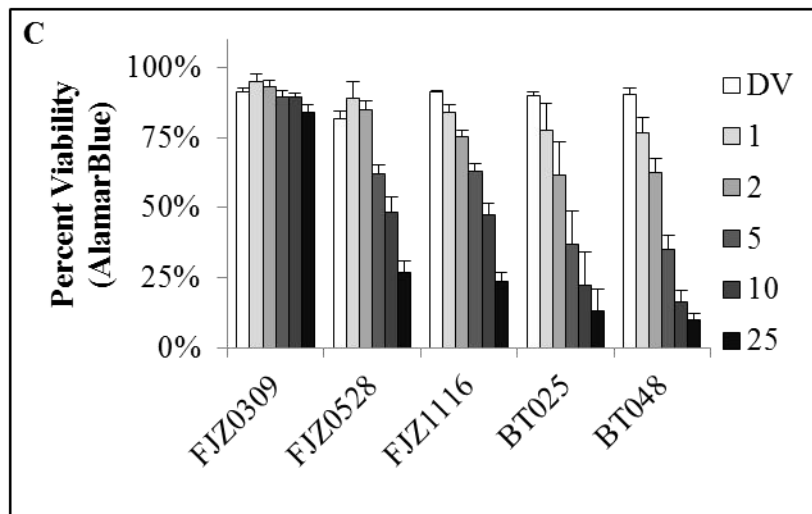
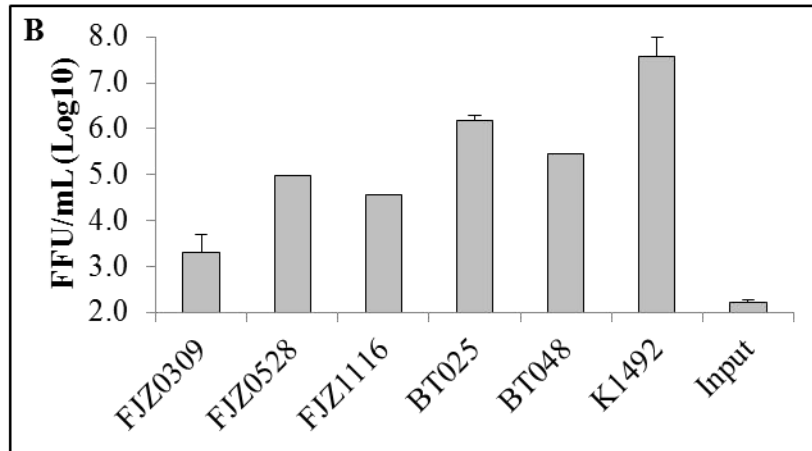
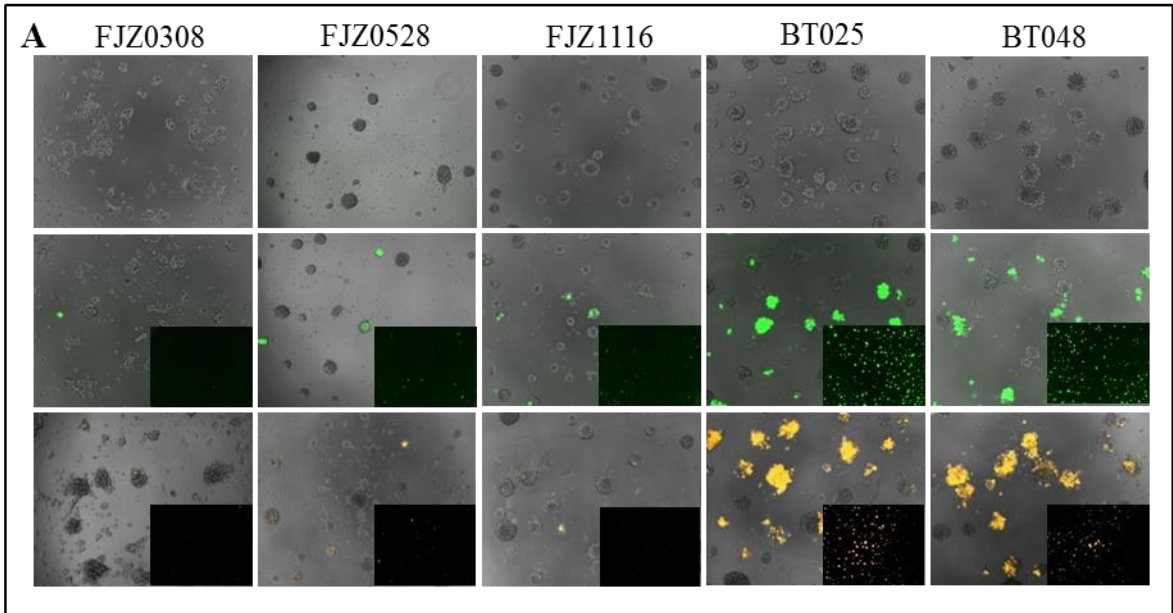


Figure 3.11: Murine BTIC lines FJZ0309, FJZ0528, and FJZ1116 and human BTIC lines BT025 and BT048 in response to Myxoma virus treatment *in vitro*. **A** - 1.0×10^4 cells were plated in a 96-well plate overnight, and then treated with vMyx-GFP or vMyx-RFP the next day. Photomicrographs of mBTIC or hBTIC lines not infected (top) infected with 5 MOI of vMyx-GFP (middle) or 5 MOI of vMyx-RFP (bottom). Phase-contrast with fluorescent overlay photomicrographs at 100X magnification and inlay pictures at 25X magnification taken at 120 hours post-infection. **B** – 2.5×10^4 cells plated in 24-well plates and infected with vMyx-GFP the following day. Supernatant and cells harvested and virus titred on BGMK cells as described previously. Error bars represent standard deviation (n=2). **C** - 1.0×10^4 cells were plated in a 96-well plate overnight and then treated with different MOIs of vMyx-GFP. Viability was read at 120 hours post-infection via fluorescent AlamarBlue assay (n=4). DV was at equivalence of 5 MOI.

3.3. Discussion

The first half of this chapter explores the use of a panel of primary, serum-cultured syngeneic mouse glioma cell lines to determine the mechanisms of treatment failure with our candidate oncolytic virus. As we have previously shown in syngeneic rodent models,²²⁰ MYXV treatment demonstrates neither replication nor survival benefit in these orthotopically grafted murine gliomas *in vivo*, despite being sensitive to MYXV-mediated cell death and viral replication *in vitro*. This is in stark contrast to what we have found in xenograft models with traditional human glioma cell lines²⁵³ and with freshly cultured patient neurospheres,³²⁵ where we found robust viral replication and survival benefit from MYXV treatment when these cells are grown in immunodeficient mice. This MYXV treatment failure in syngeneic gliomas is also in contrast to the situation for other classes of cancer localized outside the brain. For example, disseminated pancreatic cancer in the peritoneal cavity, where MYXV virotherapy is most effective against syngeneic murine Pan02 tumours in C57Bl/6 mice, compared to the reduced efficacy against the same cells engrafted into the intraperitoneal cavity of immunodeficient mice.³¹²

The murine glioma lines we used in this manuscript are derived from spontaneous

low-to-high grade gliomas that arose in *Trp53*^{+/-}/*Nf1*^{+/-} C57Bl/6 mice.^{127,131,133} As such, these lines fill an underrepresented niche in the experimental glioma therapeutics field that is of special interest to investigators interested in oncolytic viruses, immunotherapies, and/or stromal contributions to treatment. In this model, tumourigenesis is initiated by loss-of-heterozygosity at the *Trp53* and *Nf1* loci, leading to the development of low-grade astrocytomas, which can progress to diffusely infiltrative high-grade gliomas.¹²⁷ The relevance of the tumour suppressors *Trp53* and *Nf1* to glioma biology has been robustly validated in comprehensive genomic studies. Recent characterization of the mutational profiles of high-grade human gliomas by the Cancer Genome Atlas (TCGA) Research Network demonstrated that 23% of patient samples harboured somatic *NF1* inactivating mutations or deletions, of which 64% represented *NF1* heterozygous deletions.³²⁸ The relevance of *NF1* to human high-grade gliomas was further validated when the TCGA identified *NF1* as the defining mutation for the mesenchymal subtype of glioblastoma in a multi-dimensional genomic analysis.¹² Mutation of the human p53 gene, *TP53*, is the most frequent genetic alteration in precursor low-grade astrocytomas (present in 60% of cases)³²⁹ and was also shown to be frequently mutated in both the mesenchymal subtype and classical subtype of glioblastoma.¹² In addition to *TP53* and *NF1* mutations, prior *in vitro* characterization of the *Trp53*^{+/-}/*Nf1*^{+/-} C57Bl/6-derived cell lines revealed concomitant over-expression of commonly amplified receptor tyrosine kinases, including EGFR and PDGFR α .¹³³ The accumulation of aberrations in gene expression accurately recapitulates the clinical progression from low- to high-grade gliomas in patients, whereby loss of p53 function in low-grade astrocytomas precedes further genetic and gene expression changes that

ultimately lead to progression and development of high-grade gliomas.³²⁹ We consider it very important to preclinically test OV_s in cell lines that contain relevant genomic alterations, as these changes may ultimately determine the susceptibility to viral infection, viral replication, and viral-mediated cell death.

Secondly, these lines arose in C57Bl/6 mice, and thus are ‘graftable’ into the most common immunocompetent laboratory mouse strain. The power of using this strain of mouse is the numerous transgenic and knockout animals available, allowing for the interrogation and modelling of glioma-stromal interactions that can influence tumour-development and treatment response. Utilizing transgenic mice for the precise and complete ablation of specific aspects of the immune system or other aspects of the glioma microenvironment (ie, ECM components) allows for comprehensive studies that can interrogate exactly how these therapies work and can be improved.

Discovering minimal MYXV infection in the tumour *in situ* with no sustained viral replication, although not surprising, is worrisome if we extrapolate this data for the clinical use of virotherapy of gliomas and other brain cancers. Of the currently completed clinical trials of OV_s in glioma, only two,^{221,249} both with a neuroattenuated HSV, were designed to investigate viral infection and possible replication in the tumour. These results, with a combined total of 21 patients with their tumours resected or biopsied 2-9 days post-intratumoural virus inoculation, only found recovery of functional virus in three cases. Further, IHC staining for viral proteins was only found in 4 of the 21 patients. In contrast, both of these strains of HSV produced robust viral infection or replication and/or measurable efficacy in mouse subcutaneous or orthotopic xenografts.^{238,255} Interestingly, HSV-G207, as well as other unarmed HSV-strains, was

found to provide measurable survival benefit in an orthotopic syngeneic B6D2F1 glioma model, albeit only when infecting small tumours early after implantation.²⁵⁷ Notably, this study showed that *in vivo* viral clearance kinetics closely mimicked what occurs in our model, and, ultimately, what was seen in patients. Collectively, this suggests to us that syngeneic models more closely recapitulate the clinical experience with OV therapy for gliomas, and further understanding and optimization of these therapies should be robustly interrogated using these or similar syngeneic systems as we advance these treatments.

A potential limitation of this model is the ‘mesenchymal’ drift that seems to have occurred in these cells lines, such that the grafted tumours appear to be more of a gliosarcoma than a truly infiltrative astrocytoma from which they originated.^{127,128,131} Gliosarcomas are an uncommon GBM variant with biphasic glial and mesenchymal components.^{8,330} Interestingly, a current theory on the origin of gliosarcomas is that they arise from the abnormal differentiation of glioblastoma cells *in situ*.^{8,330} This, paired with the knowledge that human primary glioma cell lines cultured in serum selects an anomalous mesenchymal-type cell, one which no longer adequately represents the tumours from which they were derived,^{162,323,324} led us to believe that the serum culturing of cancer cell lines were leading to this transformation to a gliosarcoma-like orthograft.

To circumvent this problem in human lines, it has been shown that growing primary tumours as neurospheres¹⁵⁵ retains the genetic and phenotype integrity of the gliomas from which they were derived.^{308,318,319} Given the work we perform in the laboratory is only as relevant to the human condition as our models are, we attempted to build a syngeneic glioma mBTIC model that would retain the original characteristics of the spontaneous tumour it was grown in whilst being capable of being orthotopically grafted

into immunocompetent mice. As such, we derived cell lines from NPcis astrocytoma-bearing mice cultured under neurosphere conditions. These cells retained neural-stem cell markers, multi-lineage differentiation and formed tumours *in vivo* in immunocompetent C57Bl/6 mice that, at least superficially, recapitulate the tumours from which they were derived. Much work still has to be done to confirm these mBTIC are indeed *bona fide* cancer stem-like cells, but what has been begun in this chapter is a solid foundation to move forward.

The method of confirming the presence of a brain lesion prior to culturing cells from these mice was done to lessen the possibility that we were transforming ‘normal’ neural-stem cells from the mice in culture. However, even though these neural stem cells are already heterozygous for *Nf1* and *Tp53*, we failed to create a cell culture from one questionable lesion, suggesting that spontaneous transformation of these cells *in vitro* is difficult. This has been previously suggested with cultures from these mice.¹³³ Also of note is the low discovery-rate of neoplastic lesions in the NPcis mice, which have been reported to have greater than 70% penetrance in this strain of mouse.¹²⁸ This could be explained by the cutting of coronal sections that cover small proportions of the brain per section as opposed to sagittal sections. Also, my rudimentary neuropathology skills may have resulted in overlooking some more subtle lesions.

Of concern in this study is the origin of the original tumours themselves. NPcis mice are prone to both lymphomas and histiocytic tumours, both of which are capable of infiltrating the CNS. Detailed staining of these tumours along with a final neuropathology review will ultimately decide the origins of these tumours; however, the following observations strongly suggest they were malignant gliomas. Firstly, all malignant gliomas

(low and high grade) are known to express glial fibrillary acidic protein (GFAP; a CNS-lineage marker) to some degree,⁸ as do the two tumours we examined. Secondly, the infiltrative nature of these tumours suggests they are of glial origin, as non-glial tumours growing in the brain are often non-infiltrative.⁸ Thirdly is the ubiquitously high expression of OLIG2 in these lines. OLIG2 is an oligodendrocyte lineage specific transcription factor,³³¹ and while OLIG2 expression in human astrocytomas and other gliomas has been controversial,^{332,333} it is currently a hallmark of the proneural subclass of GBMs along with PDGFR α and other oligodendrocytic markers.^{12,13} Considering that the original characterization of the NPcis gliomas found that 22 of 23 tumours had high expression of PDGFR α *in situ*,¹³³ and our lines express OLIG2, and likely have loss of *Trp53*, strongly suggests that these tumours and resulting mBTIC lines are belong to the proneural subclass. This is curious, however, as *Nf1* deletions and mutations are rarely are found in the proneural class, and are mostly of the mesenchymal class.¹² This, of course, will have to be verified through analysis of the original tumours and expression analysis of the mBTIC lines. Of note, however, is that this classification should be expected in the NPcis mouse model, as it has recently been shown in lineage tracing experiments that *Nf1*^{-/-}*Trp53*^{-/-} mouse models of astrocytoma have oligodendrocyte-precursor cells, and transcriptome analysis matches to a proneural designation.¹⁴⁴

Of note here is the possibility that our culture conditions are not ideal for this particular phenotype of glioma. At the time these studies started, standard procedures for culturing neural stem cells were followed,¹⁵⁵ procedures that have been done with human primary tumours at our institution. This includes the addition of EGF to our culture media and not PDGF α , which in retrospect seems much more relevant. Indeed, EGFR

expression in the original NPcis lines derived in serum was shown to be a consequence of cell culture.¹³³ Perhaps the excess EGF, or more importantly the lack of PDGF α , supplied in the media may have or will change these lines. However, it has been shown that human BTICs can proliferate through their own autocrine growth factors,³⁰⁸ suggesting that maybe they can produce their own PDGF. Future studies should isolate these tumours in neural-stem cell media with the additional supplementation of PDGF α , or, considering that these lines have been stored at such low passage (~2-3), perhaps the addition of PDGF α to these lines during future use could help sustain their genetic integrity and phenotype.

What is worrisome is the change that we may already be seeing in the FJZ0309 mBTIC line. This tumour stained quite strongly for GFAP initially, however the cells are losing or already lost this marker. Further, preliminary immunostaining performed early after culture showed robust GFAP staining in this line (*data not shown*). We are unsure if this change is in response to a change in antibody, as GFAP has many clones, or if this line is succumbing to culture-induced changes. Indeed, it has recently been shown that hBTIC cultures may also suffer from ‘mesenchymal drift’ suggesting that factors in addition to serum may be responsible this abnormal transformation.³³⁴

As mentioned, further work must be done with these lines, and of much interest would be the characterization and comparison of the original tumours and the derived cell lines in terms of the markers and receptors they express. Further work looking more closely at the multilineage differentiation potential must also be performed. However, in addition to just the differentiated phenotypes observed by phase-contrast microscopy, the staining of the OLIG2, TUJ1 and/or GFAP markers within the neurospheres suggest that

this is indeed occurring. It is not unusual to find these differentiation markers within a neurosphere, as some of these markers might represent cells that have already committed down a particular lineage. The current paradigm suggests that even within a BTIC culture, only a fraction of these cells are the putative cancer stem cells, while the remaining cells in the neurosphere represent partially committed/partially differentiated cells.^{161,300,319}

The resistance of these lines to Myxoma virus is quite striking, and FJZ0309 is the most resistant line encountered in the Forsyth lab. It appears that MYXV is having problems infecting these mBTICs, not replicating in them. This was demonstrated by both early and late viral gene expression in these cells, in addition to the functional viral replication observed. Perhaps this is suggesting that there is some extracellular matrix proteins expressed by these mBTICs that is eventually lost as a consequence of passage in serum. Indeed, a single preliminary experiment passaging FJZ0309 in High Sucrose DMEM with 10% FBS for 5 passages, demonstrated that these cells strongly change their phenotype, becoming a homogenous lawn of cells that looked very similar to the conventional NPCis lines we use. These ‘differentiated’ FJZ0309 cells were readily infected by MYXV (*data not shown*). Alternatively, given the heterozygous nature of these neurospheres, perhaps only a certain lineage within these spheres is able to be infected.

It is unknown what the mechanism of this mBTIC resistance may be and how it is relevant to OV therapy for gliomas. As mentioned, we have already used patient-derived human BTIC cultures and shown that Myxoma virus treatment is functional *in vitro* and *in vivo*,³⁰⁰ albeit these BTIC cultures had been passaged quite extensively. Several OVs

have also been studied in BTIC models *in vitro* and *in vivo*, including herpes virus,³²¹ adenovirus,^{335,336} and vaccinia virus²¹⁷, and all these studies demonstrated the capacity of OVs to be efficacious in this model system. Further studies will have to be performed to interrogate whether this is a mouse-specific phenomenon.

This study, although still in its initial stages, shows promise in achieving its goal of producing a set of mBTIC lines that produce relevant, heterozygous and infiltrative glioma capable for use in preclinical studies in immunocompetent animals.

4. THE ROLE OF TYPE-I INTERFERON IN MEDIATING TREATMENT FAILURE IN NPcis PRECLINICAL GLIOMA MODELS

4.1. Introduction

Moving forward with the syngeneic lines we characterized that were sensitive to MYXV *in vitro* but resistant to replication and killing *in vivo*, we next investigated possible mechanisms in mediating the treatment failure in these models. These studies were begun by investigating the potential role Type-I Interferon could play on treatment. Of note, almost all of the work presented below is published in two papers by Zemp et al.^{300,337}

Type-I interferon (**IFN α/β**) is the quintessential anti-viral cytokine, being able to mediate anti-viral responses in a variety of cell types. Further, it is a fundamental part of the anti-viral immune response in the CNS, as shown by IFN α/β -receptor deficient mice having increased neurovirulence, CNS viral load and/or mortality to many viruses, including West Nile²²¹ and Sindbis²⁵¹ viruses as well as viruses commonly used in OV therapies such as HSV,²⁴⁷ MV,²⁴⁹ and VSV.^{338,339}

Expression of IFN α/β is mediated through recognition of conserved molecular patterns unique to pathogens (pathogen-associated molecular patterns; **PAMPs**) which are recognized by a number of host inter- and extracellular pattern-recognition receptors (**PRRs**). The CNS, and the brain parenchyma especially, are unique in terms of the PRRs that they express. In the periphery, it is thought that only the specialized professional immunocytes, such as dendritic cells (**DCs**) and macrophages, constitutively display large complements of PRRs; however, in the brain, microglia and astrocytes, and to a lesser extent neurons, express many PRRs. Toll-like receptors (**TLR**) are one group of PRR,

having membrane-bound extracellular members (TLR-2, -4, -5, -6) and endosomal membrane-bound intracellular members (TLR-3, -7, -8, -9).³⁴⁰ Generally speaking, these extracellular TLRs are involved in sensing bacterial PAMPs, while the intracellular TLRs recognize foreign nucleic acids, such as viral or bacterial genomes. Of these viral sensing TLRs, mouse and human microglia and astrocytes constitutively express TLR-3, TLR-7, and TLR-9.^{341,342} Further, astrocytes and microglia constitutively express RIG-I and Mda-5, cytosolic PRRs that are very important in the recognition of viral double stranded RNA.^{58,343} Taken together, the constitutive expression of these PRRs indicate that the brain is poised to mount a robust antiviral ‘counterattack’ once viral genomic material is recognized.

Resident astrocytes and microglial are the chief IFN α/β producing cells in the CNS.³⁴⁴⁻³⁴⁶ The production of IFN α/β in these cells starts with the initial recognition of a virus by a PRR, which activates a signaling cascade that culminates in the phosphorylation and dimerization of interferon regulatory factor (IRF)-3. This causes nuclear translocation of IRF3, and production of the IFN β . This early IFN is then secreted to signal in an autocrine and paracrine manner to the IFN α/β receptor (IFNAR1/IFNAR2) which utilizes TYK2 (IFNAR1) and JAK1 (IFNAR2) to phosphorylate STAT1 and STAT2 to stimulate the formation of the ISGF3 complex (STAT1/STAT2/IRF9) to turn on IFN stimulated genes (**ISGs**) and IRF7. Many of these ISGs have direct anti-viral activity, attenuating host metabolism and limiting viral replication. IRF7 plays an important role in a IFN α/β positive feedback-loop, whereby PRR activation in a cell with IRF7 results in an amplified production of IFN α/β that includes the production of all or many of ~13 human IFN α s as well as IFN β .²⁴⁴

Aberrant IFN α/β signalling has been proposed to be one mechanism by which specific OV infection in cancer cells may function. It has been proposed that during transformation tumor cells lose their ability to mount an anti-viral response to IFN α/β .³⁴⁷⁻³⁴⁹ However, in our hands, rat²²⁰ and human gliomas²⁶² retain their ability to be protected from OV infection by exogenous IFN α/β , leaving this a potentially significant therapeutic obstacle in the clinic. Further, when examining the roles of IFN α/β on OV therapy, only syngeneic models can be used as Type-I¹¹⁰⁻¹¹² interferons are not cross-reactive between species; therefore, any IFN α/β derived from the microglia or astrocytes in response to viral infection in the brain would not be recognized by a human orthoxenograft, perhaps over-estimating OV efficacy in xenograft models (**Figure 4.1**).

In this Chapter, **it was hypothesized that Type-I interferon signalling plays a major role in Myxoma virus treatment failure *in vivo***. The **main objectives** of these studies were to: **1) Confirm *in vitro* that IFN α/β acts in a species-specific manner in our glioma models and to investigate if NPcis cell lines are protected from MYXV infection by exogenous murine IFN α/β ; 2) Determine if IFN α/β signalling occurs in the glioma microenvironment following intratumoural MYXV treatment and that this is mediating MYXV treatment efficacy.**

Here, it was confirmed that human glioma cell lines and mouse glioma cell lines are unresponsive to heterospecific IFN β , and show that NPcis mouse glioma cell lines are exquisitely sensitive to protection from MYXV infection with exogenous murine IFN β *in vitro*. Interestingly, however, IFN α/β production was not detected by following the infection of NPcis cells *in vitro* using both transcript and protein analysis, yet they retain the ability to produce IFN α/β to other stimuli. This lack of IFN α/β production in response

to a viral infection was intriguing, and could potentially be an important factor clinically, thus this investigation was continued in conventional human glioma cells lines, human brain-tumour initiating cell cultures, and untransformed human cell cultures. Our data suggested that IFN α/β was not produced in any of these lines in response to Myxoma infection.

This apparent lack of production of IFN α/β *in vitro* did not preclude its role *in vivo*, as several cell types in the CNS and periphery are capable of making IFN α/β . However, K1492 tumours infected with a high dose of MYXV did not produce any measurable mIFN α or mIFN β . To confirm the lack of a role of IFN α/β *in vivo*, an interferon insensitive K1492 cell line was engineered through shRNA knock-down of IRF9. IRF9 is a central mediator of IFN α/β signalling, a member of the ISG3 transcription factor complex, directing STAT1/STAT2 to genes containing interferon stimulated elements (**ISRE**). This IRF9 knockdown cell line had identical viral infection and clearance kinetics as the wildtype or scrambled controls, strongly suggesting that IFN α/β is not involved in MYXV infection *in vivo*.

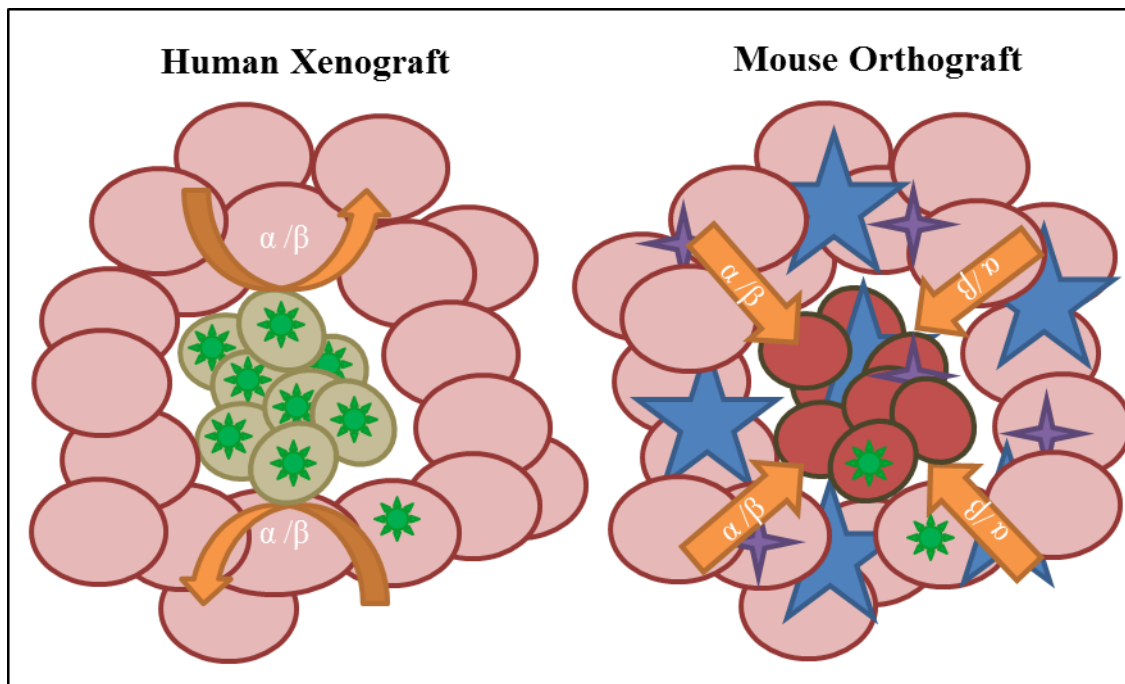
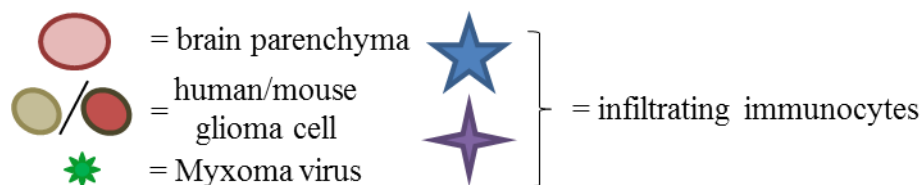


Figure 4.1: Differences between xenograft and syngeneic glioma models that could explain the resistance to Myxoma therapy *in vivo*. Human xenografts lack some of the interactions with the tumour stroma that are conserved in syngeneic mouse orthografts. For example, anti-viral type-I interferon produced by the tumour stroma will not activate human IFN α/β receptors on glioma xenografts due to species specific limitations in that signalling axis. Conversely, syngeneic murine orthografts will retain these interactions, as well as other interactions with immune cell components that may be lacking in xenografts.



4.2. Results

4.2.1. *Species-specificity of type-I interferon and protection of NPcis cell lines by exogenous type-I interferon*

It has long been known that human cells are non-responsive to murine IFN α/β ,¹¹⁰⁻¹¹² in fact, heterospecific expression of the mouse interferon receptors in primate cell lines lead to their identification and cloning.^{110,113} To start our foray into the role of IFN α/β in MYXV-treatment resistance, it was confirmed that murine IFN α/β did not function on human cells lines. For this, human and mouse IFN β was tested on HEK-Blue™ IFN α/β Cells (Invivogen), which has a secreted embryonic alkaline phosphatase (SEAP) reporter gene under the control of the human ISG54 promoter. Only human IFN β resulted in the colorimetric change indicating the engagement of IFN α/β signalling (**Figure 4.2 A**). Next, confirmation of this specificity using our standard human (U87) and murine (K1492) glioma cell lines was explored. This was achieved by creating a reporter construct that would express firefly luciferase in the presence of IFN α/β signalling (described in **Chapter 2.5.2**). Here it was shown that interferon-induced luciferase expression occurred in a dose dependent manner only when using homospecific IFN β (**Figure 4.2 B**). With these results and the support of the literature, it could be concluded that in our models, mouse and human IFN α/β is not reactive across species.

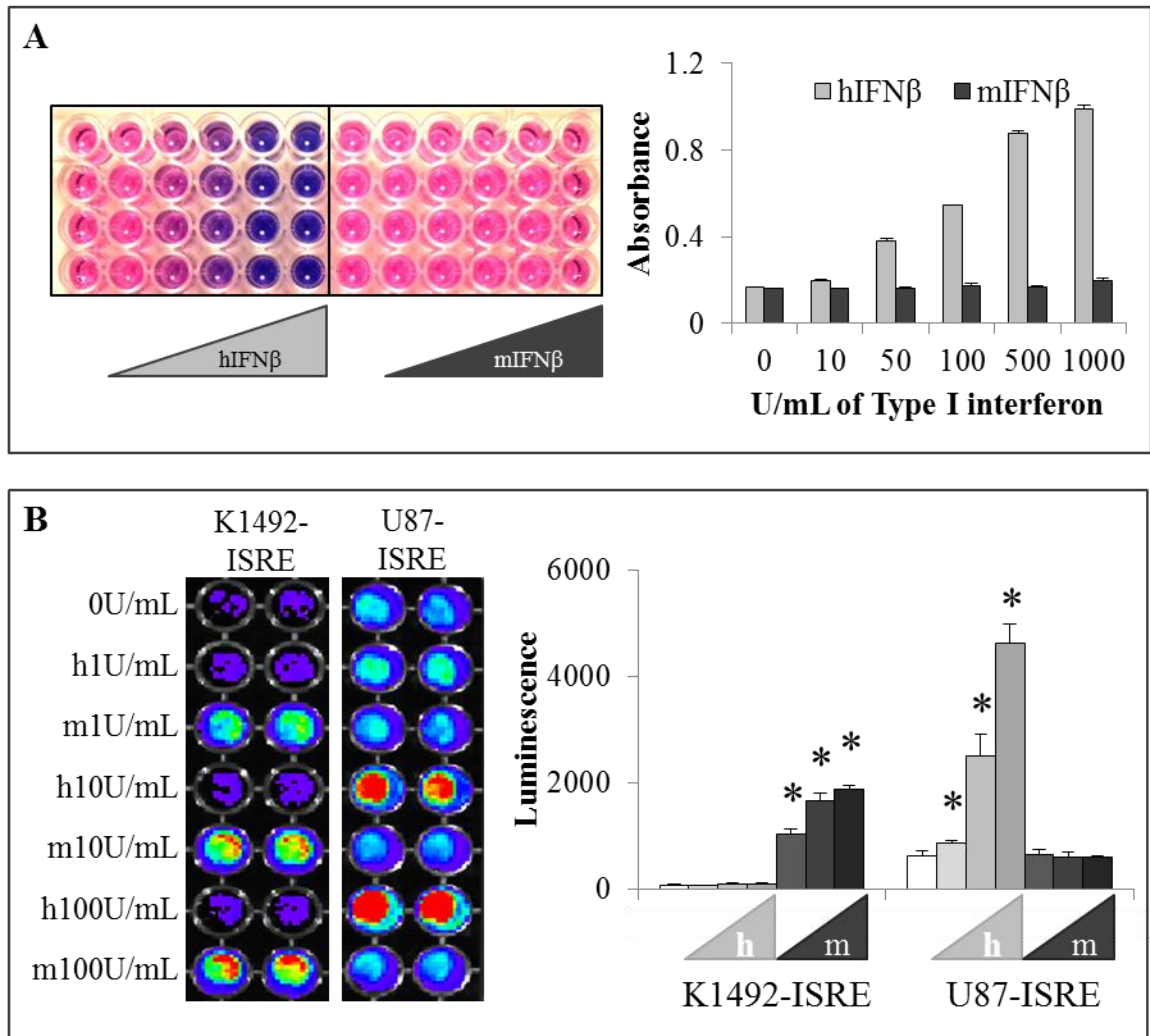


Figure 4.2: Type-I Interferon is not cross-reactive between human and murine glioma lines. **A)** Specificity of mouse and human IFN using the HEK-Blue system (InvivoGen) which uses an interferon specific promoter upstream of SEAP to detect human IFN. Graph is quantitated picture where error bars represent standard deviation between wells (n=4 of internal replicates). **B** – Mouse or human IFN β on K1492 or U87 lines which stably express an ISRE::FLUC construct. Graph is quantified from representative picture (left). Error bars represent standard deviation and asterisks p<0.05 (t-test) between groups respective to the no interferon control (n=4).

Next, it was determined if the NPCis cell lines were protected from MYXV viral infection *in vitro*, as it has previously been suggested that transformed cells have lost their ability to respond to IFN α/β signalling.^{113,350} Surprisingly, all the tested lines were protected by exogenous mIFN β with as little as 1 U/mL of mIFN β (**Figure 4.3 A, B**). This demonstrated that mIFN α/β production from the tumour or stroma in syngeneic models had the potential to protect tumour cells from viral infection.

4.2.2. NPCis cell line type-I interferon production in response to MYXV *in vitro* or *in vivo*

Next, the IFN α/β response to MYXV infection of the NPCis glioma lines was assessed *in vitro*. First, the B16-Blue™ IFN α/β Cells detection system (Invivogen) was employed to detect murine IFN α/β production by these lines. This system is the murine counterpart to the HEK-Blue system described above. The strength of this system allows the simultaneous assay of all IFN α/β production. Surprisingly, MYXV infection with 1.0 MOI did not produce any IFN α/β 24 hours after infection in any of the NPCis cell lines (**Figure 4.4 A**). This was not due to these line's inability to produce IFN α/β , as both 1.0 MOI of VSV Δ 51 and 1.0 μ g/mL of polyI:C delivered via lipofectamine significantly induced IFN α/β reporter gene activity. Interestingly, naked polyI:C given extracellularly did not elicit a response in these cells, suggesting that the intracellular dsRNA sensing machinery such as RIG-I/MDA5 was mediating the IFN response to polyI:C.^{238,255}

To confirm these results, reverse-transcriptase PCR was performed on lines K1492 and K1861 (**Figure 4.4 B**), and found identical results. After 24-hours of exposure to 1.0 MOI MYXV, both lines had no significant transcriptional activation of the IFN β and IFN α 4 genes, while both VSV Δ 51 or intracellular polyI:C, produced robust IFN α/β

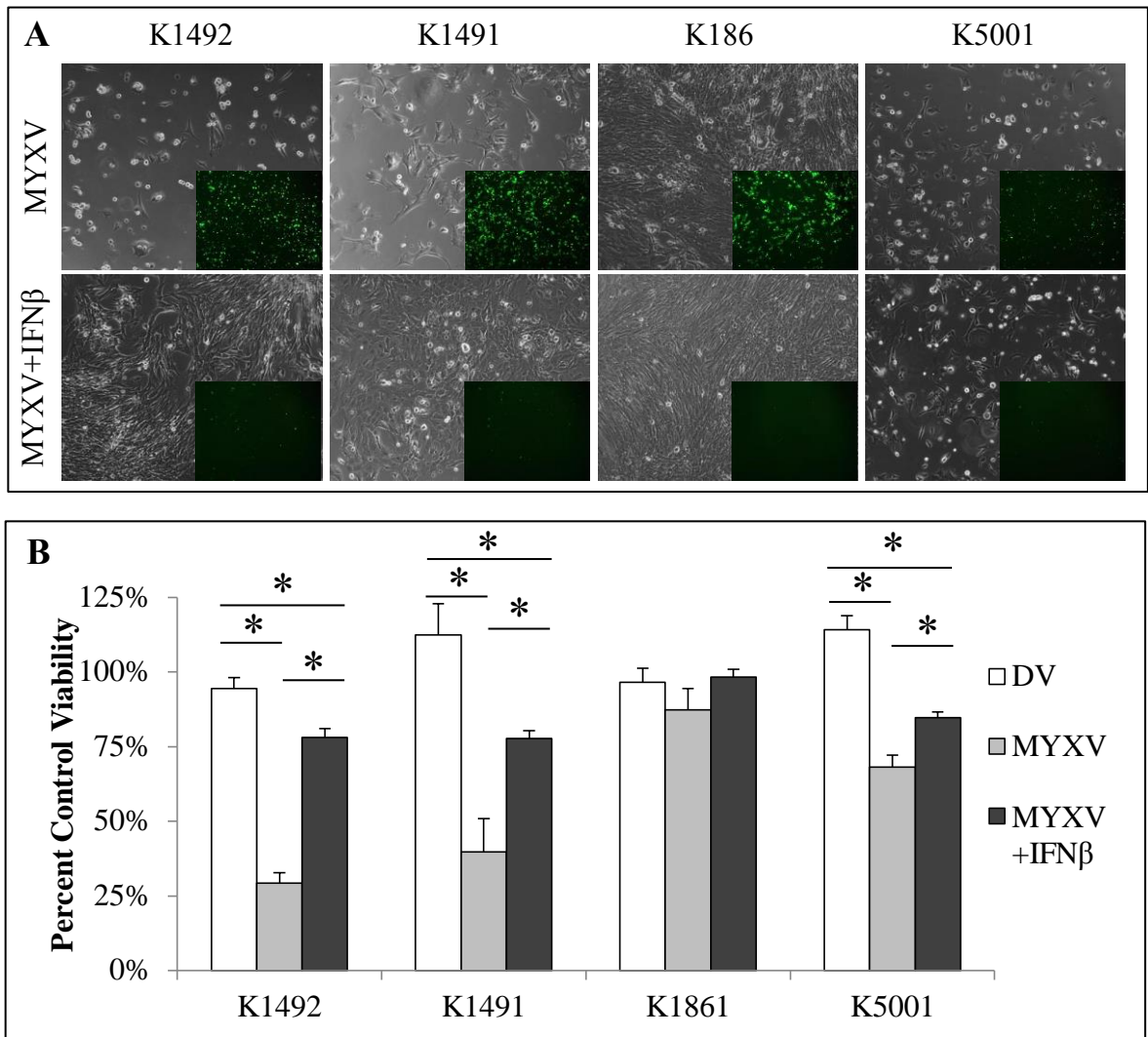


Figure 4.3: *NPcis* cell lines are protected by exogenous murine *IFN* β . **A** – *NPcis* cell lines infected for 48 hpi with 1.0 MOI vMyx-GFP (top row; 100X phase/contrast, 25X GFP inlay) or 1.0 MOI vMyx-GFP pretreated 6 hours with 1.0 units of mouse *IFN* β (bottom row; 100X phase/contrast, 25X GFP inlay). **B** – Percent viability corresponding to controls (MYXV and DV to no treatment control; MYXV + IFN to IFN alone control) of *NPcis* cell lines at 48 hpi with 1.0 MOI vMyx-GFP or 1.0 MOI vMyx-GFP pretreated with 1.0 units mouse *IFN* β for 6 hours as measured by Alamar blue. Error bars represent standard error and asterisks $p < 0.05$ (t-test) compared to control (n=4).

responses. The time point of 24 hpTx also allowed for auto/paracrine IFN α/β signalling, and showed that only K1861 had transcriptional activation of interferon-stimulated genes IRF7, ISG15 and CXCL10. The activation of these genes in the absence of functional IFN production suggests that perhaps these are activated upon infection independent of IFN α/β production^{351,352} or that perhaps Type-I interferon was being produced at levels beneath our detection level (~1U/mL). Interestingly, this only occurred in the resistant K1861 cell line and, thus, could be part of the mechanism mediating its *in vitro* resistance. Interestingly, IFIT2 (the murine homologue of ISG56) was constitutively active in both lines.

Given the apparent lack of IFN α/β produced by the lines in response to MYXV infection *in vitro*, it was important to determine if stromal IFN α/β production might have been produced *in vivo*. IFN α/β production was measured *in vivo* by ELISA in MYXV-treated K1492-bearing C57Bl/6 mice. Interestingly, we could not find a robust IFN α/β response following intracranial MYXV injection (**Figure 4.5 A**); this is particularly striking in comparison to the response to a small amount of naked polyI:C (5 μ g) administered intracranially. Given the negative outcome of the experiment, with all the controls acting as they should, it was deemed sufficient to end this after only testing two animals per group; and thus no statistics could be performed on this experiment.

We next investigated if the K1492-ISRE::FLUC cell line was orthotopically grafted in C57Bl/6 mice to establish if interferon-induced luciferase activity could be monitored *in vivo*. Unfortunately, this construct gave a surprisingly high background when implanted, and was not responsive to even the positive control polyI:C, which the ELISA demonstrated to elicit a IFN α/β response *in vivo* (**Figure 4.5 A**). This high

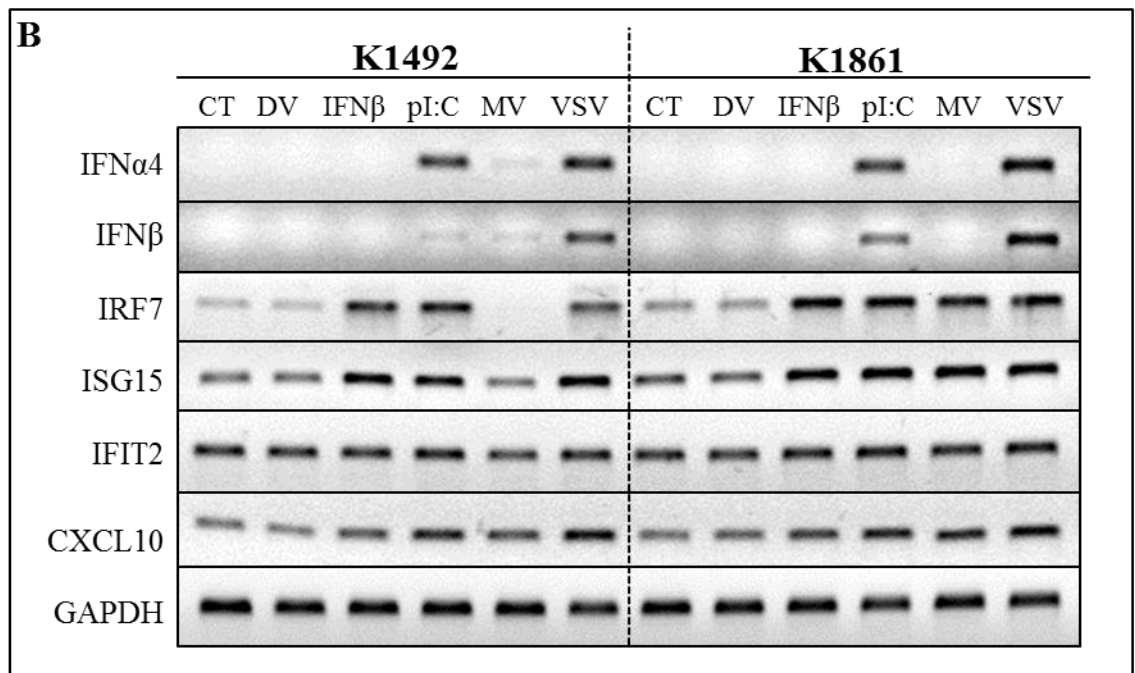
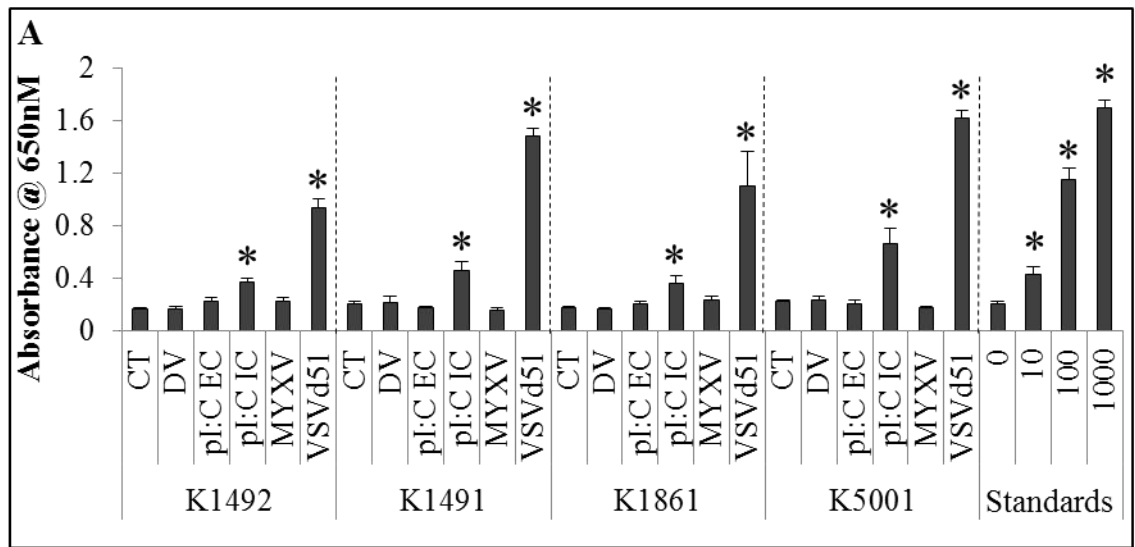


Figure 4.4: NPcis cell lines do not produce any functional type-I interferon to Myxoma virus in vitro yet retain the ability to produce type-I interferon to other stimuli. . **A** – Type-I interferon production in NPcis cell lines in response to 1.0 MOI vMyx-GFP (MYXV), 1.0 MOI of oncolytic vesicular virus (VSV-Δ51), 25 μg/μL delivered extracellularly (pI:C EC), 1.0 μg/μL polyI:C delivered by intracellularly via lipofectimine (pI:C IV), UV-inactivated MYXV (DV) or no treatment (CT) as measured using the HEK-Blue system 24 hpi. Error bars represent standard error and asterisks p<0.05 compared to control (t-test, n=4). **B** – Reverse-transcriptase (RT)-PCR of type-I interferons and type-I interferon responsive genes in K1492 and K1861 lines in response to 1.0 MOI vMyx-GFP (MYXV), 1.0 MOI of oncolytic vesicular virus (VSV-Δ51), 1.0 μg/μL intracellular polyI:C (pI:C), 10 Units of exogenous mouse IFNβ (IFNβ), UV-inactivated MYXV (DV) or no treatment (CT).

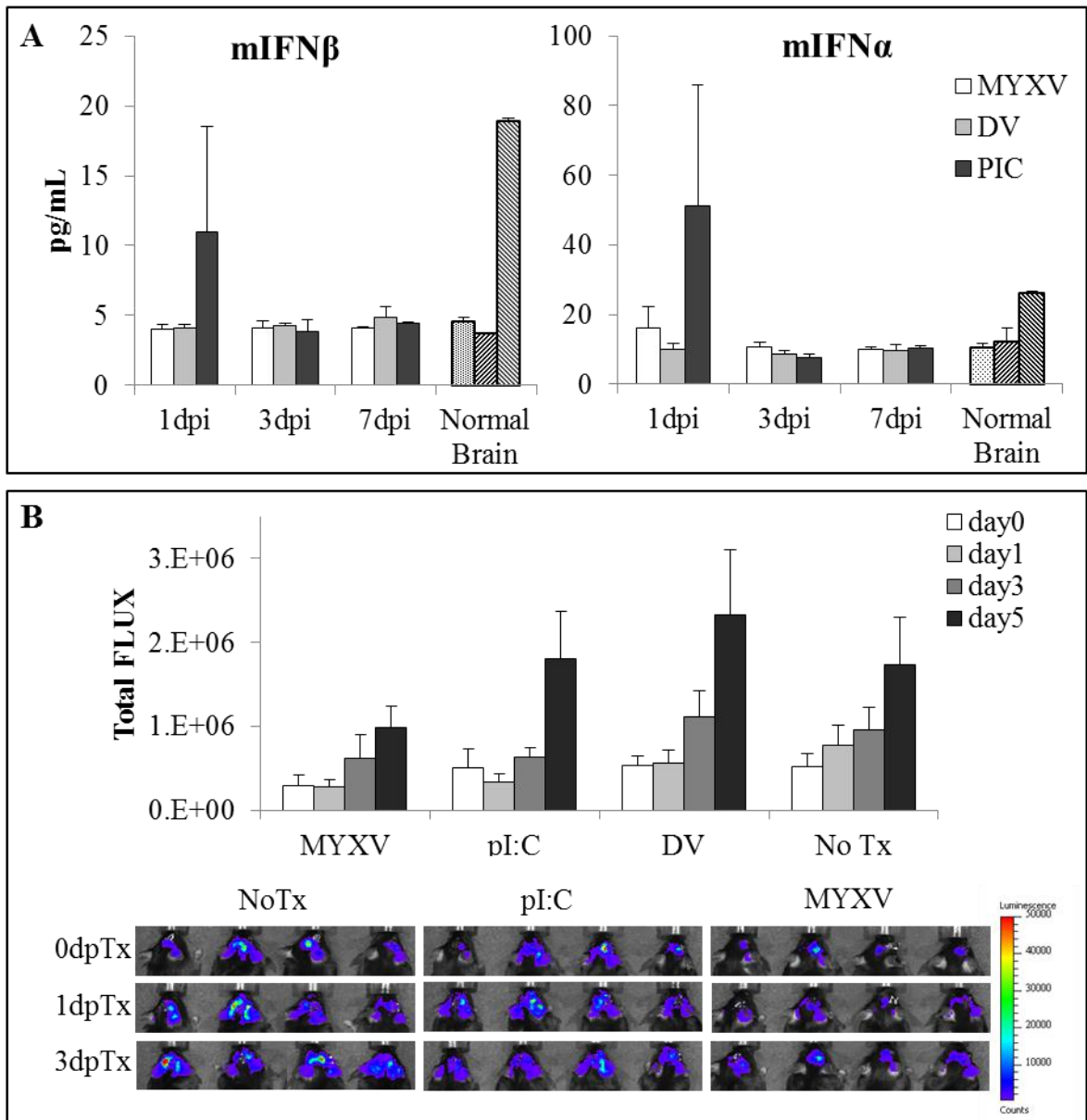
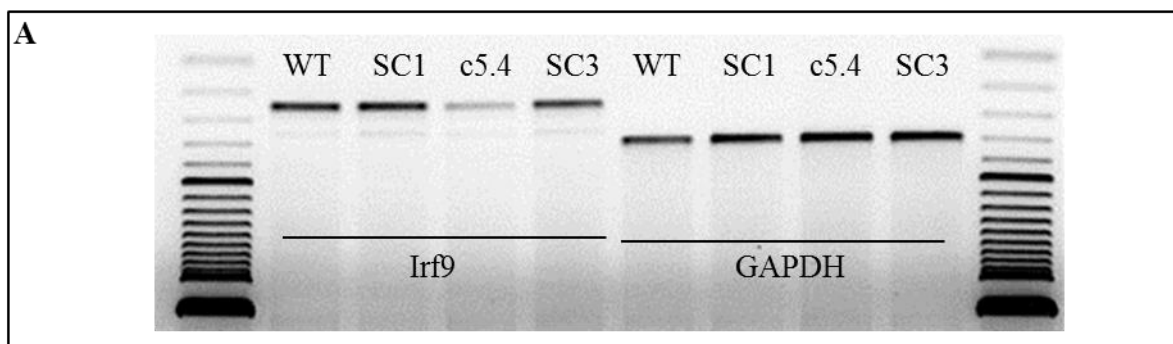


Figure 4.5: *Type-I Interferon is not produced in the K1492 glioma microenvironment in vivo.* **A** - ELISA of mouse IFN β and mouse pan IFN α from 14 day K1492 tumours 1, 3 or 7 days post intracranial administration of 5×10^6 PFU MYXV (MYXV), UV-inactivated MYXV (DV) or 5 μ g of naked polyI:C (pI:C), n=2 per time point. Stippled bar represents no treatment K1492 tumour at 14, 15, 17, and 21 days combined (n=2 per time point). Left-slashed bars are normal mouse brain (n=2) and right-slashed bars are normal mouse brain 'spiked' with 15 pg and 20 pg of IFN β or IFN α , respectively. Error bars represent deviation. **B** -K1492-ISRE::FLUC treated at 14 dpi with intracranial administration of 5×10^6 PFU vMyx-GFP (MYXV; n=10 at 0 and 1 dpTx, n=8 at 3 dpTx, n=6 at 5 dpTx), UV-inactivated MYXV (DV n=9 at 0 and 1 dpTx, n=7 at 3 dpTx, n=5 at 5 dpTx), 5 μ g of naked polyI:C (pI:C n=9 at 0 and 1 dpTx; n=7 at 3 dpTx; n=5 at 5 dpTx), or No treatment (NoTx; n=8 at 0 and 1 dpTx, n=6 at 3 dpTx, n=4 at 5 dpTx). Luciferase measured (Total FLUX) from region-of-interest around the entire mouse skull following treatment.

background suggested that IFN α/β signalling was already engaged in the K1492 tumour while in the *in vivo* microenvironment.

4.2.3. Creation of interferon insensitive NPCis cell lines through IRF9 knockdown

To show definitively that IFN α/β production by the tumour or the stroma was not involved in mediating the *in vivo* resistance to MYXV, K1492's ability to respond to IFN α/β was reduced by silencing IRF9 with an shRNA construct transduced via lentiviral infection (Creation of lines see **Chapter 2.5.3**). Knockdown of IRF9, as a central mediator of IFN signalling, would also attenuate any anti-viral crosstalk from Type-II and III IFN produced by the tumour or stroma, which could also possibly mediate this resistance. IRF9 was successfully knocked-down in K1492 (**Figure 4.6A**), which resulted in a functional loss of transcriptional activity at interferon-response elements (ISRE) as measured by the K1492 ISRE::FLUC cell line (**Figure 4.6 B**). Importantly, this IRF9 knockdown resulted in a dramatic loss of the protection provided by the application of exogenous IFN β *in vitro* (**Figure 4.6 C**). Thus, these modified K1492 tumours when implanted into the brains of C57Bl/6 mice would be insensitive to IFN α/β .



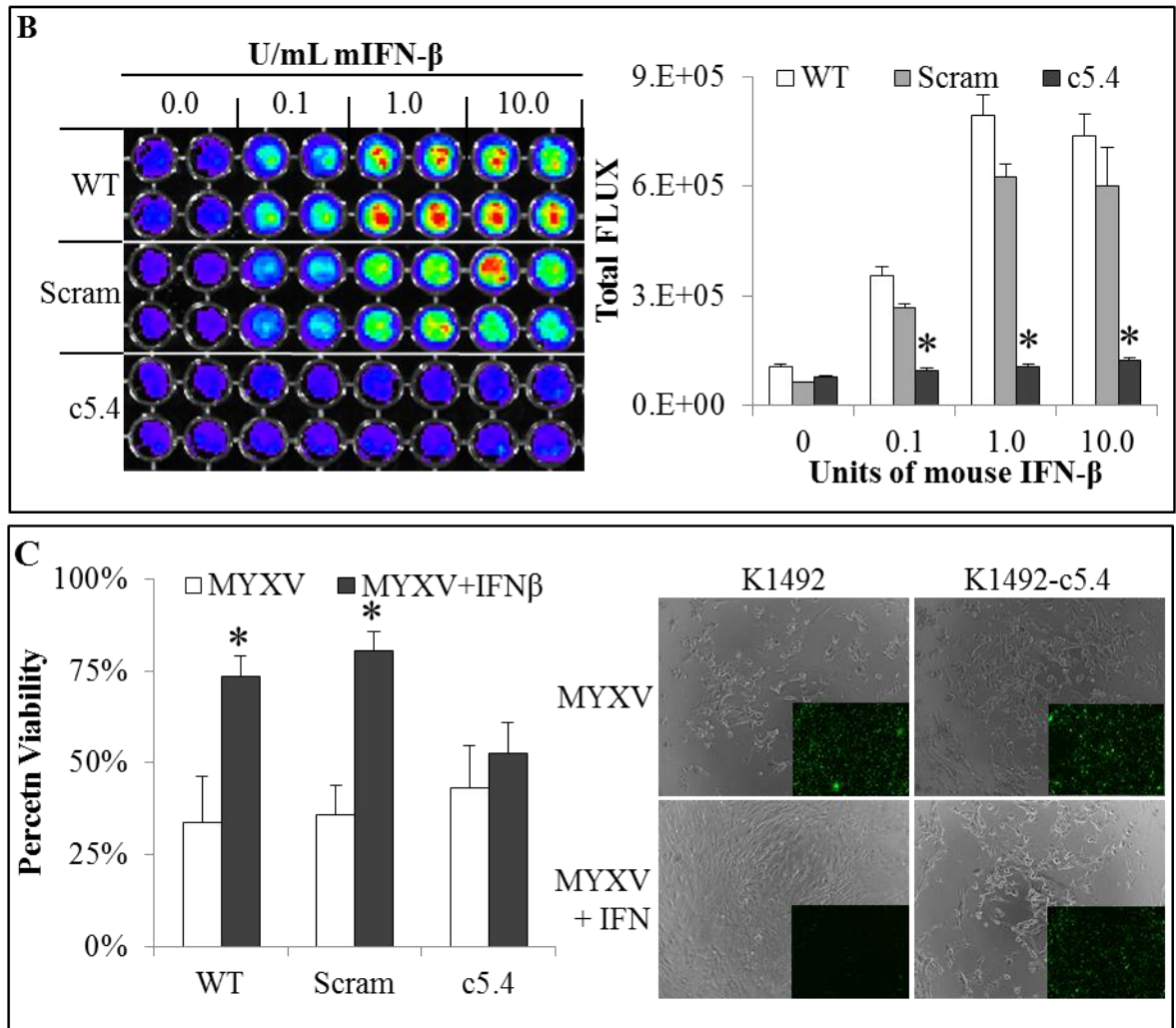
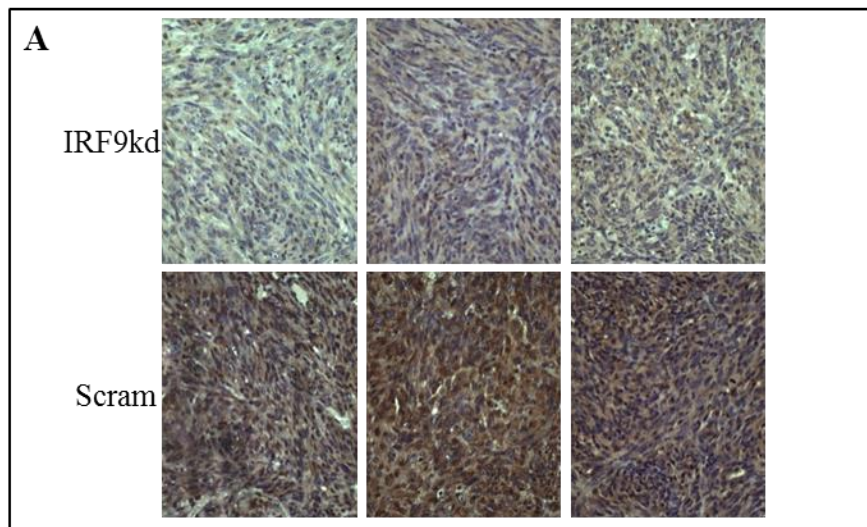


Figure 4.6: *IRF9* knockdown results in loss of protection of type-I interferon in K1492 in vitro. **A** – RT-PCR of *IRF9* message level after stable transduction of *IRF9* shRNA (c5.4), scrambled control (SC1 and SC3) or wildtype (WT) K1492. **B** – Luciferase activity of an interferon-inducible FLUC construct stably transfected into *IRF9* knockdown (c5.4), scrambled control (Scram) or wildtype cells (WT) K1492 cells 8 hours after the addition of exogenous mIFN β . Error bars represent standard error and asterisks $p < 0.05$ when compared to WT K1492 (t-test, $n = 3$). **C** – K1492 knockdown construct or controls 48 hpi with 1.0 MOI vMyx-GFP with or without the pre-treatment with 1.0 U of mouse IFN β as measured by AlamarBlue. Error bars represent standard error and asterisks $p < 0.05$ when compared MYXV alone (T-test, $n = 4$). Photomicrographs of MYXV infection with/without 1 U/mL IFN β in K1492 wildtype (WT) or *IRF9* knockdown (c5.4; top row; 100X phase/contrast, 25X GFP inlay).

To determine if ablating IFN α/β signalling in the tumour *in vivo* would allow for more robust viral infection and/or replication of MYXV *in vivo*, IRF9 knockdown or its scrambled control K1492 was implanted in C57Bl/6 mice. Importantly, the knockdown persisted *in vivo* as shown by immunohistochemistry for IRF9 (**Figure 4.7 A**). Treatment with vMyx-FLuc resulted in no change in survival (35 days for no treatment versus 30 days for MYXV treatment in Scram-K1492 (Log-rank Mantel-Cox test; p=0.8279) and 35 days for no treatment versus 36 days for MYXV treatment in IRF9kd-K1492 (Log-rank Mantel-Cox test; p=0.6406); **Figure 4.7 B**), with no change in viral FLUC (**Figure 4.7 C**). Collectively, the observations of no significant IFN α/β production *in vitro* and no apparent induction of IFN α/β *in vivo*, with no change in replication kinetics in IFN α/β -insensitive gliomas suggested to us that the swift clearance and control of MYXV in these gliomas in immunocompetent mice is independent of anti-viral IFN α/β signalling.



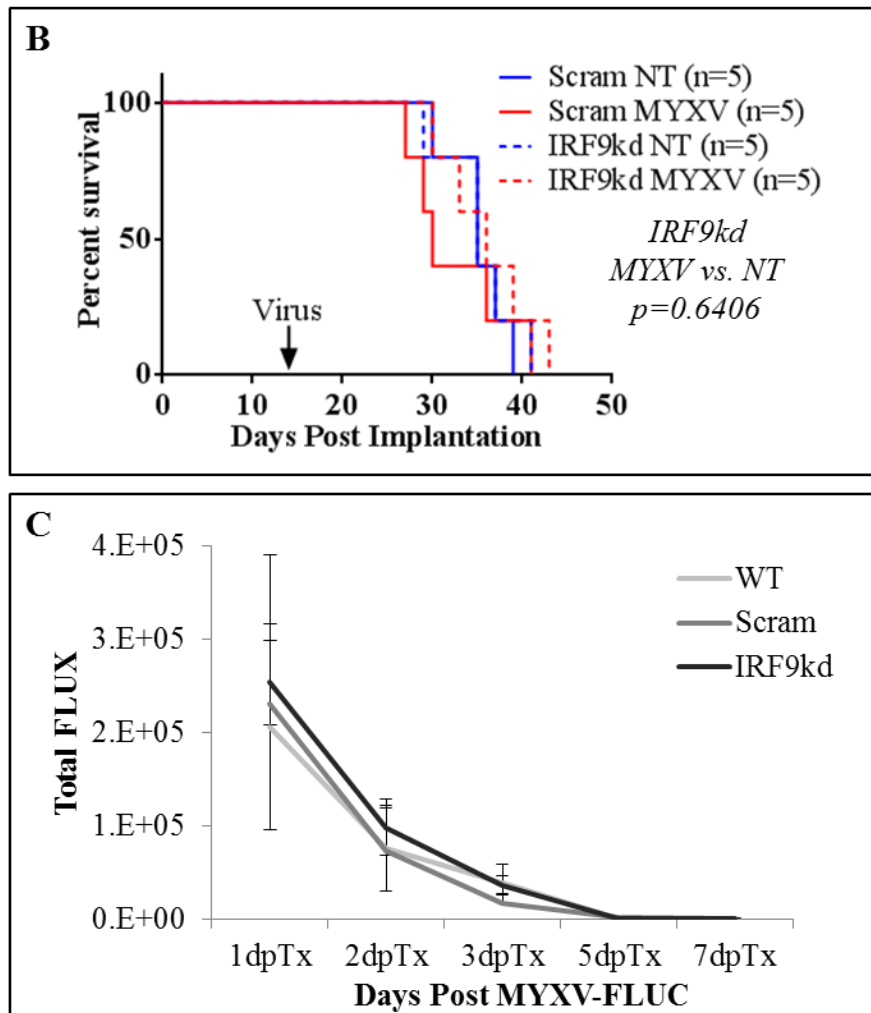


Figure 4.7: *K1492 IRF9 knockdown persists in vivo, but makes no difference in viral replication or treatment efficacy.* **A** – Immunohistochemical confirmation of IRF9 knockdown clone c5.4 (IRF9KD) or Scrambled control (Scram) in K1492 tumours 14 days post-implantation (200X). **B** – Survival of animals implanted with 5×10^4 K1492 c5.4 (IRF9kd) or Scrambled control (Scram) in C57Bl/6 mice receiving 5×10^6 PFUs vMyx-FLUC (MYXV) or no treatment (NT) on at 14 dpi. **C** – Luciferase measured (Total FLUX) from region-of-interest around the entire mouse skull following 5×10^6 PFUs vMyx-FLUC in K1492 control (WT), scrambled control (Scram) or IRF9 knockdown (IRF9kd) at 14 dpi (n=5). Error bars represent standard error.

4.2.4. Testing human cell lines for type-I interferon production following Myxoma virus infection

To test if the inability of MYXV to produce an IFN α/β response extended beyond the murine glioma cell lines, a variety of human cell lines were tested for a similar response. This work was published in Zemp *et al.*, 2013.³⁰⁰ The conventional human glioma cell line U251 was tested for IFN α/β production by RT-PCR at 12 hours post-treatment and the HEK-Blue interferon detection system for functional IFN α/β production at 24 hours post-treatment. RT-PCR for IFN α/β and IFN responsive genes found that only a small band of IFN $\alpha 4$ was detected with MYXV, although this did not seem to elicit a functional IFN α/β response as measured by a lack of autocrine signalling to activate transcription of IRF7, ISG15 or MX1, as seen with the polyI:C treatment (**Figure 4.8 A**). This was confirmed by the HEK-Blue assay revealing no detected IFN α/β secreted in the U251 culture. U251 did, however, retain an ability to respond to extracellular polyI:C at both the transcriptional and functional levels. MYXV was also unable to produce a IFN α/β response in the U87 cell line (**Fig, 4.8 B**); however, this experiment was not designed to show if U87 was able to produce IFN α/β to other stimuli, but does demonstrate that IFN α/β signalling is intact through the stimulation of IRF7, ISG15 and ISG56 in response to 50 U/mL of exogenous IFN α .

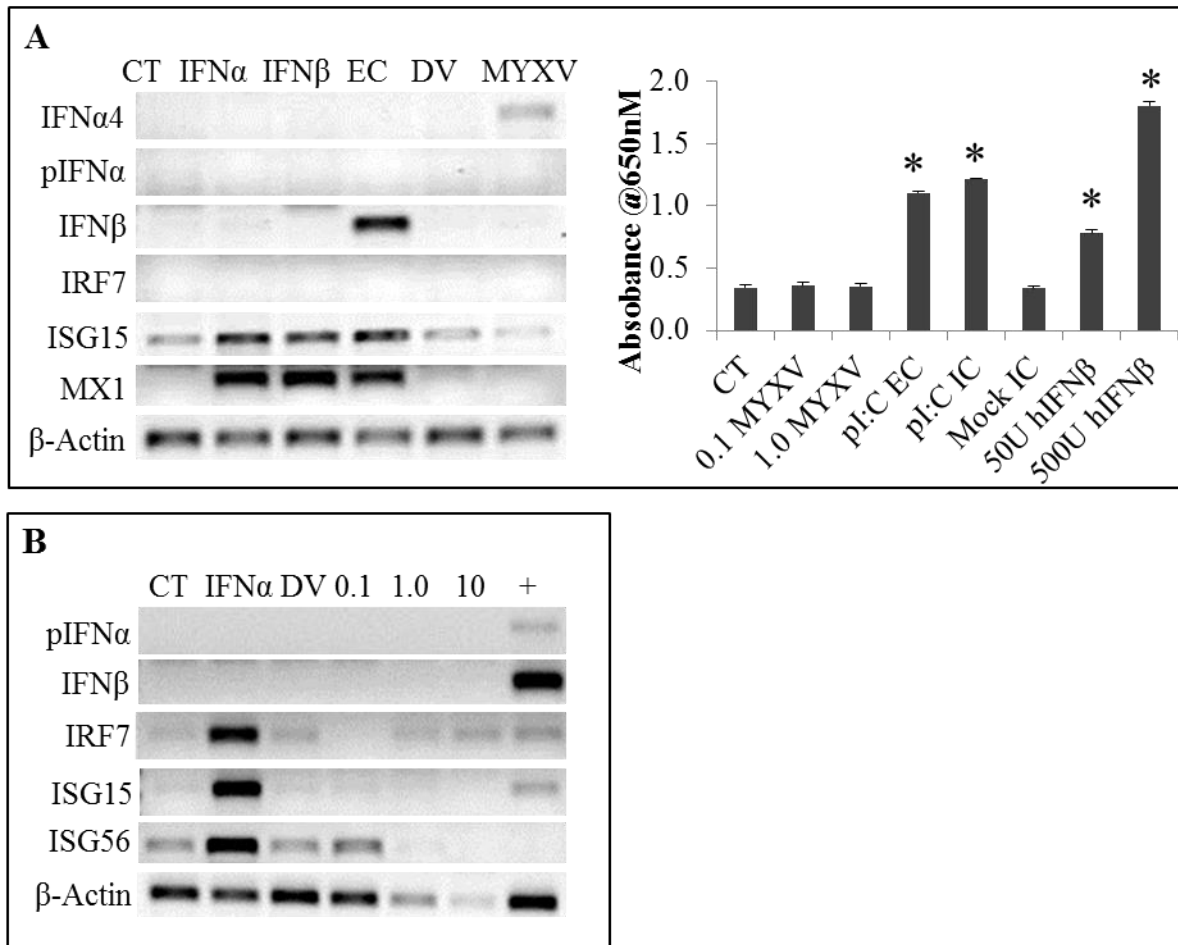


Figure 4.8: Conventional glioma cell lines do not produce type-I interferon in response to Myxoma virus. **A - Left:** RT-PCR of U251 glioma cell line 24 hours post-stimulation (CT-control; IFN α – 100 U/mL IFN α ; IFN β – 100 U/mL IFN β ; EC – 25 μ g/mL of extracellular Poly I:C; DV – Dead Myxoma virus; MV – 1.0 MOI Myxoma virus; VSV – 1.0 MOI Vesicular stomatis virus Δ 51) for type-I interferon and type-I interferon stimulated genes. **Right:** Absorbance readings of HEK-Blue Assay (Invivogen) measuring secreted type-I interferon from U251 cells 24 hours post-treatment in response to vMyx-GFP (MYXV), 25 μ g/uL delivered extracellularly (pI:C EC), 1.0 μ g/uL polyI:C delivered by intracellularly via lipofectimine (pI:C IV), UV-inactivated MYXV (DV) or no treatment (CT). Asterisks indicate significant difference ($p < 0.05$) from control (CT) as measured by t-test ($n = 4$). Error bars indicate standard error. **B –** RT-PCR of U87 glioma cell lines in response to 0.1, 1.0, 10 MOI of vMyx-GFP (MYXV), UV-inactivated virus (DV), or 50 U/mL of IFN α . + indicates PCR positive control for IFN response, and is LPS stimulated THP1 monocytic cell line.

Next, the ability of primary glioma neurosphere cultures to produce IFN α/β was examined. These lines are derived from human gliomas cultured under neurosphere conditions, and, as such, retain stem cell-like properties. Our laboratory refers to these cultures as brain-tumor-initiating cells (**BTICs**). These patient-derived BTICs express stem cell markers, self-renew, and have multi-lineage differentiation.^{4,161,300,308,319,320} These lines are considered to be more appropriate than conventional cell lines for preclinical testing as they accurately recapitulate the original tumour expression patterns, mutational status, and glioma phenotypes *in vivo*.^{318,319} Further, we have found that these cultures are more resistant to MYXV infection than conventional glioma cell lines.³⁰⁰ Interestingly, as with the conventional cell lines, these human BTICs did not produce IFN in response to MYXV infection either at the level of message, as measured by RT-PCR, or secreted protein, as measured by HEK-Blue assays (**Fig 4.9**). BT012, BT025 and BT048 produced IFN α/β in response to VSV Δ 51 and/or extracellular polyI:C at the transcriptional level, but only BT012 and BT025 produced functional IFN α/β . Further, BT012 was able to produce IFN α/β in response to extracellular polyI:C, while BT025 only produced in response to VSV Δ 51. BT042 seemed to have lost its ability to produce IFN α/β to these stimuli. All lines did show responsiveness to exogenously applied 10 U/mL of IFN β at the transcriptional level. This variation in IFN α/β production and anti-viral sensing methods displays the power of using patient-BTIC cultures, as these different responses many associate with different mutational statuses that define particular cohorts of patients. However, despite their inherent differences, these lines universally fail to respond to MYXV infection with an IFN α/β response.

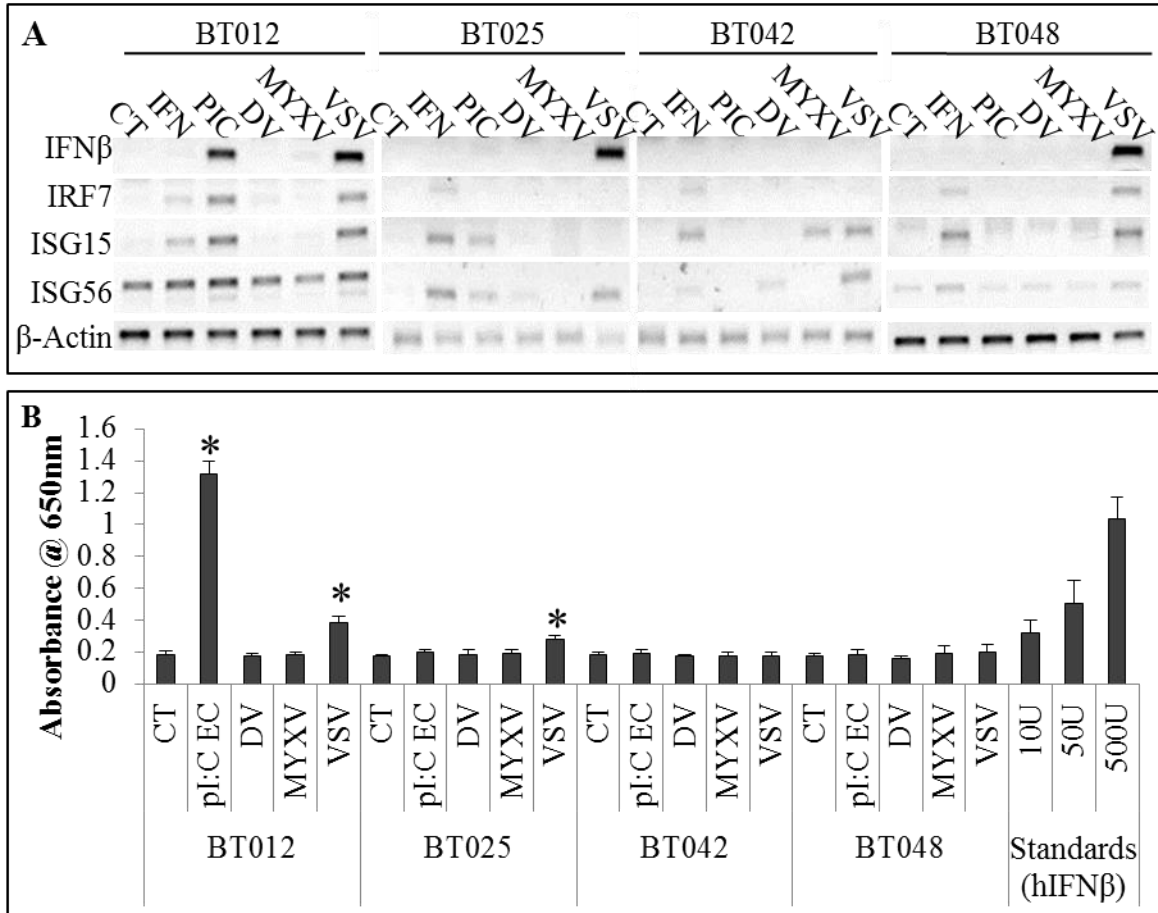


Figure 4.9: Human brain tumour-initiating cell lines do not produce type-I interferon in response to Myxoma virus. **a)** RT-PCR of BTIC lines 24 hours post-stimulation (CT-control; IFN – 10 U/mL IFN β ; PIC – 25 μ g/mL extracellular polyI:C; DV – Dead MYXV virus; MYXV – 1.0 MOI vMyx-GFP; VSV – 1.0 MOI of Δ 51- Vesicular Stomatitis Virus) for type-I interferon and type-I interferon stimulated genes. **b)** Absorbance readings of HEK-Blue Assay (Invivogen) measuring secreted type-I interferon from BTICs 24-hours post-treatment (asterisks indicate significant difference from control (CT) as measured by T-test; n=4). Error bars indicate standard error.

Finally, non-transformed human cell lines were assessed for their ability to respond to MYXV with an IFN α/β response. Interestingly, it has been suggested in the literature that transformed cells are compromised in their innate anti-viral responses.^{113,257} First, the HS68 human fibroblast cell line was examined. Again, by both RT-PCR and the HEK-Blue assay at 24 hours post-treatment, MYXV did not induce an IFN α/β response,

but the cell line was able to produce IFN α/β to the oncolytic virus VSV Δ 51 (RT-PCR) and intracellular polyI:C (HEK-Blue; **Figure 4.10 A**), as well as extracellular polyI:C (HEK-Blue, *data not shown*). This lack of production of IFN α/β was not a consequence of failure of MYXV to enter these cells, as early gene expression was observed as measured by GFP under the control of the early/late synthetic Vaccinia virus promoter in vMyx-GFP (**Figure 4.10 C**). To take this a step further and examine a primary CNS cell-type, low-passage human foetal astrocytes were obtained and infected with MYXV or given polyI:C. Again, MYXV was unable to induce a IFN α/β response, but these cells were able to produce IFN α/β in response to both intracellular and extracellular polyI:C as measured by the HEK-Blue system (**Figure 4.10 B**). The same results were obtained with 0.1, 1, 5, 10 MOI MYXV at 6, 12, 24 and 48hrs (*data not shown*). Again, MYXV was able to enter these cells and initiate early gene expression as measured by GFP expression after 24 hours post-infection (**Figure 4.10 C**). These diverse examples of cell types retaining the ability to produce IFN α/β to other oncolytic viruses or viral nucleic acid homologues, but not MYXV, strongly indicates to us two possibilities: MYXV is not recognized by these cell types through lack of an approximate receptor, and/or MYXV is capable of shutting down the initiation of the anti-viral response.

It seems unlikely that so many diverse cell types would lack the necessary PRRs to recognize MYXV infection. Further, it has been shown that primary human macrophages can detect MYXV through the RIG-I pathway,³⁴⁸ which our data suggests is functional in the NPCis cell lines, U251, 3 of the 4 BTIC lines, HS68, and human foetal astrocytes. Preliminary experiments investigating whether MYXV is able to block IFN α/β production were performed. Here, NPCis cell lines, as well as in human

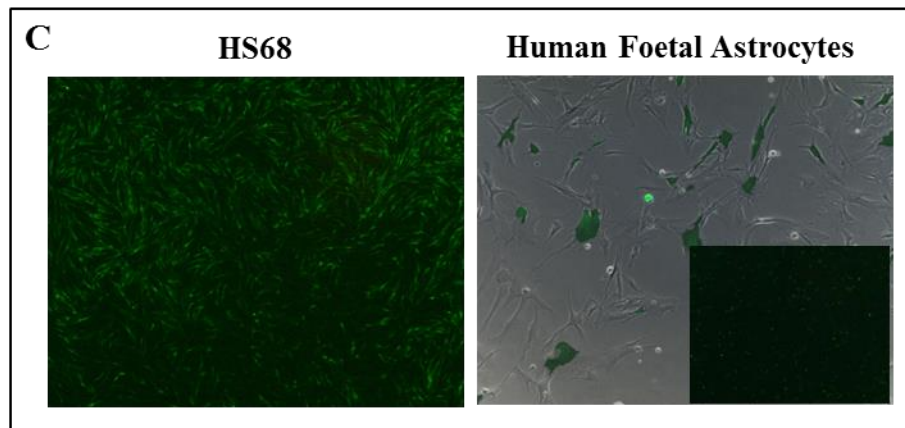
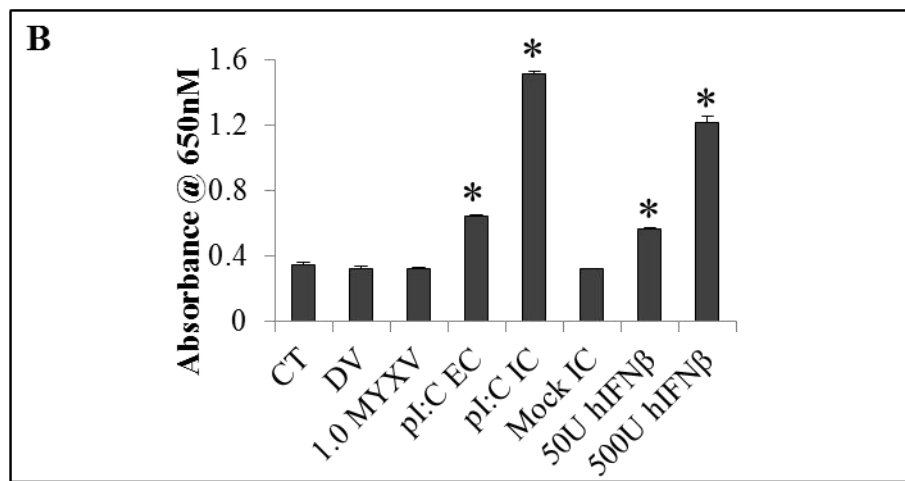
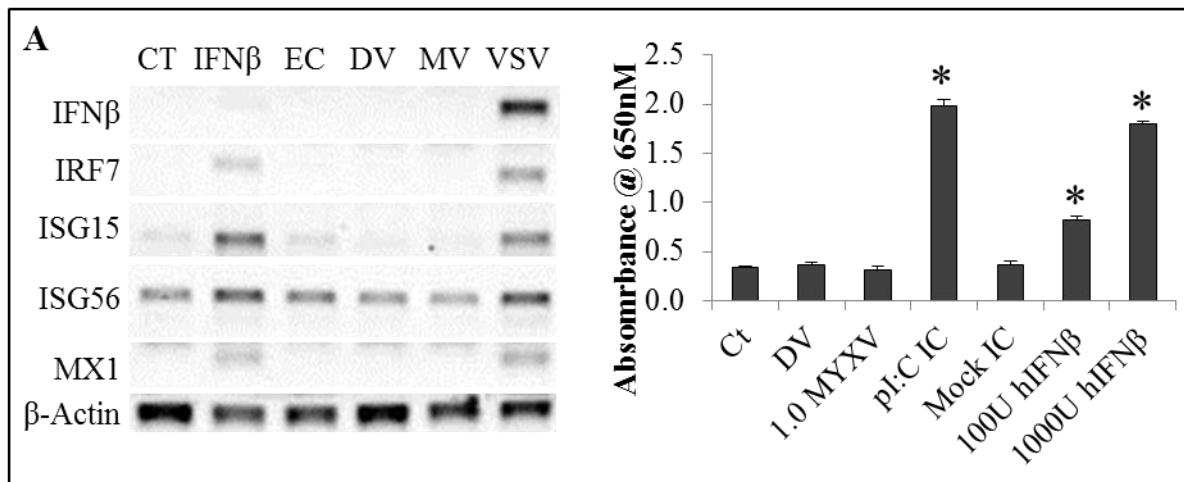


Figure 4.10: Non-transformed human cell types do not produce type-I interferon in response to Myxoma virus. **A** – Left: RT-PCR of HS68 human fibroblast cell line 24 hours post-stimulation (CT-control; IFN – 100 U/mL IFN β ; EC – extracellular Poly I:C, 25 μ g/mL; DV – Dead Myxoma virus; MV – 1.0 MOI vMyx-GFP; VSV – 1.0 MOI of Vesicular Stomatitis virus mutant Δ 51) for type-I interferon and type-I interferon stimulated genes. Right: Absorbance readings of HEK-Blue Assay (Invivogen) measuring secreted type-I interferon from HS68 cells 24-hours post-treatment (n=4).

Error bars display standard error, asterisks indicate significance ($p < 0.05$, t-test, $n = 4$). **B** - Absorbance readings of HEK-Blue Assay (Invivogen) measuring secreted type-I interferon from foetal human astrocytes 24-hours post-treatment ($n = 4$). Error bars display standard error, asterisks indicate significance ($p < 0.05$, t-test, $n = 4$). **C** - MYXV is capable of infecting HS68 cell lines (1.0 MOI, 24hpi, 25X mag.) and human foetal astrocytes (1 MOI, 24hpi, 100X magnification phase/contrast, 25X GFP inlay) *in vitro*.

fibroblasts (HS68) and BTICs (BT012), infected with MYXV were unable or severely inhibited in their ability to produce IFN α/β to polyI:C (*data not shown*). This suggested that MYXV indeed may be able to repress the induction of IFN α/β ; however, these results were too preliminary to present in this work.

4.3. Discussion

This chapter interrogates the role of type-I interferon (IFN α/β) signalling in MYXV treatment failure in *in vitro* and *in vivo* in the syngeneic NPCis cell lines described in **Chapter 3**. This cytokine was of special interest, as it has a number of properties that suggest that it would be an important factor in oncolytic virus therapy in syngeneic glioma preclinical models. Firstly, IFN α/β is an important cytokine mediating viral resistance in vertebrates, directly inhibiting anti-viral responses as well as orchestrating other cell types of the innate and adaptive immune response.³⁵³ Importantly, IFN α/β is important in protecting the central nervous system from infection, as IFN α/β receptor knockout mice have been shown to have increased neurovirulence, CNS viral load and/or mortality to many viruses, including West Nile²²¹ and Sindbis²⁵¹ viruses as well as viruses commonly used in OV therapies such as HSV,²⁴⁷ MV,²⁴⁹ and VSV.^{338,339} Thus, given the nature of this cytokine in protecting the 'normal' CNS from viral infection and

encephalitis, it seems a delicate cytokine to try and manipulate with OV therapy for CNS cancers.

Secondly, and as confirmed in this chapter, IFN α/β displays exquisite heterospecificity between murine and human systems, presenting a large problem with testing anti-viral tumour-stroma interactions in mouse orthoxenografts. There has been much development in the area of tumour-stroma interactions dictating treatment resistance, with much recent interest in how hepatocyte growth factor can mediate BRAF-inhibitor resistance in melanoma.^{338,354} Although growth factors are largely thought to be cross-reactive between mouse and human, many chemokines and cytokines have species-specific interactions, such as Type-I¹¹⁰⁻¹¹² and Type-II¹¹³ interferons and members of the TNF α family¹¹⁵ and CSF family.¹¹⁴ These interactions may be of great importance to therapeutic outcome, especially for immune-based therapies such as oncolytic viruses. Thus, models where these interactions are conserved should become part of the standard for preclinical testing. Some would argue that this discrepancy in interferon signalling in xenografts may not be of consequence in cancer cells, as compromised IFN α/β signalling occurs during transformation.^{348,355} This may be the case in some cell lines, but the glioma lines described in the literature,^{220,262,325,356,357} the NPCis cell lines, and nearly all the human lines we investigated, have retained their ability to both produce and respond to IFN α/β . This is one of the main reasons for the pursuit of IFN α/β 's anti-proliferative and pro-apoptotic effect as a glioma therapeutic in the clinic,³⁵⁸ as well as in other cancers.¹⁸⁹ IFN α/β has additional immunomodulatory functions, and has long been known to stimulate NK- and T-cell responses, mediating trafficking, proliferation and cytotoxic responses of these cells.¹⁹¹⁻¹⁹⁵ Indeed, it could be suggested that if MYXV did

mount a robust IFN α/β response in the glioma microenvironment, we may see some indirect therapeutic response in these syngeneic models through the cytostatic/pro-apoptotic effects of IFN α/β on the tumour and/or through stimulating anti-tumour NK and T cell responses.

The lack of an IFN α/β response *in vitro* is an interesting finding, as several studies have reported that MYXV has indeed induced an IFN α/β response. This was first shown in primary mouse embryonic fibroblasts (MEF).³⁵⁹ This study demonstrated that primary MEFs were resistant to MYXV infection which was accompanied by an IFN α/β response, while immortalized MEFs lost their ability to produce IFN α/β and were permissive to MYXV infection and replication. This loss of IFN α/β production was not a result of losing the ability to produce IFN α/β , as exogenously applied dsRNA could still produce IFN α/β that could subsequently protect these cells from infection. Further, it was demonstrated that pre-infection of the immortalized MEFs with MYXV would stop the induction of IFN α/β by intracellular administered dsRNA or dsDNA, suggesting that MYXV was selectively abrogating IFN production by antagonizing the intracellular nucleic acid sensing pathways. This study suggests that the immortalization of MEFs results in the loss of an IFN-inducing MYXV-sensing pathway that MYXV is incapable of disrupting.

This study begged the question as to which PPR receptors are utilized to recognize MYXV. This was first demonstrated in primary human macrophages, where it was demonstrated that the cytoplasmic RNA sensors RIG-I and MDA5 pathway was responsible for recognizing MYXV infection and producing IFN α/β in an IRF3-dependent manner.³⁶⁰ TLRs were found to play no role. It may seem peculiar that

intracellular dsRNA sensing proteins are responsible for responding to a dsDNA virus, but this is not unfounded. dsDNA viruses produce dsRNA transcription intermediates, while host RNA polymerase III proteins have been shown to convert cytosolic dsDNA to dsRNA to be sensed through this machinery.³⁶¹

Conversely, both murine³⁶² and human³⁶³ primary plasmacytoid dendritic cells (specialized dendritic cells for the production of IFN α/β in the periphery²⁶²) were shown to produce IFN α/β . In mice, this was shown to be through a TLR9-MYD88 dependent pathway, which further required the transcription factor IRF7 but was independent of IRF3, TLR3 and RIG-I/MDA-5 signalling. In human plasmacytoid dendritic cells specific TLRs were not investigated, but the TLR7, 8 or 9 pathway was implicated through inhibition of endosomal TLR signalling inhibiting the IFN response.

It appears that human macrophages and dendritic cells use fundamentally different pathways to recognize MYXV. Additionally, murine plasmacytoid dendritic cells utilize a unique method of interferon production, which is perhaps dendritic cell dependent, as these are the only cells that constitutively express high levels of IRF7.³⁶⁴ Discovering which PRR method is used to sense MYXV is likely to be cell type-specific, which would be further complicated in tumour cells that can have unpredictable protein expression. This is not to say that our glioma lines are incapable of recognizing MYXV, as they respond to infection primarily through robust CXCL10 and CXCL1 response (*data not shown*).

Comparing these studies to what we have seen in our NPCis lines and human cancer cell lines *in vitro* is complex. The first study suggests that the immortalization of murine

cells results in the loss of IFN production to MYXV, and being as our glioma lines are certainly transformed, this relates to our studies and perhaps parallels this work. Interestingly, it has been shown the murine melanoma cell lines³⁶⁵ as well as human neuroblastoma cell lines (*personal communication*) do not induce a IFN α/β to MYXV infection, perhaps indicating that transformation is an important mediator of IFN α/β production to MYXV. Of note, however, is that we found that primary human astrocytes were also incapable of mounting a IFN α/β response to MYXV.

The lack of robust MYXV-induced IFN α/β response *in vivo* in the mouse glioma microenvironment is an interesting observation, and suggests that an IFN α/β response is not necessary to protect the tumour from MYXV infection. This is contrary to what has been seen with intracranial MYXV inoculation before. In the aforementioned study using murine melanoma cell lines, MYXV treatment of these tumours implanted in the brain of RAG1^{-/-} C57Bl/6 mice found a mild IFN β response *in vivo* at 24 hpTx. This suggests that the milieu of infiltrating leukocytes in the brain-melanoma microenvironment produce different cytokine expression profiles to intracranial MYXV infection than the brain-glioma microenvironment of the orthografted NPCis line. This could be a consequence of either the different tumour type or the use of RAG1^{-/-} animals in the melanoma experiment.

Further, it has previously been shown that STAT1-deficient mice on the 129Sv/Ev background rapidly succumb to intracranial injections of MYXV,³⁶⁶ suggesting that IFN α/β signalling is important in protecting against MYXV neurovirulence in this strain of mouse. Perhaps this is a result of inherent differences between the 129Sv/Ev and C57Bl/6 background of mouse, which have shown strain-specific effects in models of

HSV viral encephalitis^{10,367} and experimental autoimmune encephalomyelitis.^{368,369} However, STAT1 is not solely involved in IFN α/β signalling, and it would be interesting to look at MYXV neurovirulence in C57BL/6 mice deficient in *Ifnar1* or *Irf9*, which would specifically ablate IFN α/β signalling in these animals.

Of important note is that our experiment examining *in vivo* IFN α/β production in the K1492 microenvironment must be interpreted with caution, as only 2 animals per group were analyzed. Perhaps future investigation could be performed looking at interferon-inducible genes in the glioma microenvironment through IHC or RT-PCR following MYXV infection, although this would be complicated by the fact that these genes are often up-regulated in gliomas *in situ*^{370,371} and as suggested by our ISRE::FLUC data. Strongly supporting our data is the IRF9 knockdown experiments in the K1492 line. This experiment demonstrates that the NPcis line is no longer able to induce the anti-viral state in response to IFN α/β , and as these lines have no change in viral infection or treatment efficacy, it further suggests that IFN α/β is playing little to no role in protecting these tumours from MYXV infection.

5. IMMUNOCYTE-MEDIATED MECHANISMS OF MYXOMA VIRUS TREATMENT RESISTANCE IN NPc15 ORTHOTOPIC MODELS

5.1. Introduction

The previous chapters demonstrate that K1492 is a suitable model for preclinical testing of oncolytic Myxoma virus and that treatment failure is likely independent of the production of type-I interferon. Therefore, in this chapter I tested **the hypothesis that Myxoma virus treatment failure is caused by the swift clearance of the virus by resident or treatment-recruited immunocytes.**

As there has been no previous work interrogating the NPc15 orthograft microenvironment, and very little work looking at how immunocytes change in glioma models in response to MYXV treatment, these studies began with a blank slate. The **main objective** of this chapter was to immunophenotype the K1492 glioma microenvironment before and after MYXV treatment in C57Bl/6 mice to find potential immunocytes mediating MYXV tumour clearance. The **secondary objectives** were to utilize systems to ablate candidate immunocyte populations in order to test subsequent hypotheses that these cell types mediate MYXV treatment resistance.

The glioma microenvironment is complex, with tumour cell interactions with other glia, extracellular matrix proteins, vasculature, and infiltrating immune cells. Among these glioma infiltrating immune cells, brain-resident microglia and infiltrating peripheral monocytes/macrophages (glioma-infiltrating monocytes/macrophages; **GIMs**) have been the best described in glioma patients,¹⁸⁻²² with some reports suggesting they make up to one-third of the tumour mass.⁴⁵ Microglia are the central nervous system's primary immunocyte which populate the CNS during development and remain as a brain resident

macrophage. Under non-pathogenic conditions, microglia are considered quiescent, but are actually incessantly sampling the CNS for injury or pathogen presence. Activation of these cells through pathogen or damage-associated molecules or through recruitment by chemokines results in an activated phenotype with increased proliferation, motility, phagocytic activity, and cytokine/growth factor secretion. Activation of microglia is a continuum, with unactivated 'ramified' microglia possessing small bodies and long tendrill-like processes, intermediate states that include the shortening and bulking of the processes and cell body, and full activation results in an amoeboid phenotype that is morphologically and immunohistochemically indistinguishable from recruited peripheral monocytes.^{46,50} These glioma-infiltrating macrophage/microglia are thought to be recruited by the tumour, functioning in enhancing glioma growth through secreting growth factors,⁹¹ pro-invasion matrix-metalloproteases,^{87,89} and pro-angiogenic factors.⁹² Importantly, these tumour-recruited microglia/macrophage populations were previously shown to mediate oncolytic HSV efficacy in syngeneic rat glioma models.^{218,219}

Immunophenotyping the K1492 microenvironment at the time of MYXV treatment found that there was a substantial infiltration of both microglia and peripheral monocytes. The microglia surrounded the glioma and were fully activated, amoeboid cells, while GIMs were found within the tumour itself. These tumour-associated microglia were lost following Myxoma virus administration, while additional peripheral monocytes were recruited following treatment. It was determined that all tumour-resident and treatment recruited peripheral monocytes were trafficked to the tumour via CCR2, similar to what has been found in other CNS pathologies.^{199,200,202,203,372} Myxoma virus administration in CCR2-deficient animals resulted in a significantly more intratumoural infection for the

first 3 days after treatment which then rapidly returned to wildtype levels and was cleared by 5 to 7 days post-treatment. Tumour-resident microglial recruitment and activation was unaffected in these animals. This strongly suggested that these resident or recruited monocytes play a critical role in determining infection or early replication rates and resulted in longer survival in treated animals. Ablation of circulating monocytes with clodronate liposomes did not phenocopy the results in the CCR2-deficient mice, strongly suggesting that it was the macrophages already in the tumour that were mediating initial viral infection/clearance. To further test this hypothesis, a diphtheria toxin (**DT**) inducible system to target peripheral monocytes and, presumably, tumour-resident macrophages and microglia was employed. DT administration was found to ablate peripheral monocyte recruitment in addition to microglia in the tumour-bearing hemisphere, and resulted in a substantial increase in viral infection. This suggested that microglia may also play a role in mediating viral infection and clearance. In order to determine if this approach could be used to increase viral replication clinically, we evaluated the monocyte/macrophage/microglia activation inhibitor Minocycline hydrochloride,³⁷³⁻³⁸⁰ and found it significantly elevated viral infection in the tumour-bearing hemisphere. This study suggests that this therapeutic approach to could potentially enhance initial OV infection of gliomas in patients.

Despite the initial increase in infection rates in the CCR2-deficient animals, there was still an abrupt viral clearance occurring at 3 days-post treatment. The initial immunophenotyping experiments found that in addition to the tumour-resident and recruited peripheral monocyte and microglial populations, there was also a large recruitment of T, NKT and NK cell populations that were recruited in elevated numbers

in the CCR2-deficient mice. The NK populations were of specific interest, as these had recently been shown to be important in mediating swift viral clearance from orthotopic xenograft models treated with oncolytic HSV.^{232,233} To test the hypothesis that T and NK cell populations limited viral replication and clearance in the tumours, IL2R γ -deficient mice were utilized. The IL2R γ receptor is necessary for the maturation of NK cells, and for the activation and clonal expansion of lymphocytes.^{381,382} K1492-bearing IL2R γ ^{-/-} mice had increased viral infection with sustained MYXV virus infection in the tumour that persisted until death. These mice had a >20% increase in survival over non-treated animals. These results suggested that either the T cell or NK cell populations were important in mediating the clearance of MYXV from the CNS and the tumour.

To further investigate which of these cell types could be important in this clearance, RAG1-deficient animals were used to specifically ablate T and B-cell populations.³⁸³ These mice had identical early viral clearance kinetics as wildtype mice, but were delayed in their ability to clear a small amount of viral infection from what appeared to be the tumour stroma. MYXV treatment had no treatment benefit in these animals. To target NK and NKT cell populations, a neutralizing antibody was used; however, this too did not result in any change in viral infection or survival. Further studies are needed to delineate if it is a combined effort of both NK and T cell populations that are mediating clearance in these animals or if this is another IL-2-family mediated mechanism.

Using IL2R γ and RAG1 animals provided a unique opportunity to investigate whether U87 orthoxenografts, which have been shown to be 'cured' with a single injection of MYXV,²⁵³ had similar inhibiting factors as the K1492 model. Surprisingly, U87-bearing animals had similar viral clearance kinetics as K1492-bearing RAG1

animals. U87 orthografted into RAG1^{-/-}/IL2Rγ^{-/-} double knockout mice had a sustained viral infection and replication with a 25% increase in animal survival. Surprisingly, these U87 tumours were nearly completely infected with virus at time of sacrifice. These results suggest that the clearance mechanisms may be similar in orthoxenografts, but more importantly demonstrates that MYXV treatment alone is not sufficient to achieve cures in animals, and strongly suggests that the immune system plays an important role in mediating MYXV oncolytic efficacy.

Taken together, the results in this chapter show that resistance to Myxoma virus infection and replication in syngeneic animals is a complex and multi-faceted mechanism. However, it was shown that tumour-resident monocytes, and possibly microglia, play a critical role in mediating the initial infection and replication of Myxoma, while a combination of both T and NK cell populations mediate clearance from the K1492 and U87 orthografts (**Figure 5.1**).

5.2. Results

5.2.1. The K1492 tumour microenvironment after Myxoma virus treatment

First analysed was the composition of the K1492 tumour microenvironment with or without MYXV treatment. Of particular interest were the microglia and recruited monocyte/macrophage (**GIM**) populations, as these are known to be recruited and activated in glioma models and glioma patients.^{21,22,45} It is not possible to differentiate an activated microglia from a GIM by microscopic appearance or histology, and thus these studies rely heavily on flow cytometric analysis of immunocytes isolated from the brains of perfused mice. Traditional neuroimmunological studies classify immunocytes in the

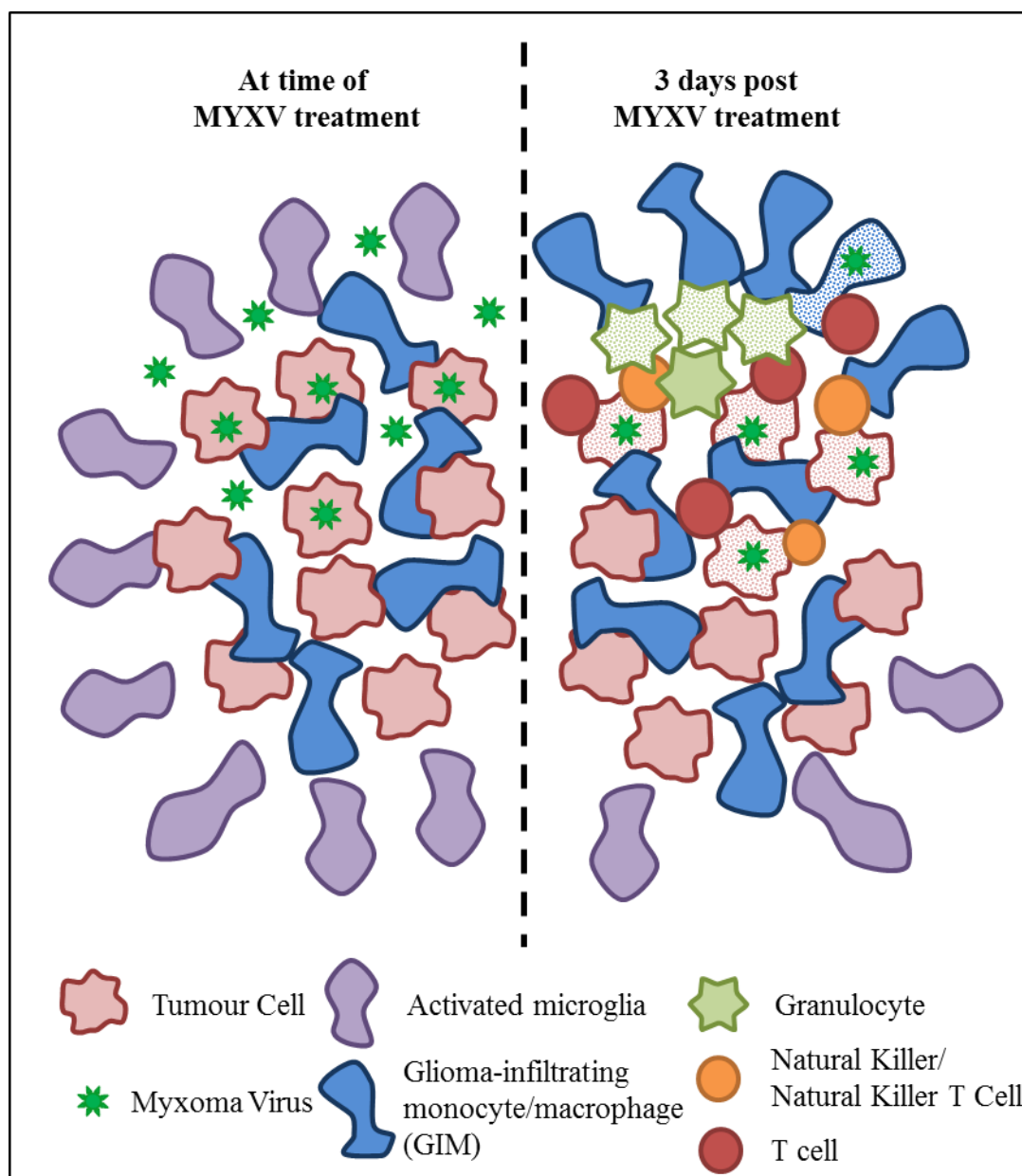


Figure 5.1: *Hypothesized mechanism for Myxoma virus treatment resistance.* The glioma microenvironment is inundated with activated microglial around the tumour and glioma-recruited monocytes/macrophages from the periphery. These tumour resident immunocytes cells function to phagocytize Myxoma virus upon viral administration, limiting how many tumour cells are infected. This infection is followed by an immediate neutrophil ingress, followed by the recruitment of additional peripheral monocytes that are likely involved in safely removing these neutrophils. This inflammatory microenvironment becomes lethal for the microglia, and they die off. NK, NKT and T cells are recruited to the tumour with significant numbers at 3 days post-infection, collaborating in overlapping functions to remove viral infected cells, including virally infected tumour cells (stippled cells signify dying cell).

brain according to their CD45 expression levels and CD11b status. For example, CD45^{low}CD11b⁺ are considered microglia, CD45^{high}CD11b⁺ cells are considered GIMs, and CD45^{high}CD11b⁻ cells are infiltrating lymphocytes.^{46,67} These studies began by examining these cell types, with the addition of a T-cell marker, CD3ε, as T cells can play important roles in tumour and viral immunology.

All flow cytometry in the following sections utilized C57Bl/6 mice implanted with 5×10^4 K1492 cells in the right striatum, and then treated with vMyx-GFP (MYXV) or left untreated (NoTx) at 12 days post-tumour implantation (**dpi**), unless otherwise noted. Animals were then sacrificed, immunocytes purified, and flow cytometry performed 3 days post treatment (3 dpTx; 15 dpi). These time-points were chosen to coincide with the initial characterisation of the K1492 model where animals were treated at 14 dpi with MYXV (**Chapter 3**). Given the process involved in isolating immunocytes from the brain, it would be difficult to compare 0 dpTx mice from 3 dpTx mice on separate days with separate purifications; thus, mice were treated or not at 12 dpi and then sacrificed at 15 dpi, 3 dpTx. This allowed for harvesting, processing and measuring these groups simultaneously. Further, 3 dpTx was determined as a relevant time-point as the previous studies through MYXV-FLUC, viral recovery, and IHC of viral proteins (**Figure 3.4**) showed that there was still MYXV in the tumour at this time, but was in the process of being cleared (less virus than 1 dpTx but more than 5 or 7 dpTx). Thus, any cell types present at this 3 dpTx could be implicated in mediating viral clearance. Finally, all mice were assayed by flow cytometry individually and results displayed as a mean of all mice.

Comparing the normal mouse brain to the untreated 15 dpi K1492 brain demonstrates the inflammatory nature of the gliomas. Here, a nearly 2-fold increase in CD45^{low}CD11b⁺

microglia can be seen (t-test, $p < 0.05$, **Figure 5.2 A**), making up 67% of the total CD45 cells found in the tumour-bearing hemisphere compared to the near 100% of the control, non-tumour mouse (**Figure 5.2 B**). By flow cytometry, we can see that many of these microglia are activated by their increasing levels of CD45 and CD11b.⁴⁶ This was confirmed by immunohistochemistry for IBA1, a monocyte/macrophage/microglial specific marker, whereby a 'gradient of activation' can be seen as the microglia migrate closer to the tumour (**Figure 5.3 A**). Also within the untreated K1492 glioma were CD45^{high} peripheral immunocytes. These consisted of a population of CD45^{high}CD11b⁺ GIMs, making up 24% of the total CD45 cells in the tumour-bearing hemisphere, (**Figure 5.2 A/B**) and the majority of the CD45^{high} cells. However, amongst these CD45^{high} infiltrating cells is also a small population of CD3⁺ T-cells, which made up 4% of the total immunocytes in the non-treated glioma-bearing hemisphere. (**Figure 5.2 A/B**) All of these were significantly increased in relation to their corresponding cell type in the untreated, non-tumour-bearing animals (t-test, $p < 0.05$).

Three days following Myxoma treatment, the microenvironment of the glioma changes dramatically. Unexpectedly, there is a significant loss of CD45^{low}CD11b⁺ microglia, returning to levels seen in the normal mouse brain. (**Figure 5.2 A/B**) This loss of CD45^{low}CD11b⁺ cells is accompanied by the recruitment of additional peripheral CD45^{high} cells, reaching levels nearly 2-fold over the untreated glioma. These CD45^{high} cells consisted largely of CD11b⁺ cells (76%), but also contained a further number of CD3⁺ T-cells, which was 22% of CD45^{high} cells and 12% of the CD45⁺ immunocytes. (**Figure 5.2 A/B**) Additionally, a population of cells straddling the CD11b gate in the CD45^{high} compartment was seen. Again, all of these groups of immunocytes were

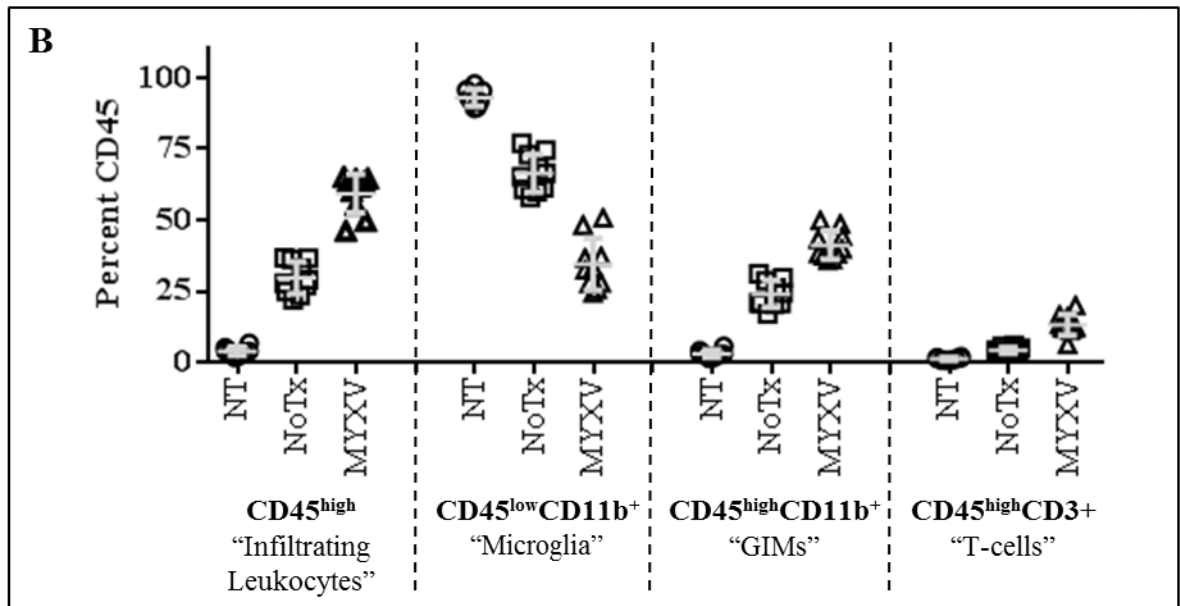
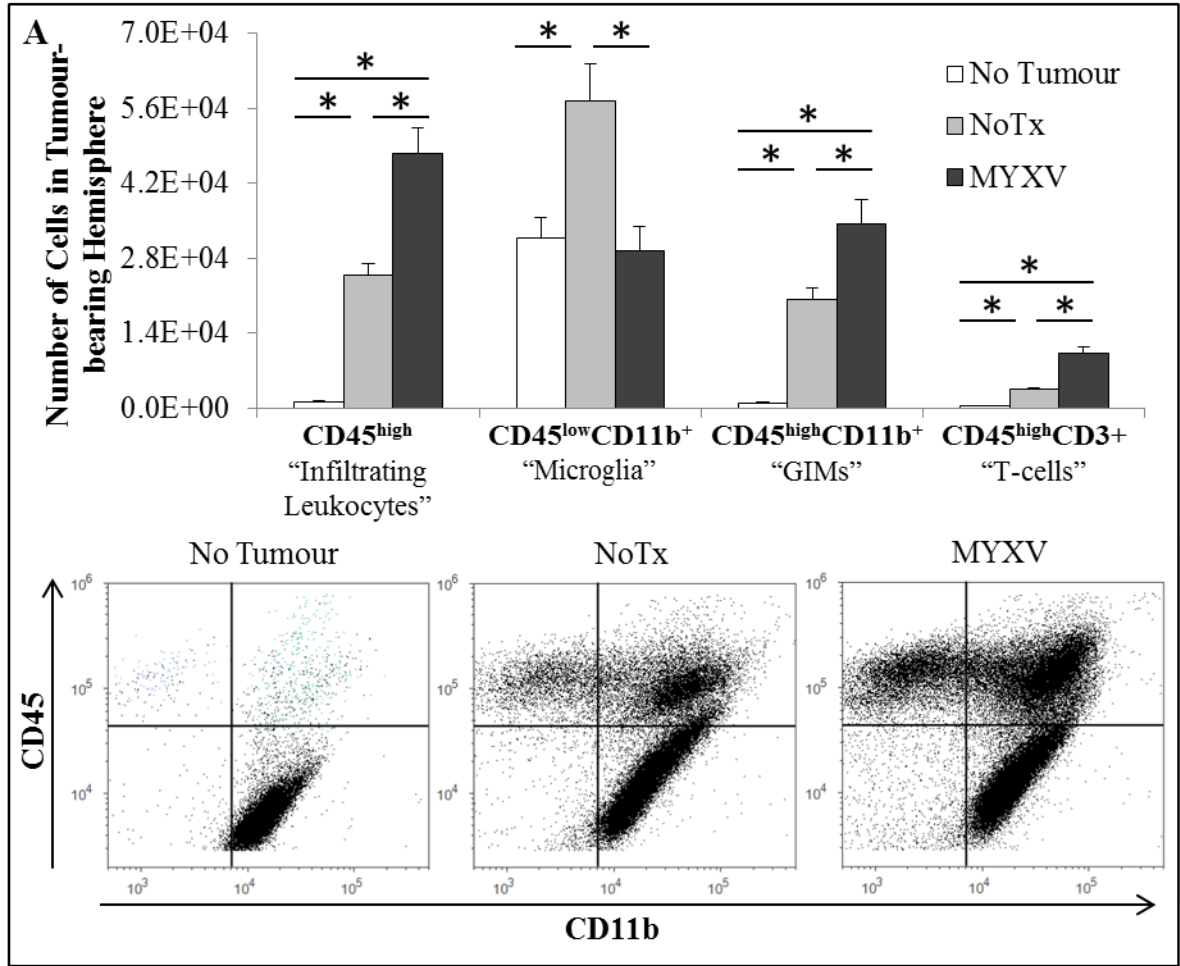


Figure 5.2: Immunophenotyping of the K1492 glioma microenvironment by flow cytometry with or without Myxoma virus treatment. C57Bl/6 mice implanted with K1492 cells and analyzed by flow cytometry at 15 days-post implantation, 3 days post-treatment with Myxoma virus (MYXV, n=10) or untreated (NoTx, n=10). Non-tumour bearing mice were used as a control (NT, n=6). Mice were assayed individually data shown as a mean of all mice. **A** – Quantified numbers of each cell type isolated from the tumour-bearing hemisphere (*top*) with representative scatter plot of CD45-PE and CD11b-PerCP-Cy5.5 (*bottom*). Error bars represent standard error, and asterisks indicate statistical difference via T-test ($p < 0.05$). **B** – Scatter graph of isolated immunocytes as a percent of the total CD45 population present in the tumour-bearing hemisphere.

significantly elevated over the no tumour control and the untreated K1492 tumour, except for the MYXV-treated $CD45^{\text{low}}CD11b^+$ microglia which was significantly lower than the K1492 alone and did not differ from the no tumour control (t-test, $p < 0.05$).

The loss of microglia in response to MYXV could be attributed to either cell death or a shift in markers, perhaps masking them as the $CD45^{\text{high}}CD11b^+$ GIMs up-regulated in the treatment groups. However, it is not thought that microglia activate CD45 to the ‘high’ levels seen in peripheral cells,^{46,67} suggesting that these cells are dying in response to the virus. Interestingly, areas of necrosis are seen in the tumour margins following MYXV treatment starting at 3 dpTx and are especially prevalent at 7 dpTx (**Figure 5.3**). These tumour margins are where a number of IBA1 positive microglia and/or GIMs accumulate, suggesting that this loss of microglia is an inflammation-induced microglia cell death. One could speculate this death was due to microglial infection by MYXV, yet there was no detection of GFP⁺ cells in the FITC channel in CD45⁺ cells, at least suggesting that MYXV cannot initiate early genome replication in any immunocytes in the brain at 3 dpTx. It is more likely that these microglia are succumbing to activation-associated cell death³⁸⁴⁻³⁸⁶ in response to viral infection. This perhaps exacerbated considering the already activated phenotype seen in these stromal microglia.

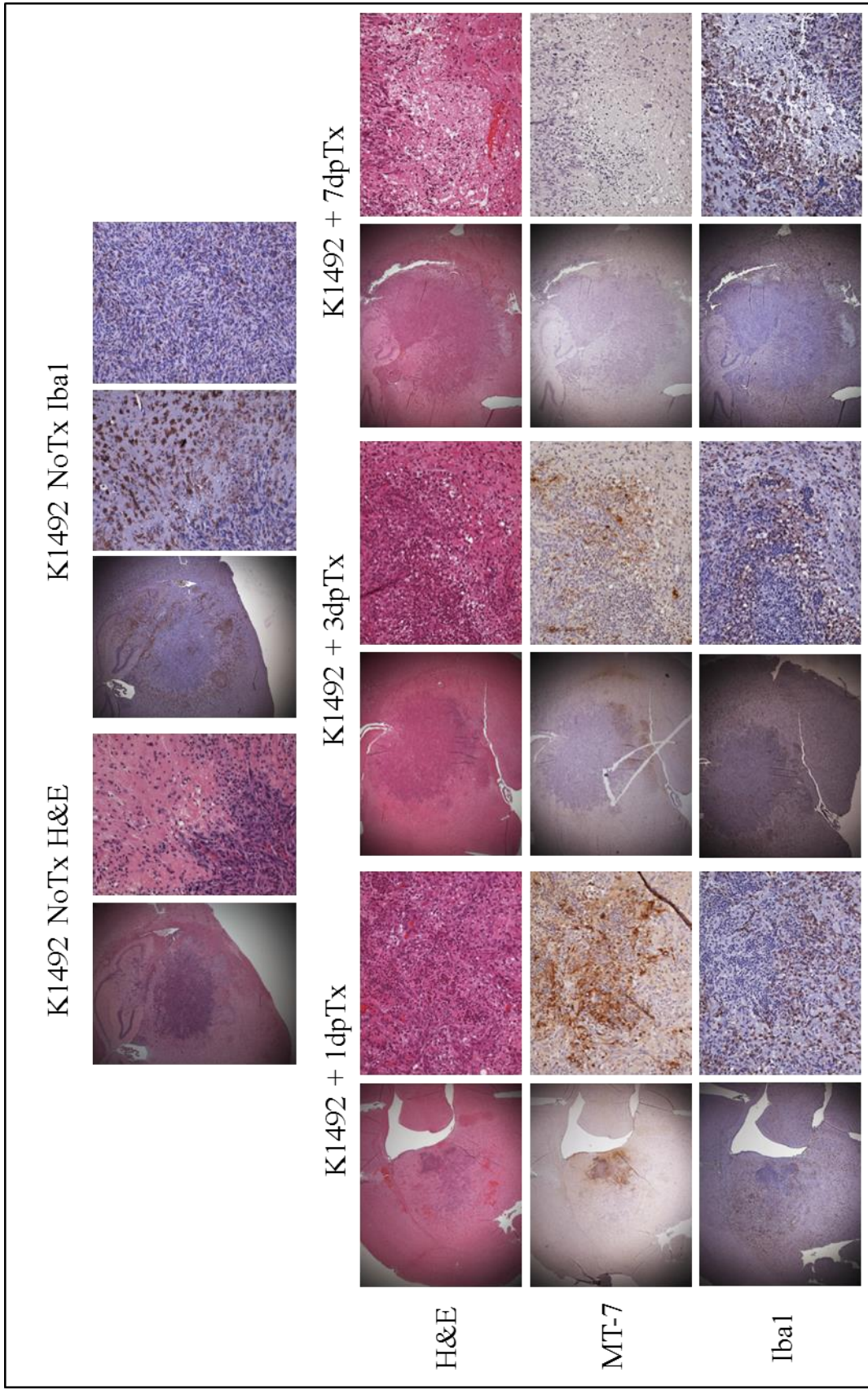


Figure 5.3: *K1492 orthografts in C57Bl/6 mice are highly infiltrated by microglia and macrophages.* C57Bl/6 mice were implanted with K1492 cells and treated with Myxoma at 14 days post-implantation. Formalin-fixed paraffin sections were stained using Hematoxylin and Eosin (H&E) or immunohistochemical for Myxoma virus early protein MT-7 or for the microglial/macrophage marker IBA1. (First row 25X; Second row 200X). K1492 NoTx Iba1 200x panels represent within tumour (left) and adjacent to tumour (right).

Given that MYXV is administered intratumourally, it was important to assess if this response was due to the injection itself or as part of an injury response. However, the injection of the same volume of PBS intratumourally did not result in any elevated CD45^{high} cells or loss of the CD45^{low}CD11b⁺ population (**Figure 5.4**), suggesting that the above changes were a direct result of intratumoral viral administration. This is not surprising as sterile injury in the brain is an acute response that is often resolved very quickly. Further, the sheer number of immunocytes in the K1492 tumour may mask any response persisting at 3 dpTx with PBS.

It was interesting to see such a robust CD3⁺ cell population only three days following MYXV treatment. In addition to traditional T-cells, CD3 could also be present on a population of CD161⁺ T-cells (NKT), innate T cells capable of performing NK cell-like functions such as IFN γ secretion and antigen independent cytotoxicity. To further characterize the CD45^{high}CD3⁺ population, and determine the presence of NK and NKT cells within the population of CD45^{high} cells recruited to the tumour at 3 dpTx, further flow cytometry immunophenotyping experiments were performed with the addition of the CD161(NK1.1) antibody. In these experiments, and all subsequent experiments looking at NK cells by flow cytometry, only the small and dense lymphocytes were gated on, with subsequent gating on CD45^{high} and then measured for CD161 and/or CD3 (**Supplementary Figure 1**).

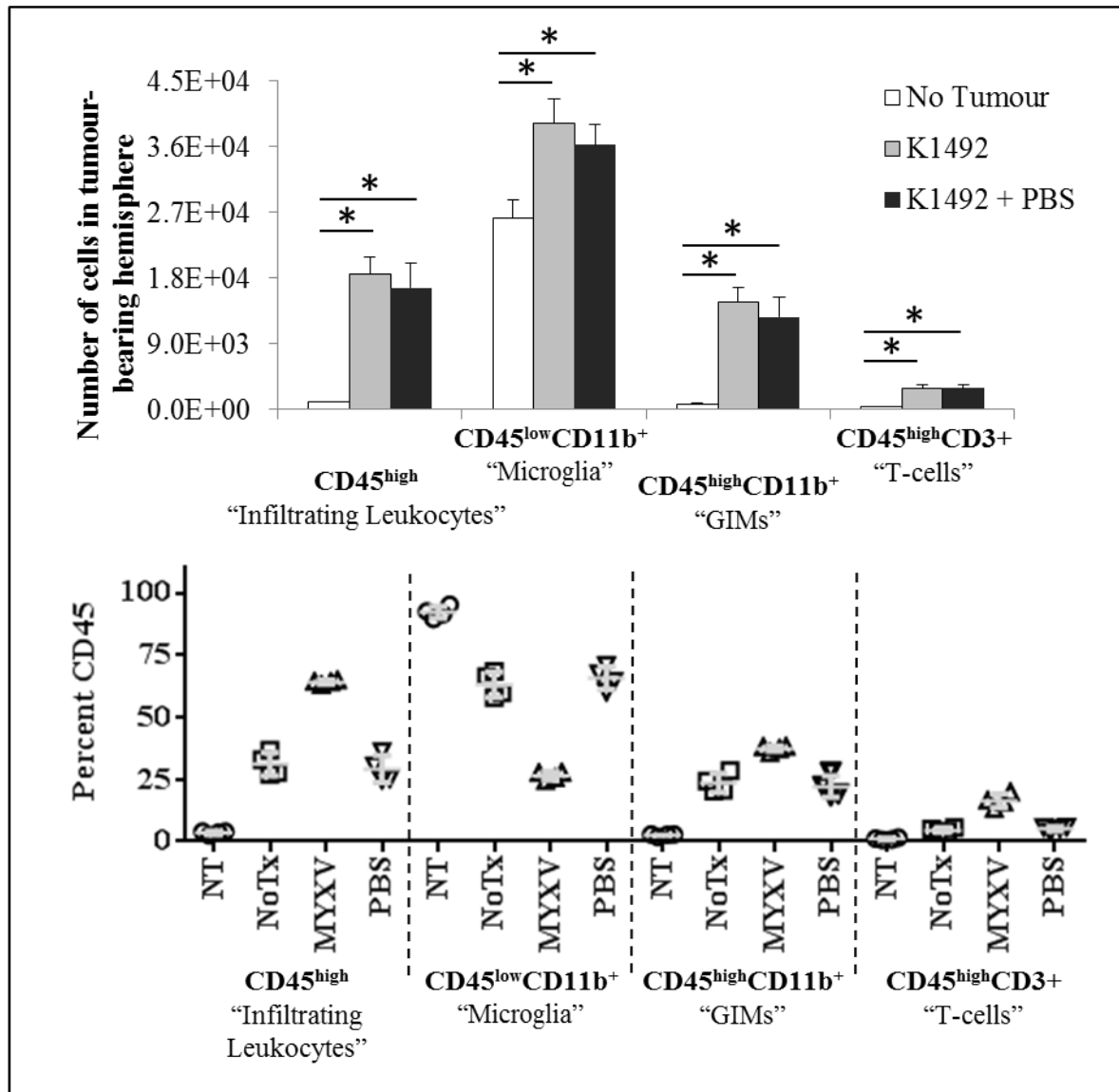


Figure 5.4: Immunophenotyping of the K1492 glioma microenvironment in response to sterile injury. C57Bl/6 mice implanted with K1492 cells and analyzed by flow cytometry at 15 days-post implantation, 3 days post-treatment with intracranial PBS (PBS, n=4) or untreated (NoTx, n=4). Non-tumour bearing mice were used as a control (NT, n=4). Quantified numbers of each cell type isolated from the tumour-bearing hemisphere (top). Error bars represent standard error, and asterisks indicate statistical difference via 2-way t-test ($p < 0.05$). Scatter graph of isolated immunocytes as a percent of the total CD45 population present in the tumour-bearing hemisphere compared to Myxoma treatment (bottom).

This was to reduce the background staining from the CD161(NK1.1) antibody. It was surprising to see a small population of tumour-resident NK ($CD45^{\text{high}}CD161^+CD3^-$) and T ($CD45^{\text{high}}CD161^-CD3^+$) cells. (**Figure 5.5 A**) One could speculate on the nature of the T cells within the tumour, as T-regulatory cells have been known to populate other mouse glioma models³⁸⁷ and human gliomas;⁴³ however, NK cells are considered to be involved in anti-tumour immunity, and perhaps their presence could be indicative of an immune response to combat the grafted glioma. All NK, NKT and T cells significantly increased in the MYXV treated mice (t-test, $p < 0.05$). The increase in NK cells was especially interesting, as they have been known to be involved in mediating neurovirulence^{388,389} as well as oncolytic HSV resistance in human glioma xenografts.^{232,233} To confirm that these were indeed NK cells within the treated and non-treated brain, an addition experiment using a double stain of CD161(NK1.1) and CD49b(DX5) was performed and confirmed the presence of NK cells in treated and untreated K1492 tumours. (**Figure 5.5 B**)

Given the inflammatory nature of gliomas with a compromised blood-brain barrier and leaky vasculature, coupled with the intense inflammation associated with intracerebral viral injection, it was very plausible that the $CD45^{\text{high}}CD11b^+$ component of K1492 gliomas with or without treatment could be composed of cells other than GIMs. $CD11b^+$ is an integrin associated with a number of cell types in addition to microglia and monocytes/macrophages, including granulocytes, NK cells, dendritic cells and some T cell subtypes.^{390,391} Thus, further analysis of the $CD11b^+$ populations in the K1492

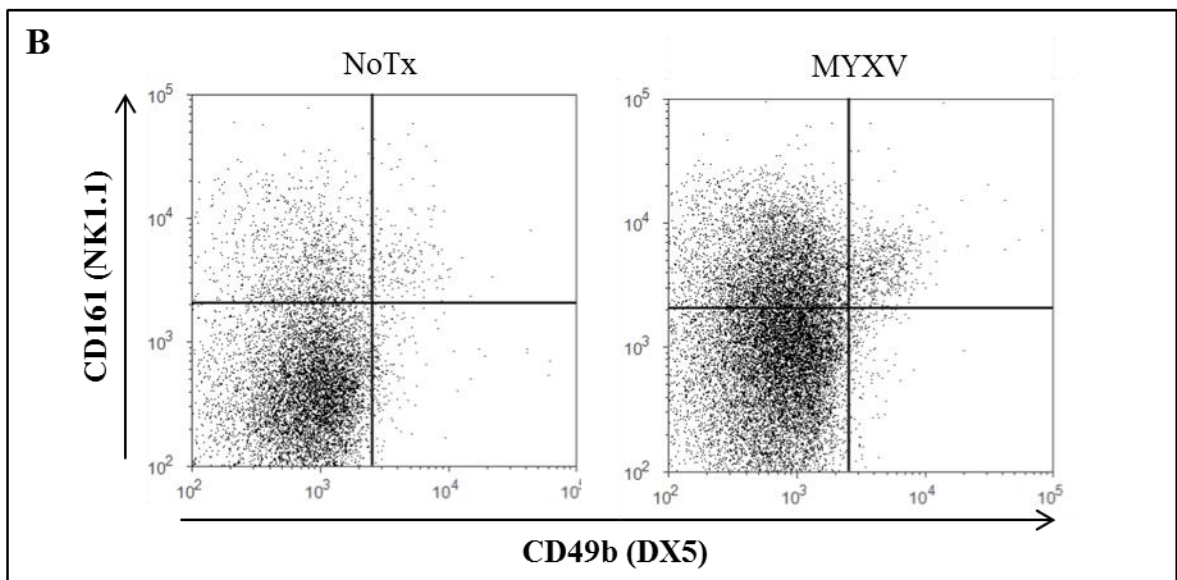
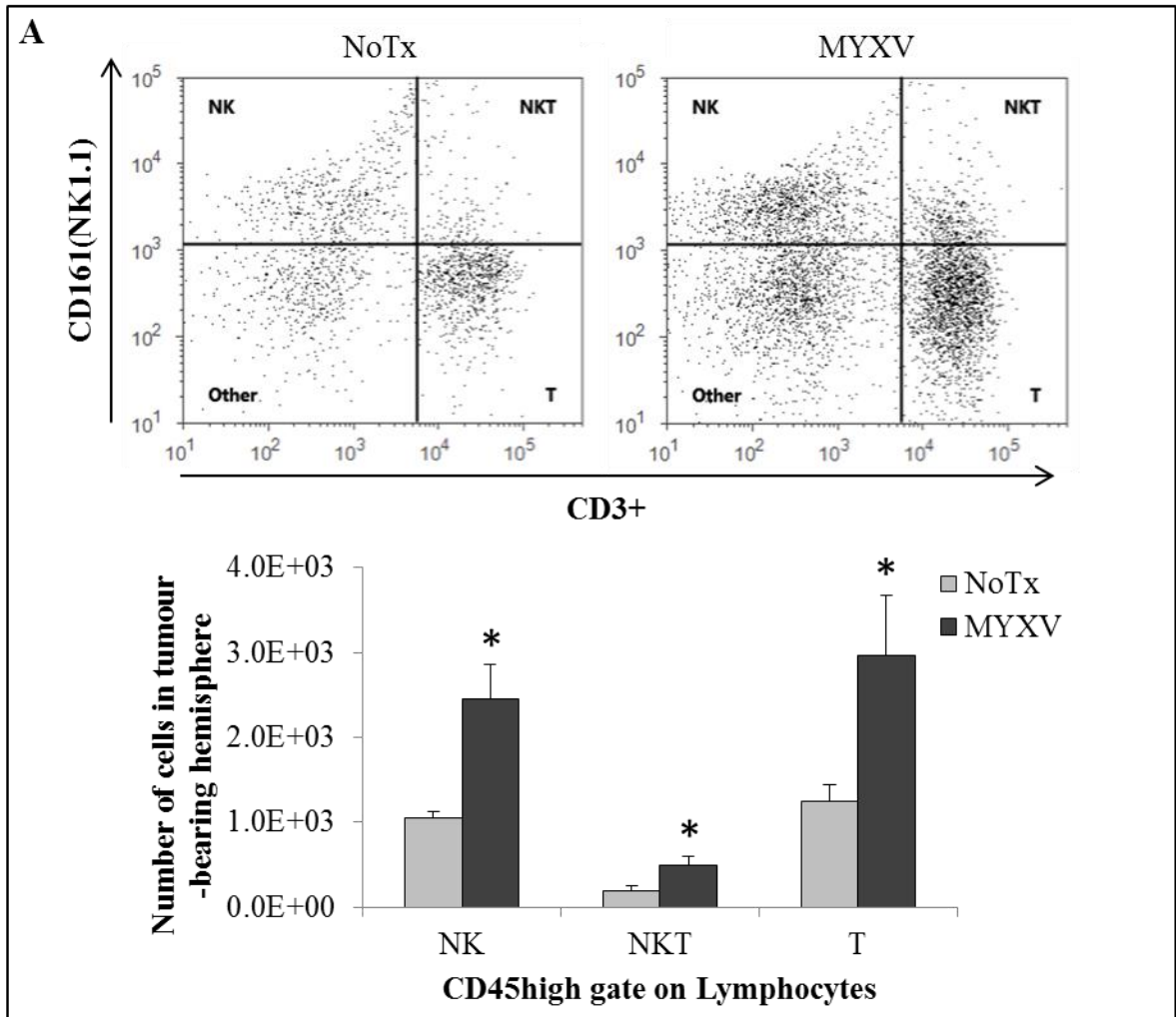


Figure 5.5: *Tumour-resident and recruited NK cells in K1492 treated with Myxoma virus.* C57Bl/6 mice implanted with K1492 cells and analyzed by flow cytometry at 15 days-post implantation, 3 days post-treatment with Myxoma virus (MYXV) or untreated (NoTx). **A** – Scatter plot of CD161(NK1.1)-PE-Cy7 and CD3 ϵ -APC gated on lymphocytes population and CD45^{high} (*top*), and quantified numbers of each cell type isolated from the tumour-bearing hemisphere (*bottom*). Error bars represent standard error and asterisks represent significance between MYXV (n=6) and NoTx (n=6; t-test, p<0.05). **B** – Scatter plot of subsequent experiment staining for NK cells using a double stain of CD161(NK1.1)-PE-Cy7 and CD49b(DX5)-FITC gated on lymphocyte population.

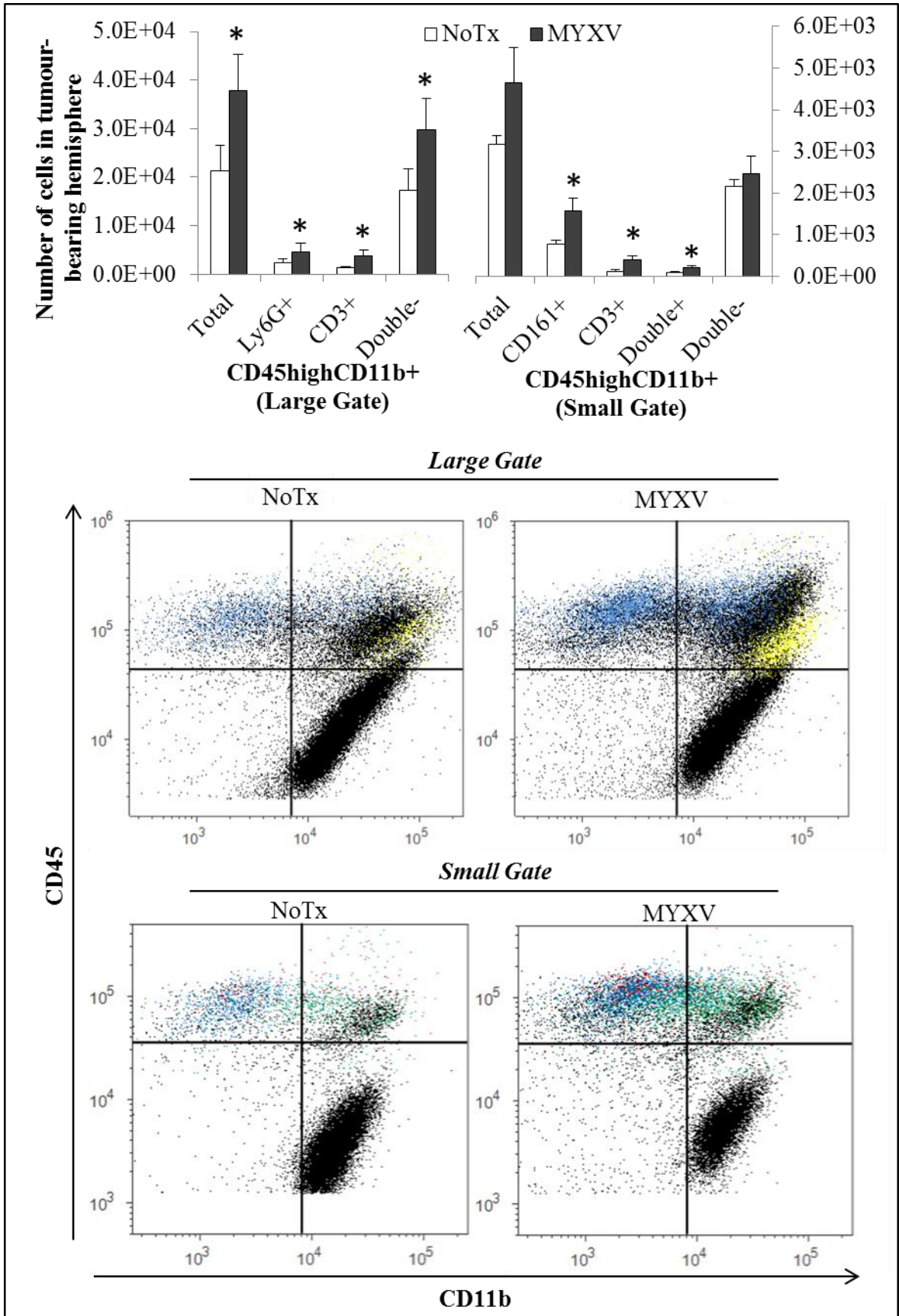
tumours with or without MYXV treatment was conducted. It was found that within the untreated glioma the majority of the CD45^{high}CD11b⁺ cells were negative for Ly6G (granulocytes), CD3 (T cells), albeit there was a small population of CD161⁺CD3⁻ NK cells (**Figure 5.6**). Although we did not employ other myeloid markers such as F4/80 or Ly6C, it was concluded that these cells were indeed GIMs as the IBA1 staining within the tumour was extensive (**Figure 5.3**) and because of subsequent experiments that ablated these cell types. Staining for CD115⁺ cells was negative (*data not shown*).

However, within the treated K1492-bearing hemisphere, there were a number of different cell types noted. Firstly, there was a significant increase in CD11b⁺CD3⁺ cells, suggesting there is a population of CD11b⁺ T cells. Although controversial, CD11b up-regulation has to been shown to occur on cytotoxic T cells after viral challenge,³⁹⁰⁻³⁹² suggesting that these cell types may be playing a role in mediating viral clearance. Verifying the authenticity of these cells as a T cell subset was subsequent experiments using transgenic IL2R γ ^{-/-} that lacked this population and RAG1^{-/-} mice that lacked all CD3⁺ cells (*data in subsequent section*).

Also within the ‘Large-Gate’ of CD45^{high}CD11b⁺ was a population of Ly6G (1A8)⁺ cells, which represents granulocytic cells. Although not stained for specifically,

these cells can be identified in the H&E sections through their polymorphonuclear morphology, and are seen in high numbers at 1 dpTx, and decrease significantly at 3 dpTx and are cleared by 7 dpTx (**Figure 5.3**). It is unclear whether the presence of these cells is a result of the administration injury or viral inoculation, as neutrophils respond rapidly to sites of injury in the brain. However, the CD45^{high}CD11b⁺Ly6G⁺ population has a very distinctive staining pattern in the CD45CD11b scatter plots, (**Figure 5.6 - yellow**) allowing for the estimation of its presence in the PBS injury experiment carried out. This experiment did not seem to contain this population of cells, which is corroborated by an unchanged number in the CD45^{high}CD11b⁺ population between no treatment and PBS administration (**Figure 5.4**), suggesting that these granulocytes at 3 dpTx are a consequence of viral infection of the tumour. Of note in these sections, granulocytes appeared very early, in great numbers by 1 dpTx, but were largely gone in most IHC slides by 3 dpTx, despite their presence by flow cytometry. Interestingly, in areas where virus was still present by IHC, concomitant neutrophil presence was still noted. Further, these areas of neutrophil accumulation were surrounded by IBA1⁺ cells that appeared to have a 'foamy' appearance, indicative of activated macrophages, perhaps suggesting macrophages are playing a role removing these scavengers (**Figure 5.6 B**).

Finally, amongst the 'Small Gate' CD45^{high}CD11b⁺ was a population of CD161⁺CD3⁻ NK cells, and these were the cells that appear to straddle the CD11b boundary observed previously. (**Figure 5.6 - green**) An interesting observation within the 'Small Gate' group is a population of CD161⁻CD3⁻ cells that does not seem to change in response to



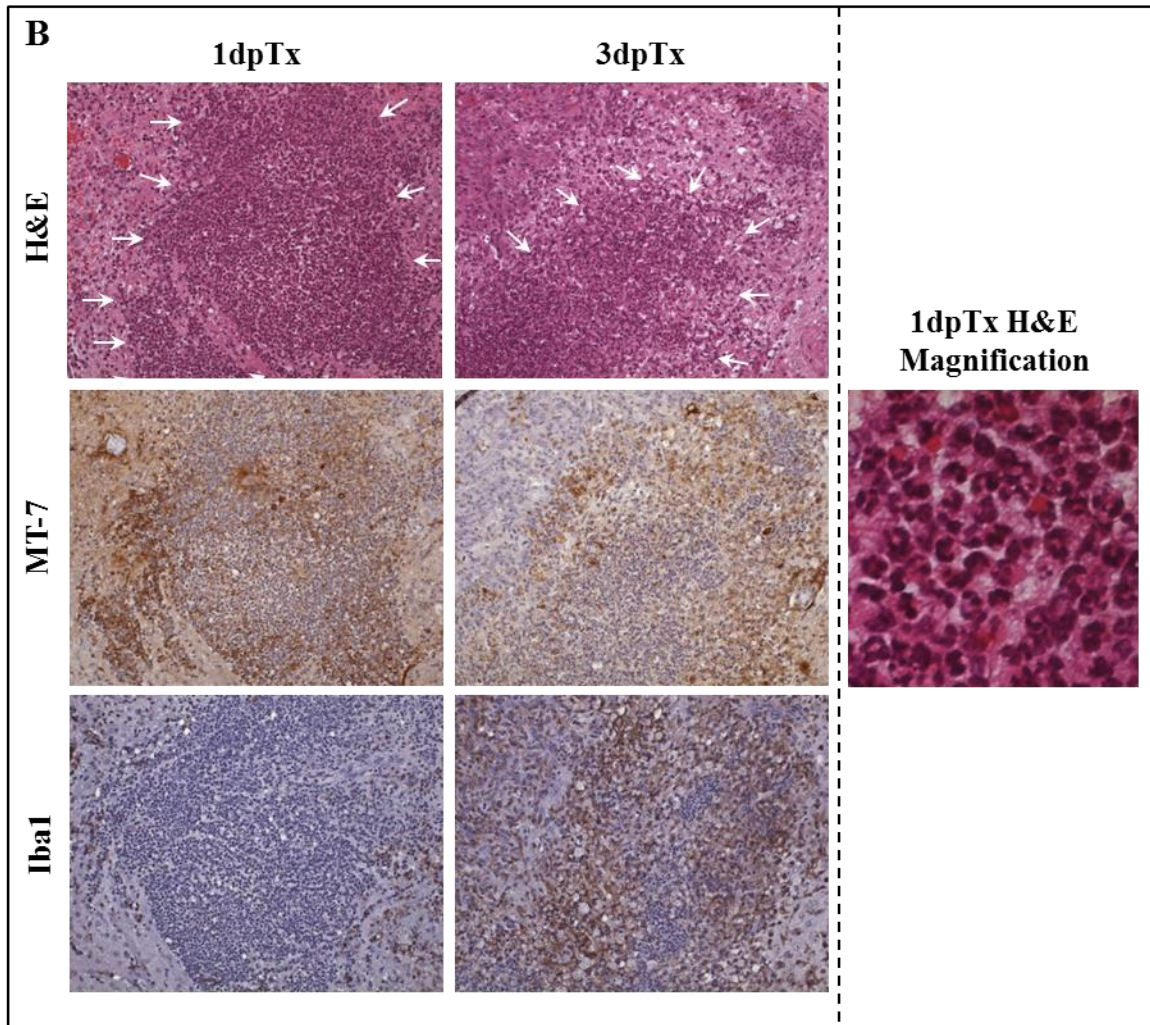


Figure 5.6: The recruited population of $CD45^{high}CD11b^{+}$ in Myxoma treated K1492 tumours consists of monocytes, granulocytes NK cells and T cells. The $CD45^{high}CD11b^{+}$ populations were further broken down into granulocytes (Ly6C[1A8], Yellow), T cells (CD3, Blue), NK cells (CD161[NK1.1], Green), NKT cells (Double+, Red) and monocytes (negative for these markers, Black). All of these populations significantly increased in Myxoma treated animals (n=6, t-test, $p < 0.05$; Top) and formed distinct populations in the $CD45CD11b$ scatter plot (bottom). **B** - Formalin-fixed paraffin sections were stained using Hematoxylin and Eosin (H&E) or immunohistochemical for Myxoma virus early protein MT-7 or for the microglial/macrophage marker IBA1. Granulocytes are identified by polymorphonuclear phenotype. (50X magnification). White arrows show areas of intense infiltration of polymorphonuclear cells. Far left picture is 400X displaying polymorphonuclear phenotype.

viral treatment; however, subsequent experiments identify these as monocytes. Finally, it can be seen in this figure that the population of CD161⁺CD3⁺ NKT cells, although small, was mostly contained in the CD45^{high}CD11b⁻ population (**Figure 5.6 - red**).

As with human gliomas, these appeared to be highly inflamed tumours, consisting of a range of recruited immunocytes. To delve deeper into the pre-treatment K1492 microenvironment, the cytokines and chemokines that are present at the time of infection and possibly responsible for recruiting these tumour-resident cells, were analyzed by a 32-plex ELISA. Supernatants to test for ELISA were prepared by taking tumour-bearing hemispheres in 500 μ L of PBS, homogenized, spun and filtered. The results are a combination of mice from 2 separate K1492-implantation experiments. Comparing non-tumour bearing to 14 dpi K1492-bearing C57Bl/6 mice revealed that 9 cytokines or chemokines were significantly up-regulated in the K1492 microenvironment (Mann-Whitney, $p < 0.05$; **Figure 5.7 A**). The most up-regulated of these was the chemokines CXCL10 (2646 pg/mL) and CCL2 (430 pg/mL), which are often elevated under neuroinflammatory conditions. Interestingly, IL-6 (87 pg/mL),³⁹³ CXCL1 (138 pg/mL)³⁹⁴ and LIF (28 pg/mL)³⁸ have been shown to play a role in glioma proliferation and/or invasion. Granulocyte-related chemokines CSF-3 (33 pg/mL), CCL11 (117 pg/mL), CXCL1 (138 pg/mL) and CXCL2 (225 pg/mL) are strongly represented in this analysis. Future experiments looking into how this cytokine/chemokine milieu changes in response to intracranial Myxoma treatment will be very interesting, and could explain the infiltration of some of the cell types we are seeing recruited to the tumour following treatment.

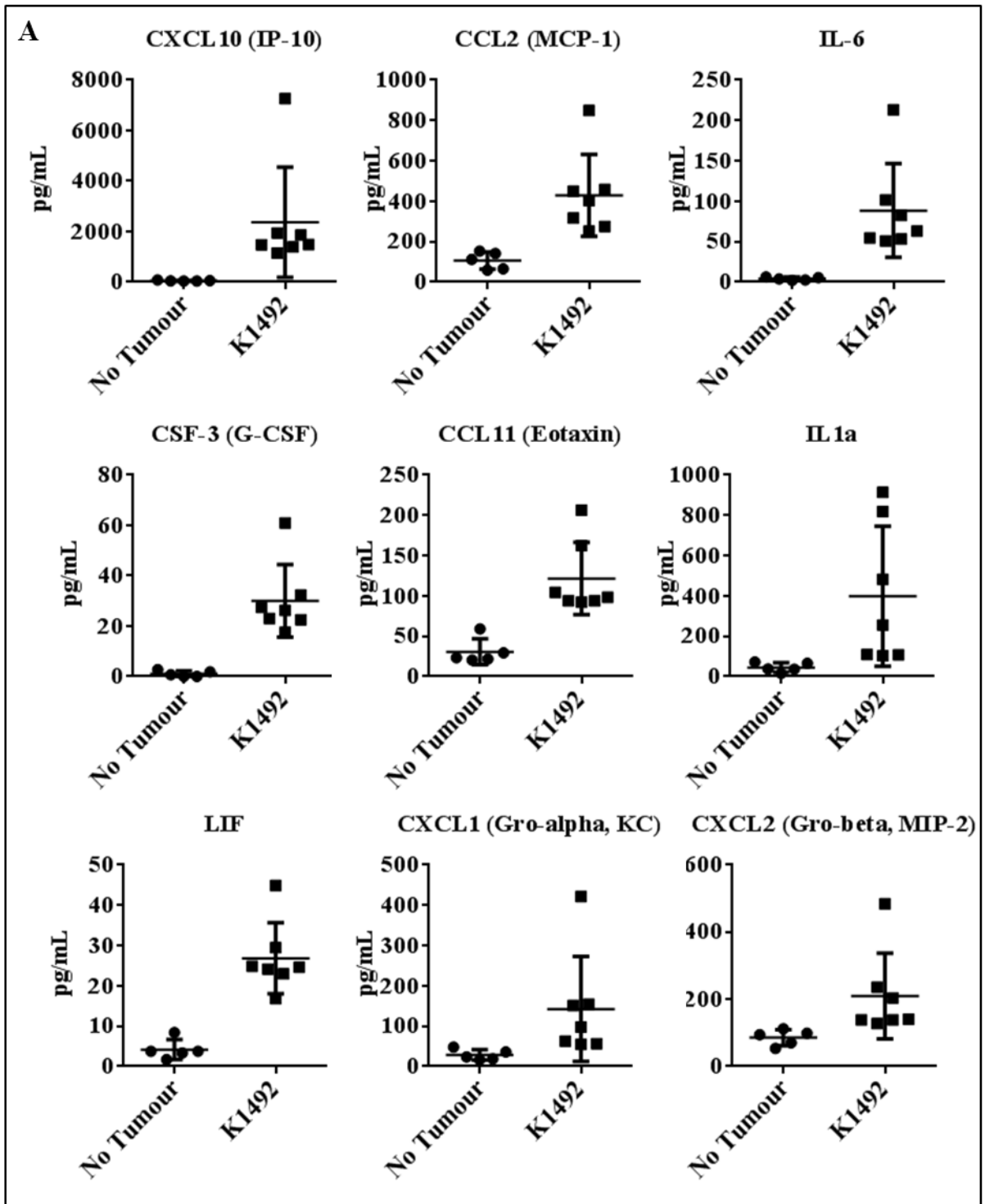


Figure 5.7: Cytokine and Chemokines significantly regulated in the K1492-glioma microenvironment. A – Significantly regulated cytokines and chemokines (Mann-Whitney, $p < 0.05$) in a mouse 32-plex ELISA for naïve C57Bl/6 (No Tumour, $n = 5$) and 14 dpi K1492-bearing hemisphere C57Bl/6 (K1492, $n = 7$).

These experiments provided some interesting insight as to the nature of the CD45^{high}CD11b⁺ population in our untreated and treated groups. Of particular note, is that many of the cell populations identified, GIMs (LargeGateCD45^{high}CD11b⁺Ly6G⁻CD3⁻), granulocytes (LargeGateCD45^{high}CD11b⁺Ly6G⁺CD3⁻), and NK cells (SmallGateCD45^{high}CD11b⁺NK1.1⁺CD3⁻) had very specific locations within the CD45/CD11b plot, which further confirmed their authenticity. Further, cytokine profiling the glioma microenvironment can give us clues as to the nature of these tumours *in situ*.

5.2.2. *The role of resident and recruited monocytoïd cells in mediating Myxoma virus treatment failure in the K1492 model*

Given that the largest population of cells infiltrating the untreated and treated K1492-tumour bearing hemisphere was CD45^{low}CD11b⁺ microglia and CD45^{high}CD11b⁺ GIMs, these were the first populations targeted for testing their role in mediating MYXV clearance and treatment failure. Interestingly, compared to the K1492 tumours, there was limited microglia and/or GIMs seen in U87-bearing CB17-SCID mice (**Figure 5.8 A**), which have previously been shown to have robust MYXV replication and can be cured with a single injection of MYXV.²⁵³ This is not a consequence of mouse strain, as K1492 grafted in CB17-SCID mice seem to have comparable microglial and GIM infiltration to C57Bl/6 mice as measured by IBA1 staining and intracranial MYXV treatment of K1492-bearing CB17-SCID mice had no treatment benefit (Log-Rank Mantel-Cox, p=0.7418; **Figure 5.8 B**). Of note, there is no inflammatory signature in the U87 xenografts with very little regulation of cytokines/chemokines compared to K1492 in SCID mice, which resembles the C57Bl/6 signature (*data not shown*).

Given the large tumour recruitment of GIMs to the K1492 glioma, and the high levels of CCL2 found in the K1492 microenvironment, we hypothesized that recruitment of these GIMs to the glioma was mediated through the CCL2-CCR2 pathway. Importantly, peripheral monocyte recruitment to the CNS has been shown to use this loop in other CNS pathologies such as experimental autoimmune encephalitis,¹⁹⁹ ischemic injury,²⁰⁰ and West Nile²⁰² and HSV²⁰³ viral encephalitis.

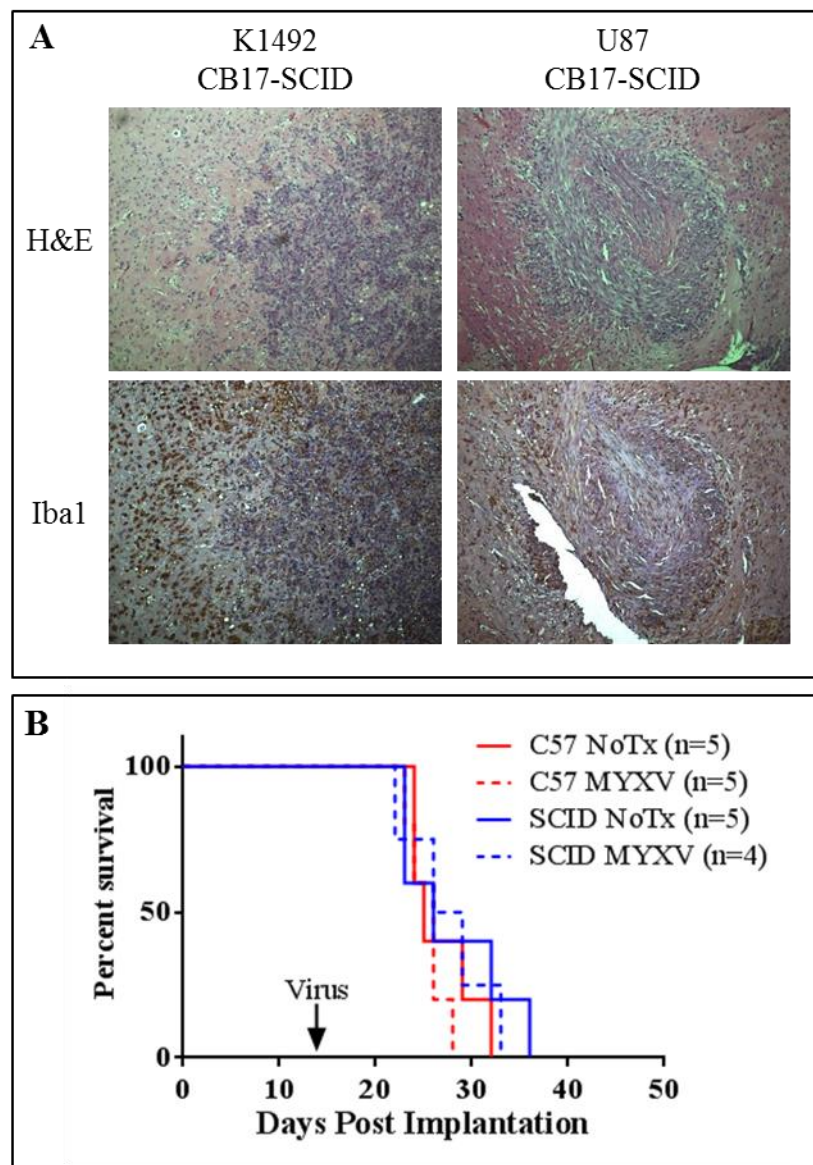


Figure 5.8: *K1492 orthografts in CB17-SCID mice have similar microglial and monocyte infiltration to C57Bl/6, but U87 lacks extensive infiltration. A - CB17-SCID mice were implanted with K1492 or U87 cells and harvested at 14 or 21 dpi, respectively, and stained with H&E or the microglial/macrophage marker IBA1 (100X magnification). B – K1492 implanted into C57Bl/6 (C57) or CB17-SCID (SCID) mice and treated with vMyx-FLuc (MYXV) or not treated (NoTx) on 14 dpi (Log-Rank Mantel-Cox, p=0.7418).*

Looking at K1492 cells in culture, they constitutively expressed CCL2, which increased nearly 2-fold in response to exogenously applied EGF 24 hours after treatment (**Figure 5.9**). Although a trend toward increasing CCL2 in response to FGF and PDGF was found, there was not a significant increase measured by ELISA. These results were confirmed by RT-PCR. Collectively, this suggest that the K1492 tumour may be recruiting peripheral monocytes through CCL2 secretion, and that this may, in part, be regulated though growth factors found in the tumour microenvironment.

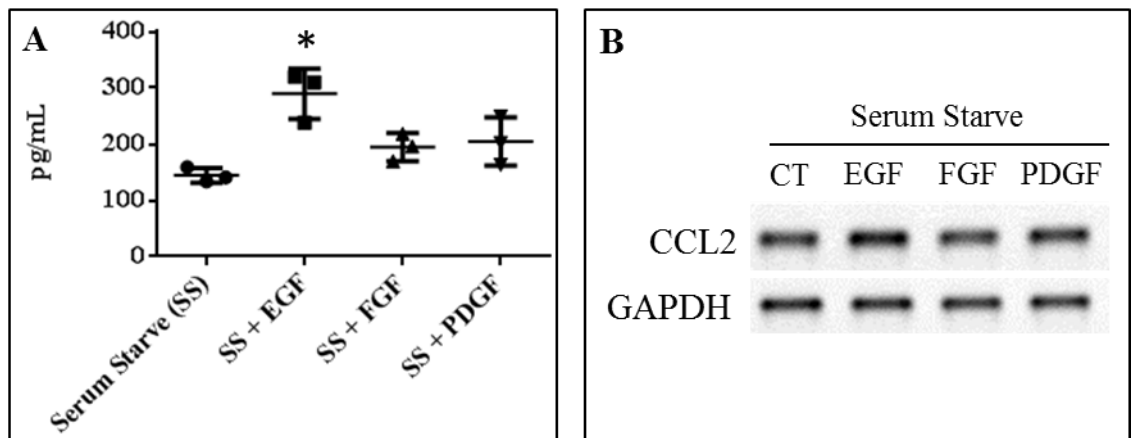
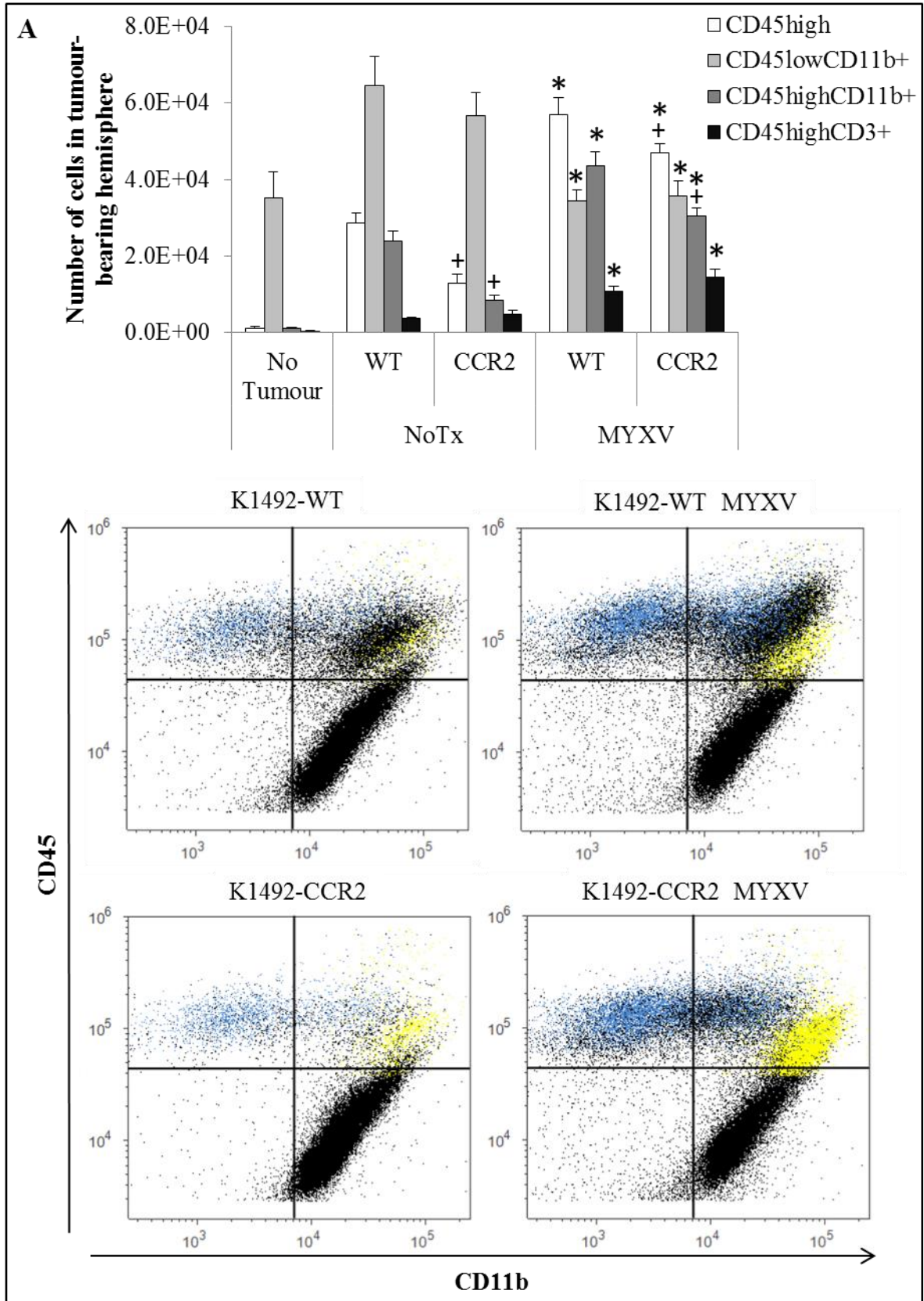


Figure 5.9: *CCL2 in the glioma microenvironment may in part be tumourally-derived and regulated by growth factor signalling. K1492 cells in vitro were serum-starved for 24 hrs and then given 10 ng/mL of EGF, FGF, or PDGF and supernatants collected for ELISA (A) or cells collected for RT-PCR (B) 24 hrs later to determine CCL2 expression levels.*

To test if CCL2-CCR2 signalling was indeed involved in recruiting GIMs, and whether these cells mediated MYXV infection of gliomas, CCR2^{-/-} mice implanted with K1492 were assayed by flow cytometry as previously described. In untreated K1492-bearing CCR2^{-/-} mice, it was found that the CD45^{high}CD11b⁺ population was dramatically reduced, almost three fold lower than wildtype mice (**Figure 5.10 A**), and of this population many were identified as Ly6G⁺ granulocytes (39.7%, yellow) or CD3⁺ T cells (12.0%, blue). Further, a large population of cells straddling the CD11b⁺ border (NK cells) was seen, suggesting that the GIM population was essentially abolished (**Figure 5.10 A**). The infiltrating CD45^{low}CD11b⁺ microglial and CD45^{high}CD3⁺ T-cell populations were unchanged in these mice.

In response to MYXV treatment, all cell types in the CCR2^{-/-} mice significantly increased (t-test, p<0.05). The CD45^{high}CD11b⁺ populations was also increased (**Figure 5.10 A**), albeit this did not increase to the extent seen in the wildtype mice (t-test, p<0.05). However, within the CD45^{high}CD11b⁺ population, it could be seen that the majority of the recruited cells were not monocytes, but mainly CD45^{high}CD11b⁺Ly6G⁺ granulocytes (**Figure 5.10 A/B, yellow**), and the double negative CD45^{high}CD11b⁺ group was significantly reduced. Interestingly, increased neutrophil recruitment to the CNS in replacement of monocytes in CCR2^{-/-} mice has been shown previously,³⁷² suggesting that this is a conserved neuroinflammatory response. However, the question remains, is this an increase in neutrophil recruitment or failure to remove neutrophils from the CNS? In our IHC studies, after the initial massive influx of neutrophils at 1 dpTx, by 3 dpTx the remaining neutrophils are surrounded by ‘foamy’ IBA1⁺ cells, indicative of phagocytic macrophages (**Figure 5.6**). It is conceivable that these macrophages, whether there are



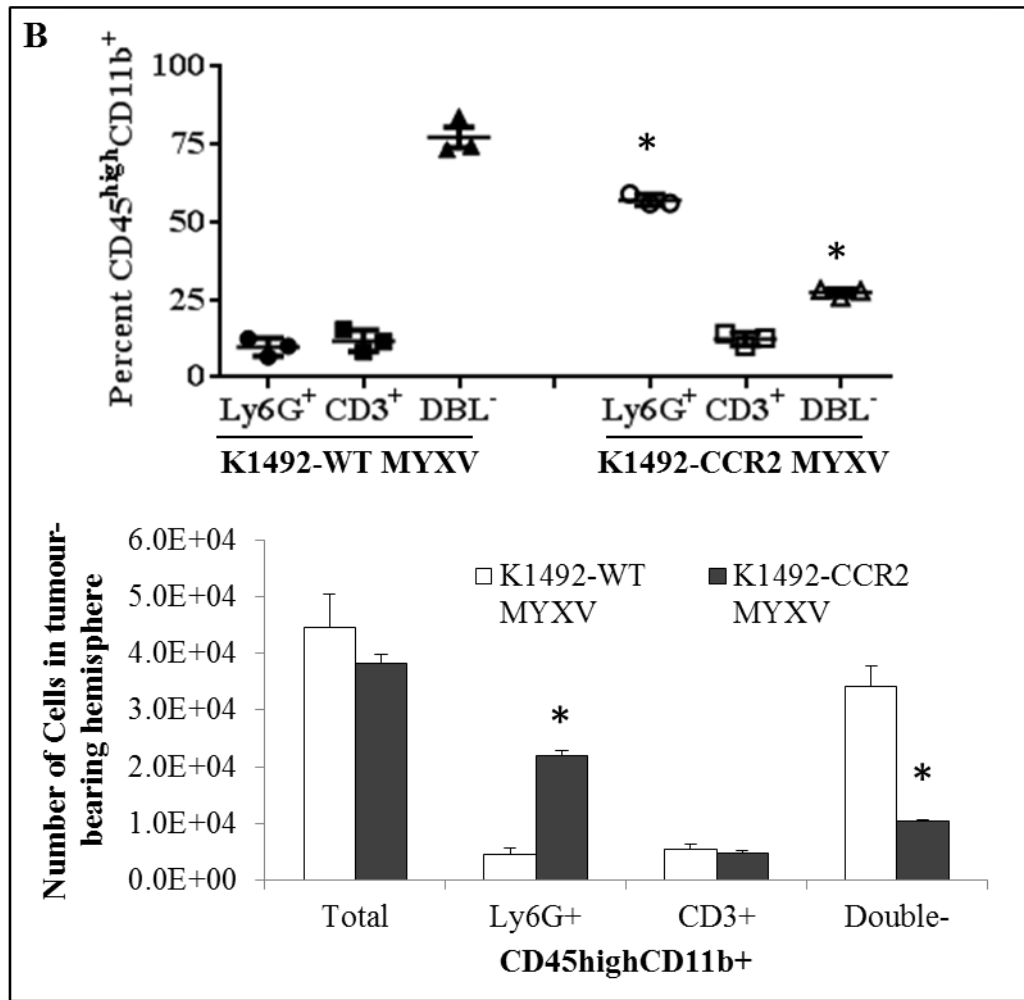


Figure 5.10: CCR2-deficient mice fail to recruit any peripheral monocytes/macrophages to the K1492 tumour before or after Myxoma treatment. Wildtype (WT) or CCR2-deficient (CCR2) C57Bl/6 mice implanted with K1492 cells and analyzed by flow cytometry at 15 days-post implantation, 3 days post-treatment with Myxoma virus (MYXV) or untreated (NoTx). **A** - Quantified numbers of each cell type isolated from the tumour-bearing hemisphere (*top*) accompanied by the CD45/CD11b scatter plot (*bottom*) highlight the cell populations that also stain for Ly6G (granulocytes, yellow) and CD3 (T cells, blue). Error bars represent standard error and asterisks represent significant differences within mouse strain but between treatment groups. Plus signs represent significant differences between mouse strains within treatment groups (n=6, t-test, p<0.05). **B** - Scatter graph of percent of CD45^{high}CD11b⁺ populations were further broken down into granulocytes (Ly6G[1A8]) and T cells (CD3) or neither (DBL-) between WT and CCR2-deficient mice after Myxoma treatment. Error bars indicate standard error while asterisks indicate significant difference between cell types of different mouse strain (n=3, t-test; *top*). Quantified numbers of the CD45^{high}CD11b⁺ populations of each cell type isolated from the tumour-bearing hemisphere (*bottom*). Error bars indicate standard error while asterisks indicate significant difference between cell types of different mouse strain (n=3, t-test).

recruited out of the tumour or from the periphery, are responsible for the safe-destruction of these scavenging neutrophils,³⁹⁵⁻³⁹⁷ as their autolysis could be tremendously toxic to the neurons and glia in the CNS. The CD11b^{high}CD3⁺ population did not change between mice (**Figure 5.10 A/B, blue**).

To confirm this loss of GIMs in the CCR2^{-/-} mice, formalin-fixed, paraffin-embedded samples of wildtype or CCR2^{-/-} K1492-bearing animals were stained with IBA1 (**Figure 5.11**). There was a very similar staining pattern of IBA1⁺ amoeboid cells, which in the CCR2^{-/-} mice must represent the activated microglial population. What was different between these mice was the number of IBA1⁺ cells within the K1492 glioma, with the CCR2^{-/-} mice having next to no tumour-infiltrating IBA1⁺ cells.

This provides strong evidence that the IBA1⁺ cells surrounding the K1492 cells are the tumour-resident microglial population, while the IBA1⁺ cells within the tumour were GIMs. Interestingly, a very similar scenario was seen in another study monitoring oncolytic HSV in a syngeneic rat glioma model, where peripherally recruited monocytes were found within the tumour while microglia remained surrounding the tumour border.²¹⁹

Finally, NK, NKT and T cell recruitment in CCR2^{-/-} mice was examined using the CD161(NK1.1) and CD3 antibodies in the CD45^{high} small gated population. Judging by the scatter pattern alone in the CD45/CD11b plots, there was an obvious population straddling the CD11b boundary (**Figure 5.10 A**), which was previously shown as the CD161⁺CD3⁻ NK cell population (**Figure 5.5**). CCR2^{-/-} mice did indeed have a significant recruitment of NK, NKT and T cells at 3 dpTx with MYXV (t-test, p<0.05;

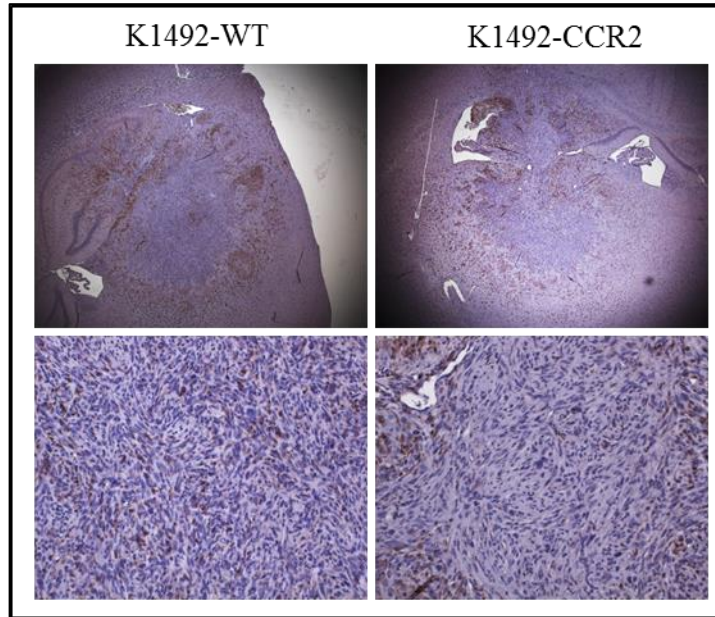
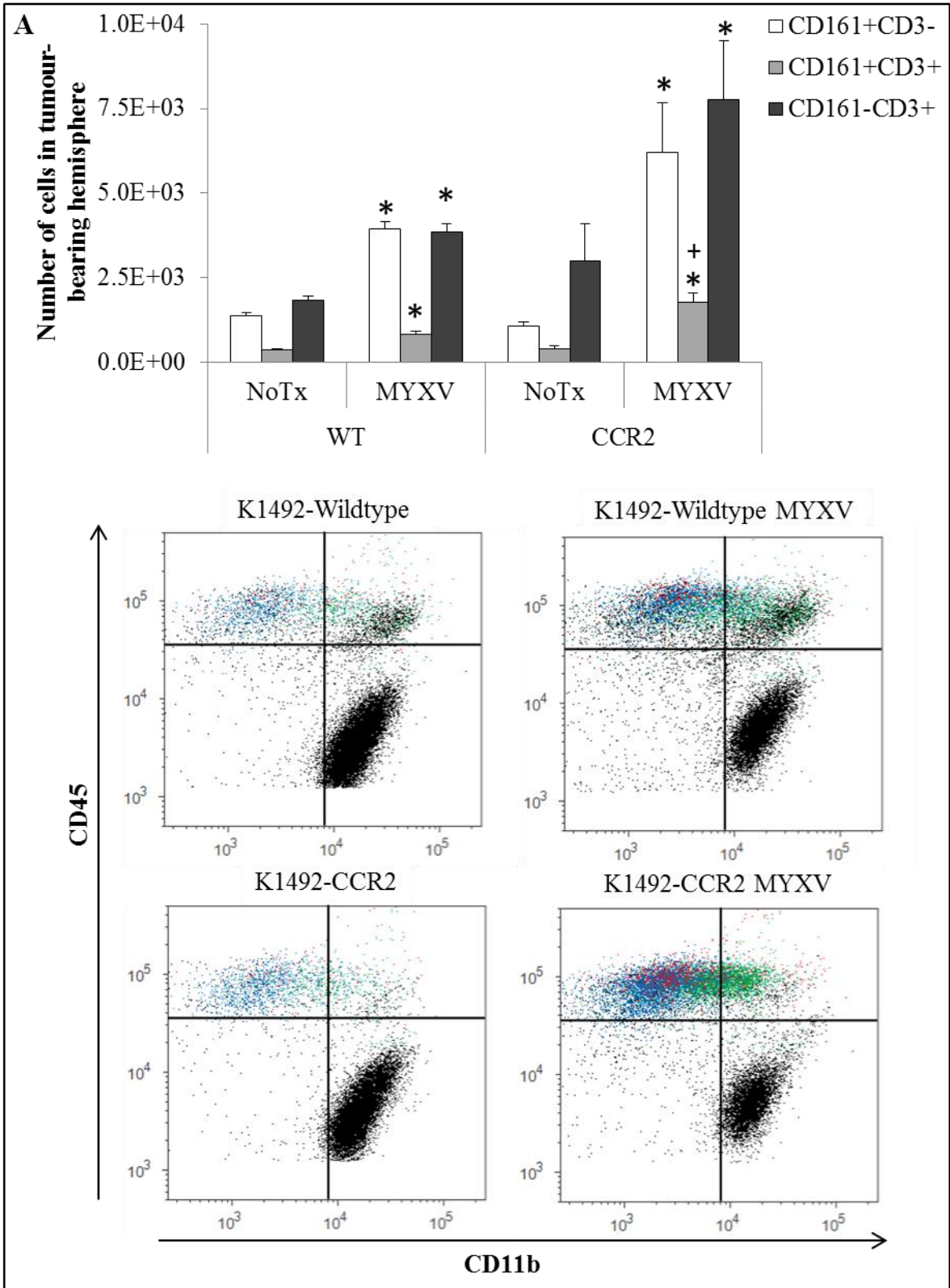


Figure 5.11: *CCR2-deficient mice have unaffected microglial activation and tumour-recruitment but are largely devoid of monocyte/microglia within the K1492 glioma.* C57Bl/6 wildtype or CCR2 deficient mice were implanted with K1492 and harvest at 14 days post-injection. Formalin-fixed paraffin sections were stained using microglial/macrophage marker IBA1 (Top row 25X; Second row 200X).

Figure 5.12), a response that seemed exaggerated compared to the wildtype controls, but was only significantly in the $CD45^{\text{high}}CD161^+CD3^+$ population of NKT cells. It was important to demonstrate that these cell types are not-inhibited in trafficking to the tumour, as CCR2-mediated recruitment has been shown for NK cell populations.^{398,399} Of note here was the absence of the SmallGate $CD45^{\text{high}}CD11b^+CD161^-CD3^-$ population seen in the wildtype controls, suggesting that these were small, 'ungranular' monocytes.

Further investigation into whether the $CCR2^{-/-}$ mice were indeed recruiting more NK cells than the wildtype was performed (**Figure 5.12 B**). This additional experiment using CD161(NK1.1) and CD49b(DX5) antibodies alone found overall the number of NK cells was decreased compared to the previous experiment, but there was a significantly increased number of recruited NK cells in the $CCR2^{-/-}$ mice compared to the



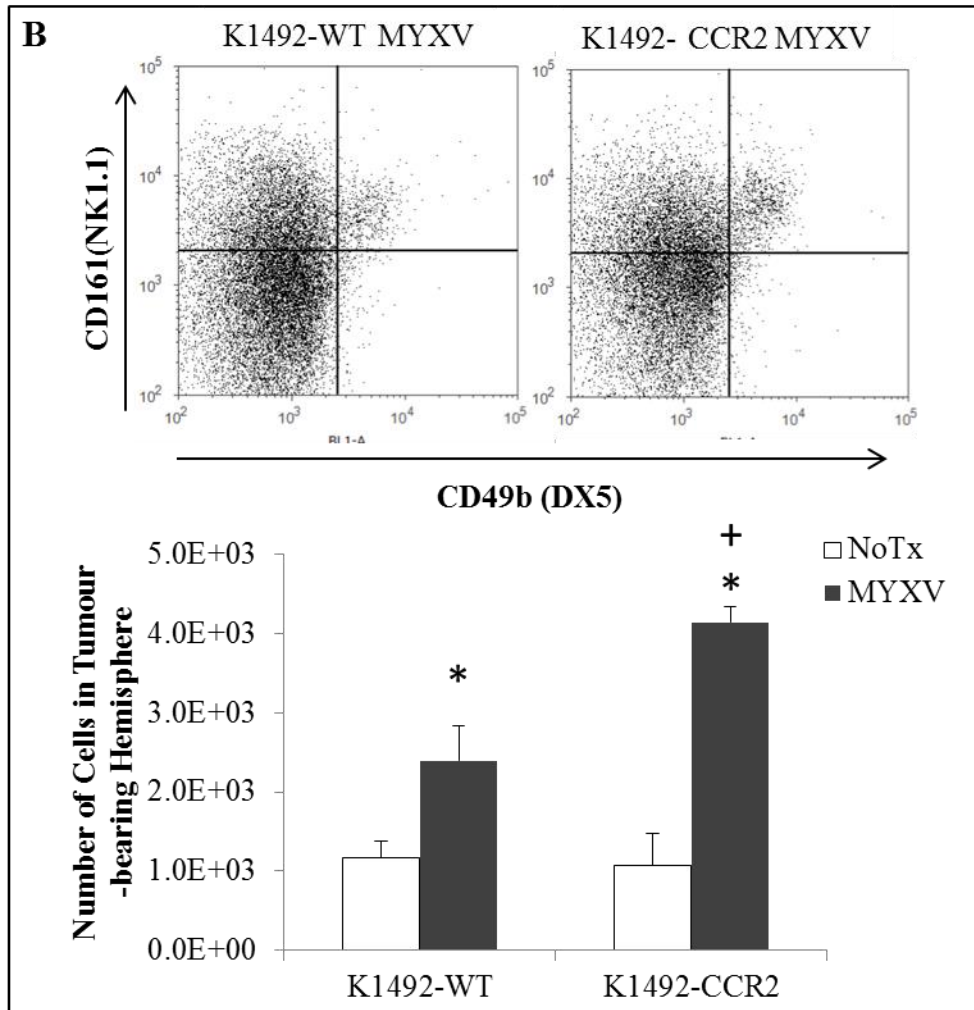
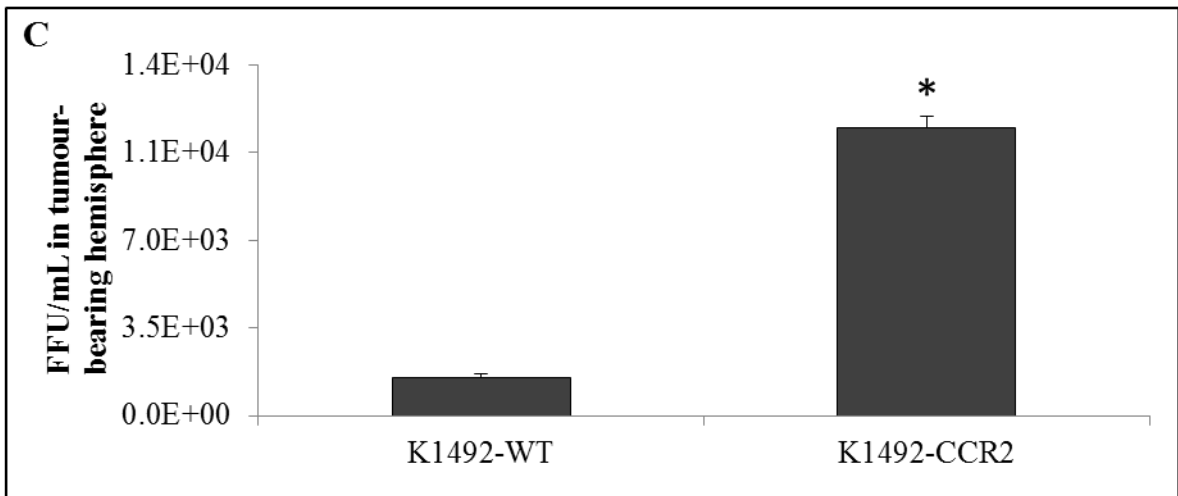
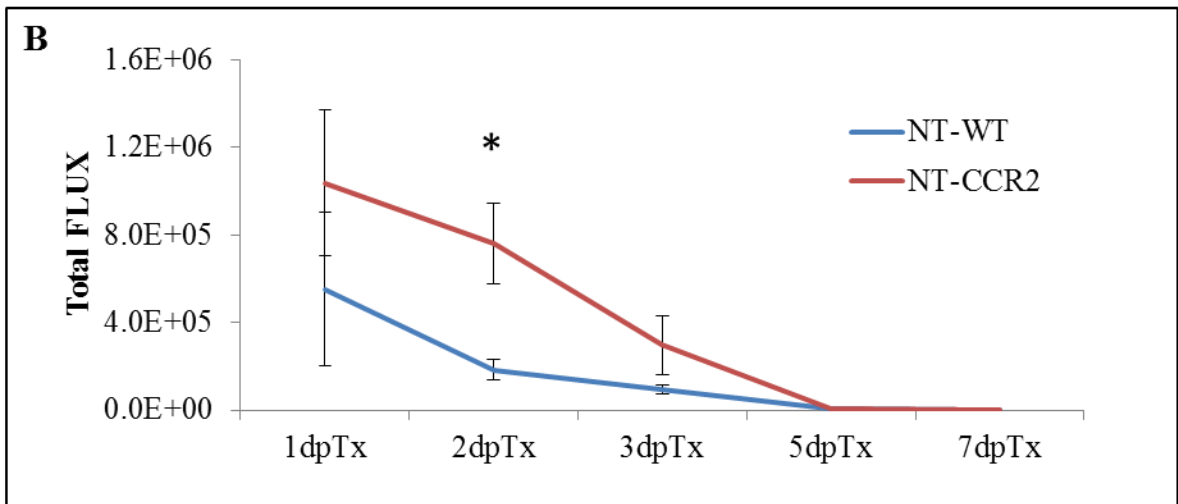
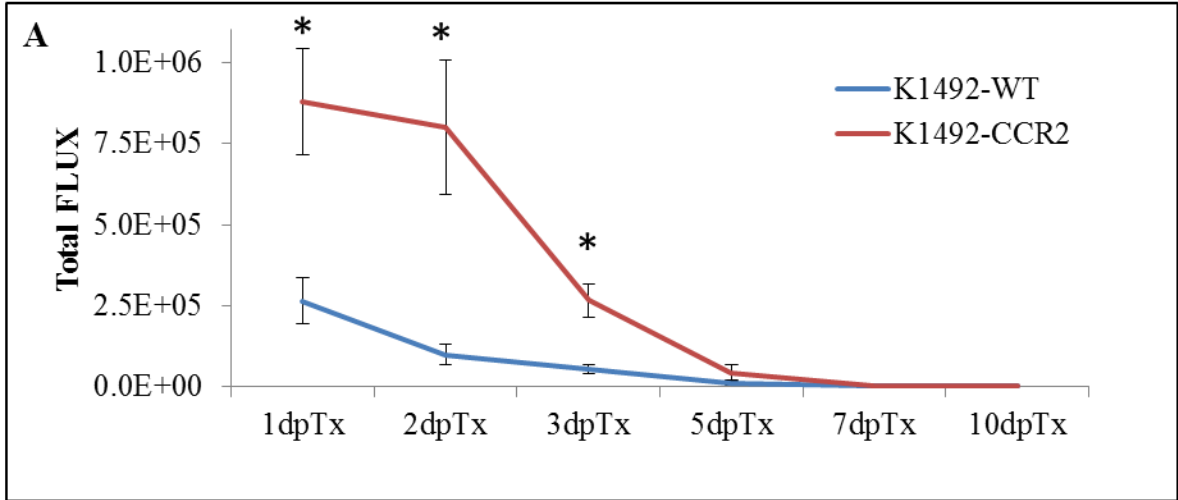


Figure 5.12: *CCR2*-deficient have an exaggerated recruitment of NK, NKT and T cells to the K1492 glioma in response to Myxoma treatment. Wildtype (WT) or *CCR2*-deficient (*CCR2*) C57Bl/6 mice implanted with K1492 cells and analyzed by flow cytometry at 15 days-post implantation, 3 days post-treatment with Myxoma virus (MYXV) or untreated (NoTx). Initial live gating was around small lymphocyte population followed by interrogation of the CD45^{high} population within this gate. **A** - Quantified numbers of each cell type isolated from the tumour-bearing hemisphere (*top*) accompanied by the CD45/CD11b scatter plot (*bottom*) highlight the cell populations that also stain for NK cells (CD161⁺CD3⁻, green), CD161⁻CD3⁺ (T cells, blue), and CD161⁺CD3⁺ (NKT cells, red). Error bars represent standard error and asterisks represent significant differences within mouse strain but between treatment groups. Plus signs represent significant differences between mouse strains within treatment groups (n=3, t-test, p<0.05). **B** - Scatter plot of subsequent flow cytometry experiment using only the CD161(NK1.1) and CD49b(DX5) antibodies to look at NK cell populations recruited to K1492 gliomas 3 dpTx. (*top*) Quantified CD161⁺CD49b⁺ data from this experiment (*bottom*). Error bars represent standard error and asterisks represent significant differences within mouse strain but between treatment groups. Plus signs represent significant differences between mouse strains within treatment groups (n=3, t-test, p<0.05).

wildtype-mice (t-test, $p < 0.05$).

Given the lack of resident and recruited GIMs in the $CCR2^{-/-}$ K1492 tumours, but retention of all the other glioma-infiltrating immunocytes, the role these cells played in viral clearance kinetics and treatment efficacy was then examined. Real-time monitoring of viral infection using vMyx-FLuc determined that initial infection and clearance at 1, 2 and 3 days post infection was 3.5-, 8.1-, and 5.0-fold increased over K1492-bearing wildtype mice (Mann-Whitney, $p > 0.05$; **Figure 5.13 A**), but returned to wildtype levels by 5 dpTx. This was not entirely attributed to the delay of off-target infection in non-tumour bearing $CCR2^{-/-}$ mice. There was an elevated signal in these mice, with a significant time-point at 2 dpTx, but this was only 4.1-fold higher than non-tumour-bearing wildtype controls (**Figure 5.13 B**), suggesting that the additional viral luciferase signal was occurring within the tumour. Unfortunately, the tumour and non-tumour bearing experiments were not performed in parallel and cannot be directly compared. These viral clearance kinetics were examined with a viral recovery experiment from wildtype or $CCR2^{-/-}$ K1492-bearing animals (**Figure 5.13 C**). Here we found that MYXV titres at 3 dpTx were over 10-fold greater than what was seen in wild-type, suggesting that the $CCR2^{-/-}$ K1492-bearing mice were inhibited in clearing MYXV from the tumour.

MYXV treatment of 14 dpi tumours resulted in a small, but significant increase in treatment efficacy, living on average 4 days longer (15%) than non-treated $CCR2^{-/-}$ animals (27 dpi NT $CCR2^{-/-}$ versus 31 dpi MYXV $CCR2^{-/-}$; $p = 0.0079$, Mantel-Cox Log Rank; **Figure 5.13 E**). K1492 tumours in wildtype versus $CCR2^{-/-}$ mice had nearly identical survival (26 vs. 27 dpi, respectively, $p = 0.3274$, Mantel-Cox Log Rank). Non-tumour-bearing $CCR2^{-/-}$ mice did not succumb to viral infection (**Figure 5.13 D**).



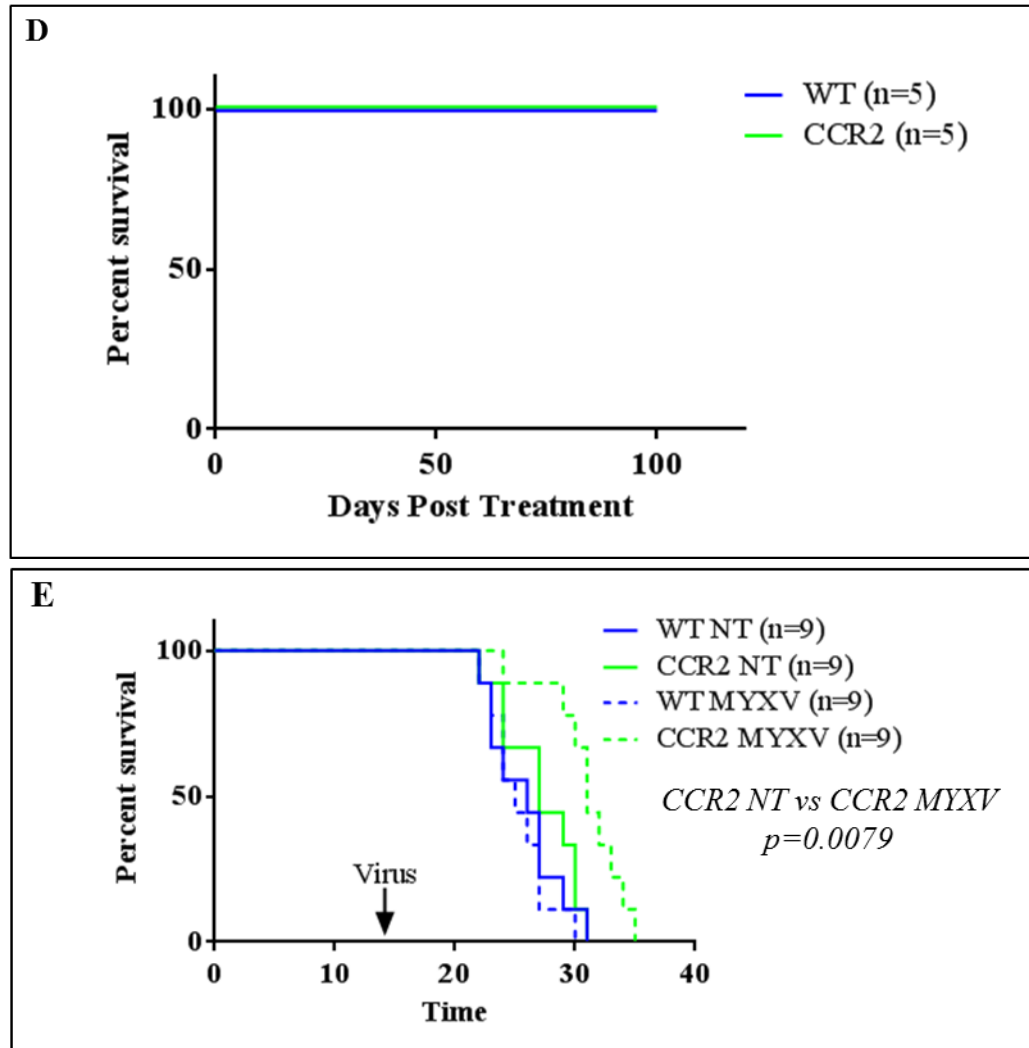


Figure 5.13: CCR2-deficient mice have a significant increase in the amount of infection, but not replication occurring after Myxoma virus administration which translates into a mild increase in survival of treated animals. **A** - Wildtype or CCR2^{-/-} C57Bl/6 mice implanted with K1492 cells were treated at 14 dpi with 5.0×10^6 PFUs of vMyxv-FLuc and monitored for viral infection. Error bars represent standard error and asterisks represent significantly difference (K1492-WT n=9, K1492-CCR2 n=10; Mann-Whitney Test, $p > 0.05$). **B** - A subsequent experiment looking at bioluminescence from non-tumour bearing wildtype (NT-WT) and CCR2^{-/-} animals (NT-CCR2) infected with 5.0×10^6 PFUs of vMyx-FLuc. Error bars are standard error and asterisks represent significantly different (NT-WT n=5, NT-CCR2 n=5; Mann-Whitney Test, $p > 0.05$). **C** - Viral recovery assay from wildtype (K1492-WT) or CCR2^{-/-} (K1492-CCR2) bearing 14 day K1492 tumours and infected with 1.5×10^7 PFU vMyx-FLuc 3 days post-treatment. Error bars represent standard error and asterisk represents significant difference (n=3/group; t-test, $p < 0.05$). **D** - Survival of wildtype (WT) or CCR2^{-/-} (CCR2) C57Bl/6 mice treated with 5.0×10^6 PFUs of vMyxv-FLuc (MYXV). **E** - Survival of wildtype (WT) or CCR2^{-/-} (CCR2) C57Bl/6 mice implanted with K1492 cells were treated at 14 dpi with 5.0×10^6 PFUs of vMyxv-FLuc (MYXV) or untreated (NT).

Results from the flow cytometry experiments suggested that MYXV-treatment resulted in very few if any recruited monocytes from the periphery in $CCR2^{-/-}$ mice (**Figure 5.10 A/B**). To confirm that these did not play a role in this phenotype, an experiment to ablate peripheral monocytes was conducted. Clodronate liposomes (CL) have been used to specifically target peripheral macrophages⁴⁰⁰ as well as circulating monocytes,⁴⁰¹ while being unable to cross the blood-brain barrier⁴⁰² would leave microglia and GIMs unaffected. First examined was the population of cells recruited to the MYXV-treated K1492 tumours in C57Bl/6 mice treated with CL or liposomes alone (Vehicle). For these experiments, CL or Vehicle was administered intravenously via tail vein the day before (-1 dpTx), the day of (0 dpTx) and one day following MYXV treatment (1dpTX). Animals were then sacrificed and immunocytes analyzed in the tumour-bearing hemisphere 3 dpTx. It was observed that CL treatment resulted in the ablation of MYXV-recruited $CD45^{high}CD11b^{+}Ly6g^{-}$ GIMs to the tumour after treatment (**Figure 5.14; Supplementary Figure 2**), but resulted in a significant increase in $CD45^{high}CD11b^{+}Ly6g^{+}$ granulocytes (t-test, $p < 0.05$). Unfortunately, these experiments did not utilize CD3 or CD161 antibodies so the populations of T and NK cells cannot be readily analyzed; however, $CD45^{high}CD11b^{-}$ cells were unchanged in the CL treated mice, while the ‘straddling’ population, previously shown to be NK cells, remained. It is these cell types that likely resulted in the upwards trend of the $CD45^{high}CD11b^{+}Ly6g^{-}$ cells. This, coupled with what the literature has shown in the past, it was concluded that CL can deplete monocyte recruitment to the K1492 glioma in C57Bl/6 mice.

Next, the identical experiment was performed except MYXV infection was followed in real time using vMyx-FLuc. In this experiment, we found that the viral

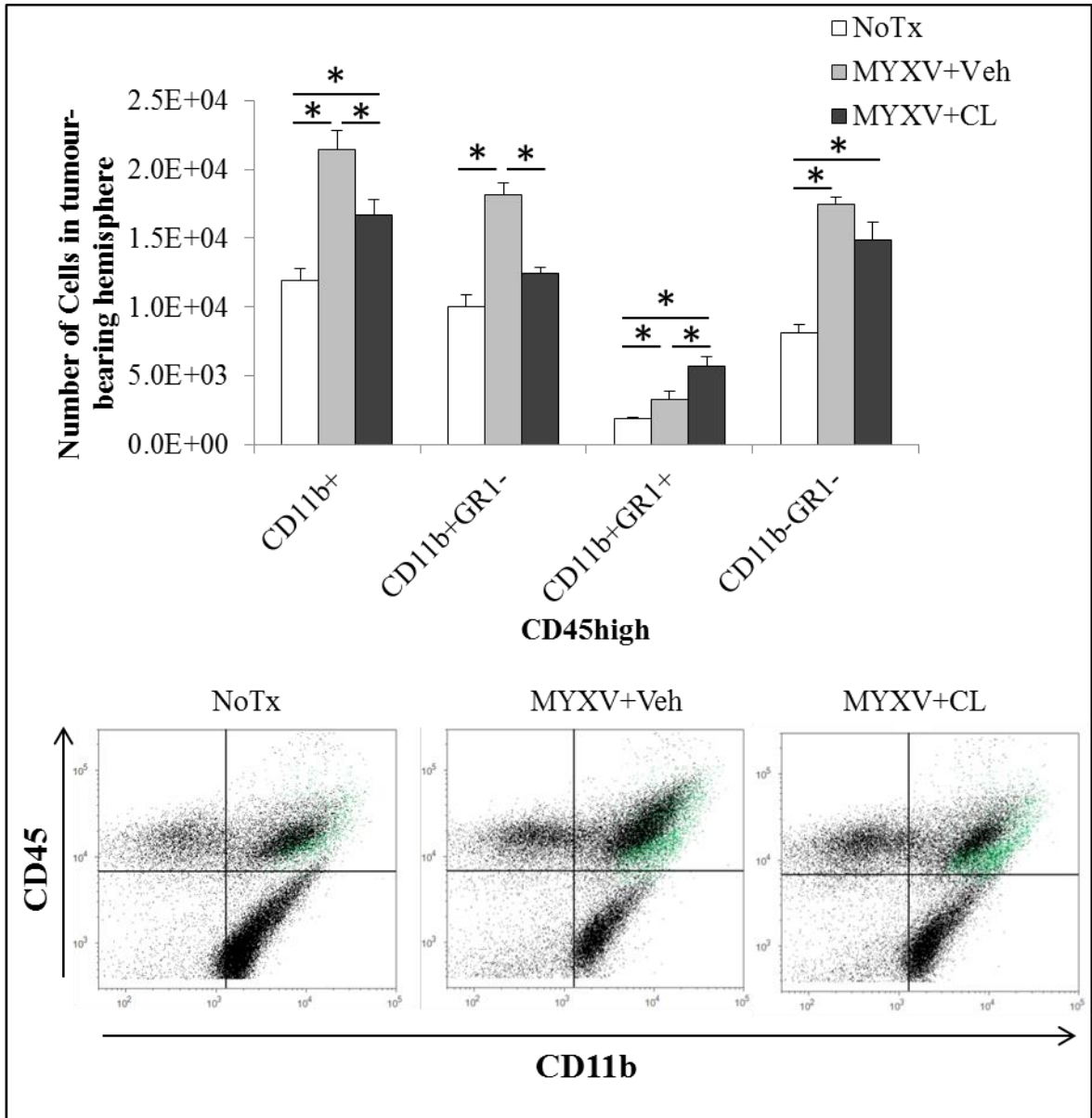


Figure 5.14: Clodronate liposome administration results in depletion of peripheral monocyte infiltration at three days post Myxoma virus administration. Wildtype C57Bl/6 mice implanted with K1492 cells were treated at 11, 12, and 13 dpi with Clodronate liposomes (CL) or vehicle (Veh) and with Myxoma virus administration at 12dpi. Tumour infiltrating immunocytes analyzed by flow cytometry at 15 days-post implantation, 3 days post-treatment with Myxoma virus (MYXV) or untreated (NoTx). Quantified numbers of each cell type isolated from the tumour-bearing hemisphere (*top*) of the CD45^{high} population of cells. Error bars represent standard error and asterisks represent significant differences between treatment groups. (n=4, t-test, p<0.05). CD45/CD11b scatter plot (*bottom*) highlight the lack of monocyte infiltration and enhanced CD11b+Ly6g+ (green) from the periphery in CL treated mice.

clearance kinetics were statistically identical between the two samples (Mann-Whitney, $p > 0.05$), however viral clearance appeared to be partially delayed in the CL group at 5 and 7 dpTx (**Figure 5.15 A**). There was no significant change in survival between the Vehicle and CL treated groups following MYXV treatment (25dpi vs 28.5 dpi, respectively. Log-rank Mantel-Cox $p = 0.3039$; **Figure 5.15 B**).

The results from the $CCR2^{-/-}$ mice and Clodronate liposome experiments strongly suggest that it is the tumour-resident GIMs, not treatment recruited GIMs that are mediating the initial infection and replication of Myxoma virus in the K1492 model. Given that microglia are also activated and recruited to the K1492 tumour, we tried to target these cell types as well as GIMs. Here, these populations were targeted using an inducible system for monocyte/macrophage ablation herein referred to as CD11b::DTR mice. These transgenic mice contain the human diphtheria toxin receptor (**DTR**; heparin-binding epidermal growth factor-like, HB-EGF) under the control of the CD11b promoter.⁴⁰³ DT has a $< 100,000X$ affinity for murine HB-EGF than human cells, making them much more resistant to diphtheria toxin.^{315,316} Thus, the $CD11b^{+}$ cells in the CD11b::DTR mice were specifically susceptible to DT administration. Interestingly, it has been shown that only the monocyte/macrophage $CD11b^{+}$ cells within the mouse are targeted, while CD11b expressing granulocytes, NK and NKT cells were unaffected.^{317,403} This, however, was not confirmed in this study. Importantly, DT has been shown to cross the blood-brain barrier,⁴⁰⁴ and that administration in CD11b::DTR mice can ablate microglia.^{124,405} Finally, unlike other inducible models using viral tyrosine kinase and ganocyclovir,⁴⁰⁶ DT can target terminally differentiated cells, thus providing the opportunity to target already active tumour-resident microglia and

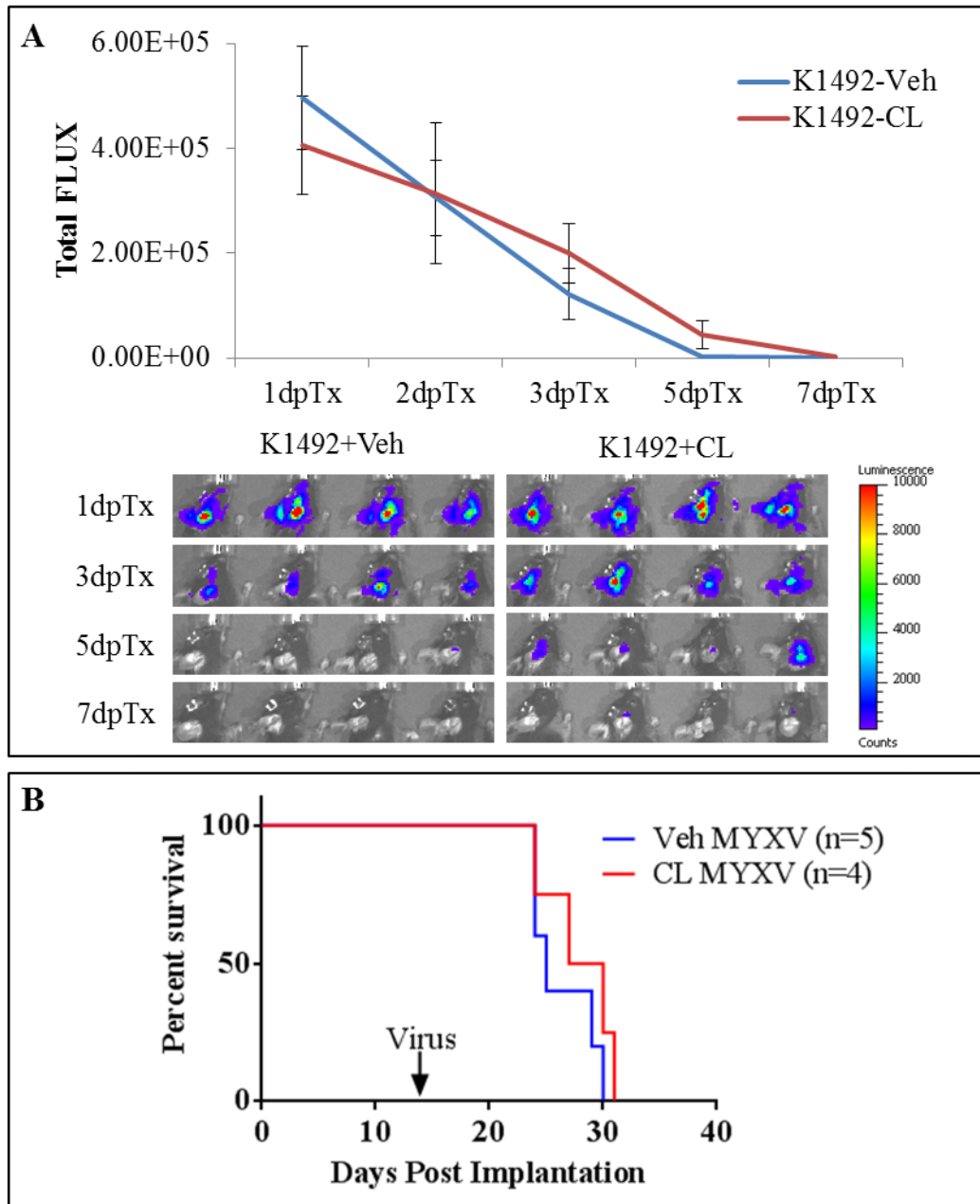


Figure 5.15: Ablation of peripheral monocytes results in no significant change in viral luciferase or survival in K1492 glioma-bearing mice. Wildtype C57Bl/6 mice implanted with K1492 cells were treated at 11, 12, and 13 dpi with Clodronate liposomes (CL) or vehicle (Veh) and Myxoma virus administration at 12dpi were followed for viral luciferase expression using the Xenogene imaging system (**A**; $n=5/\text{group}$, Mann-Whitney Test, all point $p>0.05$). These mice were then followed for survival (**B**); one CL animal was removed from group as it was sacrificed due to symptoms likely unrelated to tumour burden (Log-rank Mantel-Cox $p=0.3039$).

macrophages. DT administration was found to be very toxic to the CD11b::DTR mice. Transgenic mice, but not wildtype mice, rapidly lost weight and succumbed to the toxin by 8 dpTx at the 10 ng/g dose and by 4-5 dpTx at the 25 ng/g dose (**Figure 5.16 A**). Despite this toxicity, it appeared there was a window of opportunity to measure the microglial/GIM ablation on MYXV treatment in the K1492 model (**Figure 5.16 B**).

Flow cytometry of infiltrating immunocytes in the CD11b::DTR mice at 14 dpi of K1492 (0 dpTx) and after two doses of DT found that the resident CD45^{high}CD11b⁺ GIM population was unaffected by the DT yet the CD45^{low}CD11b⁺ microglial population was reduced by over 2-fold (t-test, $p < 0.05$; **Figure 5.17 A**). Three days post MYXV treatment, DT in the transgenic mice was able to ablate the recruitment of CD45^{high}CD11b⁺ cells compared to either the wildtype control or the wildtype mice treated with DT, although DT treatment in wildtype mice had a significantly lower CD45^{high}CD11b⁺ compared to the no treatment control (t-test, $p < 0.05$). Further, the loss of microglia persisted in the transgenic mice, although the loss of microglia normally seen in MYXV-treated mice was not observed in these experiments. Overall, these experiments demonstrated that DT administration in CD11b::DTR mice can significantly target microglial cells and halt the recruitment of peripheral CD45^{high}CD11b⁺ cells.

Viral infection and early replication in these animals was assessed by following the bioluminescent of the vMyx-FLuc virus. Virus was administered at 14 dpi, following DT injections on 11 dpi and 13 dpi, and then followed by another DT injection at 15 dpi (**Figure 5.17 B**). Viral luciferase activity in these animals was significantly elevated at 1, 2 and 3 dpTx over the control non-treated mice (Mann-Whitney, $p < 0.05$), suggesting that

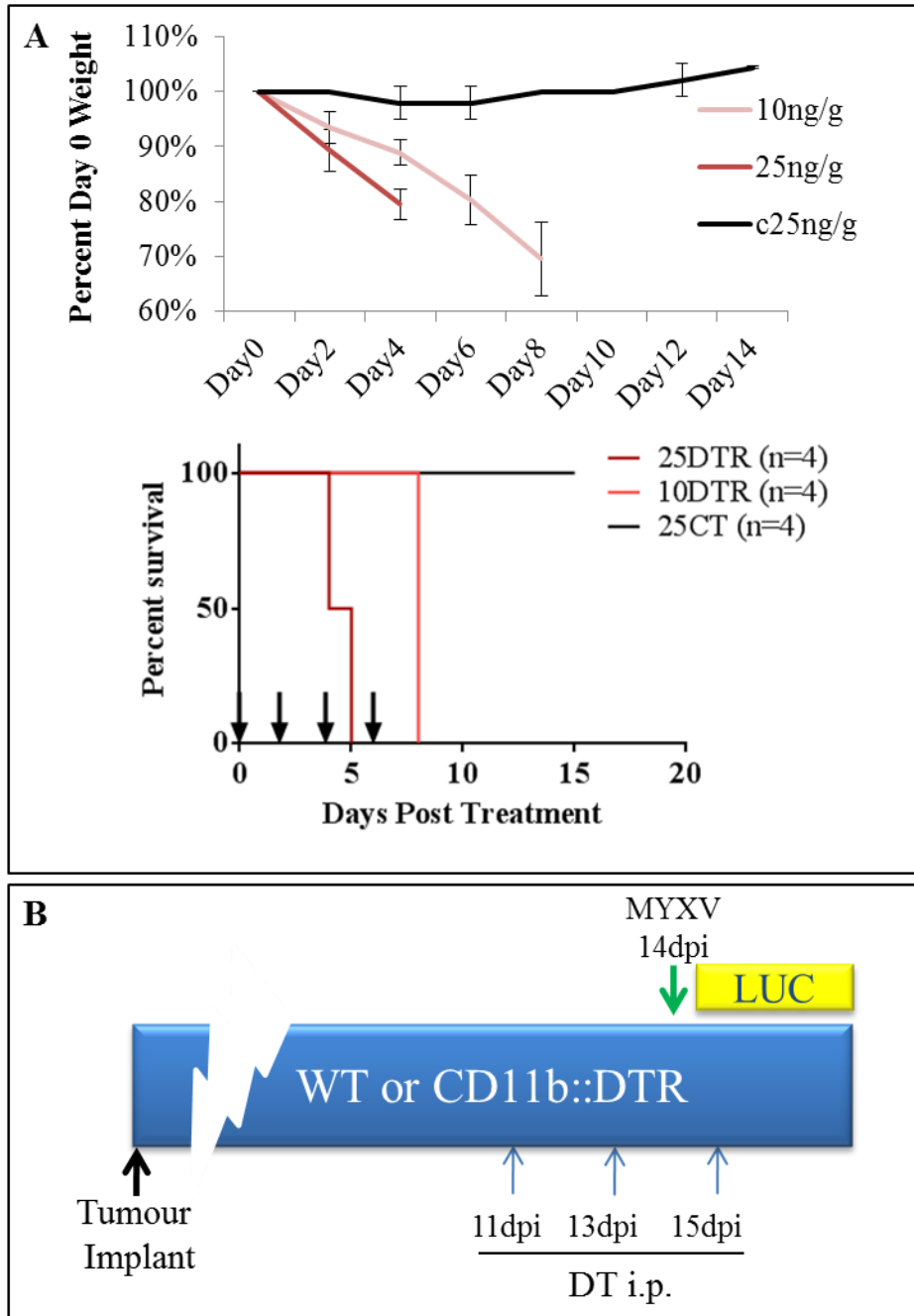


Figure 5.16: *CD11b::DTR* mice display toxicity to diphtheria toxin administration. C57Bl/6 mice given intraperitoneal injections of diphtheria toxin every second day for a total of four doses were assessed for toxicity by weight (**A**; top) at 10 ng/g and 25 ng/g in *CD11b::DTR* mice or wildtype mice at 25ng/g (c25 ng/g). Transgenic animals succumbed to DT poisoning at the 25 ng/g (25DTR) and 10 ng/g (10DTR) doses while wildtype mice were unaffected at 25 ng/g (25CT). **B** - The experimental design for the *CD11b::DTR* mice experiments with MYXV comprised of 10ng/g DT administered at 11, 13 and 15 dpi and vMyx-FLuc given at 14 dpi. Mice were followed for 3 days for viral luminescence until the animals succumbed to DT poisoning.

either the resident microglia or recruited $CD45^{high}CD11b^{+}$ cells could be responsible in mediating either initial viral infection or viral clearance. Of note here is the lack of a control experiment examining whether ablating these cell types would increase viral FLUC in non-tumour bearing mice, or an assessment of the other cell types that are affected by DT administration.

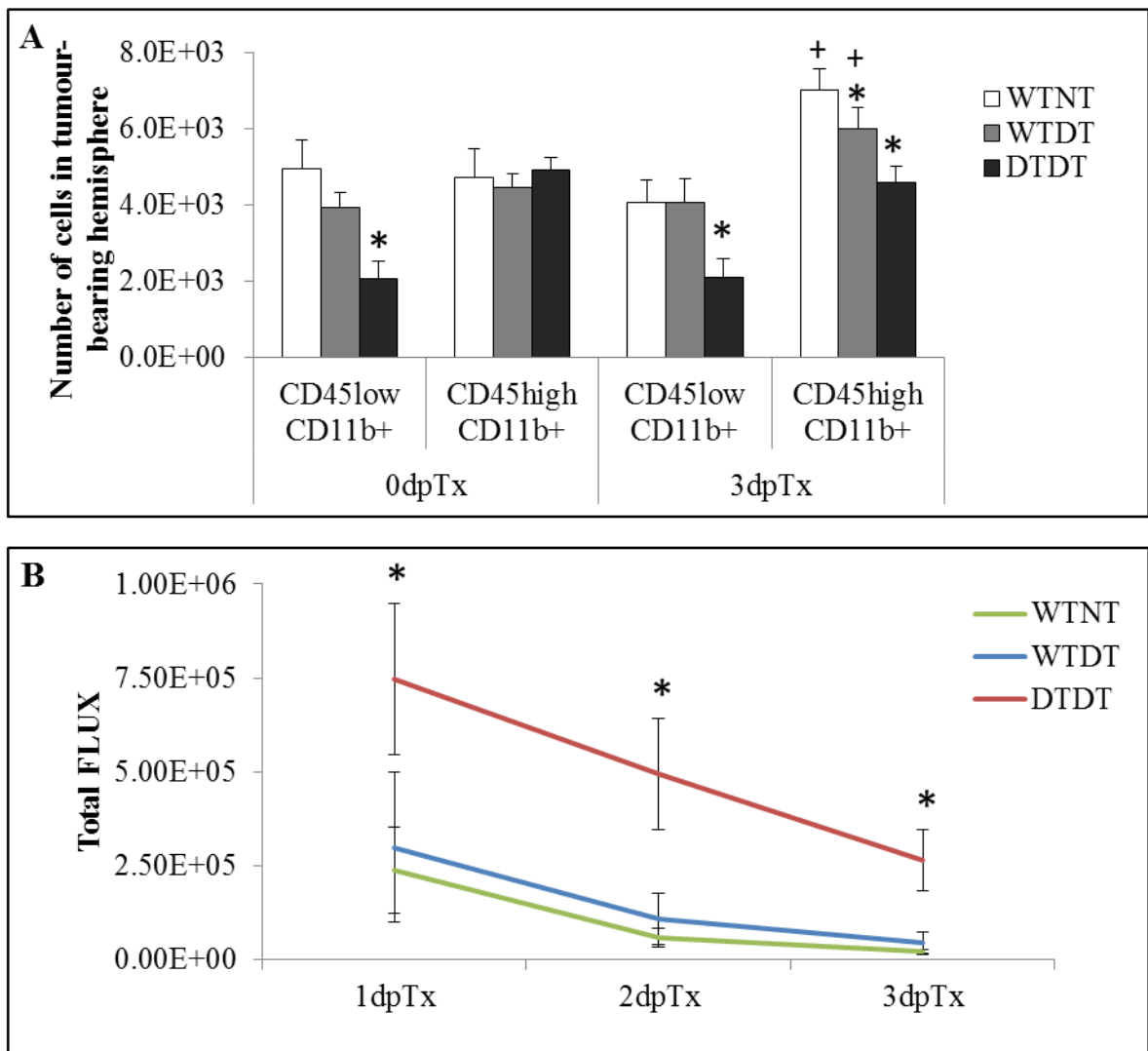


Figure 5.17: *CD11b::DTR mice bearing K1492 gliomas have resident glioma-infiltrating microglia and recruited CD45^{high}CD11b⁺ ablated after diphtheria toxin administration. Loss of these cell types results in significant increase in Myxoma luciferase expression.* Wildtype (WT) or CD11b::DTR (DT) C57Bl/6 mice implanted with K1492 cells were treated at 11, 13, and 15 dpi with 10ng/g diphtheria toxin (DT) or not (NT) and had Myxoma virus administration at 14pdi. Animals were sacrificed and tumour infiltrating immunocytes analyzed by flow cytometry at 17 days-post implantation, 3 days post-treatment with Myxoma virus. **A** - Quantified numbers of microglia (CD45^{low}CD11b⁺) and infiltrating peripheral immunocytes (CD45^{high}CD11b⁺) from the tumour-bearing hemisphere. Error bars represent standard error and asterisks represent significant differences between treatment groups within time point while pluses represent significant differences between time points. (n=6, t-test, p<0.05). **B** – Real-time monitoring of viral infection with luciferase using vMyx-FLuc for the three days following intracranial viral administration. Error bars represent standard error and asterisks represent significant differences (Mann-Whitney, p<0.05; WTNT n=6, WTDT n=5, DTDT n=7).

Considering the role that CCR2-recruited GIMs, and perhaps recruited microglia, play in mediating the initial clearance and possible infection of oncolytic MYXV, it was prudent to check how relevant these cells are outside of our orthograft system. Granted the K1492 cell line has had minimal passages, < 10-15, these have still been passaged in serum and then grafted into the brain of C57Bl/6 mice. To test if the recruitment of these microglia and GIMs were in fact a consequence of tumourogenesis and not cell culture, we looked at NPcis mice bearing spontaneously arising astrocytomas. Specific details about these glioma-bearing NPcis mice can be seen in **Chapter 3**. Two spontaneous astrocytomas, a high grade and mid-high grade astrocytoma, were stained for the microglia/macrophage marker IBA1 (**Figure 5.18**). Although inherently different staining patterns were found, both tumours had marked infiltration of IBA1⁺ cells. The high-grade glioma was intensely infiltrated with highly activated microglia and/or GIMs, while the low-grade had substantial infiltration but seemingly less activated microglia. These results strongly suggest that microglial and GIM recruitment in this model is a consequence of tumourgenesis, just as reported in the literature for human gliomas.

All the work done in this chapter thus far suggests that the ability to pharmacologically inhibit the activation or activity of glioma infiltrating microglia and GIMs could greatly enhance early infection rates in OV therapy in glioma patients. This could be difficult to accomplish, mainly because these cells are already somewhat activated while at the same-time being resident in the glioma, limiting therapeutic delivery. Minocycline tetrachloride is a member of the tetracycline family of antibiotics, but itself has some very interesting properties above and beyond antimicrobial activity.

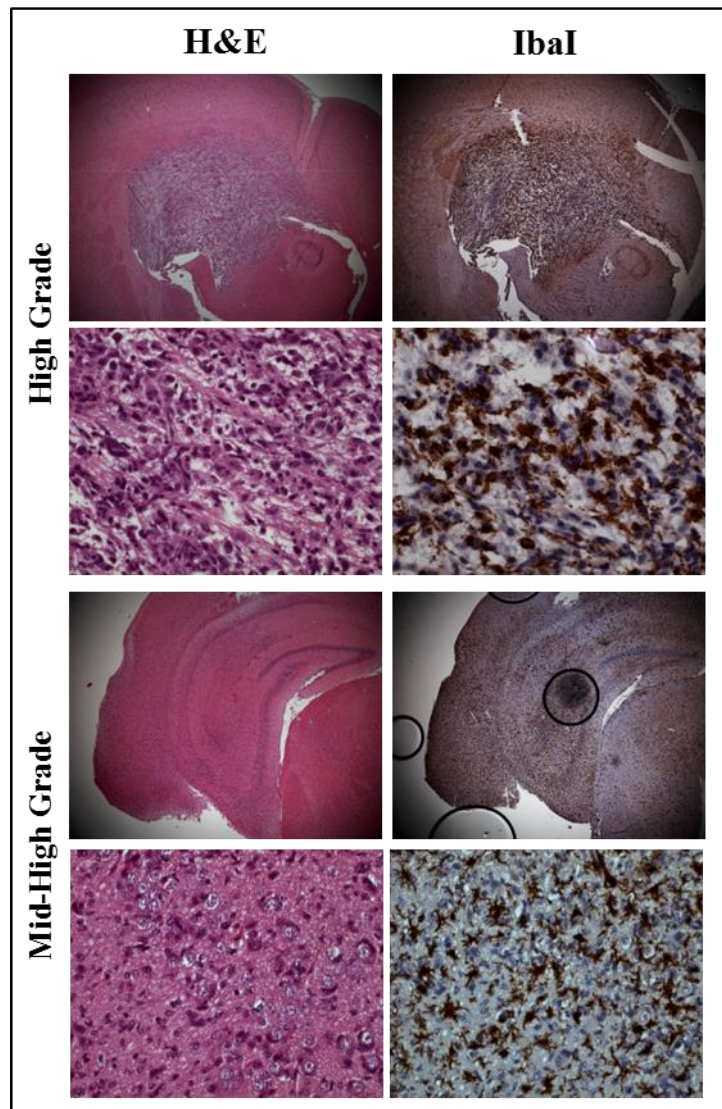


Figure 5.18: *Spontaneous NPcis gliomas in C57Bl/6 mice have microglia and/or monocyte activation and recruitment that may correlate with grade of the tumour.* C57Bl/6 mice heterozygous for Nf1 and Tp53 inactivating mutations spontaneously develop astrocytomas. Two such spontaneous astrocytomas, a high grade (*top*) and low grade (*bottom*) were stained with haematoxylin and eosin (H&E) or with the microglia/macrophage marker IBA1. (Top picture 25X magnification, bottom picture 200X magnification).

Of specific interest are the anti-inflammatory properties, including the inhibition of activity of both microglia and monocytes/macrophages.³⁷⁵⁻³⁷⁹ As such, an experiment administering minocycline to K1492-bearing C57Bl/6 mice in an attempt to inhibit the anti-viral activities of the tumour-resident microglia and GIMs was conducted. The dosing regimen was complicated, as reaching therapeutically relevant doses in mice can be challenging. Animals were started at 50 mg/Kg twice a day starting at 10 dpi for two days (10-11 dpi), then 50 mg/Kg once a day for 5 days (12-16 dpi), and then dropped on a maintenance dose of 25 mg/Kg for 3 days (16-19 dpi). Viral administration was given at 14 dpi. Following real-time viral infection by monitoring luciferase activity from vMyx-FLuc found that minocycline administration resulted in a nearly identical trend to the CCR2^{-/-} mice, with an elevation of viral luciferase at days 1, 2 and 3 dpTx, but catching up to the untreated by 5 dpTx (**Figure 5.19 A**); however, due to the variability in the response, only 2 dpTx was significantly different from the control at >10-fold luminescent intensity (Mann-Whitney, p<0.05). These mice were also monitored for survival, but there was no significant efficacy seen with either minocycline alone or minocycline and MYXV (Vehicle, 24 dpi; minocycline, 26 dpi; MYXV, 25.5 dpi; MYXV + minocycline, 24 dpi; p=0.8630, Mantel-Cox Log Rank; **Figure 5.19 B**). Of note, however, was the toxicity of the minocycline in these mice, perhaps confounding the survival study (lethargic, stopped grooming; *data not shown*). Based on this

preliminary study, further work interrogating minocycline combination therapy with OV6s in glioma is warranted, and should start with confirmation of enhanced viral infection within the glioma.

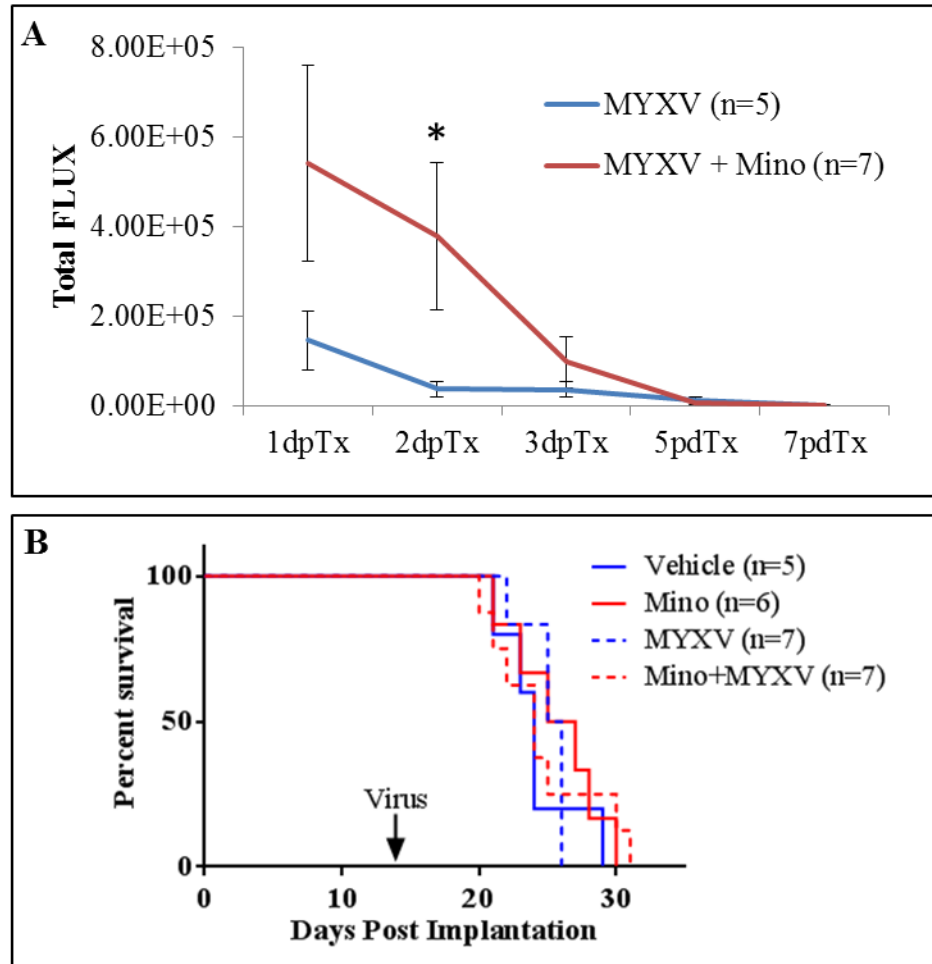


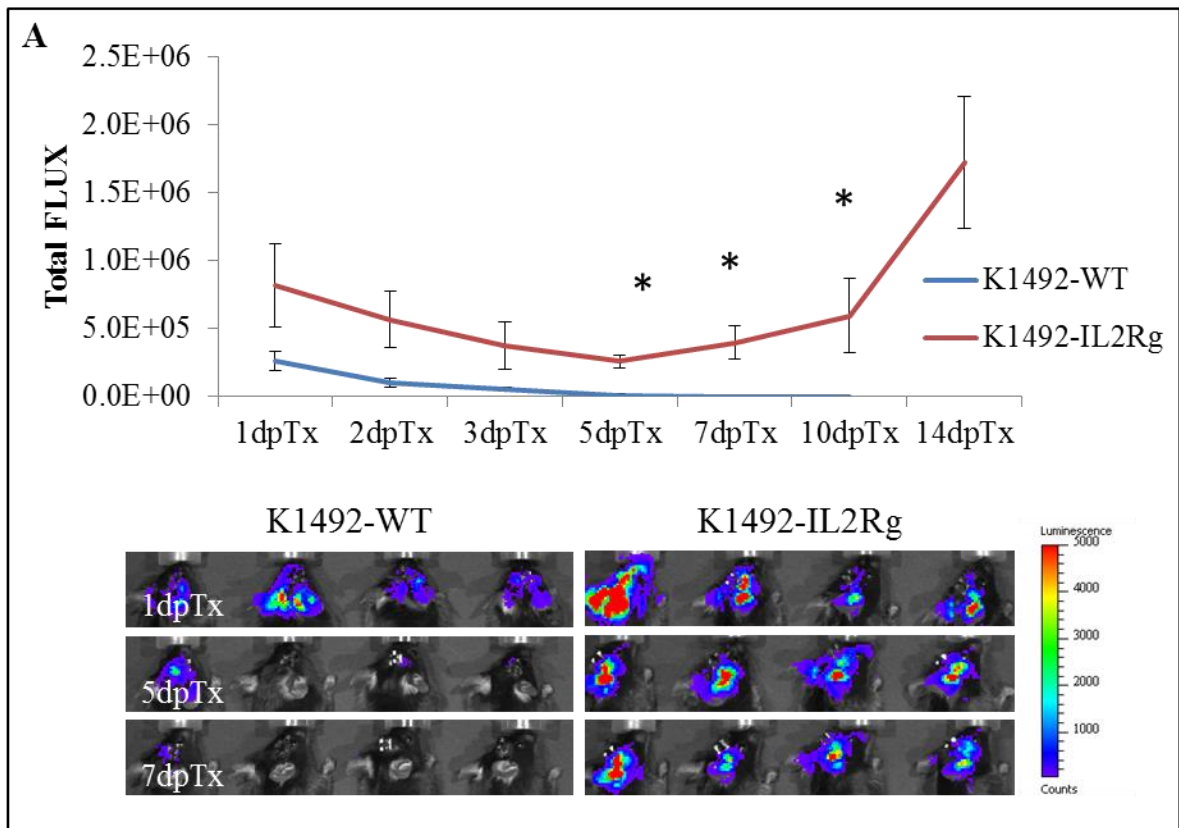
Figure 5.19: Minocycline administration in the K1492 model enhances early Myxoma virus infection but does not result in survival benefit. Wildtype C57Bl/6 mice implanted with K1492 cells were treated with Minocycline (Mino) or 50 mg/Kg twice a day starting at 10-11 dpi, 50 mg/Kg once a day from 12-16 dpi, and then 25 mg/Kg from 17-20 dpi or with DMSO (Vehicle). Viral administration was given at 14 dpi. **A** - Real-time monitoring of viral infection with bioluminescence using vMyx-FLuc. Error bars represent standard error and asterisks represent significant differences (Mann-Whitney, $p < 0.05$; MYXV $n=5$, MYXV+Mino $n=7$). **B** - Survival of animals treated with this regimen (Log-rank, Mantel-Cox, $p=0.8630$).

5.2.3. *The role of NK, NKT and T cells in mediating Myxoma virus treatment failure in the K1492 model*

The above data section demonstrated that inhibiting or ablating the K1492-resident microglial or GIM populations can amplify early infection of MYXV. Nevertheless, all the studies eventually cleared MYXV, returning to untreated/non-transgenic levels by 5-7 dpTx. This suggests that there is an additional cell type recruited to the tumour mediating this clearance and inhibiting viral spread. Looking at the immunophenotyping experiments in the wildtype and $CCR2^{-/-}$ mice demonstrated that the next populations of interest should be the NK, NKT and T cell populations, as these are present at 3 dpTx and present in enhanced numbers in the $CCR2^{-/-}$ mouse that are clearing a larger infection. The NK populations were of particular interest, as they have recently been shown to be important in mediating swift viral clearance from orthoxenograft glioma models treated with oncolytic HSV.^{232,233}

To address this, $IL2R\gamma^{-/-}$ mice were implanted with K1492, treated with MYXV and monitored for viral infection, clearance and treatment benefit. These were excellent mice to start with as these severely immunocompromised mice are devoid of NK cells and have very limited numbers of poorly functioning T- and B- lymphocytes.^{381,382} We used K1492-bearing $IL2R\gamma^{-/-}$ mice treated with vMyx-FLuc at 14 dpi, and followed real-time viral gene expression in these animals. Initial viral luminescence at 1 dpTx, 2 dpTx and 3 dpTx was elevated when compared to the wildtype control (**Figure 5.20 A**), albeit this was variable and non-significant (Mann-Whitney, $p>0.05$). However, this elevated viral luciferase expression persisted through the life of the animals, and increased as the animals began to perish from tumor burden, significantly increasing over control at 5, 7

and 10 dpTx (Mann-Whitney, $p < 0.05$). Intracranial vMyx-FLuc administration in naïve $IL2R\gamma^{-/-}$ displayed a similar phenotype, albeit, as with the $CCR2^{-/-}$ mice, the levels of FLUC were not as elevated as in the tumour-bearing animals (**Figure 5.20 B**), suggesting the additional luminescence was coming from tumoural infection. MYXV treatment in these animals resulted in an increase in survival, with MYXV treated $IL2R\gamma^{-/-}$ mice having a >20% increase in survival over untreated mice (23.5 dpi NoTx vs 28.5 dpi MYXV, $p = 0.0002$, Mantel-Cox Log Rank; **Figure 5.20 C**). Naïve $IL2R\gamma^{-/-}$ mice did not succumb to viral infection (**Figure 5.20 D**).



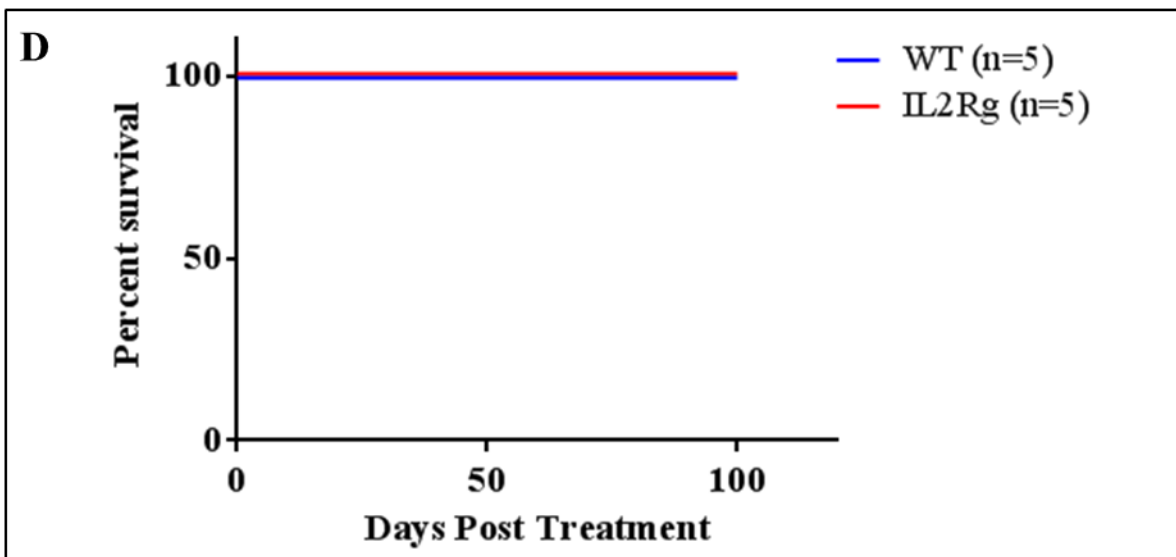
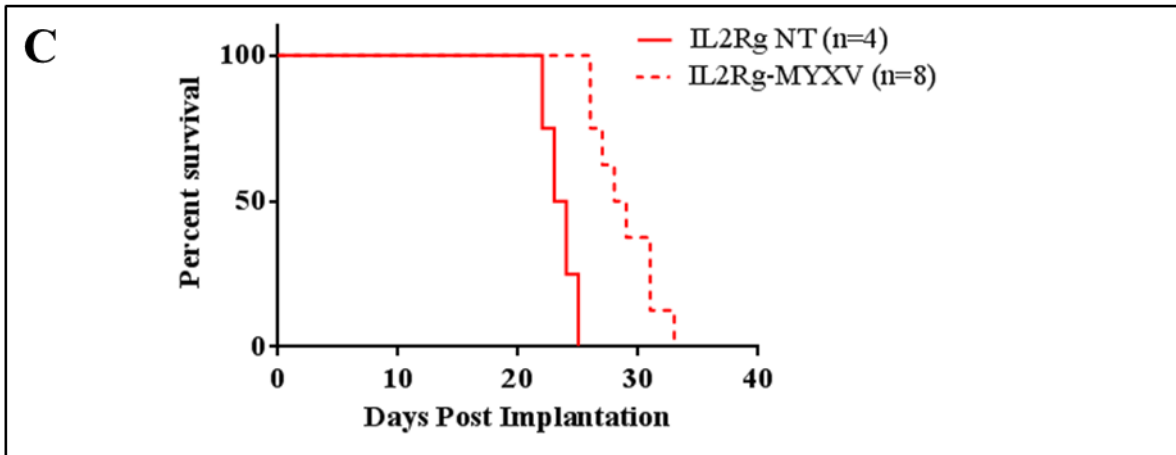
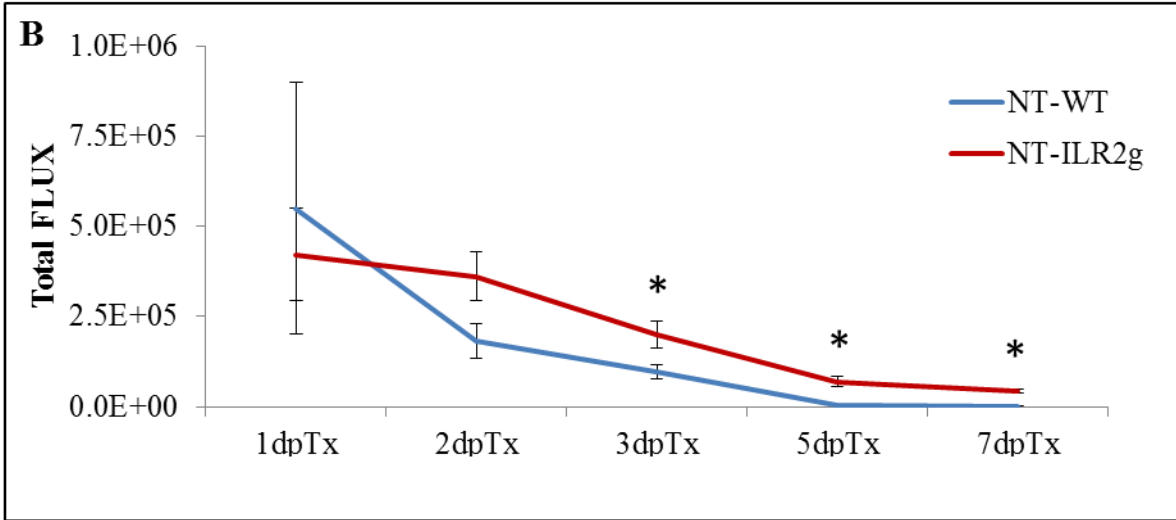
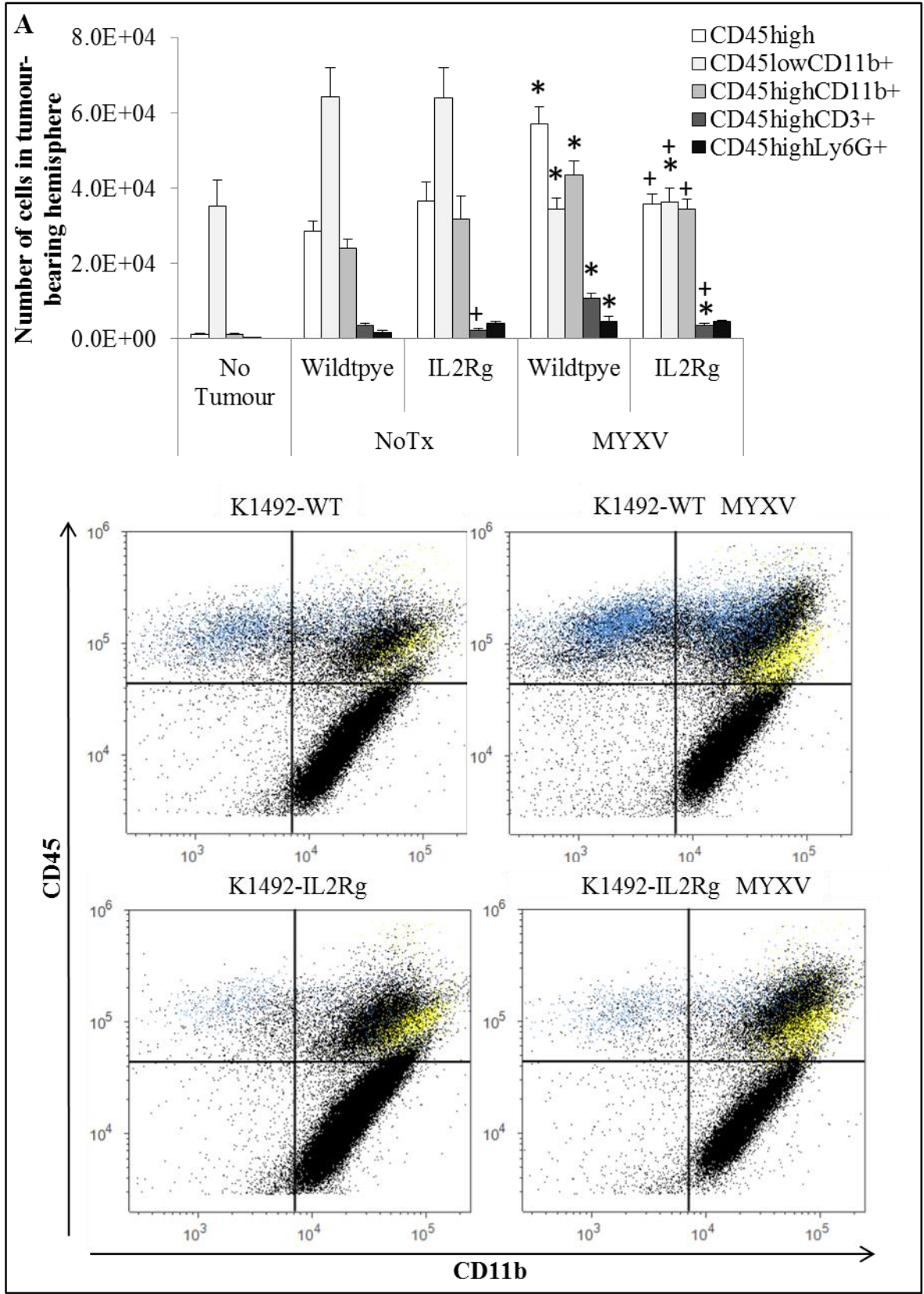


Figure 5.20: *K1492 gliomas implanted in immunodeficient IL2R γ -deficient mice have a persistent tumour infection that results in an increase in survival benefit.* IL2R γ ^{-/-} or wildtype (WT) C57Bl/6 mice implanted with K1492 cells were treated with Myxoma virus on 14 dpi. **A** - Real-time monitoring of viral infection with luciferase using vMyx-FLuc. Error bars represent standard error and asterisks represent significant differences (Mann-Whitney, $p < 0.05$; K1492-WT $n = 9$, K1492-IL2R γ $n = 8$). **B** - A subsequent experiment looking at bioluminescence from non-tumour bearing wildtype (NT-WT) and IL2R γ ^{-/-} animals (NT-IL2R γ) infected with 5.0×10^6 PFUs of vMyx-FLuc. Error bars are standard error and asterisks represent significantly different (NT-WT $n = 5$, NT-CCR2 $n = 5$; Mann-Whitney Test, $p > 0.05$). **C** - Survival of K1492-bearing IL2R γ animals treated with Myxoma at 14 dpi (Log-rank, Mantel-Cox, $p = 0.0002$). **D** - Survival of non-tumour bearing IL2R γ animals treated with Myxoma.

It was exciting to find a persistent viral infection in a syngeneic glioma model, as this was the goal of these studies. To interrogate this further, it was important to try and delineate how the loss of IL2R γ was allowing for this persistent infection. First determined was the cell type composition of these tumours before and after MYXV treatment by flow cytometry, as we had done previously. Interestingly, the untreated K1492 glioma microenvironment did not dramatically change in the IL2R γ ^{-/-} mice, (**Figure 5.21 A**) having comparable levels of microglial proliferation/activation and infiltrating CD45^{high}CD11b⁺ numbers. Only the CD45^{high}CD3⁺ population was significantly lower than wildtype (t-test, $p < 0.05$), but still present, suggesting that the glioma was able to recruit immature T cells. However, MYXV treatment resulted in a dramatic change in immunocyte composition in the glioma at 3dpTx compared to the wildtype. There was a complete lack of CD45^{high} infiltration in these animals. This was expected in terms of the NK and T cells shown to be significant contributors to this number in wildtype mice, but there also was a lack of what appeared to be the recruited peripheral monocyte population (**Figure 5.21 A, bottom**). Further, the CD45^{high}CD11b⁺Ly6g⁺ did not change between the untreated and treated tumours, albeit



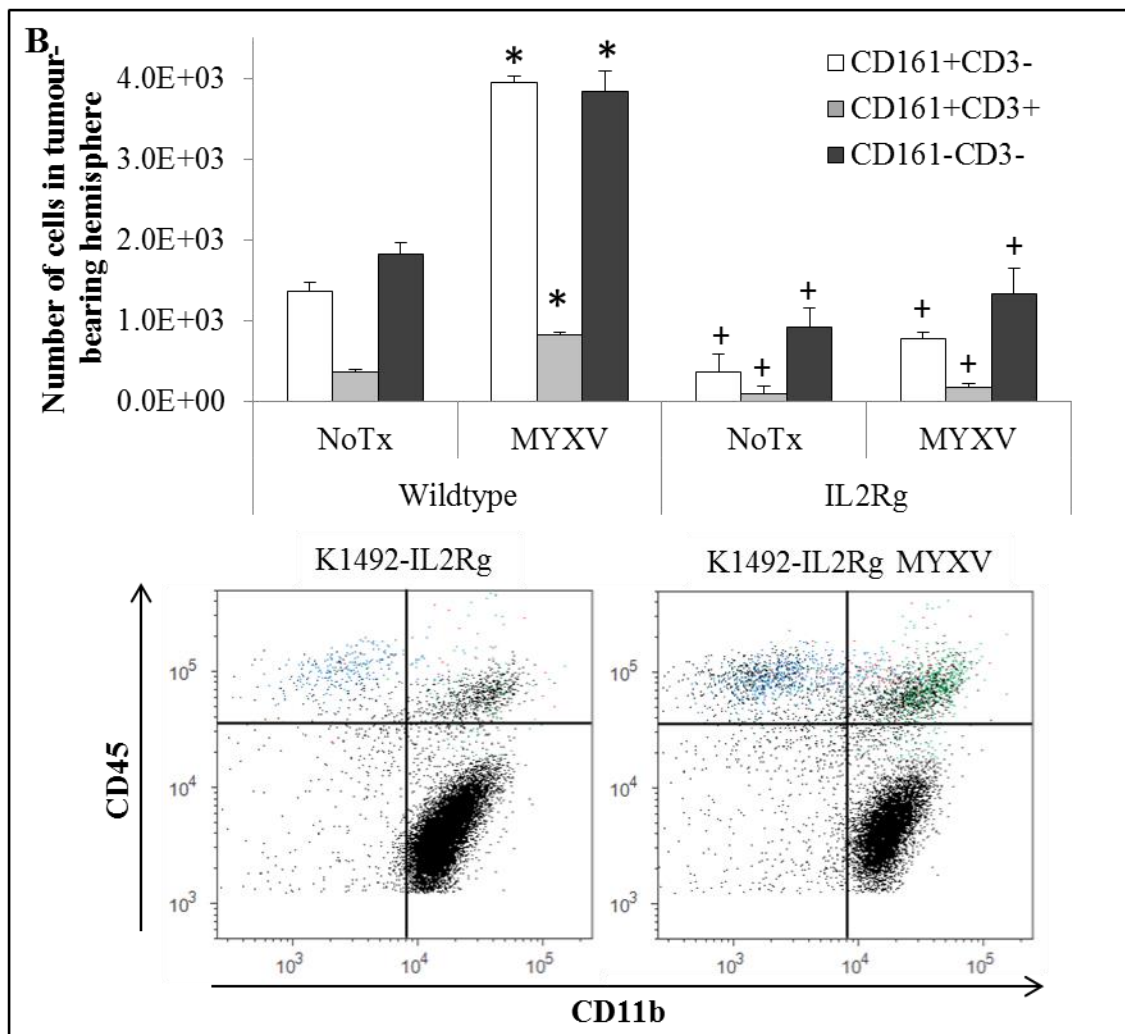


Figure 5.21: Immunophenotyping the K1492 glioma microenvironment in *IL2R γ* -deficient mice shows no recruitment of peripheral immunocytes in response to Myxoma treatment. Wildtype (WT) or *IL2R γ* -deficient (*IL2R γ*) C57Bl/6 mice implanted with K1492 cells and analyzed by flow cytometry at 15 days-post implantation, 3 days post-treatment with Myxoma virus (MYXV) or untreated (NoTx). **A** - Quantified numbers of each cell type isolated from the tumour-bearing hemisphere (*top*) accompanied by the CD45/CD11b scatter plot (*bottom*) highlight the cell populations that also stain for Ly6g (granulocytes, yellow) and CD3 (T cells, blue). Error bars represent standard error and asterisks represent significant differences within mouse strain but between treatment groups. Plus signs represent significant differences between mouse strains within treatment groups (n=6, t-test, p<0.05; CD45^{high}Ly6g⁺ n=3). **B** - Initial live gating around small lymphocyte population followed by interrogation of the CD45^{high} population within this gate. Quantified numbers of each cell type isolated from the tumour-bearing hemisphere (*top*) accompanied by the CD45/CD11b scatter plot (*bottom*) highlight the cell populations that also stain for NK cells (CD161⁺CD3⁻, green), CD161⁻CD3⁺ (T cells, blue), and CD161⁺CD3⁺ (NKT cells, red). Error bars represent standard error and asterisks represent significant differences within mouse strain but between treatment groups. Plus signs represent significant differences between mouse strains within treatment groups (n=3, t-test, p<0.05)

there was a trend to an elevated number of these cells in non-treated tumours. Activation-induced microglial death still occurred in these animals. Of note, there was very minimal, if any CD3⁺ staining in the CD45^{high}CD11b⁺ gate, suggesting that if these cells are indeed staining activated, dividing T cells, this was not occurring in these animals, which one would expect. Notably absent from the CD45CD11b scatter plots was the population of NK cells straddling the CD11b⁺ boundary. This was expected in this strain of mice, and their absence was confirmed experimentally (**Figure 5.21 B**). Examining the ‘small gate’ lymphocytes, there was only a very small background of CD161(NK1.1) staining (**Figure 5.21, bottom**) that did not change in response to MYXV treatment. T cell numbers did not change in response to MYXV. Finally, we confirmed the lack of the NK cell population using a double-staining CD161(NK1.1)/CD49b(DX5; *data not shown*).

Given the severe immunocompromised nature of the IL2R γ ^{-/-} mice, and the many cell types that can be affected through loss of IL-2-family signalling, more specific techniques were employed to try and delineate the cell types responsible for this phenotype. Firstly, the NKT and T populations were targeted using RAG1^{-/-} mice that are completely devoid of any lymphocytes, including all B cell populations, but have fully functional NK cell populations.³⁸³ Flow cytometry of K1492-RAG1 treated and untreated animals showed the complete ablation of the entire CD3⁺ population in tumours (**Figure 5.22 A**). RAG1^{-/-} animals retained their ability to recruit NK cells upon MYXV treatment (**Figure 5.22 B**).

Monitoring real-time viral infection with the vMyx-FLuc virus found viral clearance very slightly delayed in RAG1^{-/-} animals, with a significant increase in virus luciferase at

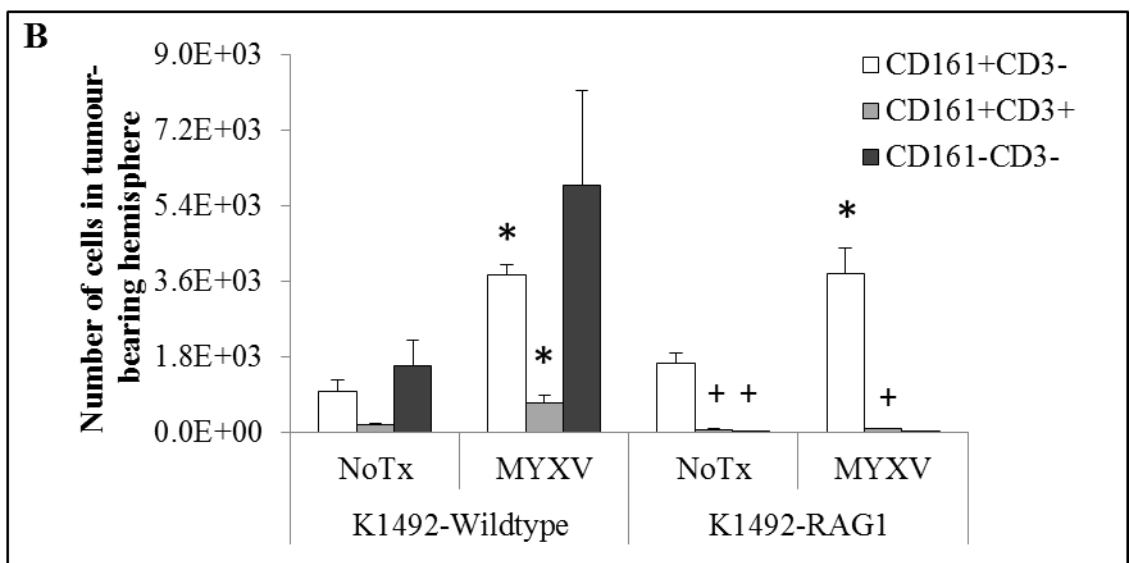
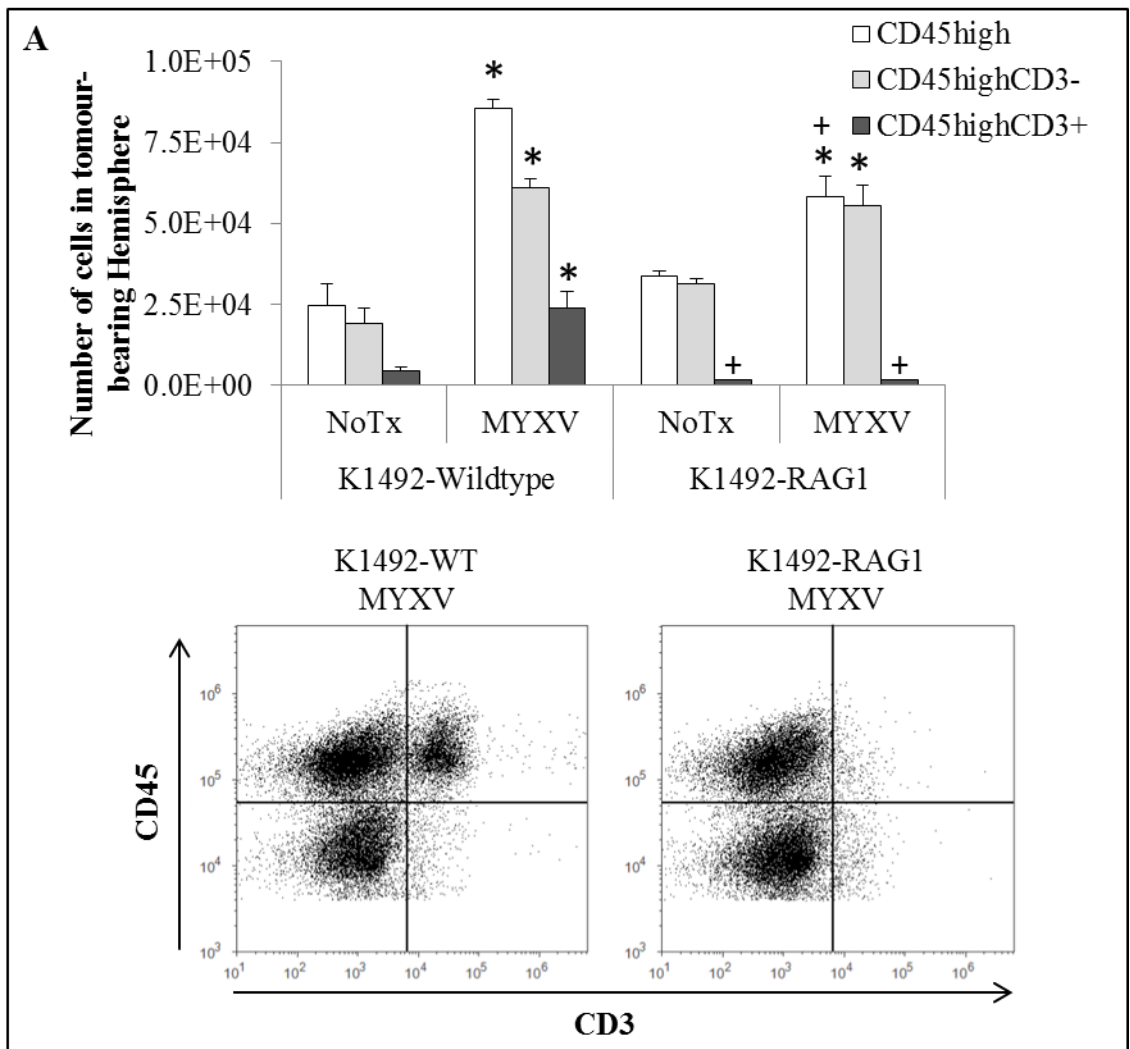
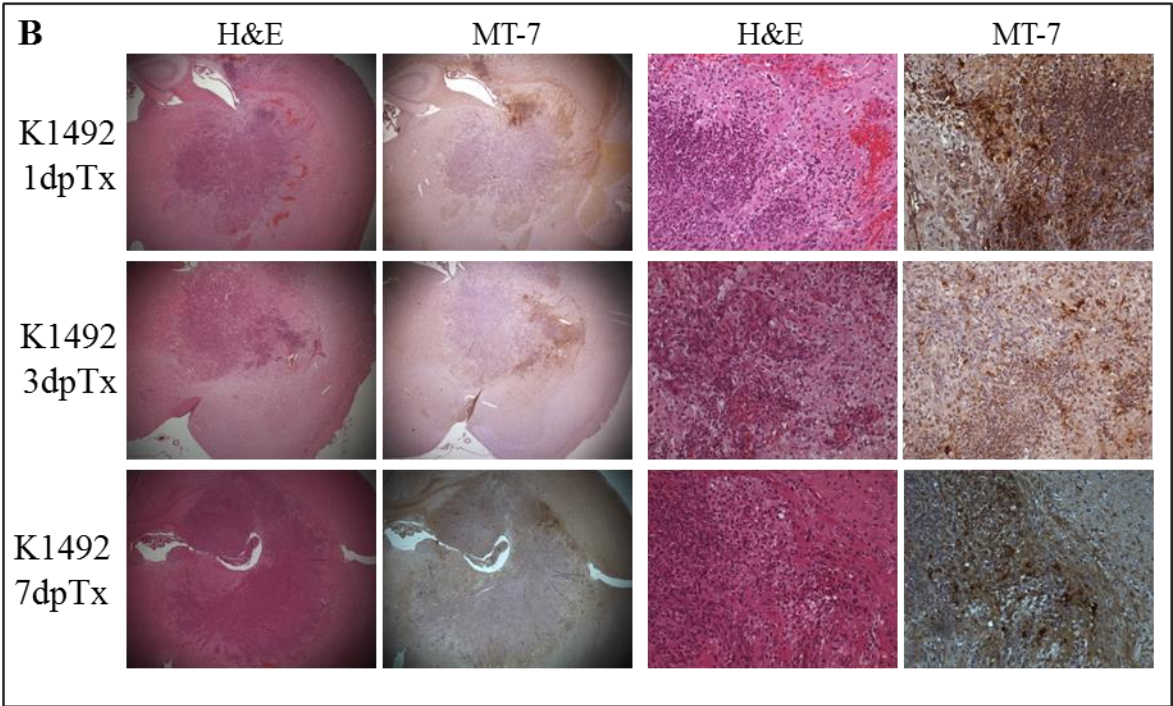
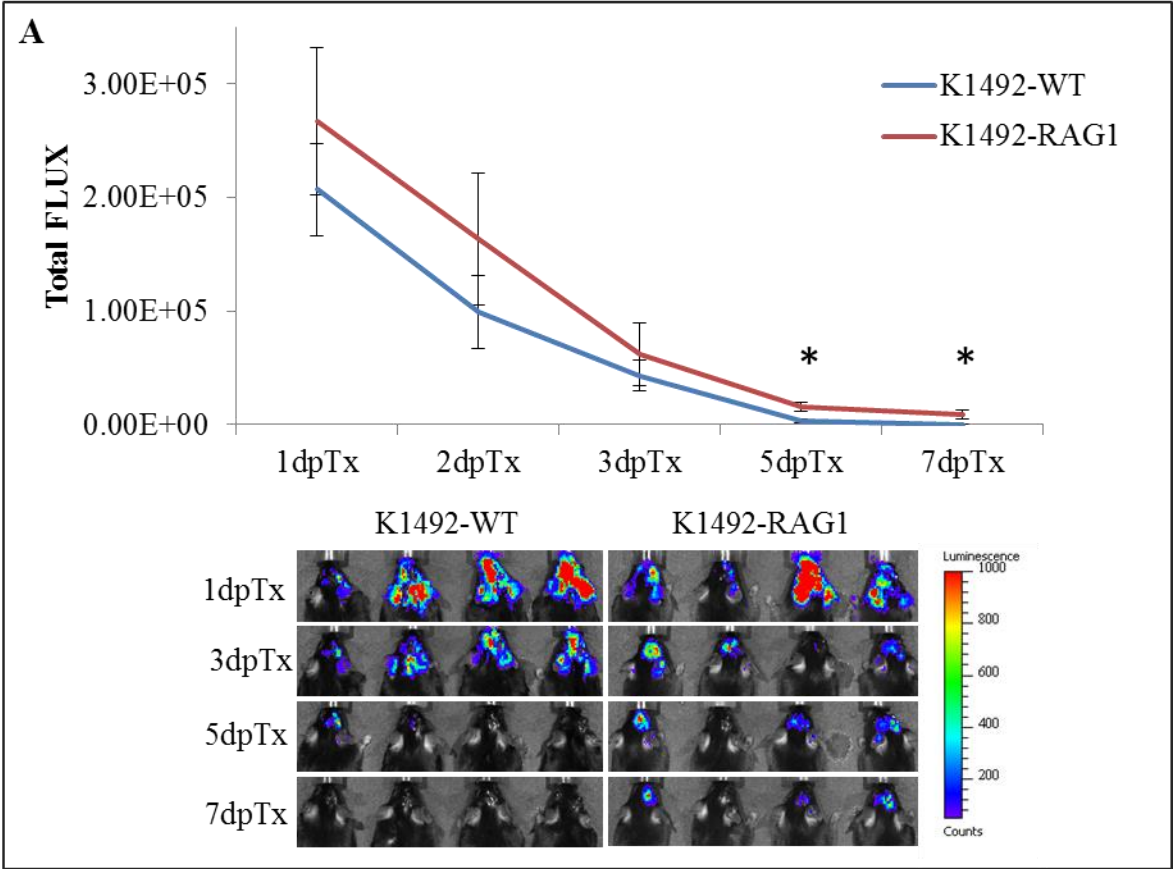


Figure 5.22: *RAG1*-deficient animals are devoid of all CD3 populations in the K1492 microenvironment before or after Myxoma treatment, but the NK cell population remains the same. Wildtype (WT) or *RAG1*-deficient (*RAG1*) C57Bl/6 mice implanted with K1492 cells and analyzed by flow cytometry at 15 days-post implantation, 3 days post-treatment with Myxoma virus (MYXV) or untreated (NoTx). **A** - Quantified numbers of each cell type isolated from the tumour-bearing hemisphere (*top*) accompanied by the CD45/CD3 scatter plot (*bottom*). Error bars represent standard error and asterisks represent significant differences within mouse strain but between treatment groups. Plus signs represent significant differences between mouse strains within treatment groups (n=3, t-test, p<0.05). **B** – Initial live gating around small lymphocyte population followed by interrogation of the CD45^{high} population within this gate. Quantified numbers of each cell type isolated from the tumour-bearing hemisphere of NK cells (CD161⁺CD3⁻), CD161⁻CD3⁺ (T cells), and CD161⁺CD3⁺ (NKT cells). Error bars represent standard error and asterisks represent significant differences within mouse strain but between treatment groups. Plus signs represent significant differences between mouse strains within treatment groups (n=3, t-test, p<0.05).

5 and 7 dpTx (Mann-Whitney, p<0.05; **Figure 5.23 A**). This delay in viral clearance from the tumour was seen at 3 dpTx through immunohistochemistry for MYXV protein MT-7 (**Figure 5.23 B**), where more MT-7 was seen than in wildtype animals (**Figure 5.3**).

Viral protein was also detected at 7 dpTx by IHC, although this seems to be infection of the area surrounding tumour. Interestingly, there seems to be intensely staining cells at 7 dpTx. This small delay in complete clearance was also seen in viral recovery experiments, whereby there was elevated functional virions recovered from the tumour-bearing hemisphere at 3 and 5 dpTx (t-test, p<0.05; **Figure 5.23 C**), but despite viral protein present at 7 dpTx, there was no recovery of functional virions, suggesting that the residual infection seen at 7 dpTx is not replicating. Survival studies with the *RAG1*^{-/-} animals found that despite this small delay in viral clearance, there was no change in treatment efficacy with either single or double (*data not shown*) intracranial viral



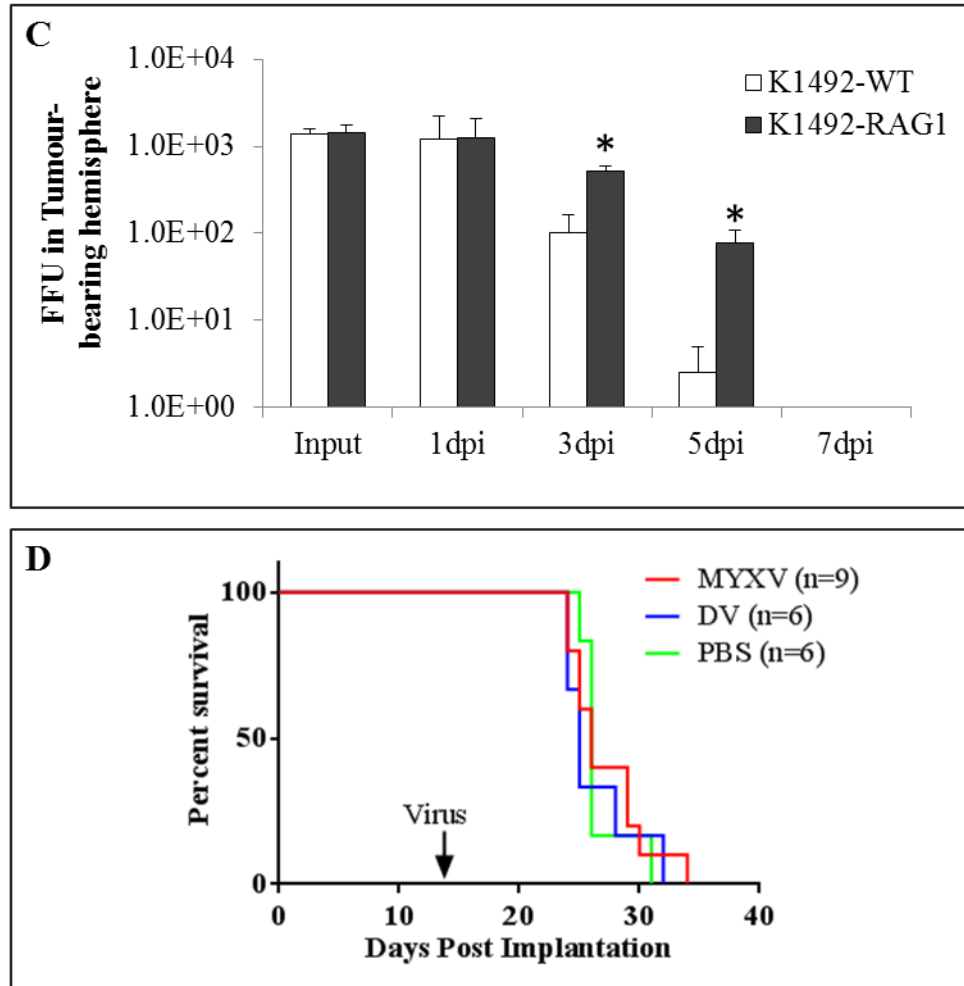


Figure 5.23: *RAG1*-deficient mice have a subtle impediment to viral clearance from the *K1492* glioma but this does not translate to a change in treatment efficacy. *RAG1*-deficient (K1492-RAG1) or wildtype C57Bl/6 (WT-K1492) mice implanted with K1492 cells were treated with Myxoma virus on 14 dpi. **A** - Real-time monitoring of viral infection with luciferase using vMyx-FLuc. Error bars represent standard error and asterisks represent significant differences (Mann-Whitney, $p < 0.05$; K1492-WT and K1492-RAG1, 1 dpTx $n = 19$, 2-3 dpTx $n = 10$, 5-7 dpTx $n = 8$). **B** - Formalin-fixed paraffin embedded sections of *RAG1*-deficient animals bearing K1492 and treated with MYXV were cut and stained with haematoxylin and eosin (H&E) for early viral protein MT-7 (left, 25X magnification, right 200X magnification). **C** - Survival of *RAG1* animals treated with Myxoma (MYXV), UV-inactivated virus (DV) or PBS at 14 dpi (Log-rank, Mantel-Cox, $p = 0.8242$).

injections (26 dpi MYXV vs 25 dpi DV vs 26 dpi PBS; Log-rank Mantel-Cox, $p = 0.8242$; **Figure 5.23 D**).

To be certain that the residual T cells found in the $IL2R\gamma^{-/-}$ mice were not functioning in any way, or that the serum IgM found in $IL2R\gamma^{-/-381}$ and not found in $RAG1^{-/-383}$ was not contributing to this phenotype, a pilot study using double knockout $IL2R\gamma^{-/-}RAG1^{-/-}$ mice was conducted. There was no enhancement of viral luciferase (**Figure 5.24 A**) or survival in these animals over the $IL2R\gamma^{-/-}$ animals (26.5 dpi Wildtype-MYXV, 31 dpi $IL2R\gamma$ -MYXV, 33 dpi $RAG1$ - $IL2R\gamma$ -MYXV. Log-rank Mantel Cox between $IL2R\gamma$ and $RAG1/IL2R\gamma$, $p=0.2069$; **Figure 5.24 B**). The results in the $RAG1^{-/-}$ animals suggested that T and/or NKT cells play a small role in the delayed viral clearance observed in the $IL2R\gamma^{-/-}$ mice, but were not on their own unable to phenocopy the results found in the $IL2R\gamma^{-/-}$ mice.

Next targeted was the NK cell compartment using an ablation study using functional grade anti-CD161(NK1.1) antibodies. A pilot study to test the ability of the antibody to deplete NK cells found that a single intraperitoneal injection of 200 μ g of the CD161(NK1.1) antibody resulted in a $>75\%$ depletion of $CD161(NK1.1)^+$ cells in the spleen (**Figure 5.25 A**). The literature reported that a single injection of 100 μ g could result in ablation greater than 7 days,⁴⁰⁷ but given the inflammation induced by the viral injection, two doses of the CD161(NK1.1) antibody or the isotype control were given at 12 dpi (-2 dpTx) and 15 dpi (1 dpTx) for the subsequent studies. Real-time viral luciferase from the vMyx-FLuc virus was monitored, but no change in viral luciferase was found with the CD161(NK1.1) antibody treatment (**Figure 5.25 B**). Further, this did not result in any change in survival (Log-rank Mantel-Cox, $p=0.6205$; **Figure 5.25 C**).

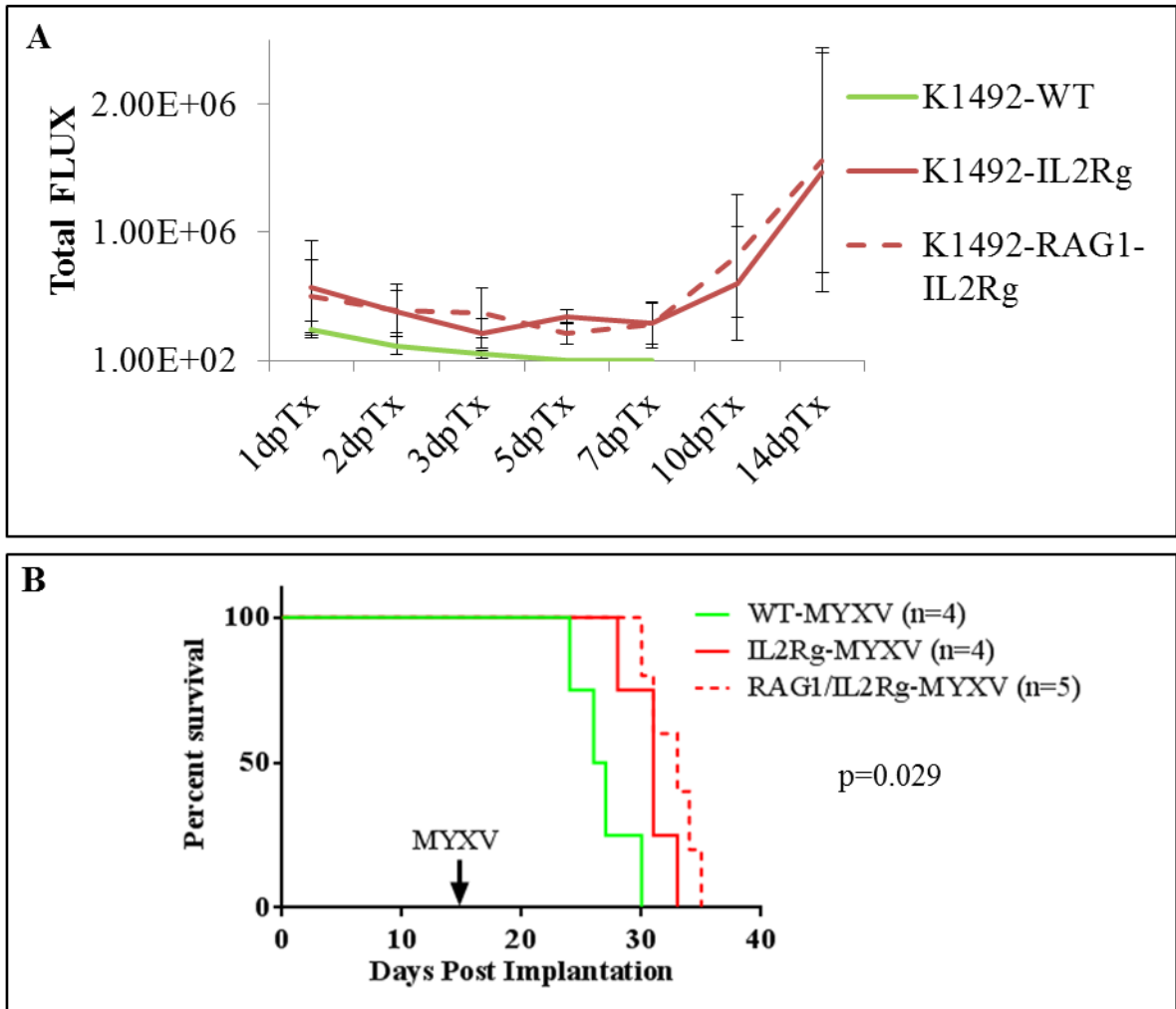


Figure 5.24: *IL2R γ* -deficient and *IL2R γ* -Rag-deficient mice have identical viral clearance kinetics and similar survival benefit in response to Myxoma virus treatment. *IL2R γ* ^{-/-}, *RAG1*^{-/-}/*IL2R γ* ^{-/-}, or wildtype (WT) C57Bl/6 mice implanted with K1492 cells were treated with Myxoma virus on 14 dpi. **A** - Real-time monitoring of viral infection with luciferase using vMyx-FLuc. Error bars represent standard error and asterisks represent significant differences (Mann-Whitney, $p < 0.05$; K1492-WT $n = 4$, K1492-*IL2R γ* $n = 4$, K1492-RAG1-*IL2R γ* $n = 5$). **B** - Survival of *IL2R γ* ^{-/-}, *RAG1*^{-/-}/*IL2R γ* ^{-/-}, or wildtype (WT) C57Bl/6 mice implanted with K1492 and treated with Myxoma virus at 14 dpi (Log-rank Mantel-Cox, $p = 0.029$).

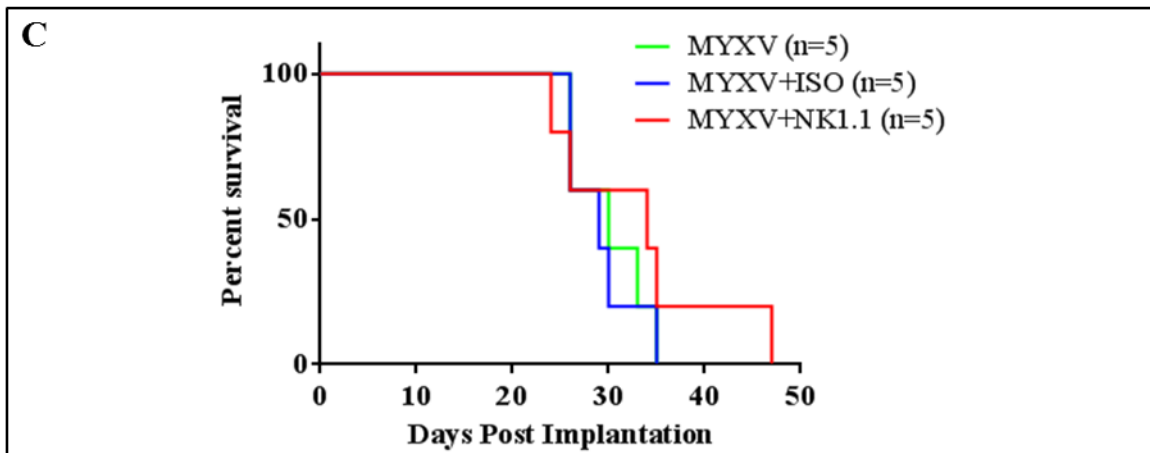
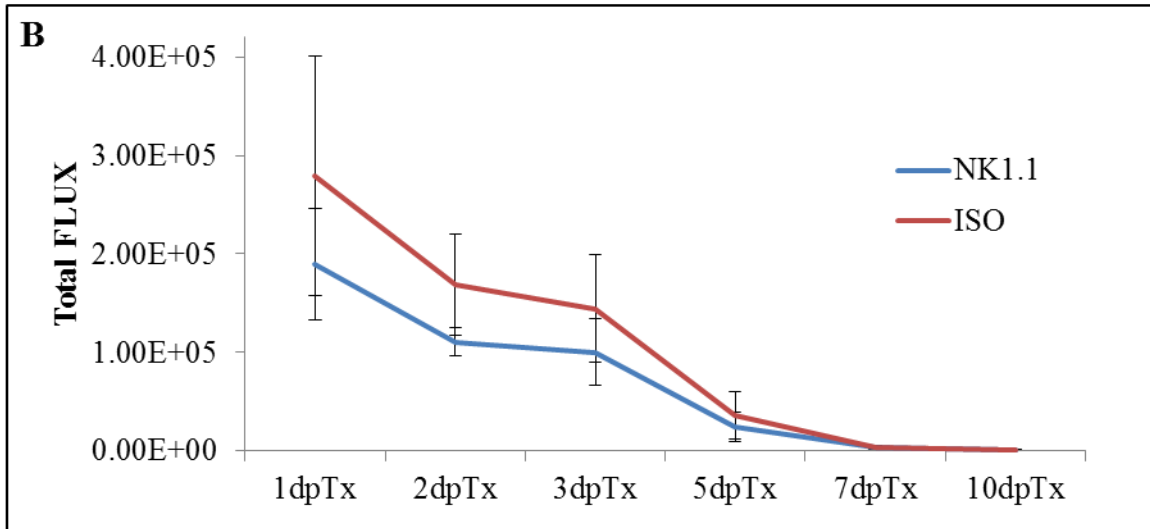
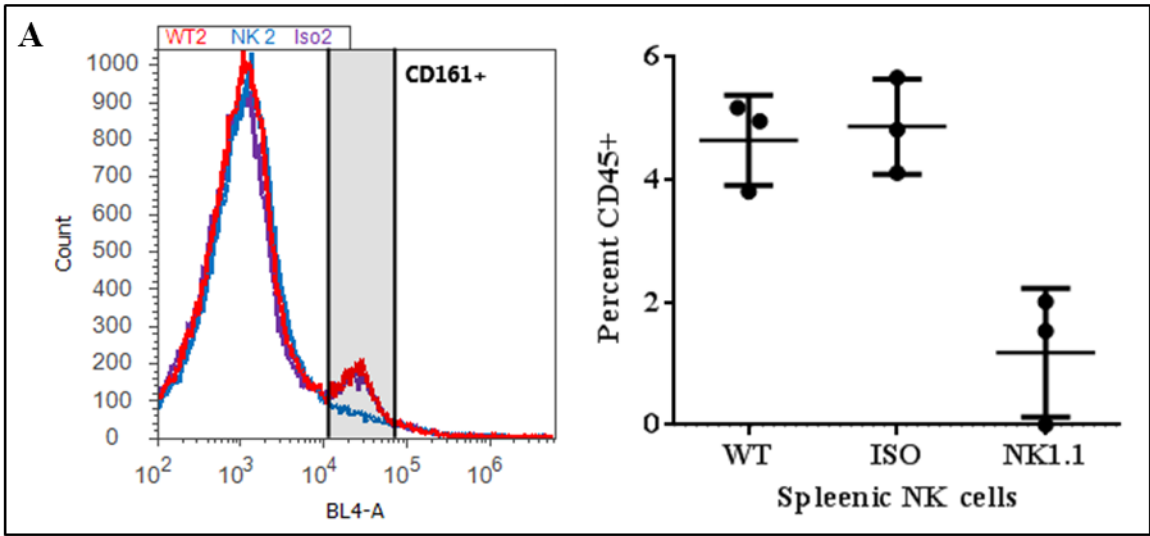
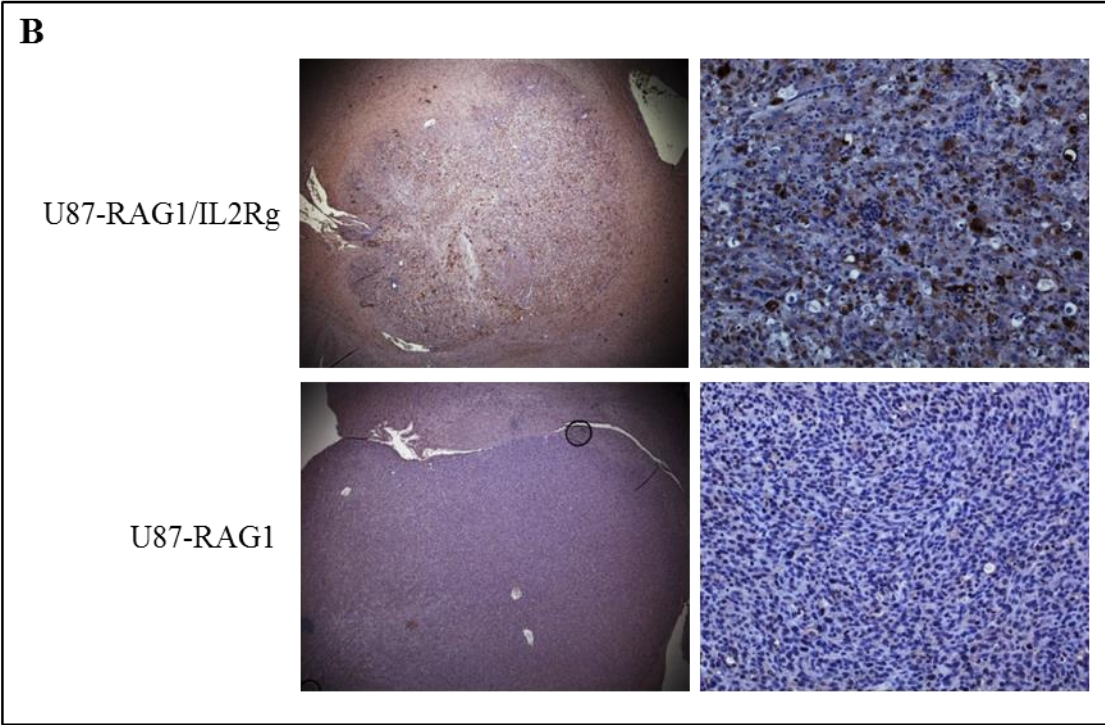
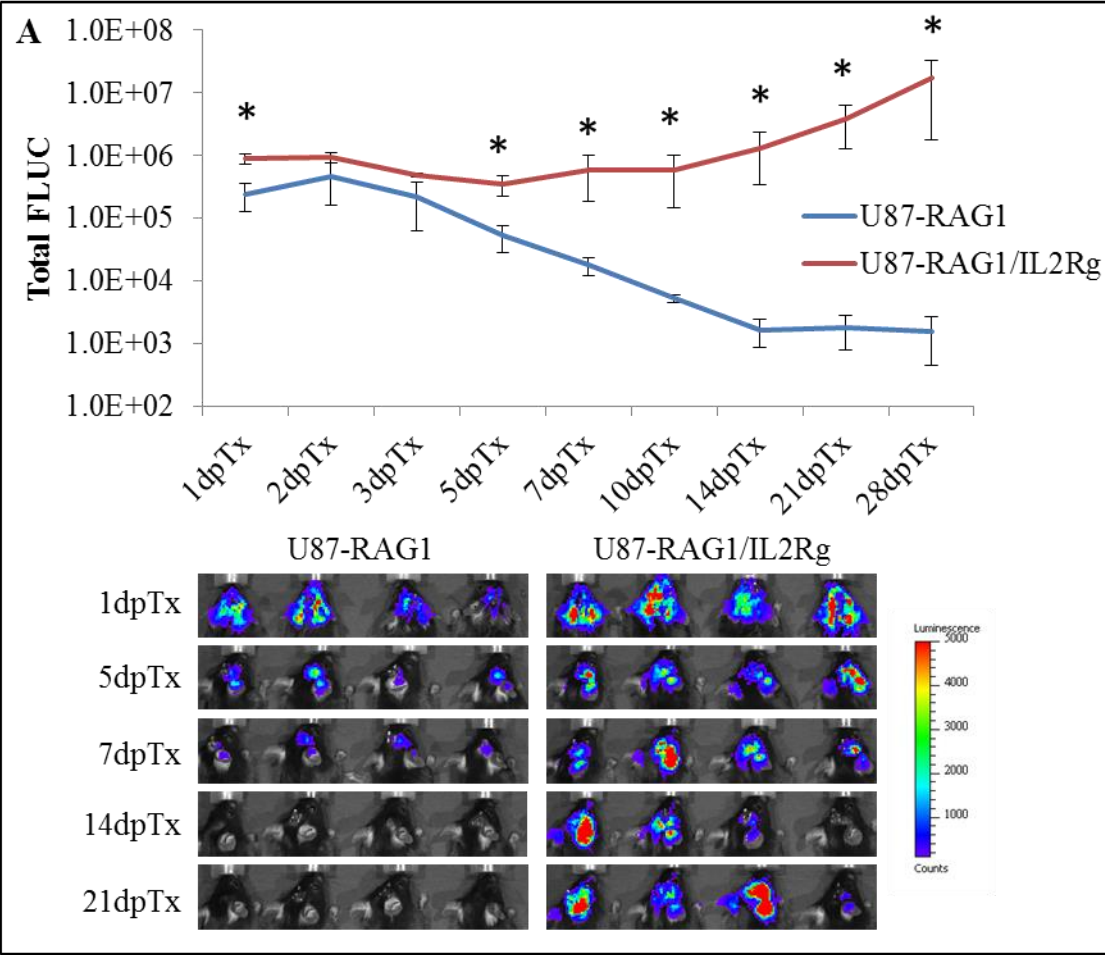


Figure 5.25: Ablation of peripheral NK cells does not change viral luciferase clearance from K1492-bearing CD57Bl/6 mice, nor change treatment efficacy. **A** - Naïve C57B/6 animals treated with a single intraperitoneal injection of a functional grade anti-CD161(NK1.1) antibody, spleens were removed and 1.0×10^6 cells measured by flow cytometry for CD161(NK1.1)⁺ cells. C57Bl/6 mice implanted with K1492 cells were treated with CD161(NK1.1) antibody or Isotype control (Iso) on 12 dpi and 15 dpi (- 2 and 1 dpTx). Myxoma virus administered at 14 dpi. **B** - Real-time monitoring of viral infection with bioluminescence using vMyx-FLuc. Error bars represent standard error and asterisks represent significant differences (Mann-Whitney, $p > 0.05$, NK1.1 $n=5$, Iso $n=5$). **C** - Survival comparison of CD161(NK1.1), Isotope control (Iso) or No treatment animals given vMyx-FLuc at 14 dpi. (Log-rank Mantel-Cox, $p=0.6205$).

The use of RAG1^{-/-} and IL2R γ ^{-/-}/RAG1^{-/-} animals provided a unique opportunity to measure the effect of these knockout animals bearing U87 xenografts, previously shown to be cured with a single injection of MYXV in either nude²⁵³ or SCID animals. Surprisingly, U87 xenografts in RAG1^{-/-} mice had very similar viral clearance kinetics as K1492-RAG1^{-/-} as measured by viral luciferase (**Figure 5.26 A**). Further, U87-IL2R γ ^{-/-}/RAG1^{-/-} had MYXV infection in the tumour that persisted and increased in the animals until they died from tumour burden. Examination by IHC for viral protein MT-7 at death found that only the U87-IL2R γ ^{-/-}/RAG1^{-/-} animals had tumoural infection at death. In fact, nearly the entire tumour was infected with virus (**Figure 5.26 B**). Interestingly, U87-RAG1^{-/-} did not result in statistical treatment efficacy (49 dpi NoTx vs 67 dpi MYXV; Log-rank Mantel-Cox $p=0.2017$; **Figure 5.26 C**). Of note, however, is that the NoTx and MYXV were not done in parallel. The U87-IL2R γ ^{-/-}/RAG1^{-/-} treated with MYXV resulted in >25% significant increase in survival (46.5 dpi NoTx vs 60 dpi MYXV; Log-rank Mantel-Cox $p=0.0169$; **Figure 5.26 D**).



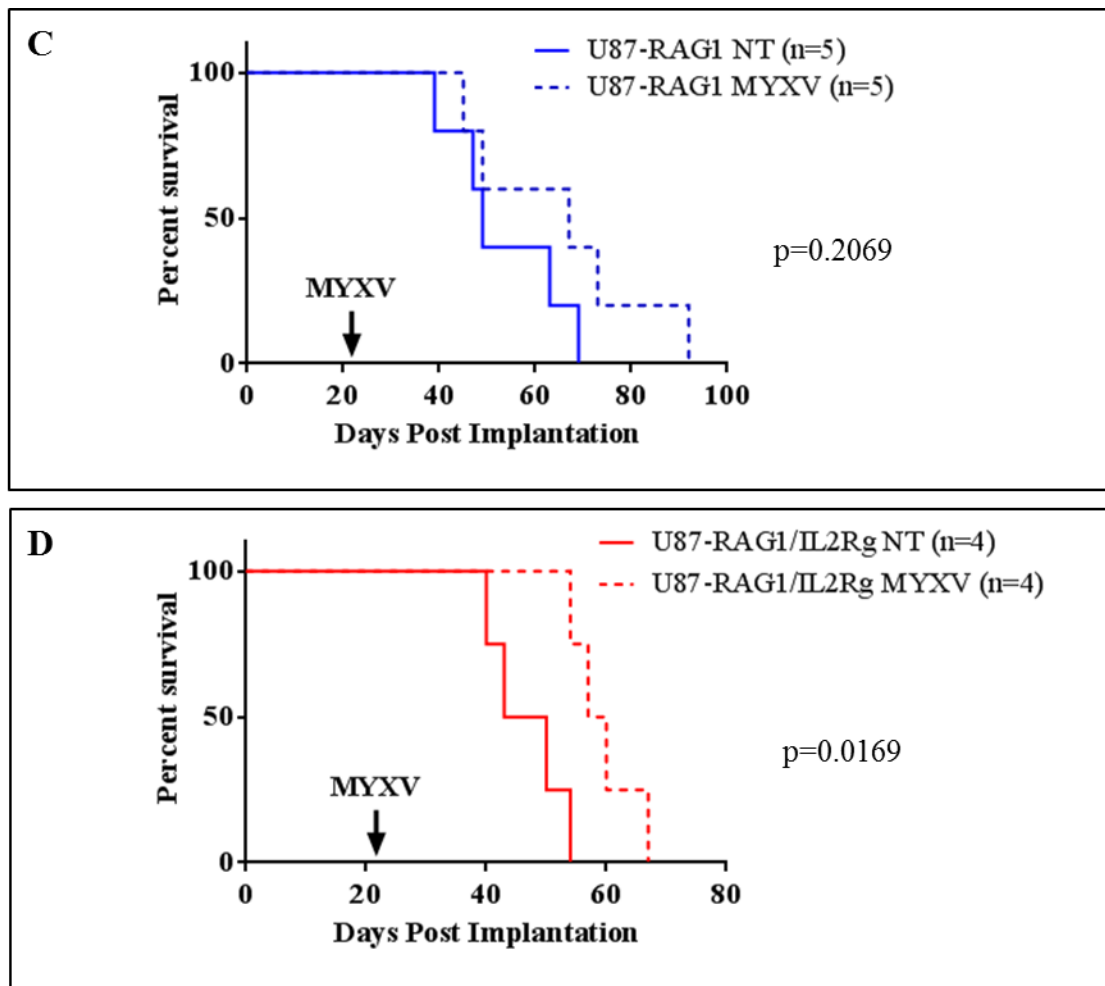


Figure 5.26: U87 orthoxenografts in $Rag1^{-/-}$ or $Rag1/IL2R\gamma^{-/-}$ mice show similar trends of viral clearance kinetics and treatment efficacy in the K1492 model. $Rag1^{-/-}$ or $Rag1/IL2R\gamma^{-/-}$ C57Bl/6 mice implanted with U87 cells were treated with Myxoma virus on 21 dpi. **A** - Real-time monitoring of viral infection with luciferase using vMyx-FLuc. Error bars represent standard error and asterisks represent significant differences (Mann-Whitney, $p < 0.05$; U87-RAG1-IL2R γ $n=4$; U87-RAG1 $n=5$). **B** - U87-RAG1-IL2R γ or U87-RAG1 mice had brains removed after death, formalin fixed, and stained for Myxoma virus protein MT-7 (Left, 25X magnification; Right, 200X magnification) **C/D** - Survival of U87-IL2R $\gamma^{-/-}$ (Log-rank Mantel-Cox, $p=0.2069$) and U87-RAG1 $^{-/-}$ /IL2R γ (Log-rank Mantel-Cox, $p=0.0169$) mice treated with Myxoma virus at 21 dpi on not (NT). Of note, the U87-RAG1 NT and U87-RAG1 MYXV curves were not generated simultaneously, and thus caution must be taken when interpreting these results.

5.3. Discussion

The human glioma microenvironment is complex, with tumour cell interactions with other glia, extracellular matrix proteins, vasculature, and infiltrating immune cells. Although all of these interactions could, and likely do, play some role in determining oncolytic virus therapy efficacy in patients and animal models, the infiltrating immunocyte population is a logical place to investigate mechanisms to improve viral infection, replication and OV-mediated tumour-cell death.

The glioma infiltrating immunocyte population is diverse, including an array of T cells, including T_{regs} ⁴⁰⁸ and $CD8^+$ T cells,^{20,409} NK cells,^{20,410} and neutrophils.⁴¹¹ However, the most numerous infiltrating immune cells in human glioma is microglia and monocytes/macrophages.^{21,22,45} Indeed, there have been reports suggesting these cells can potentially make up to one-third of the tumour mass.⁴⁵ The K1492 syngeneic tumours used in these studies has a similar make-up to what has been reported in human glioma, containing resident T ($CD3^+$), NK ($CD161^+$) and granulocytes ($Ly6C^+$), but it is dominated by infiltrating microglia and recruited peripheral monocytes/macrophages (GIMs). These cells make up >90% of the total immune infiltrate, with GIMs making up 75% of the peripheral $CD45^{\text{high}}$ cells. The multiplex ELISA analysis of the microenvironment has significantly elevated chemokines for each of the major chemokines commonly known to recruit these cells, with NK and T cell potentially recruited through the high levels of CXCL10, granulocytes through CXCL1, MIP2, CCL11, and G-CSF, and monocytes through CCL2. In fact, we confirmed the dependence of GIM infiltration on CCR2, which implicates CCL2 in this process, albeit other CCR2 chemokines were not measured. Microglia have been reported to be recruited

to sites of CNS inflammation through a variety of chemokines depending on the pathology studied, although CCL2 and CX3CL1 appear to be the major chemokines reported in the literature.^{46,61,412} Our studies suggest that the activation and immigration of microglia in the K1492 model is independent of CCR2, suggesting that CCL2 or other CCR2 chemokines are not involved in this process.

What is perplexing is the overrepresentation of neutrophil chemokines expressed in the K1492 microenvironment, albeit many of these were not regulated to the degree seen in CXCL10 and CCR2. Given the granulocyte population is small in the K1492-bearing CNS, this suggests that perhaps these chemokines are playing alternative roles in gliomagenesis, as has been shown for CXCL1³⁹⁴ and G-CSF⁴¹³ having roles in tumour autocrine signalling inducing proliferation and migration.

These studies demonstrated that peripheral monocyte recruitment to the K1492 tumours is dependent on CCR2, perhaps mediated, in part, by growth-factor regulated CCR2 expression by the tumour. Although monocyte recruitment to the CNS through CCR2 has been shown in other CNS pathologies,^{199,200,202,203,372} this is the first time that this has been shown in a mouse model of glioma. It has been established that GIMs play a role in enhancing glioma growth through secreting growth factors⁹¹, pro-invasion matrix-metalloproteases,^{87,89} and pro-angiogenic factors.⁹² This is substantiated by many studies that have correlated increased microglial/GIM infiltration to poor survival in glioma patients;^{69,414} thus, it is surprising that these tumours appeared to develop at the same rate in wildtype mice. Perhaps this is a consequence of deriving these lines in cell culture, whereby these K1492 cells have 'learned' how to live and grow in a contrived environment such that these cells no longer need recruited cells for their sustained growth

in vivo. Alternatively, perhaps the persistence of the activated microglia in the CCR2-deficient mice fulfils this role in these animals. Nevertheless, it would appear that spontaneously arising NPCis tumours are very efficient at recruiting these cell types, with both the high-grade and mid-high-grade tumour displaying an increase in IBA1 staining. Of interest is the difference in staining pattern. IBA1⁺ cells in the high-grade glioma appear amoeboid and highly activated such that we cannot differentiate them as microglia or GIMs through IHC alone. In contrast, the IBA1 staining in the ‘mid-high-grade’ tumour has much less accumulation of the amoeboid IBA1⁺ cells, but substantial infiltration of ‘fuzzy’ microglia, suggesting a state of intermediate microglial activation.⁴⁶ This has been reported in human glioma patients, whereby the level of activation, as judged by the highly activated, amoeboid phenotype increases with glioma grade.^{50,65,66} Speculation into the differences between activation state of these cells in relation to the differing roles they play in gliomagenesis and tumour progression could lead down many paths; however, thinking of the damage and disruption of the high-grade glioma versus the subtle-infiltrating low-grade lesion could play an important part in this activation. The presence of activated microglia in spontaneous models and what has been published in the literature in patients collectively suggests that microglial and GIM infiltration in human patients and the spontaneous model are important players in gliomagenesis, and a possible hurdle in OV therapy for glioma.

A surprising result was the loss of microglia in response to MYXV infection; however, this may be a clue as to how Myxoma clearance is occurring in the K1492-bearing brain. There are several lines of evidence in this chapter that suggests that this loss of microglia is in fact due to microglial cell death, and not a shift of cells from the

CD45^{low/intermediate} to CD45^{high}. Other than the literature suggesting that this rarely occurs,^{46,67} experiments with the CCR2-deficient mice devoid of infiltrating monocytes does not show a shift to CD45^{high}CD11b⁺Ly6g⁻ cells, yet still has comparable levels of microglial activation and subsequent loss of microglia in response to Myxoma treatment. Similarly, there was no difference seen in microglial activation within the tumour or microglial loss after therapy in the clodronate liposome treated mice, which failed to have a significant increase in CD45^{high}CD11b⁺Ly6g⁻. These data strongly suggest that this loss of CD45^{low/intermediate}CD11b⁺ cells is not due to a shift to the CD45^{high}CD11b⁺ population.

Perhaps the most convincing evidence that this loss of the CD45^{low/intermediate}CD11b⁺ population is at least in part caused by death of microglia is the areas of necrosis surrounding the tumours beginning at 3 dpTx., that are especially predominant at 7 dpTx. These areas surrounding the tumour were shown to stain heavily with IBA1 positive cells, and based on the CCR2^{-/-} studies that are devoid of GIMs but retain this staining, are likely composed mostly of microglia. These areas of necrosis also occur in the areas of viral M-T7 staining at 3 dpTx, which seems to be dominant around the periphery of the tumour. This suggests that the mechanisms of viral clearance are destructive and result in large areas of cell death where infected cells are present. This could suggest that microglia are important in immediately scavenging virus or virally-infected tumour cells followed by their targeted cell death by cytotoxic effector cells, an idea supported by the large infiltration of T, NKT, and NK cells entering the tumour at this time. As nicely as this model would fit, experiments with the IL2R γ -deficient mice, which are devoid of functional T cells and NK cells, still exhibit congruent losses of this microglial population and areas of necrosis (*data not shown*). This seems to suggest that this loss is

a consequence of microglial hyperactivation leading to activation-associated cell death,³⁸⁴⁻³⁸⁶ or perhaps simply the death of microglial that are infected with Myxoma without resulting in early gene expression. Without further studies, it is difficult to speculate further on the loss of these microglia.

This poses an interesting question: how is ablation or inactivation of microglia and/or GIMs enhancing preliminary viral infection? In this study, we demonstrate that CCR2-deficient mice are devoid of GIM infiltration yet have unaffected microglial infiltration/activation. Interestingly, as we noted above, it appeared that the GIMs were located within the tumour itself while the activated microglia were seen surrounding the tumour. A very similar scenario was seen in another study monitoring oncolytic HSV in a syngeneic rat glioma model, where peripherally recruited monocytes were found within the tumour while microglia remained surrounding the tumour border.²¹⁹ In this model however, the peripheral monocytes within the tumour are recruited upon oncolytic administration and ablation of these circulating monocytes resulted in increased viral infection in the tumour. In contrast, in our studies, clodronate liposomes did not have a significant effect on viral luminescence, perhaps because the K1492 tumours are already inundated with these GIMs. However, although non-significant, there was a trend to elevated levels of luminescence at 5 days-post infection, but this could be attributed to the loss of peripheral macrophages that assist in NK cell recruitment from the thymus.⁴¹⁵

The authors of the aforementioned study,²¹⁹ and a similar additional study,²¹⁸ suggest that it is the phagocytic activities of microglia and GIMs that are initially mediating increased tumour infection. Indeed, the amoeboid shape of the microglia around the tumour coincides with an activation state that is defined by enhanced abilities

in phagocytosis. This may also be suggested in the rather unimpressive viral recovery experiments, which demonstrated that despite a large tumoural increase in infection, functional replication was not occurring, and in the end the virus is cleared at the same rate as wildtype K1492 tumours. If more tumoural infection was occurring as a result of decreased scavenging by GIMs, this could trigger a stronger recruitment response for the cell types involved in removing infected cells in the CNS. This may be demonstrated by the increased NKT and NK cells infiltrating the tumours in these animals. This scavenging hypothesis is supported by a collaboration looking at systemic Myxoma administration in a liver infection model. In the absence of Kupffer cells, liver resident macrophages, Myxoma was better able to infect hepatocytes, suggesting that these resident macrophages were an active buffer between the virus and the functioning cells of the organ.⁴¹⁶ However, other possibilities remain for explaining this increased infection in the absence of GIMs. This could be a result of immediate production of anti-viral cytokines, or roles these cells may play in recruiting other important immunocytes through chemokine production or even through helping facilitate entry through the blood-brain-barrier. The latter scenario seems less likely as it was found that recruitment of T, NK and NKT cells to these tumours was enhanced in the CCR2-deficient animals. This is important considering these cells have been shown to use CCR2 for trafficking.^{222,417,418}

Of interest, however, is the small elevation of viral luciferase in the non-tumour bearing CCR2-null mice, possibly suggesting that either CCR2 recruitment of peripheral cells are necessary for initial control of viral infection in the non-tumour brain. Alternatively, it could be suggesting that CCR2 is necessary for the proliferation and recruitment of microglia in instance where astrogliosis and/or microgliosis is not already

present in the brain. Future studies will have to delineate exactly how these GIMs are mediating this process, but our current line of reasoning holds that they are acting to immediately scavenge virus in the K1492 microenvironment, preventing tumoural infection.

Minocycline tetrachloride is a member of the tetracycline family of antibiotics, but itself has some very interesting immunosuppressive properties, and are best known for their ability to inhibit the activation of both microglia and monocytes/macrophages.³⁷⁴⁻³⁸⁰ The exact mechanism of activation inhibition in monocytoïd cells is not entirely understood, but studies have shown that minocycline can inhibit iNOS production,³⁷⁵ cytokine/chemokine secretion,^{374,375,378} and MHC-II expression;³⁸⁰ however phagocytosis, at least of amyloid- β plaques, remains unaffected.³⁷³ Although further studies need to be performed to ensure that minocycline administration was indeed enhancing tumoural infection and not just inhibiting viral clearance from the normal brain, the potential of minocycline with OV_s as a combination therapy could be quite fruitful, in addition to the antiglioma effects seen by minocycline itself.^{376,419}

The next cell types looked at were the lymphoid cell types, consisting of the recruited T, NK and NKT populations upon Myxoma administration. The persistent infection in the tumour in the IL2R γ -null animals strongly suggests that these cells play a critical role in mediating viral clearance, as does the peak levels of IFN γ at 3 days post-infection, when viral luciferase is sharply dropping in wildtype K1492-bearing animals. Further, considering the RAG1-deficient animals only had a minor delay in viral clearance, this strongly suggests that the NK cell population is playing a critical role. This

has been shown previously in using oncolytic HSV, whereby immediately recruited NK cells caused ‘premature’ viral clearance from the tumour before significant oncolytic activity could occur.²³³ This clearance was based off of the up-regulation of NK cell activation receptors NKp30 and NKp46 on HSV-infected glioma cells, resulting in a targeted cytotoxic degranulation of NK cells and clearance of the virus and tumour cell. It is very conceivable that a similar situation is occurring in our model, as we have very recently shown that NK cell adjuvant therapy improves MYXV-mediated killing of U87 cells *in vitro* and *in vivo*; however, in our model, this was shown to be mediated through down-regulation of MHC-I by Myxoma virus protein M153.²³⁴ Future studies investigating how NK cells could be mediating swift OV clearance from the brain by looking at NK cell cytotoxicity and the change in activation and inhibition ligands on tumour cells are warranted.

However, NK cells cannot be the sole players responsible for this swift clearance, as depletion of NK cells using the anti-CD161(NK1.1) antibody resulted in no change in viral luciferase or treatment efficacy. This could be due to a number of reasons, the first being technical. It is possible that the ~75% peripheral NK cell depletion achieved was not sufficient to stop all the antiviral activities; however, we employed two doses in our viral infection/replication studies at -2 and +1 days-post treatment, which should deplete all circulating NK cells. Secondly, it is possible that the small population of tumour-resident cells, which may not be targeted by the antibody, could be facilitating this viral clearance. NK cell populations in the tumour before and after CD161(NK1.1) treatment should be conducted in future studies. Most interestingly, however, is the possibility that the T cell populations, resident or recruited, play a role in this early viral clearance.

Perhaps the NK, NKT and T cell populations jointly recruited play overlapping roles in this swift viral clearance, and recruiting one and not the other does not suffice in a measurable change in viral infection or treatment efficacy.

It is interesting to speculate on the nature of the T cells that are being recruited so early after infection, as most studies looking at virus specific T cell responses in the CNS begin sampling 7 days or later post-infection. However, there is literature to support the appearance of T cells in the CNS as early as 3 days post infection.^{388,420,421} Such early recruitment to the virally infected tumour suggests that perhaps these cells are playing an innate immunity role as opposed to a more classical T-cell receptor-mediated adaptive response. $\gamma\delta$ T-cells have been shown to be swiftly recruited to the CNS in response to West Nile virus infection, playing key roles in IFN γ production and antigen-independent cytotoxic activates,^{422,423} as well as playing key roles in protecting mice from HSV-1 viral encephalitis.⁴²⁴ Granted $\gamma\delta$ T-cells would have been ablated in RAG1^{-/-} mice, but these mice still had functional NK cells. Indeed, in the previous studies looking at NK cells in oncolytic HSV efficacy in xenografts, these cells would have not been present allowing NK cell depletion alone to allow for such a robust phenotype.

Perhaps the most surprising result of these studies was to find a completely infected tumour in the brain of a mouse that died from a glioma. The IL2R γ -RAG1 double-null animals bearing U87 tumours had no better increase in percent survival than the IL2R γ -null animals bearing K1492. This was startling for two reasons; first, we have cured U87 tumours before in both CB17-SCID and Nude animals,²⁵³ and only finding an increase in ~25% survival is quite underwhelming. Secondly, the entire premise of increasing achieving maximal viral replication in the tumour to achieve maximum

therapeutic efficacy is abolished. This experiment, at least in U87-IL2R γ /RAG1^{-/-} animals, exquisitely shows that cures through complete tumoural infection and oncolysis alone cannot occur. In fact, it is likely that the NK and, in the instance of the K1492 model, T cell populations are likely key to achieving efficacy in this model. Interestingly, the two previous models we achieved cures in, CB17-SCID and Nude animals, both have functioning NK cell populations.⁴²⁵ It would be interesting to see if NK cell ablation in these animals, or use of several immunocompromised animals such as NOD-SCID animals devoid of all lymphocytes and NK cells, would be able to achieve large infection rates but no cure rates. Conversely, the adoptive transfer of NK cells to IL2R γ -deficient mice with high levels tumoural infection could be a highly efficacious treatment, albeit quite contrived from the clinical scenario. It is important to bear in mind that the RAG1^{-/-} animals bearing U87 orthografts had no significant change in survival, but the experiments comparing the non-treated and treated mice were not run in parallel, making this a difficult comparison. Regardless, there was no cure in these animals, perhaps due to later viral treatment than administered previously²⁵³ or because of fewer virions administered. This is quite logical, in the presence of functioning NK cells, if the tumour was not completely infected either due to size or insufficient dose, NK cells could clear the virus before complete tumoural infection, leaving the remaining uninfected tumour to grow and eventually kill the animal.

Taken together, the results in this chapter show that resistance to Myxoma virus infection and replication in syngeneic animals is a complex and multi-faceted mechanism. However, it was shown that resident, tumour-recruited monocytes, and possibly microglia, play a critical role in mediating the initial infection of Myxoma, while

the data suggest that a combination of both T and NK cell populations mediate clearance from the K1492, and possibly U87, orthograft. Of much interest was the discovery that Myxoma virus alone is not sufficient to produce a robust 'cure' in C57Bl/6 animals, suggesting that for Myxoma virus to act to its full potential in glioma treatment we must take into consideration its value as an immunotherapeutic agent and not exclusively an oncolytic agent.

6. OVERALL IMPACT AND FUTURE DIRECTIONS

My PhD studies were instigated by two fundamental papers from the Forsyth laboratory about MYXV virotherapy for gliomas. Lun et al (2005)²⁵³ demonstrated that Myxoma virus was a very promising therapeutic for glioma therapy, with a single intracranial injection producing a robust tumour infection resulting in durable cures of mice bearing orthotopic xenografts. This was followed by Lun et al (2010),²²⁰ demonstrating that in syngeneic rat models MYXV treatment alone had no benefit with the virus rapidly being cleared from the tumour within 3 – 7 days after implantation. When comparing the results of the two studies to the clinical experience with OVIs, it was apparent that syngeneic models were better able to model the barriers to this therapy. This prompted the following hypothesis:

A fully immunocompetent glioma model will be refractory to oncolytic Myxoma virus therapy due to rapid anti-viral responses that will clear the infection before significant anti-tumour activity will occur. Inhibition of these factors to achieve viral replication and pan-tumoural infection will result in significant therapeutic benefit.

This hypothesis was set out to be tested using a set of specific Aims. Here, each one of these aims and how we met or fell short of these goals will be discussed. Also, future studies and directions will be suggested to carry this work forward.

6.1. AIM I: Characterizing relevant syngeneic glioma models

Here we set out to find and characterize syngeneic glioma lines derived from spontaneous mouse tumours with relevant human glioma genetics. The criteria were that these must be susceptible to MYXV infection and replication *in vitro*. These lines must

closely resemble the features associated with human gliomas when orthotopically implanted in syngeneic mice. Ideally, these mice would be on the C57Bl/6 background.

Thanks to Dr. Karlyne Reilly (NCI Frederick), we obtained a panel of glioma cell lines syngeneic in C57Bl/6 mice. These lines, for the most part, met the criteria laid out in Aim I. These tumours were derived from tumours deficient in *Trp53* and *Nf1*,¹³³ two of the three most mutated or deleted genes in high-grade gliomas.¹¹ Our ‘favorite’ line, K1492, was amongst the most susceptible lines to MYXV replication and viral-mediated cell death we had ever tested. It was a low passage glioma line (passage 6 when we received it) derived from the C57Bl/6 mouse background, and when implanted into C57Bl/6 mice reliably produced aggressive tumours. However, the characterization of these tumours found that they were already different from the original tumours from which they were derived. *In vivo* these tumours had both a glial and sarcomatous components, typical of the glioblastoma multiforme variant termed gliosacroma.

The treatment failure demonstrated in the K1492 cell line *in vivo*, despite the exquisite sensitivity *in vitro*, was exactly what we were hoping for. Having no treatment efficacy with swift viral clearance after infection, we could only (hopefully) improve the therapy.

Here we also attempted to establish syngeneic mouse brain-tumour initiating (mBTIC) cell lines in the C57Bl/6 background for the future preclinical testing of oncolytic Myxoma virus and other glioma therapeutics. These studies were initiated by the observed changes in phenotypes in the NPcis cell lines, presumably through serum culture. Given how it is now generally accepted that glioma neurosphere cultures are

superior to serum-derived cultures,¹⁶² it was a prudent next step to move into mouse BTIC cultures in syngeneic models. Given the growth of these neurospheres cultures, their putative multi-lineage differentiation, expression of neural stem cell markers, and their ability to form infiltrative gliomas in C57Bl/6 mice, we can confidently confirm that we have achieved our goal in this aim; however, future studies confirming the nature of these lines by looking at additional stem cell markers (CD133, CD15, NANOG, MS11, etc), staining differentiated cell types (GFAP, OLIG2, O4, TUJ1, etc), characterizing their receptor statuses *in vitro* and *in vivo*, and official neuropathology reports on both the original tumour and the orthografts are needed.

The resistance to Myxoma virus infection in these lines was a very interesting finding, and we are curious if this extends to other OV's, especially the clinically relevant HSV strains. Further, we would like to extend the findings of making these mBTIC cultures susceptible to MYXV infection after differentiation. Perhaps some media transfer experiments could initiate this or a microarray experiment before and after differentiation after several passages could provide some clues.

One of my 'dreams' for these lines includes a large drug screen of clinically relevant compounds, establishing which drugs can kill these cells *in vitro* (before and after differentiation), and then translating these findings into fully immunocompetent mice. It is easy to suppose that these drugs will function *in vivo* in mice similarly to how they do in patients, with minimal effect. These studies could then be translated into knockout mice deficient in different properties to try and delineate mechanisms for resistance. For example, how does a FJZ0309 respond to drug X in wild-type vs CCR2-deficient that

have an absence of GIMs? Indeed, these are the same kind of studies performed here in our preclinical studies with MYXV.

However, my biggest hope for glioma treatment has been through what is seen in **Figure 5.15**, where these highly infiltrative tumours are so closely associated to either GIMs or activated microglia. If we could make these cells start fighting the tumour like they have the potential to, we may be able to defeat the infiltrative nature of this disease. Perhaps cytokine-armed OV's will make a substantial contribution in this direction.

6.2. AIM II: Interrogating the role of type-I interferon in Myxoma virus treatment failure in syngeneic glioma models

This aim set out to interrogate type-I interferon (**IFN α/β**) responses in syngeneic models with Myxoma virus. It was hypothesized that these cytokines would play a key role in dictating viral infection and replication in syngeneic models. This seemed a very logical hypothesis given the species-specific nature of IFN α/β signalling, its robust anti-viral activity, and the importance of its signalling in CNS viral infections.

In vitro, the requirements for this hypothesis held true. We demonstrated that IFN α/β signalling functioned in an interspecific manner and the NPCis cell lines were exquisitely sensitive to protection from MYXV infection with exogenous IFN α/β . However, *in vivo* we found no robust IFN α/β response, suggesting that perhaps this was not an important cytokine mediating treatment efficacy. To confirm this, we created an IFN insensitive NPCis cell line that ablated tumoural-IFN α/β signalling, and these lines displayed no change in efficacy or viral infection/replication as measured by a viral-mediated FLUC transgene. These results suggested that IFN α/β did not play a role

controlling MYXV clearance from the tumour, nor in overall treatment efficacy. However, of very important note is that perhaps MYXV is being cleared very quickly from the tumour by other means (NK cells for example), and thus a robust IFN α/β response is not needed. Perhaps in the instance where we get more robust tumoural infection through knockout of the innate immune cells mediating the clearance, anti-viral IFN α/β could then become an important cytokine mediating efficacy.

The foray into IFN α/β signalling, however, did uncover a few surprising results. The fact that all the cell lines tested in this thesis could not produce IFN α/β was surprising. Future work interrogating why this is the case is warranted. In retrospect, given that MYXV is a dsDNA virus, perhaps the addition of CpG ODNs (the DNA version of polyI:C and TLR9 agonist) should have been incorporated. A recent paper looking at murine primary plasmacytoid dendritic cells, the principal IFN α/β producers of the periphery, found that MYXV infection induces IFN α/β in these cells through TLR9-MYD88 signalling.³⁶² It is conceivable, but unlikely, that all of the lines tested here were deficient in TLR9 and thus unable to sense MYXV for IFN production. Alternatively, however, RIG-I has been shown to sense MYXV in human monocytes, which we demonstrated was functional in many of our lines.³⁶⁰

It would be very interestingly to analyze how MYXV is being recognized in these human and murine glioma lines. Although not presented here, *in vitro* luminex studies on 3 of the NPcis cell lines demonstrated that these lines respond to MYXV infection with a robust CXCL10 and CXCL1 response. Further, we found that the constitutive expression of CCL2 in NPcis lines was blocked by MYXV infection. Future studies on how MYXV can induce and manipulate these chemokines could have clinical value. For example,

studies from the Chiocca lab demonstrated that *recruited* monocytes play a role in mediating oncolytic HSV infection in their syngeneic rat models.^{218,219} If this was found to be a CCL2-mediated effect, perhaps a transgenic HSV expressing the MYXV protein that can down-regulate CCL2 would achieve greater infection and replication rates in this model.

6.3. AIM III: Immunophenotyping the syngeneic glioma microenvironment before and after Myxoma therapy and identifying potential cellular mediators of treatment resistance

This aim set out to immunophenotype the syngeneic glioma microenvironment to identify candidate immune cell populations that may be mediating premature Myxoma virus clearance from the tumour. We hypothesized that tumour-resident or recruited immunocytes may be involved, and that ablating these cell populations transgenically or pharmacologically could enhance viral infection and replication in the glioma.

As with clinical high-grade gliomas, we found that the K1492 microenvironment is in a highly inflammatory state. In addition to the large infiltration of monocyte/macrophage and the activated microglia that surrounded the tumour, there were also resident populations of T cells and granulocytes. We have already discussed at length the role of macrophages and microglia in the etiology of gliomas. It would be interesting to look at these resident T cell populations, and identify their phenotype and function. As mentioned earlier, T_{regs} have been found in patients.⁴⁰⁸ However, these T cells were absent in the RAG1^{-/-} studies, with no gross changes in tumour development; however, cytotoxic T cells they could potentially regulate would also be absent. These cells would be especially important to identify if this model were to be used for other

immunotherapies such as glioma-vaccines and adoptive T cell therapy, which has been shown to be limited by T_{regs} .⁴²⁶ Also of note were the tumour-resident $CD45^{\text{high}}CD11b^+Ly6G^+$ which we loosely referred to as granulocytes. In tumours, this marker set has been used to identify a group of granulocytic myeloid-derived suppressor cells, which also have roles in mediating T cell suppression.⁴²⁷ Further immunophenotyping experiments in the K1492 microenvironment is warranted.

Further studies immunophenotyping the populations of cell recruited to the tumour after MYXV virus is also warranted. Of most interest to me is the nature of the T cells recruited at 3 days post treatment. Given the nature of the stimulus, it is easy to surmise that these may be cytotoxic killer ($CD8^+$) cells. However, it is difficult to reason that $CD8^+$ cells would be functional so early after infection in a manner that is overlapping with NK cells. It is important to consider that these may be $\gamma\delta$ T cells as they have several functions that make them possible players early in this response. Most importantly, $\gamma\delta$ T cells can target cells in the same manner as NK cells, being able to kill and induce cytotoxicity without the need for specific antigen or priming, possibly even using the using the same activating ligands as NK cells to induce cytotoxicity.^{428,429} One of the first experiments I will be conducting after I submit this thesis is to stain all my slides for $CD8$, $\alpha\beta$ TCR and $\gamma\delta$ TCR.

The other strong suggestion that these $\gamma\delta$ T cells may be involved in this early clearance is the persistent of infection seen in the $IL2R\gamma^{-/}$ gamma mice that is not recapitulated in either the $RAG1^{-/}$ mice or the NK1.1 ablation experiments. Of course it must be conceded that it is possible that the $IL2R\gamma^{-/}$ phenotype may have more wide-reaching immunosuppression beyond low T and B cell numbers/inactivity, and NK and

$\gamma\delta$ T cell absence, but it seems too unlikely for another cell type to play such a profound role in an anti-viral response. In order to assess if the NK cells and T cells recruited to the tumour are in fact playing overlapping roles to swiftly eliminate virally infected cells, the most tell-tale experiment is to do an NK ablation in the RAG1^{-/-} mice. This would eliminate all circulating NK cells in a mouse background devoid of all T (and B) cells. If this does not phenocopy the IL2R γ ^{-/-} phenotype, then there must be some factor responsible. If this is the case, the search almost becomes a needle in a haystack.

Providing the above experiment does suggest that the dual T and NK cell ablation is responsible for the immediate clearance, further experiments examining the nature of how these cells are targeting MYXV infected cells would become important. Assaying the expression and roles of NK activation/suppression ligands in these cells *in vitro* and *in vivo* after MYXV infection would be the next logical step. In fact, we have done these experiments in the U87 and U251 cell lines, demonstrating that NK cells can kill these cells lines after MYXV infection due to the down-regulation of MHCI, a NK inhibitory ligand.²³⁴

Other experiments looking at which chemokine receptors are attracting these cells could also be performed. It has long been an interest of mine to investigate how CXCR3^{-/-} mice would mediate glioma growth and respond to MYXV therapy. Finding such elevated levels in the K1492 microenvironment is especially curious, as CXCL10 recruits Th1-type cells that could be considered ‘anti-tumour.’ It has recently been shown that CXCR3 mice in the GL261 glioma model had decreased NK and NKT cell infiltrate and lower survival, which is logical. However, it was also shown that GL261 and other human cell lines used CXCL10 as a mitogen.⁴³⁰ Given this, the fact that microglia,⁴³¹ T

cells, and NK cells⁴³² can use CXCR3 for recruitment, and that our gliomas express high-levels *in vivo* makes this a ‘receptor of interest.’

Another one of the fundamental questions that remains is – considering we get recruitment of NK and T cell populations to the glioma-bearing brain, why aren’t we getting an anti-tumour activity beyond just viral clearance functions? Is this a consequence of the immunosuppressed nature of gliomas? Indeed, we have alluded to the presence of both T_{regs} and myeloid-derived suppressor cells in these tumours. Future studies using transgenic Myxoma viruses bearing transgenes of NK and T cell activating cytokines such as IL-2, IL-12, IL-15 or perhaps IFN α/β , could function to activate these cells against the tumour once recruited in response to the virus. Studies using oncolytic viruses expressing immunostimulatory molecules in glioma models have already begun in other viruses such as oncolytic HSV expressing IL-12,^{257,433} IL-4,²⁵⁶ or Flt3,²⁵⁸ oncolytic adenovirus expressing both IL-12 and B7.1,⁴³⁴ and oncolytic vaccinia virus expressing GM-CSF.²¹⁷ It will be exciting to see how these oncolytic viruses perform in the clinic. Interestingly, there is already a Myxoma virus construct expressing IL-12.⁴³⁵

The method in which GIMs are mediating enhanced tumoural infection is of great interest. Unfortunately, this could be difficult to tease out. The flow cytometry experiments demonstrated that none of the immunocytes we measured in any of the transgenic animal fluoresced in the FITC channel, which would indicate early viral gene expression through GFP. Therefore, it seems that if these GIMs were phagocytizing the virus, they are not getting infected. Perhaps immunofluorescence assays in tissue sections that would target MYXV coat-proteins could identify virus particles in the phagosomes

of these cells. Alternatively, knockout mice for various scavenging receptors could be employed.

Perhaps most importantly in this section, it seems that the overall hypothesis stated at the beginning may have to be rejected, or at least reformed. Although not in a syngeneic model, it was shown that MYXV treatment of human U87 gliomas in RAG1^{-/-} IL2R γ ^{-/-} mice could infect nearly an entire tumour, yet the mice still succumbed to tumour burden. This data strongly suggests that MYXV alone cannot mediate ‘cures’ in this strain of mice. It will be interesting to see if the IL2R γ ^{-/-} tumours have similar rates of infection. Experiments re-introducing NK cells (or maybe even $\gamma\delta$ Tcells) in both the K1492 and U87 models in these mice after allowing for significant MYXV infection could prove to have great therapeutic benefit; albeit, it is difficult to envision how this could be mimicked clinically.

In sum, the objectives of this Aim were largely met. We found that, as in the clinical scenario, the K1492 glioma is highly inundated with microglia and GIMs. We made the novel discovery that that glioma-resident monocytes/macrophages, and perhaps microglia, are responsible for limiting the initial infection of the K1492 tumours with MYXV. This may be able to be phenocopied using minocycline, although these experiments need to be expanded. We also found that we can achieve sustainable tumour infection using IL2R γ ^{-/-} mice, but neither T cell nor NK cell ablation alone could achieve the same result. Although a few key experiments remain, we consider this aim a resounding success!

6.4. Overall thoughts and conclusions

I will not reiterate myself here, this work represents more than just the past 4 years of my life and some scientific mechanisms suggesting potential barriers to MYXV therapy. It represents the transformation I have taken from the naïve plant-science MSc grad that thought doing cancer research involved squirting drugs on a dish of cells, to a PhD candidate that can contemplate the real nature of cancer, how to model it, and how to make the work we do in the lab as clinically relevant as possible.

References

- 1 Canadian Cancer Statistics 2013. Toronto, ON: Canadian Cancer Society. <http://www.cancer.ca/~media/cancer.ca/CW/cancer%20information/cancer%20101/Canadian%20cancer%20statistics/canadian-cancer-statistics-2013-EN.pdf>. Accessed May 8th, 2013.
- 2 Cancer Facts and Figures 2013. Atlanta, GA: American Cancer Society. <http://www.cancer.org/acs/groups/content/@epidemiologysurveillance/documents/document/acspc-036845.pdf>. Accessed May 8th, 2013. (2013).
- 3 Wen, P. Y. & Kesari, S. Malignant gliomas in adults. *The New England journal of medicine* **359**, 492-507, doi:10.1056/NEJMra0708126 (2008).
- 4 Chen, J., McKay, R. M. & Parada, L. F. Malignant glioma: lessons from genomics, mouse models, and stem cells. *Cell* **149**, 36-47, doi:10.1016/j.cell.2012.03.009 (2012).
- 5 Stupp, R. *et al.* Radiotherapy plus concomitant and adjuvant temozolomide for glioblastoma. *The New England journal of medicine* **352**, 987-996, doi:10.1056/NEJMoa043330 (2005).
- 6 Oertel, J., von Buttlar, E., Schroeder, H. W. & Gaab, M. R. Prognosis of gliomas in the 1970s and today. *Neurosurgical focus* **18**, e12 (2005).
- 7 DeAngelis, L. M. Anaplastic glioma: how to prognosticate outcome and choose a treatment strategy. [corrected]. *Journal of clinical oncology : official journal of the American Society of Clinical Oncology* **27**, 5861-5862, doi:10.1200/JCO.2009.24.5985 (2009).
- 8 *World Health Organization Classification of Tumours. Pathology and genetics of tumours of the nervous system.*, (IARC Press, 2000).
- 9 Dunn, G. P. *et al.* Emerging insights into the molecular and cellular basis of glioblastoma. *Genes & development* **26**, 756-784, doi:10.1101/gad.187922.112 (2012).
- 10 Cantin, E., Tanamachi, B. & Openshaw, H. Role for gamma interferon in control of herpes simplex virus type 1 reactivation. *Journal of virology* **73**, 3418-3423 (1999).
- 11 Cancer Genome Atlas Research, N. Comprehensive genomic characterization defines human glioblastoma genes and core pathways. *Nature* **455**, 1061-1068, doi:10.1038/nature07385 (2008).
- 12 Verhaak, R. G. *et al.* Integrated genomic analysis identifies clinically relevant subtypes of glioblastoma characterized by abnormalities in PDGFRA, IDH1, EGFR, and NF1. *Cancer cell* **17**, 98-110, doi:10.1016/j.ccr.2009.12.020 (2010).
- 13 Phillips, H. S. *et al.* Molecular subclasses of high-grade glioma predict prognosis, delineate a pattern of disease progression, and resemble stages in neurogenesis. *Cancer cell* **9**, 157-173, doi:10.1016/j.ccr.2006.02.019 (2006).
- 14 Sottoriva, A. *et al.* Intratumor heterogeneity in human glioblastoma reflects cancer evolutionary dynamics. *Proceedings of the National Academy of Sciences of the United States of America* **110**, 4009-4014, doi:10.1073/pnas.1219747110 (2013).

- 15 Szerlip, N. J. *et al.* Intratumoral heterogeneity of receptor tyrosine kinases EGFR and PDGFRA amplification in glioblastoma defines subpopulations with distinct growth factor response. *Proceedings of the National Academy of Sciences of the United States of America* **109**, 3041-3046, doi:10.1073/pnas.1114033109 (2012).
- 16 Hardee, M. E. & Zagzag, D. Mechanisms of glioma-associated neovascularization. *The American journal of pathology* **181**, 1126-1141, doi:10.1016/j.ajpath.2012.06.030 (2012).
- 17 Fischer, I., Gagner, J. P., Law, M., Newcomb, E. W. & Zagzag, D. Angiogenesis in gliomas: biology and molecular pathophysiology. *Brain pathology* **15**, 297-310 (2005).
- 18 Yasuda, K., Alderson, T., Phillips, J. & Sikora, K. Detection of lymphocytes in malignant gliomas by monoclonal antibodies. *Journal of neurology, neurosurgery, and psychiatry* **46**, 734-737 (1983).
- 19 Hitchcock, E. R. & Morris, C. S. Mononuclear cell infiltration in central portions of human astrocytomas. *Journal of neurosurgery* **68**, 432-437, doi:10.3171/jns.1988.68.3.0432 (1988).
- 20 Farmer, J. P. *et al.* Characterization of lymphoid cells isolated from human gliomas. *Journal of neurosurgery* **71**, 528-533, doi:10.3171/jns.1989.71.4.0528 (1989).
- 21 Hussain, S. F. *et al.* The role of human glioma-infiltrating microglia/macrophages in mediating antitumor immune responses. *Neuro-oncology* **8**, 261-279, doi:10.1215/15228517-2006-008 (2006).
- 22 Parney, I. F., Waldron, J. S. & Parsa, A. T. Flow cytometry and in vitro analysis of human glioma-associated macrophages. Laboratory investigation. *Journal of neurosurgery* **110**, 572-582, doi:10.3171/2008.7.JNS08475 (2009).
- 23 Liu, G. *et al.* HER-2, gp100, and MAGE-1 are expressed in human glioblastoma and recognized by cytotoxic T cells. *Cancer research* **64**, 4980-4986, doi:10.1158/0008-5472.CAN-03-3504 (2004).
- 24 Zhang, J. G. *et al.* Antigenic profiling of glioma cells to generate allogeneic vaccines or dendritic cell-based therapeutics. *Clinical cancer research : an official journal of the American Association for Cancer Research* **13**, 566-575, doi:10.1158/1078-0432.CCR-06-1576 (2007).
- 25 Hanahan, D. & Weinberg, R. A. Hallmarks of cancer: the next generation. *Cell* **144**, 646-674, doi:10.1016/j.cell.2011.02.013 (2011).
- 26 Facoetti, A. *et al.* Human leukocyte antigen and antigen processing machinery component defects in astrocytic tumors. *Clinical cancer research : an official journal of the American Association for Cancer Research* **11**, 8304-8311, doi:10.1158/1078-0432.CCR-04-2588 (2005).
- 27 Wiendl, H. *et al.* A functional role of HLA-G expression in human gliomas: an alternative strategy of immune escape. *Journal of immunology* **168**, 4772-4780 (2002).
- 28 Wastowski, I. J. *et al.* Human leukocyte antigen-G is frequently expressed in glioblastoma and may be induced in vitro by combined 5-aza-2'-deoxycytidine and interferon-gamma treatments: results from a multicentric study. *The American journal of pathology* **182**, 540-552, doi:10.1016/j.ajpath.2012.10.021 (2013).

- 29 Wolpert, F. *et al.* HLA-E contributes to an immune-inhibitory phenotype of glioblastoma stem-like cells. *Journal of neuroimmunology* **250**, 27-34, doi:10.1016/j.jneuroim.2012.05.010 (2012).
- 30 Kren, L. *et al.* Expression of immune-modulatory molecules HLA-G and HLA-E by tumor cells in glioblastomas: an unexpected prognostic significance? *Neuropathology : official journal of the Japanese Society of Neuropathology* **31**, 129-134, doi:10.1111/j.1440-1789.2010.01149.x (2011).
- 31 Wischhusen, J., Friese, M. A., Mittelbronn, M., Meyermann, R. & Weller, M. HLA-E protects glioma cells from NKG2D-mediated immune responses in vitro: implications for immune escape in vivo. *Journal of neuropathology and experimental neurology* **64**, 523-528 (2005).
- 32 Didenko, V. V., Ngo, H. N., Minchew, C. & Baskin, D. S. Apoptosis of T lymphocytes invading glioblastomas multiforme: a possible tumor defense mechanism. *Journal of neurosurgery* **96**, 580-584, doi:10.3171/jns.2002.96.3.0580 (2002).
- 33 Walker, D. G., Chuah, T., Rist, M. J. & Pender, M. P. T-cell apoptosis in human glioblastoma multiforme: implications for immunotherapy. *Journal of neuroimmunology* **175**, 59-68, doi:10.1016/j.jneuroim.2006.03.006 (2006).
- 34 Wintterle, S. *et al.* Expression of the B7-related molecule B7-H1 by glioma cells: a potential mechanism of immune paralysis. *Cancer research* **63**, 7462-7467 (2003).
- 35 Parsa, A. T. *et al.* Loss of tumor suppressor PTEN function increases B7-H1 expression and immunoresistance in glioma. *Nature medicine* **13**, 84-88, doi:10.1038/nm1517 (2007).
- 36 Okada, H. *et al.* Immunotherapeutic approaches for glioma. *Critical reviews in immunology* **29**, 1-42 (2009).
- 37 Gomez, G. G. & Kruse, C. A. Mechanisms of malignant glioma immune resistance and sources of immunosuppression. *Gene therapy & molecular biology* **10**, 133-146 (2006).
- 38 Penuelas, S. *et al.* TGF-beta increases glioma-initiating cell self-renewal through the induction of LIF in human glioblastoma. *Cancer cell* **15**, 315-327, doi:10.1016/j.ccr.2009.02.011 (2009).
- 39 Wick, W., Naumann, U. & Weller, M. Transforming growth factor-beta: a molecular target for the future therapy of glioblastoma. *Current pharmaceutical design* **12**, 341-349 (2006).
- 40 Tritschler, I. *et al.* Modulation of TGF-beta activity by latent TGF-beta-binding protein 1 in human malignant glioma cells. *International journal of cancer. Journal international du cancer* **125**, 530-540, doi:10.1002/ijc.24443 (2009).
- 41 Hardee, M. E. *et al.* Resistance of glioblastoma-initiating cells to radiation mediated by the tumor microenvironment can be abolished by inhibiting transforming growth factor-beta. *Cancer research* **72**, 4119-4129, doi:10.1158/0008-5472.CAN-12-0546 (2012).
- 42 Fecci, P. E. *et al.* Increased regulatory T-cell fraction amidst a diminished CD4 compartment explains cellular immune defects in patients with malignant glioma. *Cancer research* **66**, 3294-3302, doi:10.1158/0008-5472.CAN-05-3773 (2006).

- 43 Humphries, W., Wei, J., Sampson, J. H. & Heimberger, A. B. The role of tregs in glioma-mediated immunosuppression: potential target for intervention. *Neurosurgery clinics of North America* **21**, 125-137, doi:10.1016/j.nec.2009.08.012 (2010).
- 44 Crane, C. A., Ahn, B. J., Han, S. J. & Parsa, A. T. Soluble factors secreted by glioblastoma cell lines facilitate recruitment, survival, and expansion of regulatory T cells: implications for immunotherapy. *Neuro-oncology* **14**, 584-595, doi:10.1093/neuonc/nos014 (2012).
- 45 Roggendorf, W., Strupp, S. & Paulus, W. Distribution and characterization of microglia/macrophages in human brain tumors. *Acta neuropathologica* **92**, 288-293 (1996).
- 46 Kettenmann, H., Hanisch, U. K., Noda, M. & Verkhratsky, A. Physiology of microglia. *Physiological reviews* **91**, 461-553, doi:10.1152/physrev.00011.2010 (2011).
- 47 Chan, W. Y., Kohsaka, S. & Rezaie, P. The origin and cell lineage of microglia: new concepts. *Brain research reviews* **53**, 344-354, doi:10.1016/j.brainresrev.2006.11.002 (2007).
- 48 Greter, M. & Merad, M. Regulation of microglia development and homeostasis. *Glia* **61**, 121-127, doi:10.1002/glia.22408 (2013).
- 49 Soulet, D. & Rivest, S. Bone-marrow-derived microglia: myth or reality? *Current opinion in pharmacology* **8**, 508-518, doi:10.1016/j.coph.2008.04.002 (2008).
- 50 Tambuyzer, B. R., Ponsaerts, P. & Nouwen, E. J. Microglia: gatekeepers of central nervous system immunology. *Journal of leukocyte biology* **85**, 352-370, doi:10.1189/jlb.0608385 (2009).
- 51 Kreutzberg, G. W. Microglia: a sensor for pathological events in the CNS. *Trends in neurosciences* **19**, 312-318 (1996).
- 52 Nimmerjahn, A., Kirchhoff, F. & Helmchen, F. Resting microglial cells are highly dynamic surveillants of brain parenchyma in vivo. *Science* **308**, 1314-1318, doi:10.1126/science.1110647 (2005).
- 53 Wake, H., Moorhouse, A. J., Jinno, S., Kohsaka, S. & Nabekura, J. Resting microglia directly monitor the functional state of synapses in vivo and determine the fate of ischemic terminals. *The Journal of neuroscience : the official journal of the Society for Neuroscience* **29**, 3974-3980, doi:10.1523/JNEUROSCI.4363-08.2009 (2009).
- 54 Ransohoff, R. M. & Perry, V. H. Microglial physiology: unique stimuli, specialized responses. *Annual review of immunology* **27**, 119-145, doi:10.1146/annurev.immunol.021908.132528 (2009).
- 55 Choi, C. & Benveniste, E. N. Fas ligand/Fas system in the brain: regulator of immune and apoptotic responses. *Brain research. Brain research reviews* **44**, 65-81 (2004).
- 56 Davalos, D. *et al.* ATP mediates rapid microglial response to local brain injury in vivo. *Nature neuroscience* **8**, 752-758, doi:10.1038/nn1472 (2005).
- 57 Lehnardt, S. Innate immunity and neuroinflammation in the CNS: the role of microglia in Toll-like receptor-mediated neuronal injury. *Glia* **58**, 253-263, doi:10.1002/glia.20928 (2010).

- 58 Furr, S. R., Chauhan, V. S., Sterka, D., Jr., Grdzlishvili, V. & Marriott, I. Characterization of retinoic acid-inducible gene-I expression in primary murine glia following exposure to vesicular stomatitis virus. *Journal of neurovirology* **14**, 503-513, doi:10.1080/13550280802337217 (2008).
- 59 Sterka, D., Jr. & Marriott, I. Characterization of nucleotide-binding oligomerization domain (NOD) protein expression in primary murine microglia. *Journal of neuroimmunology* **179**, 65-75, doi:10.1016/j.jneuroim.2006.06.009 (2006).
- 60 Wilkinson, K. & El Khoury, J. Microglial scavenger receptors and their roles in the pathogenesis of Alzheimer's disease. *International journal of Alzheimer's disease* **2012**, 489456, doi:10.1155/2012/489456 (2012).
- 61 Ransohoff, R. M. & Cardona, A. E. The myeloid cells of the central nervous system parenchyma. *Nature* **468**, 253-262, doi:10.1038/nature09615 (2010).
- 62 Ekdahl, C. T., Kokaia, Z. & Lindvall, O. Brain inflammation and adult neurogenesis: the dual role of microglia. *Neuroscience* **158**, 1021-1029, doi:10.1016/j.neuroscience.2008.06.052 (2009).
- 63 Morantz, R. A., Wood, G. W., Foster, M., Clark, M. & Gollahon, K. Macrophages in experimental and human brain tumors. Part 2: studies of the macrophage content of human brain tumors. *Journal of neurosurgery* **50**, 305-311, doi:10.3171/jns.1979.50.3.0305 (1979).
- 64 Esiri, M. M. & McGee, J. O. Monoclonal antibody to macrophages (EMB/11) labels macrophages and microglial cells in human brain. *Journal of clinical pathology* **39**, 615-621 (1986).
- 65 Esiri, M. M. & Morris, C. S. Immunocytochemical study of macrophages and microglial cells and extracellular matrix components in human CNS disease. 2. Non-neoplastic diseases. *Journal of the neurological sciences* **101**, 59-72 (1991).
- 66 Wierzba-Bobrowicz, T., Kuchna, I. & Matyja, E. Reaction of microglial cells in human astrocytomas (preliminary report). *Folia neuropathologica / Association of Polish Neuropathologists and Medical Research Centre, Polish Academy of Sciences* **32**, 251-252 (1994).
- 67 Zhang, G. X., Li, J., Ventura, E. & Rostami, A. Parenchymal microglia of naive adult C57BL/6J mice express high levels of B7.1, B7.2, and MHC class II. *Experimental and molecular pathology* **73**, 35-45 (2002).
- 68 Cooper, L. A. *et al.* The tumor microenvironment strongly impacts master transcriptional regulators and gene expression class of glioblastoma. *The American journal of pathology* **180**, 2108-2119, doi:10.1016/j.ajpath.2012.01.040 (2012).
- 69 Engler, J. R. *et al.* Increased microglia/macrophage gene expression in a subset of adult and pediatric astrocytomas. *PloS one* **7**, e43339, doi:10.1371/journal.pone.0043339 (2012).
- 70 Mantovani, A. & Sica, A. Macrophages, innate immunity and cancer: balance, tolerance, and diversity. *Current opinion in immunology* **22**, 231-237, doi:10.1016/j.coi.2010.01.009 (2010).
- 71 Lawrence, T. & Natoli, G. Transcriptional regulation of macrophage polarization: enabling diversity with identity. *Nature reviews. Immunology* **11**, 750-761, doi:10.1038/nri3088 (2011).

- 72 Kobayashi, K. *et al.* Minocycline selectively inhibits M1 polarization of
microglia. *Cell death & disease* **4**, e525, doi:10.1038/cddis.2013.54 (2013).
- 73 Liao, B., Zhao, W., Beers, D. R., Henkel, J. S. & Appel, S. H. Transformation
from a neuroprotective to a neurotoxic microglial phenotype in a mouse model of
ALS. *Experimental neurology* **237**, 147-152,
doi:10.1016/j.expneurol.2012.06.011 (2012).
- 74 Durafourt, B. A. *et al.* Comparison of polarization properties of human adult
microglia and blood-derived macrophages. *Glia* **60**, 717-727,
doi:10.1002/glia.22298 (2012).
- 75 Pollard, J. W. Trophic macrophages in development and disease. *Nature reviews.
Immunology* **9**, 259-270, doi:10.1038/nri2528 (2009).
- 76 Zhou, X., Spittau, B. & Krieglstein, K. TGFbeta signalling plays an important
role in IL4-induced alternative activation of microglia. *Journal of
neuroinflammation* **9**, 210, doi:10.1186/1742-2094-9-210 (2012).
- 77 Ylostalo, J. H., Bartosh, T. J., Coble, K. & Prockop, D. J. Human mesenchymal
stem/stromal cells cultured as spheroids are self-activated to produce
prostaglandin E2 that directs stimulated macrophages into an anti-inflammatory
phenotype. *Stem cells* **30**, 2283-2296, doi:10.1002/stem.1191 (2012).
- 78 Kostianovsky, A. M., Maier, L. M., Anderson, R. C., Bruce, J. N. & Anderson, D.
E. Astrocytic regulation of human monocytic/microglial activation. *Journal of
immunology* **181**, 5425-5432 (2008).
- 79 Nakano, Y. *et al.* Induction of prostaglandin E2 synthesis and microsomal
prostaglandin E synthase-1 expression in murine microglia by glioma-derived
soluble factors. Laboratory investigation. *Journal of neurosurgery* **108**, 311-319,
doi:10.3171/JNS/2008/108/2/0311 (2008).
- 80 Carro, M. S. *et al.* The transcriptional network for mesenchymal transformation of
brain tumours. *Nature* **463**, 318-325, doi:10.1038/nature08712 (2010).
- 81 Zhang, L. *et al.* Stat3 inhibition activates tumor macrophages and abrogates
glioma growth in mice. *Glia* **57**, 1458-1467, doi:10.1002/glia.20863 (2009).
- 82 Hussain, S. F. *et al.* A novel small molecule inhibitor of signal transducers and
activators of transcription 3 reverses immune tolerance in malignant glioma
patients. *Cancer research* **67**, 9630-9636, doi:10.1158/0008-5472.CAN-07-1243
(2007).
- 83 Kren, L. *et al.* Production of immune-modulatory nonclassical molecules HLA-G
and HLA-E by tumor infiltrating ameboid microglia/macrophages in
glioblastomas: a role in innate immunity? *Journal of neuroimmunology* **220**, 131-
135, doi:10.1016/j.jneuroim.2010.01.014 (2010).
- 84 Magnus, T. *et al.* Microglial expression of the B7 family member B7 homolog 1
confers strong immune inhibition: implications for immune responses and
autoimmunity in the CNS. *The Journal of neuroscience : the official journal of
the Society for Neuroscience* **25**, 2537-2546, doi:10.1523/JNEUROSCI.4794-
04.2005 (2005).
- 85 Bloch, O. *et al.* Gliomas promote immunosuppression through induction of B7-
H1 expression in tumor-associated macrophages. *Clinical cancer research : an
official journal of the American Association for Cancer Research*,
doi:10.1158/1078-0432.CCR-12-3314 (2013).

- 86 Badie, B., Schartner, J., Prabakaran, S., Paul, J. & Vorpahl, J. Expression of Fas ligand by microglia: possible role in glioma immune evasion. *Journal of neuroimmunology* **120**, 19-24 (2001).
- 87 Wild-Bode, C., Weller, M. & Wick, W. Molecular determinants of glioma cell migration and invasion. *Journal of neurosurgery* **94**, 978-984, doi:10.3171/jns.2001.94.6.0978 (2001).
- 88 Markovic, D. S., Glass, R., Synowitz, M., Rooijen, N. & Kettenmann, H. Microglia stimulate the invasiveness of glioma cells by increasing the activity of metalloprotease-2. *Journal of neuropathology and experimental neurology* **64**, 754-762 (2005).
- 89 Markovic, D. S. *et al.* Gliomas induce and exploit microglial MT1-MMP expression for tumor expansion. *Proceedings of the National Academy of Sciences of the United States of America* **106**, 12530-12535, doi:10.1073/pnas.0804273106 (2009).
- 90 Ye, X. Z. *et al.* Tumor-associated microglia/macrophages enhance the invasion of glioma stem-like cells via TGF-beta1 signaling pathway. *Journal of immunology* **189**, 444-453, doi:10.4049/jimmunol.1103248 (2012).
- 91 Hoelzinger, D. B., Demuth, T. & Berens, M. E. Autocrine factors that sustain glioma invasion and paracrine biology in the brain microenvironment. *Journal of the National Cancer Institute* **99**, 1583-1593, doi:10.1093/jnci/djm187 (2007).
- 92 Arnold, T. & Betsholtz, C. The importance of microglia in the development of the vasculature in the central nervous system. *Vascular cell* **5**, 4, doi:10.1186/2045-824X-5-4 (2013).
- 93 Walton, N. M. *et al.* Microglia instruct subventricular zone neurogenesis. *Glia* **54**, 815-825, doi:10.1002/glia.20419 (2006).
- 94 Martino, G., Pluchino, S., Bonfanti, L. & Schwartz, M. Brain regeneration in physiology and pathology: the immune signature driving therapeutic plasticity of neural stem cells. *Physiological reviews* **91**, 1281-1304, doi:10.1152/physrev.00032.2010 (2011).
- 95 Komohara, Y., Ohnishi, K., Kuratsu, J. & Takeya, M. Possible involvement of the M2 anti-inflammatory macrophage phenotype in growth of human gliomas. *The Journal of pathology* **216**, 15-24, doi:10.1002/path.2370 (2008).
- 96 Hwang, S. Y. *et al.* Induction of glioma apoptosis by microglia-secreted molecules: The role of nitric oxide and cathepsin B. *Biochimica et biophysica acta* **1793**, 1656-1668, doi:10.1016/j.bbamcr.2009.08.011 (2009).
- 97 Chen, G. G. *et al.* Glioma apoptosis induced by macrophages involves both death receptor-dependent and independent pathways. *The Journal of laboratory and clinical medicine* **141**, 190-199, doi:10.1067/mlc.2003.22 (2003).
- 98 Mora, R. *et al.* TNF-alpha- and TRAIL-resistant glioma cells undergo autophagy-dependent cell death induced by activated microglia. *Glia* **57**, 561-581, doi:10.1002/glia.20785 (2009).
- 99 Kees, T. *et al.* Microglia isolated from patients with glioma gain antitumor activities on poly (I:C) stimulation. *Neuro-oncology* **14**, 64-78, doi:10.1093/neuonc/nor182 (2012).
- 100 Le, D. M. *et al.* Exploitation of astrocytes by glioma cells to facilitate invasiveness: a mechanism involving matrix metalloproteinase-2 and the

- urokinase-type plasminogen activator-plasmin cascade. *The Journal of neuroscience : the official journal of the Society for Neuroscience* **23**, 4034-4043 (2003).
- 101 Glass, R. *et al.* Glioblastoma-induced attraction of endogenous neural precursor cells is associated with improved survival. *The Journal of neuroscience : the official journal of the Society for Neuroscience* **25**, 2637-2646, doi:10.1523/JNEUROSCI.5118-04.2005 (2005).
- 102 Walzlein, J. H. *et al.* The antitumorigenic response of neural precursors depends on subventricular proliferation and age. *Stem cells* **26**, 2945-2954, doi:10.1634/stemcells.2008-0307 (2008).
- 103 Charles, N. A., Holland, E. C., Gilbertson, R., Glass, R. & Kettenmann, H. The brain tumor microenvironment. *Glia* **60**, 502-514 (2012).
- 104 Huszthy, P. C. *et al.* In vivo models of primary brain tumors: pitfalls and perspectives. *Neuro-oncology* **14**, 979-993, doi:10.1093/neuonc/nos135 (2012).
- 105 Balciunaite, G. *et al.* Wnt glycoproteins regulate the expression of FoxN1, the gene defective in nude mice. *Nature immunology* **3**, 1102-1108, doi:10.1038/ni850 (2002).
- 106 Blunt, T. *et al.* Defective DNA-dependent protein kinase activity is linked to V(D)J recombination and DNA repair defects associated with the murine scid mutation. *Cell* **80**, 813-823 (1995).
- 107 Shultz, L. D. *et al.* Multiple defects in innate and adaptive immunologic function in NOD/LtSz-scid mice. *Journal of immunology* **154**, 180-191 (1995).
- 108 Bonne-Barkay, D. & Wiley, C. A. Brain extracellular matrix in neurodegeneration. *Brain pathology* **19**, 573-585, doi:10.1111/j.1750-3639.2008.00195.x (2009).
- 109 Han, S. J., Zygourakis, C., Lim, M. & Parsa, A. T. Immunotherapy for glioma: promises and challenges. *Neurosurgery clinics of North America* **23**, 357-370, doi:10.1016/j.nec.2012.05.001 (2012).
- 110 Uze, G., Lutfalla, G., Bandu, M. T., Proudhon, D. & Mogensen, K. E. Behavior of a cloned murine interferon alpha/beta receptor expressed in homospecific or heterospecific background. *Proceedings of the National Academy of Sciences of the United States of America* **89**, 4774-4778 (1992).
- 111 Qin, X. Q., Beckham, C., Brown, J. L., Lukashev, M. & Barsoum, J. Human and mouse IFN-beta gene therapy exhibits different anti-tumor mechanisms in mouse models. *Molecular therapy : the journal of the American Society of Gene Therapy* **4**, 356-364, doi:10.1006/mthe.2001.0464 (2001).
- 112 Tada, H. *et al.* Systemic IFN-beta gene therapy results in long-term survival in mice with established colorectal liver metastases. *The Journal of clinical investigation* **108**, 83-95, doi:10.1172/JCI9841 (2001).
- 113 Gray, P. W. & Goeddel, D. V. Cloning and expression of murine immune interferon cDNA. *Proceedings of the National Academy of Sciences of the United States of America* **80**, 5842-5846 (1983).
- 114 Shanafelt, A. B., Johnson, K. E. & Kastelein, R. A. Identification of critical amino acid residues in human and mouse granulocyte-macrophage colony-stimulating factor and their involvement in species specificity. *The Journal of biological chemistry* **266**, 13804-13810 (1991).

- 115 Bossen, C. *et al.* Interactions of tumor necrosis factor (TNF) and TNF receptor family members in the mouse and human. *The Journal of biological chemistry* **281**, 13964-13971, doi:10.1074/jbc.M601553200 (2006).
- 116 Weiner, N. E. *et al.* A syngeneic mouse glioma model for study of glioblastoma therapy. *Journal of neuropathology and experimental neurology* **58**, 54-60 (1999).
- 117 Szatmari, T. *et al.* Detailed characterization of the mouse glioma 261 tumor model for experimental glioblastoma therapy. *Cancer science* **97**, 546-553, doi:10.1111/j.1349-7006.2006.00208.x (2006).
- 118 Barth, R. F. & Kaur, B. Rat brain tumor models in experimental neuro-oncology: the C6, 9L, T9, RG2, F98, BT4C, RT-2 and CNS-1 gliomas. *Journal of neuro-oncology* **94**, 299-312, doi:10.1007/s11060-009-9875-7 (2009).
- 119 Ausman, J. I., Shapiro, W. R. & Rall, D. P. Studies on the chemotherapy of experimental brain tumors: development of an experimental model. *Cancer research* **30**, 2394-2400 (1970).
- 120 Seyfried, T. N., el-Abadi, M. & Roy, M. L. Ganglioside distribution in murine neural tumors. *Molecular and chemical neuropathology / sponsored by the International Society for Neurochemistry and the World Federation of Neurology and research groups on neurochemistry and cerebrospinal fluid* **17**, 147-167 (1992).
- 121 Federspiel, M. J., Bates, P., Young, J. A., Varmus, H. E. & Hughes, S. H. A system for tissue-specific gene targeting: transgenic mice susceptible to subgroup A avian leukosis virus-based retroviral vectors. *Proceedings of the National Academy of Sciences of the United States of America* **91**, 11241-11245 (1994).
- 122 Dai, C. *et al.* PDGF autocrine stimulation dedifferentiates cultured astrocytes and induces oligodendrogliomas and oligoastrocytomas from neural progenitors and astrocytes in vivo. *Genes & development* **15**, 1913-1925, doi:10.1101/gad.903001 (2001).
- 123 Holland, E. C., Hively, W. P., DePinho, R. A. & Varmus, H. E. A constitutively active epidermal growth factor receptor cooperates with disruption of G1 cell-cycle arrest pathways to induce glioma-like lesions in mice. *Genes & development* **12**, 3675-3685 (1998).
- 124 Amankulor, N. M. *et al.* Sonic hedgehog pathway activation is induced by acute brain injury and regulated by injury-related inflammation. *The Journal of neuroscience : the official journal of the Society for Neuroscience* **29**, 10299-10308, doi:10.1523/JNEUROSCI.2500-09.2009 (2009).
- 125 Lindberg, N., Kastemar, M., Olofsson, T., Smits, A. & Uhrbom, L. Oligodendrocyte progenitor cells can act as cell of origin for experimental glioma. *Oncogene* **28**, 2266-2275, doi:10.1038/onc.2009.76 (2009).
- 126 Holland, E. C. *et al.* Combined activation of Ras and Akt in neural progenitors induces glioblastoma formation in mice. *Nature genetics* **25**, 55-57, doi:10.1038/75596 (2000).
- 127 Reilly, K. M., Loisel, D. A., Bronson, R. T., McLaughlin, M. E. & Jacks, T. Nf1;Trp53 mutant mice develop glioblastoma with evidence of strain-specific effects. *Nature genetics* **26**, 109-113, doi:10.1038/79075 (2000).
- 128 Reilly, K. M. *et al.* Susceptibility to astrocytoma in mice mutant for Nf1 and Trp53 is linked to chromosome 11 and subject to epigenetic effects. *Proceedings*

- of the National Academy of Sciences of the United States of America **101**, 13008-13013, doi:10.1073/pnas.0401236101 (2004).
- 129 Amlin-Van Schaick, J., Kim, S., Broman, K. W. & Reilly, K. M. Scram1 is a modifier of spinal cord resistance for astrocytoma on mouse Chr 5. *Mammalian genome : official journal of the International Mammalian Genome Society* **23**, 277-285, doi:10.1007/s00335-011-9380-0 (2012).
- 130 Amlin-Van Schaick, J. C. *et al.* Arlm1 is a male-specific modifier of astrocytoma resistance on mouse Chr 12. *Neuro-oncology* **14**, 160-174, doi:10.1093/neuonc/nor206 (2012).
- 131 Reilly, K. 93-118 (Springer, CNS Cancer: Models, Markers, Prognostic Factors, Targets, and Therapeutic Approaches, 2009).
- 132 Toledo, F. & Wahl, G. M. Regulating the p53 pathway: in vitro hypotheses, in vivo veritas. *Nature reviews. Cancer* **6**, 909-923, doi:10.1038/nrc2012 (2006).
- 133 Gursel, D. B. *et al.* Control of proliferation in astrocytoma cells by the receptor tyrosine kinase/PI3K/AKT signaling axis and the use of PI-103 and TCN as potential anti-astrocytoma therapies. *Neuro-oncology* **13**, 610-621, doi:10.1093/neuonc/nor035 (2011).
- 134 Bajenaru, M. L. *et al.* Astrocyte-specific inactivation of the neurofibromatosis 1 gene (NF1) is insufficient for astrocytoma formation. *Molecular and cellular biology* **22**, 5100-5113 (2002).
- 135 Bajenaru, M. L. *et al.* Optic nerve glioma in mice requires astrocyte Nf1 gene inactivation and Nf1 brain heterozygosity. *Cancer research* **63**, 8573-8577 (2003).
- 136 Dagnakatte, G. C. & Gutmann, D. H. Neurofibromatosis-1 (Nf1) heterozygous brain microglia elaborate paracrine factors that promote Nf1-deficient astrocyte and glioma growth. *Human molecular genetics* **16**, 1098-1112, doi:10.1093/hmg/ddm059 (2007).
- 137 Zhu, Y. *et al.* Early inactivation of p53 tumor suppressor gene cooperating with NF1 loss induces malignant astrocytoma. *Cancer cell* **8**, 119-130, doi:10.1016/j.ccr.2005.07.004 (2005).
- 138 Kwon, C. H. *et al.* Pten haploinsufficiency accelerates formation of high-grade astrocytomas. *Cancer research* **68**, 3286-3294, doi:10.1158/0008-5472.CAN-07-6867 (2008).
- 139 Ding, H. *et al.* Astrocyte-specific expression of activated p21-ras results in malignant astrocytoma formation in a transgenic mouse model of human gliomas. *Cancer research* **61**, 3826-3836 (2001).
- 140 Hede, S. M. *et al.* GFAP promoter driven transgenic expression of PDGFB in the mouse brain leads to glioblastoma in a Trp53 null background. *Glia* **57**, 1143-1153, doi:10.1002/glia.20837 (2009).
- 141 Chow, L. M. *et al.* Cooperativity within and among Pten, p53, and Rb pathways induces high-grade astrocytoma in adult brain. *Cancer cell* **19**, 305-316, doi:10.1016/j.ccr.2011.01.039 (2011).
- 142 Visvader, J. E. Cells of origin in cancer. *Nature* **469**, 314-322, doi:10.1038/nature09781 (2011).

- 143 Alcantara Llaguno, S. *et al.* Malignant astrocytomas originate from neural stem/progenitor cells in a somatic tumor suppressor mouse model. *Cancer cell* **15**, 45-56, doi:10.1016/j.ccr.2008.12.006 (2009).
- 144 Liu, C. *et al.* Mosaic analysis with double markers reveals tumor cell of origin in glioma. *Cell* **146**, 209-221, doi:10.1016/j.cell.2011.06.014 (2011).
- 145 Rahman, M. *et al.* The cancer stem cell hypothesis: failures and pitfalls. *Neurosurgery* **68**, 531-545; discussion 545, doi:10.1227/NEU.0b013e3181ff9eb5 (2011).
- 146 Lapidot, T., Sirard, C., Vormoor, J., Murdoch, B., Hoang, T., Caceres-Cortes, J., Minden, M., Paterson, B., Caligiuri, MA., Dick, JE. A cell initiating human acute myeloid leukaemia after transplantation into SCID mice. *Nature* **367**, 3 (1994).
- 147 Bonnet, D. & Dick, J. E. Human acute myeloid leukemia is organized as a hierarchy that originates from a primitive hematopoietic cell. *Nature medicine* **3**, 730-737 (1997).
- 148 Al-Hajj, M., Wicha, M. S., Benito-Hernandez, A., Morrison, S. J. & Clarke, M. F. Prospective identification of tumorigenic breast cancer cells. *Proceedings of the National Academy of Sciences of the United States of America* **100**, 3983-3988, doi:10.1073/pnas.0530291100 (2003).
- 149 Fang, D. *et al.* A tumorigenic subpopulation with stem cell properties in melanomas. *Cancer research* **65**, 9328-9337, doi:10.1158/0008-5472.CAN-05-1343 (2005).
- 150 Collins, A. T., Berry, P. A., Hyde, C., Stower, M. J. & Maitland, N. J. Prospective identification of tumorigenic prostate cancer stem cells. *Cancer research* **65**, 10946-10951, doi:10.1158/0008-5472.CAN-05-2018 (2005).
- 151 Dalerba, P. *et al.* Phenotypic characterization of human colorectal cancer stem cells. *Proceedings of the National Academy of Sciences of the United States of America* **104**, 10158-10163, doi:10.1073/pnas.0703478104 (2007).
- 152 Kim, C. F. *et al.* Identification of bronchioalveolar stem cells in normal lung and lung cancer. *Cell* **121**, 823-835, doi:10.1016/j.cell.2005.03.032 (2005).
- 153 Ignatova, T. N. *et al.* Human cortical glial tumors contain neural stem-like cells expressing astroglial and neuronal markers in vitro. *Glia* **39**, 193-206, doi:10.1002/glia.10094 (2002).
- 154 Singh, S. K. *et al.* Identification of human brain tumour initiating cells. *Nature* **432**, 396-401, doi:10.1038/nature03128 (2004).
- 155 Reynolds, B. A. & Weiss, S. Generation of neurons and astrocytes from isolated cells of the adult mammalian central nervous system. *Science* **255**, 1707-1710 (1992).
- 156 Villa, A., Snyder, E. Y., Vescovi, A. & Martinez-Serrano, A. Establishment and properties of a growth factor-dependent, perpetual neural stem cell line from the human CNS. *Experimental neurology* **161**, 67-84, doi:10.1006/exnr.1999.7237 (2000).
- 157 Lendahl, U., Zimmerman, L. B. & McKay, R. D. CNS stem cells express a new class of intermediate filament protein. *Cell* **60**, 585-595 (1990).
- 158 Ellis, P. *et al.* SOX2, a persistent marker for multipotential neural stem cells derived from embryonic stem cells, the embryo or the adult. *Developmental neuroscience* **26**, 148-165, doi:10.1159/000082134 (2004).

- 159 Kim, J. B. *et al.* Oct4-induced pluripotency in adult neural stem cells. *Cell* **136**, 411-419, doi:10.1016/j.cell.2009.01.023 (2009).
- 160 Molofsky, A. V., He, S., Bydon, M., Morrison, S. J. & Pardal, R. Bmi-1 promotes neural stem cell self-renewal and neural development but not mouse growth and survival by repressing the p16Ink4a and p19Arf senescence pathways. *Genes & development* **19**, 1432-1437, doi:10.1101/gad.1299505 (2005).
- 161 Chen, R. *et al.* A hierarchy of self-renewing tumor-initiating cell types in glioblastoma. *Cancer cell* **17**, 362-375, doi:10.1016/j.ccr.2009.12.049 (2010).
- 162 Lee, J. *et al.* Tumor stem cells derived from glioblastomas cultured in bFGF and EGF more closely mirror the phenotype and genotype of primary tumors than do serum-cultured cell lines. *Cancer cell* **9**, 391-403, doi:10.1016/j.ccr.2006.03.030 (2006).
- 163 Wakimoto, H. *et al.* Maintenance of primary tumor phenotype and genotype in glioblastoma stem cells. *Neuro-oncology* **14**, 132-144, doi:10.1093/neuonc/nor195 (2012).
- 164 Bao, S. *et al.* Glioma stem cells promote radioresistance by preferential activation of the DNA damage response. *Nature* **444**, 756-760, doi:10.1038/nature05236 (2006).
- 165 Salmaggi, A. *et al.* Glioblastoma-derived tumorspheres identify a population of tumor stem-like cells with angiogenic potential and enhanced multidrug resistance phenotype. *Glia* **54**, 850-860, doi:10.1002/glia.20414 (2006).
- 166 Fu, J. *et al.* Glioblastoma stem cells resistant to temozolomide-induced autophagy. *Chinese medical journal* **122**, 1255-1259 (2009).
- 167 Kelly, E. & Russell, S. J. History of oncolytic viruses: genesis to genetic engineering. *Molecular therapy : the journal of the American Society of Gene Therapy* **15**, 651-659, doi:10.1038/sj.mt.6300108 (2007).
- 168 Hoster, H. A., Zanes, R. P., Jr. & Von Haam, E. Studies in Hodgkin's syndrome; the association of viral hepatitis and Hodgkin's disease; a preliminary report. *Cancer research* **9**, 473-480 (1949).
- 169 Southam, C. M. Present status of oncolytic virus studies. *Transactions of the New York Academy of Sciences* **22**, 657-673 (1960).
- 170 Asada, T. Treatment of human cancer with mumps virus. *Cancer* **34**, 1907-1928 (1974).
- 171 Grove, J. & Marsh, M. The cell biology of receptor-mediated virus entry. *The Journal of cell biology* **195**, 1071-1082, doi:10.1083/jcb.201108131 (2011).
- 172 Allen, C. *et al.* Retargeted oncolytic measles strains entering via the EGFRvIII receptor maintain significant antitumor activity against gliomas with increased tumor specificity. *Cancer research* **66**, 11840-11850, doi:10.1158/0008-5472.CAN-06-1200 (2006).
- 173 Villa, N. Y. *et al.* Myxoma and vaccinia viruses exploit different mechanisms to enter and infect human cancer cells. *Virology* **401**, 266-279, doi:10.1016/j.virol.2010.02.027 (2010).
- 174 Johannsdottir, H. K., Mancini, R., Kartenbeck, J., Amato, L. & Helenius, A. Host cell factors and functions involved in vesicular stomatitis virus entry. *Journal of virology* **83**, 440-453, doi:10.1128/JVI.01864-08 (2009).

- 175 Russell, S. J., Peng, K. W. & Bell, J. C. Oncolytic virotherapy. *Nature biotechnology* **30**, 658-670, doi:10.1038/nbt.2287 (2012).
- 176 Deal watch: Amgen buys oncolytic virus company. *Nature reviews. Drug discovery* **10**, 166, doi:10.1038/nrd3391 (2011).
- 177 Xia, Z. J. *et al.* [Phase III randomized clinical trial of intratumoral injection of E1B gene-deleted adenovirus (H101) combined with cisplatin-based chemotherapy in treating squamous cell cancer of head and neck or esophagus]. *Ai zheng = Aizheng = Chinese journal of cancer* **23**, 1666-1670 (2004).
- 178 Gaddy, D. F. & Lyles, D. S. Oncolytic vesicular stomatitis virus induces apoptosis via signaling through PKR, Fas, and Daxx. *Journal of virology* **81**, 2792-2804, doi:10.1128/JVI.01760-06 (2007).
- 179 Cary, Z. D., Willingham, M. C. & Lyles, D. S. Oncolytic vesicular stomatitis virus induces apoptosis in U87 glioblastoma cells by a type II death receptor mechanism and induces cell death and tumor clearance in vivo. *Journal of virology* **85**, 5708-5717, doi:10.1128/JVI.02393-10 (2011).
- 180 Kanai, R. *et al.* Effect of gamma34.5 deletions on oncolytic herpes simplex virus activity in brain tumors. *Journal of virology* **86**, 4420-4431, doi:10.1128/JVI.00017-12 (2012).
- 181 Ito, H. *et al.* Autophagic cell death of malignant glioma cells induced by a conditionally replicating adenovirus. *Journal of the National Cancer Institute* **98**, 625-636, doi:10.1093/jnci/djj161 (2006).
- 182 Sova, P. *et al.* A tumor-targeted and conditionally replicating oncolytic adenovirus vector expressing TRAIL for treatment of liver metastases. *Molecular therapy : the journal of the American Society of Gene Therapy* **9**, 496-509, doi:10.1016/j.ymthe.2003.12.008 (2004).
- 183 Tong, Y. *et al.* Potent antitumor activity of oncolytic adenovirus expressing Beclin-1 via induction of autophagic cell death in leukemia. *Oncotarget* (2013).
- 184 Breitbach, C. J. *et al.* Targeting tumor vasculature with an oncolytic virus. *Molecular therapy : the journal of the American Society of Gene Therapy* **19**, 886-894, doi:10.1038/mt.2011.26 (2011).
- 185 Kirn, D. H., Wang, Y., Le Boeuf, F., Bell, J. & Thorne, S. H. Targeting of interferon-beta to produce a specific, multi-mechanistic oncolytic vaccinia virus. *PLoS medicine* **4**, e353, doi:10.1371/journal.pmed.0040353 (2007).
- 186 Benencia, F. *et al.* Oncolytic HSV exerts direct antiangiogenic activity in ovarian carcinoma. *Human gene therapy* **16**, 765-778, doi:10.1089/hum.2005.16.765 (2005).
- 187 Saito, Y. *et al.* Oncolytic replication-competent adenovirus suppresses tumor angiogenesis through preserved E1A region. *Cancer gene therapy* **13**, 242-252, doi:10.1038/sj.cgt.7700902 (2006).
- 188 Angarita, F. A., Acuna, S. A., Ottolino-Perry, K., Zerhouni, S. & McCart, J. A. Mounting a strategic offense: fighting tumor vasculature with oncolytic viruses. *Trends in molecular medicine* **19**, 378-392, doi:10.1016/j.molmed.2013.02.008 (2013).
- 189 Borden, E. C. *et al.* Interferons at age 50: past, current and future impact on biomedicine. *Nature reviews. Drug discovery* **6**, 975-990, doi:10.1038/nrd2422 (2007).

- 190 Chawla-Sarkar, M. *et al.* Apoptosis and interferons: role of interferon-stimulated genes as mediators of apoptosis. *Apoptosis : an international journal on programmed cell death* **8**, 237-249 (2003).
- 191 Biron, C. A., Nguyen, K. B., Pien, G. C., Cousens, L. P. & Salazar-Mather, T. P. Natural killer cells in antiviral defense: function and regulation by innate cytokines. *Annual review of immunology* **17**, 189-220, doi:10.1146/annurev.immunol.17.1.189 (1999).
- 192 Goodbourn, S., Didcock, L. & Randall, R. E. Interferons: cell signalling, immune modulation, antiviral response and virus countermeasures. *The Journal of general virology* **81**, 2341-2364 (2000).
- 193 Swann, J. B. *et al.* Type I IFN contributes to NK cell homeostasis, activation, and antitumor function. *Journal of immunology* **178**, 7540-7549 (2007).
- 194 Hervas-Stubbs, S. *et al.* Direct effects of type I interferons on cells of the immune system. *Clinical cancer research : an official journal of the American Association for Cancer Research* **17**, 2619-2627, doi:10.1158/1078-0432.CCR-10-1114 (2011).
- 195 Tough, D. F. Modulation of T-cell function by type I interferon. *Immunology and cell biology* **90**, 492-497, doi:10.1038/icb.2012.7 (2012).
- 196 van Horssen, R., Ten Hagen, T. L. & Eggermont, A. M. TNF-alpha in cancer treatment: molecular insights, antitumor effects, and clinical utility. *The oncologist* **11**, 397-408, doi:10.1634/theoncologist.11-4-397 (2006).
- 197 Roberts, N. J., Zhou, S., Diaz, L. A., Jr. & Holdhoff, M. Systemic use of tumor necrosis factor alpha as an anticancer agent. *Oncotarget* **2**, 739-751 (2011).
- 198 Shi, C. & Pamer, E. G. Monocyte recruitment during infection and inflammation. *Nature reviews. Immunology* **11**, 762-774, doi:10.1038/nri3070 (2011).
- 199 Huang, D. R., Wang, J., Kivisakk, P., Rollins, B. J. & Ransohoff, R. M. Absence of monocyte chemoattractant protein 1 in mice leads to decreased local macrophage recruitment and antigen-specific T helper cell type 1 immune response in experimental autoimmune encephalomyelitis. *The Journal of experimental medicine* **193**, 713-726 (2001).
- 200 Schilling, M., Strecker, J. K., Ringelstein, E. B., Schabitz, W. R. & Kiefer, R. The role of CC chemokine receptor 2 on microglia activation and blood-borne cell recruitment after transient focal cerebral ischemia in mice. *Brain research* **1289**, 79-84, doi:10.1016/j.brainres.2009.06.054 (2009).
- 201 Mildner, A. *et al.* Distinct and non-redundant roles of microglia and myeloid subsets in mouse models of Alzheimer's disease. *The Journal of neuroscience : the official journal of the Society for Neuroscience* **31**, 11159-11171, doi:10.1523/JNEUROSCI.6209-10.2011 (2011).
- 202 Lim, J. K. *et al.* Chemokine receptor Ccr2 is critical for monocyte accumulation and survival in West Nile virus encephalitis. *Journal of immunology* **186**, 471-478, doi:10.4049/jimmunol.1003003 (2011).
- 203 Boivin, N., Menasria, R., Gosselin, D., Rivest, S. & Boivin, G. Impact of deficiency in CCR2 and CX3CR1 receptors on monocytes trafficking in herpes simplex virus encephalitis. *The Journal of general virology* **93**, 1294-1304, doi:10.1099/vir.0.041046-0 (2012).

- 204 McCandless, E. E., Wang, Q., Woerner, B. M., Harper, J. M. & Klein, R. S. CXCL12 limits inflammation by localizing mononuclear infiltrates to the perivascular space during experimental autoimmune encephalomyelitis. *Journal of immunology* **177**, 8053-8064 (2006).
- 205 McCandless, E. E., Zhang, B., Diamond, M. S. & Klein, R. S. CXCR4 antagonism increases T cell trafficking in the central nervous system and improves survival from West Nile virus encephalitis. *Proceedings of the National Academy of Sciences of the United States of America* **105**, 11270-11275, doi:10.1073/pnas.0800898105 (2008).
- 206 Getts, D. R. *et al.* Targeted blockade in lethal West Nile virus encephalitis indicates a crucial role for very late antigen (VLA)-4-dependent recruitment of nitric oxide-producing macrophages. *Journal of neuroinflammation* **9**, 246, doi:10.1186/1742-2094-9-246 (2012).
- 207 Gordon, E. J., Myers, K. J., Dougherty, J. P., Rosen, H. & Ron, Y. Both anti-CD11a (LFA-1) and anti-CD11b (MAC-1) therapy delay the onset and diminish the severity of experimental autoimmune encephalomyelitis. *Journal of neuroimmunology* **62**, 153-160 (1995).
- 208 Williams, D. W., Eugenin, E. A., Calderon, T. M. & Berman, J. W. Monocyte maturation, HIV susceptibility, and transmigration across the blood brain barrier are critical in HIV neuropathogenesis. *Journal of leukocyte biology* **91**, 401-415, doi:10.1189/jlb.0811394 (2012).
- 209 Iijima, N., Mattei, L. M. & Iwasaki, A. Recruited inflammatory monocytes stimulate antiviral Th1 immunity in infected tissue. *Proceedings of the National Academy of Sciences of the United States of America* **108**, 284-289, doi:10.1073/pnas.1005201108 (2011).
- 210 Carmen, J., Gowing, G., Julien, J. P. & Kerr, D. Altered immune response to CNS viral infection in mice with a conditional knock-down of macrophage-lineage cells. *Glia* **54**, 71-80, doi:10.1002/glia.20359 (2006).
- 211 Chen, B. P., Kuziel, W. A. & Lane, T. E. Lack of CCR2 results in increased mortality and impaired leukocyte activation and trafficking following infection of the central nervous system with a neurotropic coronavirus. *Journal of immunology* **167**, 4585-4592 (2001).
- 212 Heydtmann, M. Macrophages in hepatitis B and hepatitis C virus infections. *Journal of virology* **83**, 2796-2802, doi:10.1128/JVI.00996-08 (2009).
- 213 Hashimoto, Y., Moki, T., Takizawa, T., Shiratsuchi, A. & Nakanishi, Y. Evidence for phagocytosis of influenza virus-infected, apoptotic cells by neutrophils and macrophages in mice. *Journal of immunology* **178**, 2448-2457 (2007).
- 214 Fujimoto, I., Pan, J., Takizawa, T. & Nakanishi, Y. Virus clearance through apoptosis-dependent phagocytosis of influenza A virus-infected cells by macrophages. *Journal of virology* **74**, 3399-3403 (2000).
- 215 Rigden, R. C., Carrasco, C. P., Summerfield, A. & KC, M. C. Macrophage phagocytosis of foot-and-mouth disease virus may create infectious carriers. *Immunology* **106**, 537-548 (2002).
- 216 Van Strijp, J. A. *et al.* Phagocytosis of herpes simplex virus by human granulocytes and monocytes. *Archives of virology* **104**, 287-298 (1989).

- 217 Lun, X. *et al.* Efficacy and safety/toxicity study of recombinant vaccinia virus JX-594 in two immunocompetent animal models of glioma. *Molecular therapy : the journal of the American Society of Gene Therapy* **18**, 1927-1936, doi:10.1038/mt.2010.183 (2010).
- 218 Fulci, G. *et al.* Cyclophosphamide enhances glioma virotherapy by inhibiting innate immune responses. *Proceedings of the National Academy of Sciences of the United States of America* **103**, 12873-12878, doi:10.1073/pnas.0605496103 (2006).
- 219 Fulci, G. *et al.* Depletion of peripheral macrophages and brain microglia increases brain tumor titers of oncolytic viruses. *Cancer research* **67**, 9398-9406, doi:10.1158/0008-5472.CAN-07-1063 (2007).
- 220 Lun, X. *et al.* Myxoma virus virotherapy for glioma in immunocompetent animal models: optimizing administration routes and synergy with rapamycin. *Cancer research* **70**, 598-608, doi:10.1158/0008-5472.CAN-09-1510 (2010).
- 221 Markert, J. M. *et al.* Phase Ib trial of mutant herpes simplex virus G207 inoculated pre-and post-tumor resection for recurrent GBM. *Molecular therapy : the journal of the American Society of Gene Therapy* **17**, 199-207, doi:10.1038/mt.2008.228 (2009).
- 222 Shi, F. D., Ljunggren, H. G., La Cava, A. & Van Kaer, L. Organ-specific features of natural killer cells. *Nature reviews. Immunology* **11**, 658-671, doi:10.1038/nri3065 (2011).
- 223 Hamerman, J. A., Ogasawara, K. & Lanier, L. L. NK cells in innate immunity. *Current opinion in immunology* **17**, 29-35, doi:10.1016/j.coi.2004.11.001 (2005).
- 224 Lisnic, V. J., Krmpotic, A. & Jonjic, S. Modulation of natural killer cell activity by viruses. *Current opinion in microbiology* **13**, 530-539, doi:10.1016/j.mib.2010.05.011 (2010).
- 225 Smyth, M. J. *et al.* Activation of NK cell cytotoxicity. *Molecular immunology* **42**, 501-510, doi:10.1016/j.molimm.2004.07.034 (2005).
- 226 Sentman, C. L., Olsson, M. Y. & Karre, K. Missing self recognition by natural killer cells in MHC class I transgenic mice. A 'receptor calibration' model for how effector cells adapt to self. *Seminars in immunology* **7**, 109-119, doi:10.1006/smim.1995.0015 (1995).
- 227 Hansen, T. H. & Bouvier, M. MHC class I antigen presentation: learning from viral evasion strategies. *Nature reviews. Immunology* **9**, 503-513, doi:10.1038/nri2575 (2009).
- 228 Pegram, H. J., Andrews, D. M., Smyth, M. J., Darcy, P. K. & Kershaw, M. H. Activating and inhibitory receptors of natural killer cells. *Immunology and cell biology* **89**, 216-224, doi:10.1038/icb.2010.78 (2011).
- 229 Raulet, D. H. & Guerra, N. Oncogenic stress sensed by the immune system: role of natural killer cell receptors. *Nature reviews. Immunology* **9**, 568-580, doi:10.1038/nri2604 (2009).
- 230 Lee, S. H. & Biron, C. A. Here today--not gone tomorrow: roles for activating receptors in sustaining NK cells during viral infections. *European journal of immunology* **40**, 923-932, doi:10.1002/eji.201040304 (2010).

- 231 Arase, H., Mocarski, E. S., Campbell, A. E., Hill, A. B. & Lanier, L. L. Direct recognition of cytomegalovirus by activating and inhibitory NK cell receptors. *Science* **296**, 1323-1326, doi:10.1126/science.1070884 (2002).
- 232 Alvarez-Breckenridge, C. A. *et al.* The histone deacetylase inhibitor valproic acid lessens NK cell action against oncolytic virus-infected glioblastoma cells by inhibition of STAT5/T-BET signaling and generation of gamma interferon. *Journal of virology* **86**, 4566-4577, doi:10.1128/JVI.05545-11 (2012).
- 233 Alvarez-Breckenridge, C. A. *et al.* NK cells impede glioblastoma virotherapy through NKp30 and NKp46 natural cytotoxicity receptors. *Nature medicine* **18**, 1827-1834, doi:10.1038/nm.3013 (2012).
- 234 Ogbomo, H. *et al.* Myxoma virus infection promotes NK lysis of malignant gliomas in vitro and in vivo. *PloS one* **8**, e66825, doi:10.1371/journal.pone.0066825 (2013).
- 235 Moore, A. E. Viruses with oncolytic properties and their adaptation to tumors. *Annals of the New York Academy of Sciences* **54**, 945-952 (1952).
- 236 Martuza, R. L., Malick, A., Markert, J. M., Ruffner, K. L. & Coen, D. M. Experimental therapy of human glioma by means of a genetically engineered virus mutant. *Science* **252**, 854-856 (1991).
- 237 Markert, J. M., Malick, A., Coen, D. M. & Martuza, R. L. Reduction and elimination of encephalitis in an experimental glioma therapy model with attenuated herpes simplex mutants that retain susceptibility to acyclovir. *Neurosurgery* **32**, 597-603 (1993).
- 238 Mineta, T., Rabkin, S. D., Yazaki, T., Hunter, W. D. & Martuza, R. L. Attenuated multi-mutated herpes simplex virus-1 for the treatment of malignant gliomas. *Nature medicine* **1**, 938-943 (1995).
- 239 Andreansky, S. *et al.* Evaluation of genetically engineered herpes simplex viruses as oncolytic agents for human malignant brain tumors. *Cancer research* **57**, 1502-1509 (1997).
- 240 Bischoff, J. R. *et al.* An adenovirus mutant that replicates selectively in p53-deficient human tumor cells. *Science* **274**, 373-376 (1996).
- 241 Heise, C. *et al.* ONYX-015, an E1B gene-attenuated adenovirus, causes tumor-specific cytolysis and antitumoral efficacy that can be augmented by standard chemotherapeutic agents. *Nature medicine* **3**, 639-645 (1997).
- 242 Georger, B. *et al.* Oncolytic activity of the E1B-55 kDa-deleted adenovirus ONYX-015 is independent of cellular p53 status in human malignant glioma xenografts. *Cancer research* **62**, 764-772 (2002).
- 243 Chahal, J. S., Qi, J. & Flint, S. J. The human adenovirus type 5 E1B 55 kDa protein obstructs inhibition of viral replication by type I interferon in normal human cells. *PLoS pathogens* **8**, e1002853, doi:10.1371/journal.ppat.1002853 (2012).
- 244 Zemp, F. J., Corredor, J. C., Lun, X., Muruve, D. A. & Forsyth, P. A. Oncolytic viruses as experimental treatments for malignant gliomas: using a scourge to treat a devil. *Cytokine & growth factor reviews* **21**, 103-117, doi:10.1016/j.cytogfr.2010.04.001 (2010).
- 245 Forsyth, P. *et al.* A phase I trial of intratumoral administration of reovirus in patients with histologically confirmed recurrent malignant gliomas. *Molecular*

- therapy : the journal of the American Society of Gene Therapy* **16**, 627-632, doi:10.1038/sj.mt.6300403 (2008).
- 246 Markert, J. M. *et al.* Conditionally replicating herpes simplex virus mutant, G207 for the treatment of malignant glioma: results of a phase I trial. *Gene therapy* **7**, 867-874, doi:10.1038/sj.gt.3301205 (2000).
- 247 Rampling, R. *et al.* Toxicity evaluation of replication-competent herpes simplex virus (ICP 34.5 null mutant 1716) in patients with recurrent malignant glioma. *Gene therapy* **7**, 859-866 (2000).
- 248 Harrow, S. *et al.* HSV1716 injection into the brain adjacent to tumour following surgical resection of high-grade glioma: safety data and long-term survival. *Gene therapy* **11**, 1648-1658, doi:10.1038/sj.gt.3302289 (2004).
- 249 Papanastassiou, V. *et al.* The potential for efficacy of the modified (ICP 34.5(-)) herpes simplex virus HSV1716 following intratumoural injection into human malignant glioma: a proof of principle study. *Gene therapy* **9**, 398-406, doi:10.1038/sj.gt.3301664 (2002).
- 250 Chiocca, E. A. *et al.* A phase I open-label, dose-escalation, multi-institutional trial of injection with an E1B-Attenuated adenovirus, ONYX-015, into the peritumoral region of recurrent malignant gliomas, in the adjuvant setting. *Molecular therapy : the journal of the American Society of Gene Therapy* **10**, 958-966, doi:10.1016/j.ymthe.2004.07.021 (2004).
- 251 Freeman, A. I. *et al.* Phase I/II trial of intravenous NDV-HUJ oncolytic virus in recurrent glioblastoma multiforme. *Molecular therapy : the journal of the American Society of Gene Therapy* **13**, 221-228, doi:10.1016/j.ymthe.2005.08.016 (2006).
- 252 Gromeier, M., Lachmann, S., Rosenfeld, M. R., Gutin, P. H. & Wimmer, E. Intergeneric poliovirus recombinants for the treatment of malignant glioma. *Proceedings of the National Academy of Sciences of the United States of America* **97**, 6803-6808 (2000).
- 253 Lun, X. *et al.* Myxoma virus is a novel oncolytic virus with significant antitumor activity against experimental human gliomas. *Cancer research* **65**, 9982-9990, doi:10.1158/0008-5472.CAN-05-1201 (2005).
- 254 Wilcox, M. E. *et al.* Reovirus as an oncolytic agent against experimental human malignant gliomas. *Journal of the National Cancer Institute* **93**, 903-912 (2001).
- 255 Lasner, T. M. *et al.* Therapy of a murine model of pediatric brain tumors using a herpes simplex virus type-1 ICP34.5 mutant and demonstration of viral replication within the CNS. *Journal of neuropathology and experimental neurology* **55**, 1259-1269 (1996).
- 256 Andreansky, S. *et al.* Treatment of intracranial gliomas in immunocompetent mice using herpes simplex viruses that express murine interleukins. *Gene therapy* **5**, 121-130, doi:10.1038/sj.gt.3300550 (1998).
- 257 Hellums, E. K. *et al.* Increased efficacy of an interleukin-12-secreting herpes simplex virus in a syngeneic intracranial murine glioma model. *Neuro-oncology* **7**, 213-224, doi:10.1215/S1152851705000074 (2005).
- 258 Barnard, Z. *et al.* Expression of FMS-like tyrosine kinase 3 ligand by oncolytic herpes simplex virus type I prolongs survival in mice bearing established

- syngeneic intracranial malignant glioma. *Neurosurgery* **71**, 741-748; discussion 748, doi:10.1227/NEU.0b013e318260fd73 (2012).
- 259 Wakimoto, H., Fulci, G., Tyminski, E. & Chiocca, E. A. Altered expression of antiviral cytokine mRNAs associated with cyclophosphamide's enhancement of viral oncolysis. *Gene therapy* **11**, 214-223, doi:10.1038/sj.gt.3302143 (2004).
- 260 Yang, W. Q. *et al.* Efficacy and safety evaluation of human reovirus type 3 in immunocompetent animals: racine and nonhuman primates. *Clinical cancer research : an official journal of the American Association for Cancer Research* **10**, 8561-8576, doi:10.1158/1078-0432.CCR-04-0940 (2004).
- 261 Lun, X. Q. *et al.* Efficacy of systemically administered oncolytic vaccinia virotherapy for malignant gliomas is enhanced by combination therapy with rapamycin or cyclophosphamide. *Clinical cancer research : an official journal of the American Association for Cancer Research* **15**, 2777-2788, doi:10.1158/1078-0432.CCR-08-2342 (2009).
- 262 Alain, T. *et al.* Vesicular stomatitis virus oncolysis is potentiated by impairing mTORC1-dependent type I IFN production. *Proceedings of the National Academy of Sciences of the United States of America* **107**, 1576-1581, doi:10.1073/pnas.0912344107 (2010).
- 263 Kerr, P. J. Myxomatosis in Australia and Europe: a model for emerging infectious diseases. *Antiviral research* **93**, 387-415, doi:10.1016/j.antiviral.2012.01.009 (2012).
- 264 Kerr, P. J. *et al.* Evolutionary history and attenuation of myxoma virus on two continents. *PLoS pathogens* **8**, e1002950, doi:10.1371/journal.ppat.1002950 (2012).
- 265 Barrett, J. & McFadden, G. in *Poxviruses Birkhäuser Advances in Infectious Diseases* (eds Andrew A Mercer, Axel Schmidt, & Olaf Weber) Ch. 9, 183-201 (Birkhäuser Basel, 2007).
- 266 Stanford, M. M. & McFadden, G. Myxoma virus and oncolytic virotherapy: a new biologic weapon in the war against cancer. *Expert opinion on biological therapy* **7**, 1415-1425, doi:10.1517/14712598.7.9.1415 (2007).
- 267 Zachertowska, A., Brewer, D. & Evans, D. H. Characterization of the major capsid proteins of myxoma virus particles using MALDI-TOF mass spectrometry. *Journal of virological methods* **132**, 1-12, doi:10.1016/j.jviromet.2005.08.015 (2006).
- 268 Teoh, M. L., Turner, P. V. & Evans, D. H. Tumorigenic poxviruses up-regulate intracellular superoxide to inhibit apoptosis and promote cell proliferation. *Journal of virology* **79**, 5799-5811, doi:10.1128/JVI.79.9.5799-5811.2005 (2005).
- 269 Fields, B. N., Knipe, D. M. & Howley, P. M. *Fields' Virology*. (Wolters Kluwer Health/Lippincott Williams & Wilkins, 2007).
- 270 Smallwood, S. E., Rahman, M. M., Smith, D. W. & McFadden, G. Myxoma virus: propagation, purification, quantification, and storage. *Current protocols in microbiology* **Chapter 14**, Unit 14A 11, doi:10.1002/9780471729259.mc14a01s17 (2010).
- 271 Chen, H. *et al.* Viral serpin therapeutics from concept to clinic. *Methods in enzymology* **499**, 301-329, doi:10.1016/B978-0-12-386471-0.00015-8 (2011).

- 272 Moss, B. Poxvirus cell entry: how many proteins does it take? *Viruses* **4**, 688-707, doi:10.3390/v4050688 (2012).
- 273 Cameron, C. *et al.* The complete DNA sequence of myxoma virus. *Virology* **264**, 298-318, doi:10.1006/viro.1999.0001 (1999).
- 274 Schmidt, F. I., Bleck, C. K. & Mercer, J. Poxvirus host cell entry. *Current opinion in virology* **2**, 20-27, doi:10.1016/j.coviro.2011.11.007 (2012).
- 275 Matho, M. H. *et al.* Structural and biochemical characterization of the vaccinia virus envelope protein D8 and its recognition by the antibody LA5. *Journal of virology* **86**, 8050-8058, doi:10.1128/JVI.00836-12 (2012).
- 276 Irwin, C. R. & Evans, D. H. Modulation of the myxoma virus plaque phenotype by vaccinia virus protein F11. *Journal of virology* **86**, 7167-7179, doi:10.1128/JVI.06936-11 (2012).
- 277 Chan, W. M. *et al.* Myxoma and vaccinia viruses bind differentially to human leukocytes. *Journal of virology* **87**, 4445-4460, doi:10.1128/JVI.03488-12 (2013).
- 278 Duteyrat, J. L., Gelfi, J. & Bertagnoli, S. Ultrastructural study of myxoma virus morphogenesis. *Archives of virology* **151**, 2161-2180, doi:10.1007/s00705-006-0791-2 (2006).
- 279 Rubins, K. H. *et al.* Comparative analysis of viral gene expression programs during poxvirus infection: a transcriptional map of the vaccinia and monkeypox genomes. *PLoS one* **3**, e2628, doi:10.1371/journal.pone.0002628 (2008).
- 280 Morgan, G. W. *et al.* Vaccinia protein F12 has structural similarity to kinesin light chain and contains a motor binding motif required for virion export. *PLoS pathogens* **6**, e1000785, doi:10.1371/journal.ppat.1000785 (2010).
- 281 Dodding, M. P. & Way, M. Nck- and N-WASP-dependent actin-based motility is conserved in divergent vertebrate poxviruses. *Cell host & microbe* **6**, 536-550, doi:10.1016/j.chom.2009.10.011 (2009).
- 282 Stanford, M. M., McFadden, G., Karupiah, G. & Chaudhri, G. Immunopathogenesis of poxvirus infections: forecasting the impending storm. *Immunology and cell biology* **85**, 93-102, doi:10.1038/sj.icb.7100033 (2007).
- 283 Upton, C., Mossman, K. & McFadden, G. Encoding of a homolog of the IFN-gamma receptor by myxoma virus. *Science* **258**, 1369-1372 (1992).
- 284 Lalani, A. S. *et al.* Role of the myxoma virus soluble CC-chemokine inhibitor glycoprotein, M-T1, during myxoma virus pathogenesis. *Virology* **256**, 233-245, doi:10.1006/viro.1999.9617 (1999).
- 285 Schreiber, M., Rajarathnam, K. & McFadden, G. Myxoma virus T2 protein, a tumor necrosis factor (TNF) receptor homolog, is secreted as a monomer and dimer that each bind rabbit TNFalpha, but the dimer is a more potent TNF inhibitor. *The Journal of biological chemistry* **271**, 13333-13341 (1996).
- 286 Cameron, C. M., Barrett, J. W., Mann, M., Lucas, A. & McFadden, G. Myxoma virus M128L is expressed as a cell surface CD47-like virulence factor that contributes to the downregulation of macrophage activation in vivo. *Virology* **337**, 55-67, doi:10.1016/j.virol.2005.03.037 (2005).
- 287 Cameron, C. M., Barrett, J. W., Liu, L., Lucas, A. R. & McFadden, G. Myxoma virus M141R expresses a viral CD200 (vOX-2) that is responsible for down-regulation of macrophage and T-cell activation in vivo. *Journal of virology* **79**, 6052-6067, doi:10.1128/JVI.79.10.6052-6067.2005 (2005).

- 288 Opgenorth, A., Strayer, D., Upton, C. & McFadden, G. Deletion of the growth factor gene related to EGF and TGF alpha reduces virulence of malignant rabbit fibroma virus. *Virology* **186**, 175-191 (1992).
- 289 Su, J. *et al.* Myxoma virus M11L blocks apoptosis through inhibition of conformational activation of Bax at the mitochondria. *Journal of virology* **80**, 1140-1151, doi:10.1128/JVI.80.3.1140-1151.2006 (2006).
- 290 Werden, S. J. *et al.* The myxoma virus m-t5 ankyrin repeat host range protein is a novel adaptor that coordinately links the cellular signaling pathways mediated by Akt and Skp1 in virus-infected cells. *Journal of virology* **83**, 12068-12083, doi:10.1128/JVI.00963-09 (2009).
- 291 Rahman, M. M., Mohamed, M. R., Kim, M., Smallwood, S. & McFadden, G. Co-regulation of NF-kappaB and inflammasome-mediated inflammatory responses by myxoma virus pyrin domain-containing protein M013. *PLoS pathogens* **5**, e1000635, doi:10.1371/journal.ppat.1000635 (2009).
- 292 Mansouri, M. *et al.* The PHD/LAP-domain protein M153R of myxomavirus is a ubiquitin ligase that induces the rapid internalization and lysosomal destruction of CD4. *Journal of virology* **77**, 1427-1440 (2003).
- 293 Ramelot, T. A. *et al.* Myxoma virus immunomodulatory protein M156R is a structural mimic of eukaryotic translation initiation factor eIF2alpha. *Journal of molecular biology* **322**, 943-954 (2002).
- 294 Seet, B. T. *et al.* Poxviruses and immune evasion. *Annual review of immunology* **21**, 377-423, doi:10.1146/annurev.immunol.21.120601.141049 (2003).
- 295 Spiesschaert, B., McFadden, G., Hermans, K., Nauwynck, H. & Van de Walle, G. R. The current status and future directions of myxoma virus, a master in immune evasion. *Veterinary research* **42**, 76, doi:10.1186/1297-9716-42-76 (2011).
- 296 Mossman, K. *et al.* Myxoma virus M-T7, a secreted homolog of the interferon-gamma receptor, is a critical virulence factor for the development of myxomatosis in European rabbits. *Virology* **215**, 17-30, doi:10.1006/viro.1996.0003 (1996).
- 297 J Sypula, W. F., Ma Y, Bell J, McFadden G. Myxoma virus tropism in human tumor cells. *Gen Ther Mol Biol* **8**, 11 (2004).
- 298 Lun, X. Q. *et al.* Targeting human medulloblastoma: oncolytic virotherapy with myxoma virus is enhanced by rapamycin. *Cancer research* **67**, 8818-8827, doi:10.1158/0008-5472.CAN-07-1214 (2007).
- 299 Wu, Y. *et al.* Oncolytic efficacy of recombinant vesicular stomatitis virus and myxoma virus in experimental models of rhabdoid tumors. *Clinical cancer research : an official journal of the American Association for Cancer Research* **14**, 1218-1227, doi:10.1158/1078-0432.CCR-07-1330 (2008).
- 300 Zemp, F. J. *et al.* Treating brain tumor-initiating cells using a combination of myxoma virus and rapamycin. *Neuro-oncology*, doi:10.1093/neuonc/not035 (2013).
- 301 Laplante, M. & Sabatini, D. M. mTOR signaling in growth control and disease. *Cell* **149**, 274-293, doi:10.1016/j.cell.2012.03.017 (2012).
- 302 Powell, J. D., Pollizzi, K. N., Heikamp, E. B. & Horton, M. R. Regulation of immune responses by mTOR. *Annual review of immunology* **30**, 39-68, doi:10.1146/annurev-immunol-020711-075024 (2012).

- 303 Wang, G. *et al.* Infection of human cancer cells with myxoma virus requires Akt activation via interaction with a viral ankyrin-repeat host range factor. *Proceedings of the National Academy of Sciences of the United States of America* **103**, 4640-4645, doi:10.1073/pnas.0509341103 (2006).
- 304 Stanford, M. M., Barrett, J. W., Nazarian, S. H., Werden, S. & McFadden, G. Oncolytic virotherapy synergism with signaling inhibitors: Rapamycin increases myxoma virus tropism for human tumor cells. *Journal of virology* **81**, 1251-1260, doi:10.1128/JVI.01408-06 (2007).
- 305 Shi, Y., Yan, H., Frost, P., Gera, J. & Lichtenstein, A. Mammalian target of rapamycin inhibitors activate the AKT kinase in multiple myeloma cells by up-regulating the insulin-like growth factor receptor/insulin receptor substrate-1/phosphatidylinositol 3-kinase cascade. *Molecular cancer therapeutics* **4**, 1533-1540, doi:10.1158/1535-7163.MCT-05-0068 (2005).
- 306 Cloughesy, T. F. *et al.* Antitumor activity of rapamycin in a Phase I trial for patients with recurrent PTEN-deficient glioblastoma. *PLoS medicine* **5**, e8, doi:10.1371/journal.pmed.0050008 (2008).
- 307 Sugiyama, S. *et al.* Safety and efficacy of convection-enhanced delivery of ACNU, a hydrophilic nitrosourea, in intracranial brain tumor models. *Journal of neuro-oncology* **82**, 41-47, doi:10.1007/s11060-006-9247-5 (2007).
- 308 Kelly, J. J. *et al.* Proliferation of human glioblastoma stem cells occurs independently of exogenous mitogens. *Stem cells* **27**, 1722-1733, doi:10.1002/stem.98 (2009).
- 309 Blough, M. D. *et al.* Sensitivity to temozolomide in brain tumor initiating cells. *Neuro-oncology* **12**, 756-760, doi:10.1093/neuonc/noq032 (2010).
- 310 Blough, M. D., Beauchamp, D. C., Westgate, M. R., Kelly, J. J. & Cairncross, J. G. Effect of aberrant p53 function on temozolomide sensitivity of glioma cell lines and brain tumor initiating cells from glioblastoma. *Journal of neuro-oncology* **102**, 1-7, doi:10.1007/s11060-010-0283-9 (2011).
- 311 Zemp, F. *et al.* Treating Brain Tumor-Initiating Cells Using a Combination of Myxoma Virus and Rapamycin. *Neuro-oncology* **Accepted**. **N-O-D-12-00393** (2013).
- 312 Wennier, S. T. *et al.* Myxoma virus sensitizes cancer cells to gemcitabine and is an effective oncolytic virotherapeutic in models of disseminated pancreatic cancer. *Molecular therapy : the journal of the American Society of Gene Therapy* **20**, 759-768, doi:10.1038/mt.2011.293 (2012).
- 313 Rabinovich, B. A. Y., Y. Etto, T. Chen, J.Q. Levitsky, H.I. Overwijk, W.W. Cooper, L.J. Gelovani, J. Hwu, P. Visualizing fewer than 10 mouse T cells with an enhanced firefly luciferase in immunocompetent mouse models of cancer. *Proceedings of the National Academy of Sciences of the United States of America* **105**, 4 (2008).
- 314 Brundula, V., Rewcastle, N. B., Metz, L. M., Bernard, C. C. & Yong, V. W. Targeting leukocyte MMPs and transmigration: minocycline as a potential therapy for multiple sclerosis. *Brain : a journal of neurology* **125**, 1297-1308 (2002).
- 315 Pappenheimer, A. M., Jr., Harper, A. A., Moynihan, M. & Brockes, J. P. Diphtheria toxin and related proteins: effect of route of injection on toxicity and

- the determination of cytotoxicity for various cultured cells. *The Journal of infectious diseases* **145**, 94-102 (1982).
- 316 Saito, M. *et al.* Diphtheria toxin receptor-mediated conditional and targeted cell ablation in transgenic mice. *Nature biotechnology* **19**, 746-750, doi:10.1038/90795 (2001).
- 317 Stoneman, V. *et al.* Monocyte/macrophage suppression in CD11b diphtheria toxin receptor transgenic mice differentially affects atherogenesis and established plaques. *Circulation research* **100**, 884-893, doi:10.1161/01.RES.0000260802.75766.00 (2007).
- 318 Lee J, K. S., Kotliarov Y, Li A, Su Q, Donin NM, Pastorino S, Purow BW, Christopher N, Zhang W, Park JK, Fine HA. Tumor stem cells derived from glioblastomas cultured in bFGF and EGF more closely mirror the phenotype and genotype of primary tumors than do serum-cultured cell lines. *Cancer cell* **9**, 12 (2006).
- 319 Dirks, P. B. Brain tumor stem cells: the cancer stem cell hypothesis writ large. *Molecular oncology* **4**, 420-430, doi:10.1016/j.molonc.2010.08.001 (2010).
- 320 Venere, M., Fine, H. A., Dirks, P. B. & Rich, J. N. Cancer stem cells in gliomas: identifying and understanding the apex cell in cancer's hierarchy. *Glia* **59**, 1148-1154, doi:10.1002/glia.21185 (2011).
- 321 Wakimoto, H. *et al.* Human glioblastoma-derived cancer stem cells: establishment of invasive glioma models and treatment with oncolytic herpes simplex virus vectors. *Cancer research* **69**, 3472-3481, doi:10.1158/0008-5472.CAN-08-3886 (2009).
- 322 Maes, W. & Van Gool, S. W. Experimental immunotherapy for malignant glioma: lessons from two decades of research in the GL261 model. *Cancer immunology, immunotherapy : CII* **60**, 153-160, doi:10.1007/s00262-010-0946-6 (2011).
- 323 Paulus, W., Huettner, C. & Tonn, J. C. Collagens, integrins and the mesenchymal drift in glioblastomas: a comparison of biopsy specimens, spheroid and early monolayer cultures. *International journal of cancer. Journal international du cancer* **58**, 841-846 (1994).
- 324 McKeever, P. E., Davenport, R. D. & Shakui, P. Patterns of antigenic expression of human glioma cells. *Critical reviews in neurobiology* **6**, 119-147 (1991).
- 325 Zemp, F. *et al.* Treating Brain Tumor-Initiating Cells Using a Combination of Myxoma Virus and Rapamycin. *Neuro-oncology* doi: **10.1093/neuonc/not035** (2013).
- 326 France, M. R. *et al.* Intraventricular injection of myxoma virus results in transient expression of viral protein in mouse brain ependymal and subventricular cells. *The Journal of general virology* **92**, 195-199, doi:10.1099/vir.0.026690-0 (2011).
- 327 Son, M. J., Woolard, K., Nam, D. H., Lee, J. & Fine, H. A. SSEA-1 is an enrichment marker for tumor-initiating cells in human glioblastoma. *Cell stem cell* **4**, 440-452, doi:10.1016/j.stem.2009.03.003 (2009).
- 328 Comprehensive genomic characterization defines human glioblastoma genes and core pathways. *Nature* **455**, 1061-1068, doi:nature07385 [pii] 10.1038/nature07385 (2008).
- 329 Ohgaki, H. & Kleihues, P. Genetic pathways to primary and secondary glioblastoma. *Am J Pathol* **170**, 1445-1453, doi:S0002-9440(10)61358-2 [pii]

- 10.2353/ajpath.2007.070011 (2007).
- 330 Han, S. J., Yang, I., Tihan, T., Prados, M. D. & Parsa, A. T. Primary gliosarcoma: key clinical and pathologic distinctions from glioblastoma with implications as a unique oncologic entity. *Journal of neuro-oncology* **96**, 313-320, doi:10.1007/s11060-009-9973-6 (2010).
- 331 Ono, K., Takebayashi, H. & Ikenaka, K. Olig2 transcription factor in the developing and injured forebrain; cell lineage and glial development. *Molecules and cells* **27**, 397-401, doi:10.1007/s10059-009-0067-2 (2009).
- 332 Ligon, K. L. *et al.* The oligodendroglial lineage marker OLIG2 is universally expressed in diffuse gliomas. *Journal of neuropathology and experimental neurology* **63**, 499-509 (2004).
- 333 Lu, Q. R. *et al.* Oligodendrocyte lineage genes (OLIG) as molecular markers for human glial brain tumors. *Proceedings of the National Academy of Sciences of the United States of America* **98**, 10851-10856, doi:10.1073/pnas.181340798 (2001).
- 334 Schulte, A. *et al.* A distinct subset of glioma cell lines with stem cell-like properties reflects the transcriptional phenotype of glioblastomas and overexpresses CXCR4 as therapeutic target. *Glia* **59**, 590-602, doi:10.1002/glia.21127 (2011).
- 335 Jiang, H. *et al.* Examination of the therapeutic potential of Delta-24-RGD in brain tumor stem cells: role of autophagic cell death. *Journal of the National Cancer Institute* **99**, 1410-1414, doi:10.1093/jnci/djm102 (2007).
- 336 Skog, J., Edlund, K., Bergenheim, A. T. & Wadell, G. Adenoviruses 16 and CV23 efficiently transduce human low-passage brain tumor and cancer stem cells. *Molecular therapy : the journal of the American Society of Gene Therapy* **15**, 2140-2145, doi:10.1038/sj.mt.6300315 (2007).
- 337 Zemp, F. J. *et al.* Resistance to oncolytic myxoma virus therapy in nf1(-/-)/trp53(-/-) syngeneic mouse glioma models is independent of anti-viral type-I interferon. *PloS one* **8**, e65801, doi:10.1371/journal.pone.0065801 (2013).
- 338 Straussman, R. *et al.* Tumour micro-environment elicits innate resistance to RAF inhibitors through HGF secretion. *Nature* **487**, 500-504, doi:10.1038/nature11183 (2012).
- 339 Muller, U. *et al.* Functional role of type I and type II interferons in antiviral defense. *Science* **264**, 1918-1921 (1994).
- 340 Akira, S. & Takeda, K. Toll-like receptor signalling. *Nature reviews. Immunology* **4**, 499-511, doi:10.1038/nri1391 (2004).
- 341 Paul, S., Ricour, C., Sommereyns, C., Sorgeloos, F. & Michiels, T. Type I interferon response in the central nervous system. *Biochimie* **89**, 770-778, doi:10.1016/j.biochi.2007.02.009 (2007).
- 342 Savarin, C. & Bergmann, C. C. Neuroimmunology of central nervous system viral infections: the cells, molecules and mechanisms involved. *Current opinion in pharmacology* **8**, 472-479, doi:10.1016/j.coph.2008.05.002 (2008).
- 343 De Miranda, J., Yaddanapudi, K., Hornig, M. & Lipkin, W. I. Astrocytes recognize intracellular polyinosinic-polycytidylic acid via MDA-5. *FASEB journal : official publication of the Federation of American Societies for Experimental Biology* **23**, 1064-1071, doi:10.1096/fj.08-121434 (2009).

- 344 Kallfass, C. *et al.* Visualizing production of beta interferon by astrocytes and microglia in brain of La Crosse virus-infected mice. *Journal of virology* **86**, 11223-11230, doi:10.1128/JVI.01093-12 (2012).
- 345 Roth-Cross, J. K., Bender, S. J. & Weiss, S. R. Murine coronavirus mouse hepatitis virus is recognized by MDA5 and induces type I interferon in brain macrophages/microglia. *Journal of virology* **82**, 9829-9838, doi:10.1128/JVI.01199-08 (2008).
- 346 Kapil, P., Butchi, N. B., Stohlman, S. A. & Bergmann, C. C. Oligodendroglia are limited in type I interferon induction and responsiveness in vivo. *Glia* **60**, 1555-1566, doi:10.1002/glia.22375 (2012).
- 347 Wollmann, G., Ozduman, K. & van den Pol, A. N. Oncolytic virus therapy for glioblastoma multiforme: concepts and candidates. *Cancer journal* **18**, 69-81, doi:10.1097/PPO.0b013e31824671c9 (2012).
- 348 Stojdl, D. F. *et al.* Exploiting tumor-specific defects in the interferon pathway with a previously unknown oncolytic virus. *Nature medicine* **6**, 821-825, doi:10.1038/77558 (2000).
- 349 Bartee, E., Mohamed, M. R., Lopez, M. C., Baker, H. V. & McFadden, G. The addition of tumor necrosis factor plus beta interferon induces a novel synergistic antiviral state against poxviruses in primary human fibroblasts. *Journal of virology* **83**, 498-511, doi:10.1128/JVI.01376-08 (2009).
- 350 Stojdl, D. F. *et al.* VSV strains with defects in their ability to shutdown innate immunity are potent systemic anti-cancer agents. *Cancer cell* **4**, 263-275 (2003).
- 351 Collins, S. E., Noyce, R. S. & Mossman, K. L. Innate cellular response to virus particle entry requires IRF3 but not virus replication. *Journal of virology* **78**, 1706-1717 (2004).
- 352 Noyce, R. S. *et al.* Membrane perturbation elicits an IRF3-dependent, interferon-independent antiviral response. *Journal of virology* **85**, 10926-10931, doi:10.1128/JVI.00862-11 (2011).
- 353 Stetson, D. B. & Medzhitov, R. Type I interferons in host defense. *Immunity* **25**, 373-381, doi:10.1016/j.immuni.2006.08.007 (2006).
- 354 Wilson, T. R. *et al.* Widespread potential for growth-factor-driven resistance to anticancer kinase inhibitors. *Nature* **487**, 505-509, doi:10.1038/nature11249 (2012).
- 355 Balachandran, S. & Barber, G. N. Defective translational control facilitates vesicular stomatitis virus oncolysis. *Cancer cell* **5**, 51-65 (2004).
- 356 Yuki, K. *et al.* Induction of oligodendrogenesis in glioblastoma-initiating cells by IFN-mediated activation of STAT3 signaling. *Cancer letters* **284**, 71-79, doi:10.1016/j.canlet.2009.04.020 (2009).
- 357 Yoshino, A. *et al.* Therapeutic implications of interferon regulatory factor (IRF)-1 and IRF-2 in diffusely infiltrating astrocytomas (DIA): response to interferon (IFN)-beta in glioblastoma cells and prognostic value for DIA. *Journal of neuro-oncology* **74**, 249-260, doi:10.1007/s11060-004-7316-1 (2005).
- 358 Motomura, K. *et al.* Benefits of interferon-beta and temozolomide combination therapy for newly diagnosed primary glioblastoma with the unmethylated MGMT promoter: A multicenter study. *Cancer* **117**, 1721-1730, doi:10.1002/cncr.25637 (2011).

- 359 Wang, F., Barrett, J. W., Ma, Y., Dekaban, G. A. & McFadden, G. Induction of alpha/beta interferon by myxoma virus is selectively abrogated when primary mouse embryo fibroblasts become immortalized. *Journal of virology* **83**, 5928-5932, doi:10.1128/JVI.02587-08 (2009).
- 360 Wang, F. *et al.* RIG-I mediates the co-induction of tumor necrosis factor and type I interferon elicited by myxoma virus in primary human macrophages. *PLoS pathogens* **4**, e1000099, doi:10.1371/journal.ppat.1000099 (2008).
- 361 Ablasser, A. *et al.* RIG-I-dependent sensing of poly(dA:dT) through the induction of an RNA polymerase III-transcribed RNA intermediate. *Nature immunology* **10**, 1065-1072, doi:10.1038/ni.1779 (2009).
- 362 Dai, P. *et al.* Myxoma virus induces type I interferon production in murine plasmacytoid dendritic cells via a TLR9/MyD88-, IRF5/IRF7-, and IFNAR-dependent pathway. *Journal of virology* **85**, 10814-10825, doi:10.1128/JVI.00104-11 (2011).
- 363 Cao, H. *et al.* Innate immune response of human plasmacytoid dendritic cells to poxvirus infection is subverted by vaccinia E3 via its Z-DNA/RNA binding domain. *PloS one* **7**, e36823, doi:10.1371/journal.pone.0036823 (2012).
- 364 Kawai, T. & Akira, S. TLR signaling. *Cell death and differentiation* **13**, 816-825, doi:10.1038/sj.cdd.4401850 (2006).
- 365 Thomas, D. L. *et al.* Myxoma virus combined with rapamycin treatment enhances adoptive T cell therapy for murine melanoma brain tumors. *Cancer immunology, immunotherapy : CII* **60**, 1461-1472, doi:10.1007/s00262-011-1045-z (2011).
- 366 Wang, F. *et al.* Disruption of Erk-dependent type I interferon induction breaks the myxoma virus species barrier. *Nature immunology* **5**, 1266-1274, doi:10.1038/ni1132 (2004).
- 367 Kastrukoff, L. F., Lau, A. S. & Thomas, E. E. The effect of mouse strain on herpes simplex virus type 1 (HSV-1) infection of the central nervous system (CNS). *Herpesviridae* **3**, 4, doi:10.1186/2042-4280-3-4 (2012).
- 368 Lando, Z., Teitelbaum, D. & Arnon, R. Induction of experimental allergic encephalomyelitis in genetically resistant strains of mice. *Nature* **287**, 551-552 (1980).
- 369 Gold, R., Linington, C. & Lassmann, H. Understanding pathogenesis and therapy of multiple sclerosis via animal models: 70 years of merits and culprits in experimental autoimmune encephalomyelitis research. *Brain : a journal of neurology* **129**, 1953-1971, doi:10.1093/brain/awl075 (2006).
- 370 Duarte, C. W. *et al.* Expression signature of IFN/STAT1 signaling genes predicts poor survival outcome in glioblastoma multiforme in a subtype-specific manner. *PloS one* **7**, e29653, doi:10.1371/journal.pone.0029653 (2012).
- 371 Vauleon, E. *et al.* Immune genes are associated with human glioblastoma pathology and patient survival. *BMC medical genomics* **5**, 41, doi:10.1186/1755-8794-5-41 (2012).
- 372 Saederup, N. *et al.* Selective chemokine receptor usage by central nervous system myeloid cells in CCR2-red fluorescent protein knock-in mice. *PloS one* **5**, e13693, doi:10.1371/journal.pone.0013693 (2010).

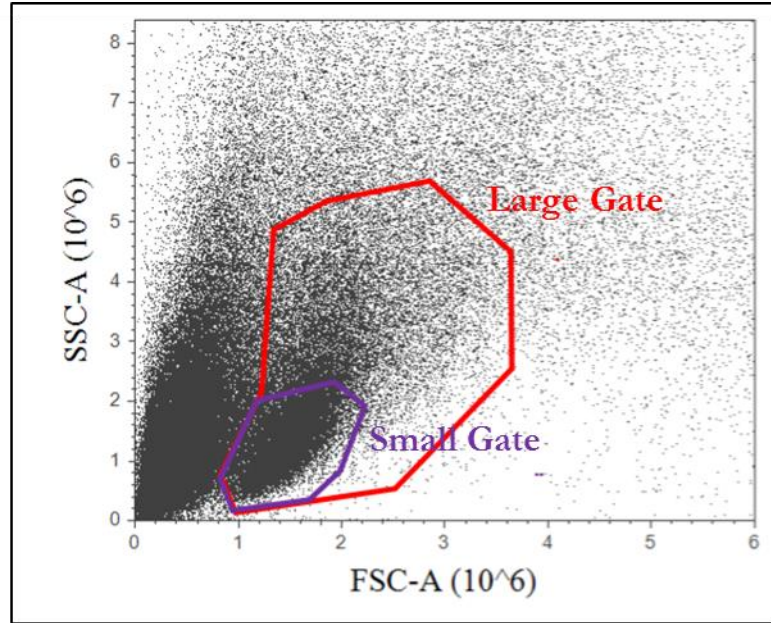
- 373 Familian, A., Eikelenboom, P. & Veerhuis, R. Minocycline does not affect amyloid beta phagocytosis by human microglial cells. *Neuroscience letters* **416**, 87-91, doi:10.1016/j.neulet.2007.01.052 (2007).
- 374 Seabrook, T. J., Jiang, L., Maier, M. & Lemere, C. A. Minocycline affects microglia activation, Abeta deposition, and behavior in APP-tg mice. *Glia* **53**, 776-782, doi:10.1002/glia.20338 (2006).
- 375 Suk, K. Minocycline suppresses hypoxic activation of rodent microglia in culture. *Neuroscience letters* **366**, 167-171, doi:10.1016/j.neulet.2004.05.038 (2004).
- 376 Markovic, D. S. *et al.* Minocycline reduces glioma expansion and invasion by attenuating microglial MT1-MMP expression. *Brain, behavior, and immunity* **25**, 624-628, doi:10.1016/j.bbi.2011.01.015 (2011).
- 377 Campbell, J. H. *et al.* Minocycline inhibition of monocyte activation correlates with neuronal protection in SIV neuroAIDS. *PloS one* **6**, e18688, doi:10.1371/journal.pone.0018688 (2011).
- 378 Tai, K., Iwasaki, H., Ikegaya, S. & Ueda, T. Minocycline modulates cytokine and chemokine production in lipopolysaccharide-stimulated THP-1 monocytic cells by inhibiting I κ B kinase alpha/beta phosphorylation. *Translational research : the journal of laboratory and clinical medicine* **161**, 99-109, doi:10.1016/j.trsl.2012.10.001 (2013).
- 379 Pang, T., Wang, J., Benicky, J. & Saavedra, J. M. Minocycline ameliorates LPS-induced inflammation in human monocytes by novel mechanisms including LOX-1, Nur77 and LITAF inhibition. *Biochimica et biophysica acta* **1820**, 503-510, doi:10.1016/j.bbagen.2012.01.011 (2012).
- 380 Nikodemova, M., Watters, J. J., Jackson, S. J., Yang, S. K. & Duncan, I. D. Minocycline down-regulates MHC II expression in microglia and macrophages through inhibition of IRF-1 and protein kinase C (PKC)alpha/betaII. *The Journal of biological chemistry* **282**, 15208-15216, doi:10.1074/jbc.M611907200 (2007).
- 381 Cao, X. *et al.* Defective lymphoid development in mice lacking expression of the common cytokine receptor gamma chain. *Immunity* **2**, 223-238 (1995).
- 382 DiSanto, J. P., Muller, W., Guy-Grand, D., Fischer, A. & Rajewsky, K. Lymphoid development in mice with a targeted deletion of the interleukin 2 receptor gamma chain. *Proceedings of the National Academy of Sciences of the United States of America* **92**, 377-381 (1995).
- 383 Mombaerts, P. *et al.* RAG-1-deficient mice have no mature B and T lymphocytes. *Cell* **68**, 869-877 (1992).
- 384 Lee, J. *et al.* Dual role of inflammatory stimuli in activation-induced cell death of mouse microglial cells. Initiation of two separate apoptotic pathways via induction of interferon regulatory factor-1 and caspase-11. *The Journal of biological chemistry* **276**, 32956-32965, doi:10.1074/jbc.M104700200 (2001).
- 385 Yun, H. J. *et al.* Daxx mediates activation-induced cell death in microglia by triggering MST1 signalling. *The EMBO journal* **30**, 2465-2476, doi:10.1038/emboj.2011.152 (2011).
- 386 Mayo, L. *et al.* Dual role of CD38 in microglial activation and activation-induced cell death. *Journal of immunology* **181**, 92-103 (2008).

- 387 Ksendzovsky, A. *et al.* Investigation of immunosuppressive mechanisms in a mouse glioma model. *Journal of neuro-oncology* **93**, 107-114, doi:10.1007/s11060-009-9884-6 (2009).
- 388 Trifilo, M. J. *et al.* CXC chemokine ligand 10 controls viral infection in the central nervous system: evidence for a role in innate immune response through recruitment and activation of natural killer cells. *Journal of virology* **78**, 585-594 (2004).
- 389 Alsharifi, M. *et al.* NK cell-mediated immunopathology during an acute viral infection of the CNS. *European journal of immunology* **36**, 887-896, doi:10.1002/eji.200535342 (2006).
- 390 Christensen, J. E., Andreasen, S. O., Christensen, J. P. & Thomsen, A. R. CD11b expression as a marker to distinguish between recently activated effector CD8(+) T cells and memory cells. *International immunology* **13**, 593-600 (2001).
- 391 McFarland, H. I., Nahill, S. R., Maciaszek, J. W. & Welsh, R. M. CD11b (Mac-1): a marker for CD8+ cytotoxic T cell activation and memory in virus infection. *Journal of immunology* **149**, 1326-1333 (1992).
- 392 Lin, Y., Roberts, T. J., Sriram, V., Cho, S. & Brutkiewicz, R. R. Myeloid marker expression on antiviral CD8+ T cells following an acute virus infection. *European journal of immunology* **33**, 2736-2743, doi:10.1002/eji.200324087 (2003).
- 393 Wang, H. *et al.* Targeting interleukin 6 signaling suppresses glioma stem cell survival and tumor growth. *Stem cells* **27**, 2393-2404, doi:10.1002/stem.188 (2009).
- 394 Zhou, Y. *et al.* The chemokine GRO-alpha (CXCL1) confers increased tumorigenicity to glioma cells. *Carcinogenesis* **26**, 2058-2068, doi:10.1093/carcin/bgi182 (2005).
- 395 Silva, M. T. Macrophage phagocytosis of neutrophils at inflammatory/infectious foci: a cooperative mechanism in the control of infection and infectious inflammation. *Journal of leukocyte biology* **89**, 675-683, doi:10.1189/jlb.0910536 (2011).
- 396 Hart, S. P., Dougherty, G. J., Haslett, C. & Dransfield, I. CD44 regulates phagocytosis of apoptotic neutrophil granulocytes, but not apoptotic lymphocytes, by human macrophages. *Journal of immunology* **159**, 919-925 (1997).
- 397 Michlewska, S., Dransfield, I., Megson, I. L. & Rossi, A. G. Macrophage phagocytosis of apoptotic neutrophils is critically regulated by the opposing actions of pro-inflammatory and anti-inflammatory agents: key role for TNF-alpha. *FASEB journal : official publication of the Federation of American Societies for Experimental Biology* **23**, 844-854, doi:10.1096/fj.08-121228 (2009).
- 398 Prinz, M. & Priller, J. Tickets to the brain: role of CCR2 and CX3CR1 in myeloid cell entry in the CNS. *Journal of neuroimmunology* **224**, 80-84, doi:10.1016/j.jneuroim.2010.05.015 (2010).
- 399 Gregoire, C. *et al.* The trafficking of natural killer cells. *Immunological reviews* **220**, 169-182, doi:10.1111/j.1600-065X.2007.00563.x (2007).
- 400 Van Rooijen, N. & Sanders, A. Liposome mediated depletion of macrophages: mechanism of action, preparation of liposomes and applications. *Journal of immunological methods* **174**, 83-93 (1994).

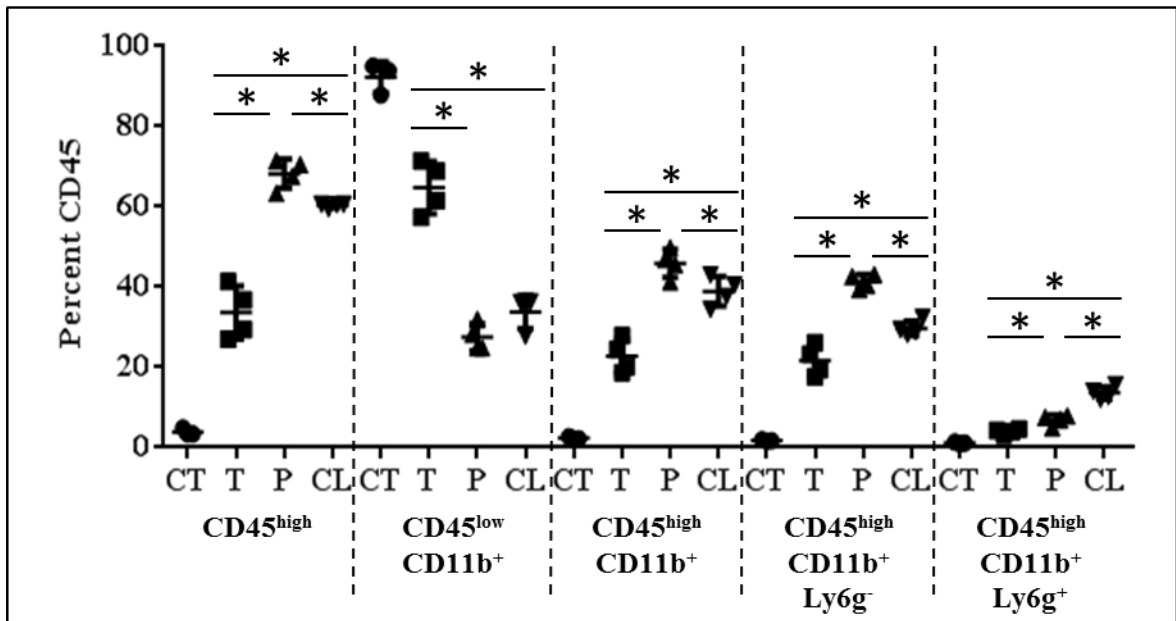
- 401 Sunderkotter, C. *et al.* Subpopulations of mouse blood monocytes differ in maturation stage and inflammatory response. *Journal of immunology* **172**, 4410-4417 (2004).
- 402 Huitinga, I., van Rooijen, N., de Groot, C. J., Uitdehaag, B. M. & Dijkstra, C. D. Suppression of experimental allergic encephalomyelitis in Lewis rats after elimination of macrophages. *The Journal of experimental medicine* **172**, 1025-1033 (1990).
- 403 Duffield, J. S. *et al.* Selective depletion of macrophages reveals distinct, opposing roles during liver injury and repair. *The Journal of clinical investigation* **115**, 56-65, doi:10.1172/JCI22675 (2005).
- 404 Buch, T. *et al.* A Cre-inducible diphtheria toxin receptor mediates cell lineage ablation after toxin administration. *Nature methods* **2**, 419-426, doi:10.1038/nmeth762 (2005).
- 405 Ueno, M. *et al.* Layer V cortical neurons require microglial support for survival during postnatal development. *Nature neuroscience* **16**, 543-551, doi:10.1038/nn.3358 (2013).
- 406 Gowing, G., Vallieres, L. & Julien, J. P. Mouse model for ablation of proliferating microglia in acute CNS injuries. *Glia* **53**, 331-337, doi:10.1002/glia.20288 (2006).
- 407 Seaman, W. E., Sleisenger, M., Eriksson, E. & Koo, G. C. Depletion of natural killer cells in mice by monoclonal antibody to NK-1.1. Reduction in host defense against malignancy without loss of cellular or humoral immunity. *Journal of immunology* **138**, 4539-4544 (1987).
- 408 Heimberger, A. B. *et al.* Incidence and prognostic impact of FoxP3+ regulatory T cells in human gliomas. *Clinical cancer research : an official journal of the American Association for Cancer Research* **14**, 5166-5172, doi:10.1158/1078-0432.CCR-08-0320 (2008).
- 409 Yang, I. *et al.* CD8+ T-cell infiltrate in newly diagnosed glioblastoma is associated with long-term survival. *Journal of clinical neuroscience : official journal of the Neurosurgical Society of Australasia* **17**, 1381-1385, doi:10.1016/j.jocn.2010.03.031 (2010).
- 410 Yang, I., Han, S. J., Sughrue, M. E., Tihan, T. & Parsa, A. T. Immune cell infiltrate differences in pilocytic astrocytoma and glioblastoma: evidence of distinct immunological microenvironments that reflect tumor biology. *Journal of neurosurgery* **115**, 505-511, doi:10.3171/2011.4.JNS101172 (2011).
- 411 Fossati, G. *et al.* Neutrophil infiltration into human gliomas. *Acta neuropathologica* **98**, 349-354 (1999).
- 412 Aguzzi, A., Barres, B. A. & Bennett, M. L. Microglia: scapegoat, saboteur, or something else? *Science* **339**, 156-161, doi:10.1126/science.1227901 (2013).
- 413 Mueller, M. M. *et al.* Autocrine growth regulation by granulocyte colony-stimulating factor and granulocyte macrophage colony-stimulating factor in human gliomas with tumor progression. *The American journal of pathology* **155**, 1557-1567, doi:10.1016/S0002-9440(10)65472-7 (1999).
- 414 Nagai, T. *et al.* Targeting tumor-associated macrophages in an experimental glioma model with a recombinant immunotoxin to folate receptor beta. *Cancer*

- immunology, immunotherapy* : *CII* **58**, 1577-1586, doi:10.1007/s00262-009-0667-x (2009).
- 415 Soderquest, K. *et al.* Monocytes control natural killer cell differentiation to effector phenotypes. *Blood* **117**, 4511-4518, doi:10.1182/blood-2010-10-312264 (2011).
- 416 Jenne, C. N. *et al.* Neutrophils recruited to sites of infection protect from virus challenge by releasing neutrophil extracellular traps. *Cell host & microbe* **13**, 169-180, doi:10.1016/j.chom.2013.01.005 (2013).
- 417 Kim, C. H., Johnston, B. & Butcher, E. C. Trafficking machinery of NKT cells: shared and differential chemokine receptor expression among V alpha 24(+)V beta 11(+) NKT cell subsets with distinct cytokine-producing capacity. *Blood* **100**, 11-16, doi:10.1182/blood-2001-12-0196 (2002).
- 418 Hodge, D. L. *et al.* MCP-1/CCR2 interactions direct migration of peripheral B and T lymphocytes to the thymus during acute infectious/inflammatory processes. *European journal of immunology* **42**, 2644-2654, doi:10.1002/eji.201242408 (2012).
- 419 Liu, W. T., Lin, C. H., Hsiao, M. & Gean, P. W. Minocycline inhibits the growth of glioma by inducing autophagy. *Autophagy* **7**, 166-175 (2011).
- 420 Bi, Z., Barna, M., Komatsu, T. & Reiss, C. S. Vesicular stomatitis virus infection of the central nervous system activates both innate and acquired immunity. *Journal of virology* **69**, 6466-6472 (1995).
- 421 McGavern, D. B., Homann, D. & Oldstone, M. B. T cells in the central nervous system: the delicate balance between viral clearance and disease. *The Journal of infectious diseases* **186 Suppl 2**, S145-151, doi:10.1086/344264 (2002).
- 422 Wang, T. *et al.* IFN-gamma-producing gamma delta T cells help control murine West Nile virus infection. *Journal of immunology* **171**, 2524-2531 (2003).
- 423 Wang, T. Role of gammadelta T cells in West Nile virus-induced encephalitis: friend or foe? *Journal of neuroimmunology* **240-241**, 22-27, doi:10.1016/j.jneuroim.2011.10.004 (2011).
- 424 Sciammas, R., Kodukula, P., Tang, Q., Hendricks, R. L. & Bluestone, J. A. T cell receptor-gamma/delta cells protect mice from herpes simplex virus type 1-induced lethal encephalitis. *The Journal of experimental medicine* **185**, 1969-1975 (1997).
- 425 Shultz, L. D., Ishikawa, F. & Greiner, D. L. Humanized mice in translational biomedical research. *Nature reviews. Immunology* **7**, 118-130, doi:10.1038/nri2017 (2007).
- 426 Vandenberk, L. & Van Gool, S. W. Treg infiltration in glioma: a hurdle for antiglioma immunotherapy. *Immunotherapy* **4**, 675-678, doi:10.2217/imt.12.64 (2012).
- 427 Gabrilovich, D. I. & Nagaraj, S. Myeloid-derived suppressor cells as regulators of the immune system. *Nature reviews. Immunology* **9**, 162-174, doi:10.1038/nri2506 (2009).
- 428 Bauer, S. *et al.* Activation of NK cells and T cells by NKG2D, a receptor for stress-inducible MICA. *Science* **285**, 727-729 (1999).

- 429 Lamb, L. S., Jr. Gammadelta T cells as immune effectors against high-grade gliomas. *Immunologic research* **45**, 85-95, doi:10.1007/s12026-009-8114-9 (2009).
- 430 Liu, C. *et al.* Chemokine receptor CXCR3 promotes growth of glioma. *Carcinogenesis* **32**, 129-137, doi:10.1093/carcin/bgq224 (2011).
- 431 Rappert, A. *et al.* CXCR3-dependent microglial recruitment is essential for dendrite loss after brain lesion. *The Journal of neuroscience : the official journal of the Society for Neuroscience* **24**, 8500-8509, doi:10.1523/JNEUROSCI.2451-04.2004 (2004).
- 432 Pak-Wittel, M. A., Yang, L., Sojka, D. K., Rivenbark, J. G. & Yokoyama, W. M. Interferon-gamma mediates chemokine-dependent recruitment of natural killer cells during viral infection. *Proceedings of the National Academy of Sciences of the United States of America* **110**, E50-59, doi:10.1073/pnas.1220456110 (2013).
- 433 Parker, J. N. *et al.* Engineered herpes simplex virus expressing IL-12 in the treatment of experimental murine brain tumors. *Proceedings of the National Academy of Sciences of the United States of America* **97**, 2208-2213, doi:10.1073/pnas.040557897 (2000).
- 434 Lee, Y. S. *et al.* Enhanced antitumor effect of oncolytic adenovirus expressing interleukin-12 and B7-1 in an immunocompetent murine model. *Clinical cancer research : an official journal of the American Association for Cancer Research* **12**, 5859-5868, doi:10.1158/1078-0432.CCR-06-0935 (2006).
- 435 Stanford, M. M., Barrett, J. W., Gilbert, P. A., Bankert, R. & McFadden, G. Myxoma virus expressing human interleukin-12 does not induce myxomatosis in European rabbits. *Journal of virology* **81**, 12704-12708, doi:10.1128/JVI.01483-07 (2007).



Supplementry Figure 1: Example of flow cytometry scatter plot with large and small gate. Representative scatter plot from flow cytometry studies demonstrating the gating for ‘live cells’ in the large gate (red) and small gate (purple).



Supplementry Figure 2: Percent CD45 of clodronate liposome experiment. Wildtype C57Bl/6 mice implanted with K1492 cells were treated at 11, 12, and 13 dpi with Clodronate liposomes (CL) or vehicle (P) and with Myxoma virus administration at 12dpi compared to not tumour (CT) or untreated K1492 (T). Tumour infiltrating immunocytes analyzed by flow cytometry at 15 days-post implantation, 3 days post-treatment with Myxoma virus (MYXV) or untreated (NoTx). Scatter plot of percent CD45. Error bars represent standard deviation and asterisks are significantly different (t-test, $p < 0.05$).

Supplementary Table 1: NPcis Litter #1. DOB: 2011.08.11

Date	Age (days)	Cause of Death/Sacrifice	Autopsy	Visible Brain Lesions	Sections
09-Dec-11	127	Huge Shoulder Necrotic Lesion	Not performed	No	No
06-Jan-12	155	Shaky walking, ataxia	large mediastinal mass ?large B-cell lymphoma?	No	No
03-Feb-12	183	Necrotic shoulder lesion. STS?	Nothing further	No	Yes (-ve)
14-Feb-12	194	Found Dead - Asymptomatic	Not performed	No	Yes (-ve)
02-Mar-12	211	Large necrotic lesion on neck, STS?	Lungs infiltrated with many white masses; enlarged spleen	No	Yes (-ve)
09-Mar-12	218	Huge hind left leg mass, weight loss STS?	Nothing further	Yes	Yes (+ve)
09-Mar-12	218	Ataxia, laboured breathing	Greatly enlarged thymus	No	Yes (-ve)

Supplementary Table 2: NPcis Litter #2. DOB: 2011.11.17

Date	Age (days)	Cause of Death/Sacrifice	Autopsy	Visible Brain Lesions	Sections
23-Mar-12	188	ataxia, weight loss and labored breathing	no visible lesions upon autopsy	No	Yes (-ve)
17-May-12	243	Massive tumour on right lower abdomen/flank	no other visible lesions upon autopsy	No	Yes (-ve)
22-May-12	248	labored breathing, hunched, lethargic	Pericardial mass	No	Yes (-ve)
26-May-12	252	Died overnight, huge inner mass (thought it was just fat)	Huge, discoloured spleen (pic) also large mass around liver (or was liver) Greatly enlarged adrenals, ?pheochromocytoma?	No	Yes (-ve)
28-May-12	254	Hyperactive, very fast breathing, skinny	Enlarged adrenals, ?bloody lungs?	Mass in ventricle; Grade II lesion in right hemisphere	Yes (+ve)

Supplementary Table 3: *NPcis* Litter #3. DOB: 2011.12.21

Date	Age (days)	Cause of Death/Sacrifice	Autopsy	Visible Brain Lesions	Sections
01-Jun-12	164	Hunched, underweight, ?ataxia?	Malocclusion likely causing symptoms, no other tumours spotted	No	Yes (?)
21-Jun-12	184	Forelimb paralysis	No obvious lesions upon autopsy	No	No
05-Sep-12	260	Complete hind limb paralysis in one leg	No obvious lesions upon autopsy	No	Yes (-ve)
21-Sep-12	276	Died overnight	-	-	-
01-Nov-12	317	Very fat but emaciated face	Major metastatic disease, very prominent in liver and lungs. Huge spleen. Large solid tumour, around liver area	No	Yes (-ve)
16-Nov-12	333	Very fat but emaciated face.... Large tumour burden	Major metastatic disease, very prominent in liver and lungs. Huge spleen.	No	Yes (+ve)

APPENDIX 1: Mouse Genotyping, Primer Sequences and shRNA sequences

1.) NPcis mice Genotyping

Primer Sets		
<i>Nfl</i> primer set		
Primer Name	Sequence	Target
oIMR8307	GGT ATT GAA TTG AAG CAC	Wild type Forward
oIMR8308	TTC AAT ACC TGC CCA AGG	Common
oIMR8309	ATT CGC CAA TGA CAA GAC	Mutant Forward
<i> Tp53</i> primer set		
Primer Name	Sequence	Target
oIMR7777	ACA GCG TGG TGG TAC CTT AT	Wild type Forward
oIMR7778	TAT ACT CAG AGC CGG CCT	Common
oIMR8306	CTA TCA GGA CAT AGC GTT GG	Mutant Forward

Volumes (μL)/Reaction		
	<i>Nfl</i>	<i>Tp53</i>
ddH ₂ O	7.80	9.30
10 PCR Mix	2.00	2.00
50mM MgCl ₂	1.00	1.00
dNTPs (10uM)	1.00	1.00
oIMR8307 / 7777	2.00	0.16
oIMR8308 / 7778	2.00	2.00
oIMR8309 / 8306	2.00	2.34
Taq (Invitrogen)	0.20	0.20

Reaction Conditions		
Temperature ($^{\circ}$ C)	Time (seconds)	
94	180	
94	30	
60	60	35X
72	60	
72	300	

Expected Band Sizes		
Primer Set	Size (bp)	
<i>Nfl</i>	Homozygote	203
	Heterozygote	203 + 350
<i>Tp53</i>	Homozygote	450
	Heterozygote	450+ 650

2.) RT-PCR Primer Sequences

<i>Mouse Primer Sets</i>	
Gene	Sequence 5' – 3'
mIFN α 4	F: GAA CAA GAG GGC CTT GAC AG R: AGG AGG TTC CTG CAT CAC AC
mIFN β	F: CAT GGC TAG GCT CAG CAC TT R: CAT TCC AAG CAG CAG ATG AA
mIRF7	F: ACA GCA CAG GGC GTT TTA TC R: GAG CCC AGC ATT TTC TCT TG
mIFIT2	F: AAG CAC CAA GTG TGG GTA GG R: CTG TGT CAA AGC GCT CAA AG
mISG15	F: AAG CAG CCA GAA GCA GAC TC R: TCG CTG CAG TTC TGT ACC AC
mCXCL10	F: CTA TCC TGC CCA CGT GTT G R: CTC TGC TGT CCA TCC ATC G
mCXCR3	F: GCA AGT TCC CAA CAA CAA GT R: CAC TGC CAA CAA TGG AAG A
mIRF9	F: AAC AGG AGC GAC AGC AAC A R: AAC TCC ACC TGC TCC ATG C
mGAPDH	F: TGT TCC TAC CCC CAA TGT GT R: TGT GAG GGA GAT GCT CAG TG

<i>Human Primer Sets</i>	
Gene	Sequence 5' – 3'
hIFN α 4	F: AGA GGC CGA AGT TCA AGG TT R: CTT GAG CCT TCT GA ACT GG
h-panIFN α	F: TGA TTT CTG CTC TGA CAA CCT C R: CAG CAG AYC TTC AAY CTC TTY A
hIFN β	F: CAT TAC CTG AAG GCC AAG GA R: CAG CAT CTG CTG GTT GAA GA
hIRF7	F: TAC CAT CTA CCT GGC TTC G R: GCT CCA TAA GGA AGC ACT CG
hISG15	F: GAC CTG ACG GTG AAG ATG CT R: GCC CTT GTT ATT CCT CAC CA
hISG56	F: TCT CAG AGG AGC CTG GCT AA R: AAG CTC TTC AGG GCT TGG TC
hMX1	F: ACC TGA TGG CCT ATC ACC AG R: TTC AGG AGC CAG CTG TAG GT
h β -Actin	F: GGA CTT CGA GCA AGA GAT GG R: GCA CTG TGT TGG CGTACA C

<i>Cloning/Sequencing Primers</i>	
Gene	Sequence 5' – 3'
ClaI-ISRE	ATC GAT TCA TGT CTG GAT CCA AGC
PfIFL-ISRE	GACGCAGTC TTTACCACC AGT ACC GGA
ISRE::FLUC Sequencing	F: GTG AAC GGA TCT CGA CGG TA R: CAC GCT CAT CTC CAA ATA CTC

3.) shRNA Sequences

<i>IRF9 shRNA Sequences</i>		
Official Name	Thesis Name	Sequence 5' – 3'
TRCN0000232234	Clone 1	CCGGCCCTACAAAAGTATATCGAATACTCGAGTATTCGATATACTTTGTAGGGTTTTTG
TRCN0000232235	Clone 2	CCGGGAGGACCAATGGCGTTGTAACTCGAGTTTACAACGCCATTGGTCCTCTTTTTTG
TRCN0000232236	Clone 3	CCGGGTCCAAAGCAACCCTACATTTCTCGAGAAAATGTAGGGTTGCTTGGAACTTTTTG
TRCN0000232237	Clone 4	CCGGGTGATGTTTCTCCTTACAATCTCGAGATTTGTAGGAGAAACATCACTTTTTG
TRCN0000257187	Clone 5	CCGGCTCAACAAGAGTCCGAAATTTCTCGAGAAAATTCGGAACTCTTGTGAGTTTTTG
#SHC002	Scram	N/A